

# **Targeted degradation of polycyclic aromatic hydrocarbons: a potential strategy for coal tar remediation**

By

© Ahmad Qublan Al-Shra'ah

A thesis submitted to the School of Graduate Studies in partial fulfillment of the requirements for the degree of Doctor of Philosophy

Department of Chemistry

Memorial University of Newfoundland

February 2018

St John's, Newfoundland and Labrador

## Abstract

The presence and degradation of coal tar deposits is of a great environmental concern due to the toxicity of many of its components especially polycyclic aromatic hydrocarbons (PAHs) on the health of humans and animals. In this work, the chemical degradation of PAHs in coal tar was investigated by using several approaches: a) chemical reduction using an acidified Mg/EtOH system; b) chemical oxidation using Fenton's reagent or peroxyacetic acid; c) thermal removal using microwave-assisted heating; and d) PAH bromination.

The reductive degradation of anthracene as a model PAH compound using Mg/EtOH in the presence of glacial acetic acid was achieved in which anthracene was converted to 9,10-dihydroanthracene. The reaction was optimized by investigating the effect of Mg concentration, co-solvent, volume of glacial acetic acid, and time on conversion yield. Experimental design methodology was used for optimizing the anthracene reduction conditions and these optimum conditions were then used for PAH reduction in coal tar. The main advantage of this approach is that the hydrogenated PAHs formed are less toxic than the parent compounds. Selective reduction of anthracene and fluoranthene in coal tar was achieved with high conversion (>90%) at room temperature within a short time (0.5 h) as determined by GC/MS and GC/FID.

Fenton's reagent ( $\text{Fe}^{2+} + \text{H}_2\text{O}_2$ ) was used to convert anthracene to 9,10-anthraquinone. The reaction was optimized by investigating the effect of the concentration of  $\text{Fe}^{2+}$ , and  $\text{H}_2\text{O}_2$ , temperature and time on the conversion % of anthracene. In addition, anthracene oxidation using peroxyacetic acid in acetic acid and  $\text{H}_2\text{SO}_4$  was also investigated. The reaction conditions were optimized by studying the influence of temperature and time on removal

% of anthracene. Experimental design methodology was used for optimizing the anthracene oxidation using Fenton's reagent or peroxyacetic acid. Fenton's reagent showed more efficiency in removal of PAHs compared to peroxyacetic acid.

Microwave-assisted thermal removal of pyrene and PAHs in coal tar was achieved using both closed and open microwave systems at low temperatures (<300 °C). The effect of microwave absorbers such as biochar, activated carbon, and TiO<sub>2</sub> on pyrene and coal tar was investigated. The volatile and non-volatile fractions from microwave heating were individually collected and dissolved in dichloromethane (DCM) then analyzed by GC-MS and GC-FID. In addition, TGA analysis of coal tar with and without additives (e.g., biochar, activated carbon, and TiO<sub>2</sub>) was investigated for additive influence.

Bromination of pyrene was achieved using hydrobromic acid/H<sub>2</sub>O<sub>2</sub> and a binary solvent, diethyl ether and methanol (1:1, v/v), 12 h. The reaction was selective, where 1-bromopyrene was formed with high yield (>95%). This reaction was also used for PAH bromination in the coal tar. The removal percentages of PAHs from coal tar increased with increasing the molar equivalents (0.25–4.00 equiv.) of the brominating reagent (HBr/H<sub>2</sub>O<sub>2</sub>), but the resulting products could not be ascertained possibly due to side reactions occurring in the coal tar mixture during the bromination reaction.

## **Acknowledgments**

First, I would like to express my sincere gratitude and appreciation to my supervisors (Drs., Yuming Zhao, and Stephanie MacQuarrie) and supervisory committee members (Drs. Martin Mkandawire and Paris Georghiou) for their guidance, patience, encouragement, motivation, and help.

I would also like to present my deepest thanks to Dr. Robert Helleur for his help in supporting this research.

I would like to extend my appreciation and thanks to Dr. Shofiur Rahman for his help.

Thank you to Linda Winsor (CCART member) for GC-MS, and Geraldine Kennedy (Lab instructor) for GC-FID.

I would like to thank Mr. Fred Baechler for providing the coal tar samples, which were collected from the pre-reclaimed abandoned Sydney Tarponds and Steel Milling Industry sites in Sydney Nova Scotia; Ms. Debi Walker of Verschuren Centre for Sustainability in Energy and the Environment for all logistical support rendered to the study. I would also like to thank Mr. Sadegh Papari for help using Design-Expert (DX9) software.

I would also thank my mother, Hamda Saroor, for her prayers and encouragement, which always makes me more motivated to achieve this research.

I would like to express my deepest and most sincere appreciation and gratitude to my dear father, Qublan Al-Shra'ah, who passed away in 2011. His memory will always be with me. Thank you very much to my sisters, brothers, all family members, and friends for their encouragement and assistance.

Finally, I would like to thank the Department of Chemistry at Memorial University of Newfoundland, and the Natural Sciences and Engineering Research Council (NSERC) of Canada for their financial support.

## Dedication

*I would like to dedicate this dissertation to my dear mother, Hamda Saroor  
and to the memory of my father, Qublan Al-Shra'ah.*

## Table of Contents

Abstract .....	ii
Acknowledgments .....	iv
Dedication .....	vi
Table of Contents .....	vii
List of Figures.....	x
List of Tables .....	xv
List of Schemes .....	xvi
List of Abbreviations.....	xviii
<b>Chapter 1. Introduction .....</b>	<b>1</b>
1.1. Background and research question .....	2
1.2. Hypothesis .....	3
1.3. Objectives .....	3
1.4. Literature review .....	4
1.4.1. Polycyclic aromatic hydrocarbons: chemical structures, sources, physical and chemical properties, and toxicity. ....	4
1.4.2. The Sydney Tar Ponds and Coke Ovens .....	9
1.4.3. Approaches for PAH degradation .....	10
1.4.3.1. Chemical reduction .....	11
1.4.3.2. Chemical oxidation .....	12
1.4.3.3. Thermal remediation.....	19
1.4.3.4. PAH bromination .....	20
1.5. Co-authorship statement .....	22
1.6. References .....	23
<b>Chapter 2. Optimizing reductive degradation of PAHs using anhydrous ethanol with magnesium catalyzed by glacial acetic acid .....</b>	<b>30</b>
Abstract .....	31
2.1. Introduction .....	32
2.2. Materials and method.....	33
2.2.1. Chemicals.....	33
2.2.2. Anthracene and coal tar reduction experiments .....	34
2.2.3. Experimental Design.....	35
2.2.4. Samples analysis .....	36
2.3. Results and discussion .....	37
2.3.1. Effect of magnesium activation.....	37
2.3.2. Effect of magnesium with ethanol .....	38
2.3.3. Anthracene reduction mechanism .....	40
2.3.4. Optimization of anthracene reduction.....	41
2.3.4.1. Screening of variables .....	41
2.3.4.2. Optimization using central composite design (CCD).....	43
2.3.5. Optimization of coal tar reduction .....	49
2.4. Conclusions .....	54

2.5. References .....	55
<b>Chapter 3. Oxidation of coal tar: Fenton’s reagent vs. peroxyacetic acid/H<sub>2</sub>SO<sub>4</sub> .....</b>	<b>59</b>
Abstract .....	60
3.1. Introduction .....	61
3.2. Materials and Methods .....	63
3.2.1. Chemicals.....	63
3.2.2. Fenton oxidation.....	63
3.2.3. Peroxyacetic acid/H <sub>2</sub> SO <sub>4</sub> oxidation.....	64
3.2.4. GC analyses .....	65
3.2.5. Experimental design.....	66
3.2.5.1. Fenton oxidation of anthracene.....	66
3.2.5.2. Peroxyacetic acid oxidation of anthracene.....	67
3.3. Results and discussion .....	67
3.3.1. Operational conditions for Fenton oxidation.....	67
3.3.2. Experimental design.....	68
3.3.2.1. Fenton oxidation of anthracene: Screening variables.....	68
3.3.2.2. Fenton oxidation of anthracene: Optimization using central composite design .....	70
3.3.2.3. Oxidation of anthracene with peroxyacetic acid: Optimization using central composite design .....	76
3.3.3. Optimization of coal tar oxidation .....	80
3.3.3.1. The effect of Fenton’s reagent .....	80
3.3.3.2. The effect of peroxyacetic acid/H <sub>2</sub> SO <sub>4</sub> .....	84
3.3.3.3. Fenton’s reagent vs. peroxyacetic acid.....	86
3.4. Conclusion .....	88
3.5. References .....	89
<b>Chapter 4. Microwave-assisted thermal removal of PAHs from coal tar .....</b>	<b>93</b>
Abstract .....	94
4.1. Introduction .....	95
4.2. Materials and methods .....	97
4.2.1. Materials.....	97
4.2.2. Experimental methods .....	97
4.2.3. GC Analysis.....	99
4.2.4. Thermogravimetric analysis (TGA) .....	100
4.3. Results and discussion .....	101
4.3.1. Operating conditioning of the microwave with carbon materials .....	101
4.3.2. Effect of microwave absorber .....	101
4.3.3. GC analyses .....	111
4.3.4. TGA analysis .....	121
4.4. Conclusions .....	124
4.5. References .....	125

<b>Chapter 5. A preliminary study for PAH bromination in coal tar using HBr-H<sub>2</sub>O<sub>2</sub></b>	128
.....	128
Abstract .....	129
5.1. Introduction .....	130
5.2. Experimental .....	131
5.2.1. Chemicals .....	131
5.2.2. Method .....	131
5.2.2.1. Pyrene bromination.....	131
5.2.2.2. Coal tar bromination.....	132
5.2.2.3. GC analysis .....	132
5.3. Results and discussion .....	133
5.3.1. Pyrene bromination .....	133
5.3.2. PAH bromination in coal tar.....	136
5.4. Conclusions .....	140
5.5. References .....	141
<b>6. Conclusions and future work .....</b>	<b>145</b>
6.1. Conclusions .....	145
6.2. Future work .....	147
6.3. References .....	150
<b>Appendices.....</b>	<b>151</b>
Appendix A. Supporting information for Chapter 1.....	151
Appendix B. Supporting information for Chapter 4.....	164
Appendix C. Supporting information for Chapter 5.....	167
References .....	169

## List of Figures

<b>Figure 1.1.</b> Chemical structures and names of 16 selected PAHs [1] .....	5
<b>Figure 2.1.</b> Effect of Mg activation and Mg particle size on reduction of anthracene in anhydrous ethanol at room temperature. A) Non-catalyzed Mg powder, B) catalyzed Mg turnings, and C) catalyzed Mg powder. The reaction conditions are 250 ppm anthracene ( $C_i$ ), 30 mg Mg, glacial acetic acid (30 $\mu$ L), and 3 h reaction time. Error bars represent the RSD%, n=3. ....	38
<b>Figure 2.2.</b> Effect of co-solvent on anthracene reduction using Mg catalyzed by glacial acetic acid (30 $\mu$ L). The inset plot represents the anthracene degradation using Mg/EtOH as a function of time. The reaction conditions are 250 ppm anthracene ( $C_i$ ), 30 mg of Mg powder, and 3 h reaction time. Error bars represent the RSD%, n=3. ....	39
<b>Figure 2.3.</b> Pareto chart for four factors (Table 2.1) effecting on anthracene reduction using magnesium activated by glacial acetic acid with anhydrous ethanol as co-solvent. ....	42
<b>Figure 2.4.</b> Normal plot of residuals (A) and predicted vs. actual values (B) of anthracene reduction in the optimization stage of the designed experiment. ....	47
<b>Figure 2.5.</b> (A) Effect of glacial acetic acid and magnesium (Mg), at constant reaction time (105 min), (B) time and Mg at constant volume of glacial acetic acid (35 $\mu$ L), and (C) time and glacial acetic acid at constant amount of Mg (20 mg) on anthracene reduction. ....	48
<b>Figure 2.6.</b> GC-FID analysis of anthracene (A) and the reaction product of anthracene reduction using Mg/EtOH system (B). The reaction conditions: 30 mg Mg concentration, 60 $\mu$ L glacial acetic acid volume, 30 min exposure time, and $C_i$ of anthracene is 250 ppm. ....	49
<b>Figure 2.7.</b> Chromatogram of GC-FID analysis of coal tar soluble in anhydrous ethanol. 0.400 g coal tar dissolved in 60 mL of anhydrous ethanol. Approximately, 66% of coal tar dissolved. Peak numbers correspond to compounds listed in Table 2.5. ....	50
<b>Figure 2.8.</b> Chromatogram of GC-FID analysis of reduction of coal tar soluble in anhydrous ethanol using Mg catalyzed by glacial acetic acid under the conditions (A, B, and C) listed in Table 2.6. Peak numbers correspond to compounds listed in Table 2.5. .	52
<b>Figure 2.9.</b> Evaluation of Mg powder catalyzed by glacial acetic acid in anhydrous ethanol for PAHs reduction in coal tar at room temperature. Reaction conditions (A, B, and C) are listed in Table 4. Error bars represents RSD%, n=3. ....	53
<b>Figure 3.1.</b> Pareto chart of the four factors (from Table 3.1) affecting anthracene oxidation with Fenton's reagent. ....	70

<b>Figure 3.2.</b> Predicted and actual values of anthracene removal (%) (A), and normal % probability vs. externally studentized residuals using CCD for optimizing the Fenton oxidation of anthracene in anhydrous ethanol (B). .....	74
<b>Figure 3.3.</b> 3D-plots of the effect of (A) time and temperature at the constant H <sub>2</sub> O <sub>2</sub> dosage (350 μL), (B) H <sub>2</sub> O <sub>2</sub> dosage and time at constant temperature (40 °C), and (C) H <sub>2</sub> O <sub>2</sub> dosage and temperature at constant time (0.5 h) on removal % of anthracene. A constant dosage (250 μL) of Fe <sup>2+</sup> (0.50 M) was used in all experiments. ....	75
<b>Figure 3.4.</b> GC-FID chromatogram of anthracene (A), and the reaction products of Fenton oxidation of anthracene (B). Reaction conditions: 250μL of Fe <sup>+2</sup> , 350 μL of H <sub>2</sub> O <sub>2</sub> , 45 °C, 0.5 h, and 2.0 mL of anthracene (250 ppm) .....	76
<b>Figure 3.5.</b> 3D-plots of the effect of time and temperature on anthracene oxidation using peroxyacetic acid/H <sub>2</sub> SO <sub>4</sub> . .....	78
<b>Figure 3.6.</b> GC-FID analysis of anthracene (A), and the reaction product of anthracene oxidation using peroxyacetic acid catalyzed by sulfuric acid (B). Reaction conditions: 5.0 mL of deionized water, 5.0 mL of H <sub>2</sub> O <sub>2</sub> , 5.0 mL of glacial acetic acid, 1.0 mL of sulfuric acid, 45 °C, 0.5 h, and 200 μL of anthracene (5.00 g/L).....	79
<b>Figure 3.7.</b> GC-FID chromatogram of coal tar in ethanol (A) and oxidation of coal tar in anhydrous ethanol (B-F). Peak numbers correspond to compounds listed in Table 3.6 and reaction conditions listed in Table 3.7. ....	82
<b>Figure 3.8.</b> Removal % of coal tar PAHS using Fenton oxidation under the conditions (B-F) listed in Table 3.7. Error bars represent RSD < 5%, n = 3. ....	84
<b>Figure 3.9.</b> GC-FID chromatogram of DCM extracts of coal tar (A) and oxidation of coal tar using different dosages of H <sub>2</sub> O <sub>2</sub> :CH <sub>3</sub> COOH:DI:H <sub>2</sub> SO <sub>4</sub> (v/v/v/v); (B) (5:5:5:1) mL, (C) 2 x (5:5:5:1) mL, and (D) 3 x (5:5:5:1) mL. Peak numbers correspond to compounds listed in Table 4. The temperature of the reaction was adjusted to be 45 °C and the time was 0.5 h. ....	85
<b>Figure 3.10.</b> Removal % of coal tar PAHs using different dosages of H <sub>2</sub> O <sub>2</sub> :CH <sub>3</sub> COOH:DI:H <sub>2</sub> SO <sub>4</sub> (5:5:5:1 v/v/v/v); (B) 16.0 mL, (C) 32.0 mL, and (D) 48.0 mL. Reaction conditions: 45 °C and 0.5 h. Error bars represent RSD < 6%, n = 3. ....	86
<b>Figure 4.1.</b> (A) CEM Discover microwave synthesis system, (B) inside microwave cavity, (C) closed microwave system, and (D) open microwave system. The clamp is used for illustration purposes only. ....	99
<b>Figure 4.2.</b> Temperature, pressure, and microwave power profile of microwave heating of pyrene (A1-C1) and pyrene with biochar (A2-C2) using a closed microwave system. .	103
<b>Figure 4.3.</b> Temperature and microwave power profile of microwave-assisted heating of pyrene (A1 and B1) and pyrene with biochar (A2 and B2) using an open microwave system. ....	103

<b>Figure 4.4.</b> Percentages of volatile, non-volatile, and gas fractions from microwave-assisted heating of pyrene/closed system (A), pyrene + biochar/closed system (B), pyrene/open system (C), and pyrene + biochar/ open system (D). Error bars represent RSD ( $n = 3$ ). .....	104
<b>Figure 4.5.</b> Pyrene recovery after microwave-assisted heating of pyrene/closed system (A), pyrene + biochar/closed system (B), pyrene/open system (C), and pyrene + biochar/ open system (D). Error bars represent RSD ( $n = 3$ ). .....	104
<b>Figure 4.6.</b> Pyrene with biochar before and after microwave-assisted heating using open system. ....	105
<b>Figure 4.7.</b> Temperature, pressure, and microwave power profiles of coal tar (A1 -A3), coal tar with biochar (B1-B3), coal tar with activated carbon (C1-C3), and coal tar with TiO <sub>2</sub> (D1-D3). All experiments were conducted in a closed microwave system at a set temperature of 190 °C. ....	107
<b>Figure 4.8.</b> Temperature, pressure, and microwave power profiles of coal tar (A1 and A2), coal tar with activated carbon (B1, B2), coal tar with biochar (C1 and C2) and coal tar with TiO <sub>2</sub> (D1 and D2). All experiments were conducted in an open microwave system at a set temperature of 300 °C. ....	108
<b>Figure 4.9.</b> Non-volatile, volatile, and gas yield (%) from microwave of coal tar and coal tar with microwave absorbers (biochar, activated carbon, and TiO <sub>2</sub> ) using a closed microwave system. The set temperature is 190 °C. Error bars represent RSD ( $n = 3$ ). ..	109
<b>Figure 4.10.</b> Non-volatile, volatile, and gas yield (%) from microwave-assisted heating of coal tar and coal tar with microwave absorbers (biochar, activated carbon, and TiO <sub>2</sub> ) using an open microwave system. The set temperature is 300 °C. Error bars represent the RSD ( $n = 3$ ). .....	109
<b>Figure 4.11.</b> Temperature and microwave power profiles of microwave-assisted heating of coal tar dissolved in anhydrous ethanol (A1 and A2), coal tar with biochar in anhydrous ethanol (B1 and B2), coal tar with activated carbon in anhydrous ethanol (C1 and C2), and coal tar with TiO <sub>2</sub> in anhydrous ethanol (D1 and D2)). Experiments were conducted using an open microwave system at a set temperature of 300 °C. ....	110
<b>Figure 4.12.</b> GC-FID analysis of pyrene (control sample), volatile and non-volatile fractions from microwave-assisted heating of pyrene with biochar using open and closed microwave systems. ....	112
<b>Figure 4.13.</b> GC-MS TIC of coal tar dissolved in DCM. Compound were identified and listed in Table 4.1. ....	114

<b>Figure 4.14.</b> GC-FID chromatograms of the combined fractions (volatile + non-volatile) from coal tar after microwave-assisted heating of coal tar (A), coal tar with biochar (B), coal tar with activated carbon (C), and coal tar with TiO <sub>2</sub> (D) using the closed microwave system at a set temperature of 190 °C. ....	116
<b>Figure 4.15.</b> GC-FID chromatograms of coal tar (A) and volatile fractions from microwave-assisted heating of coal tar (B), coal tar with biochar (C), coal tar with activated carbon (D), and coal tar with TiO <sub>2</sub> (E) using the open microwave system at a set temperature of 300 °C. ....	117
<b>Figure 4.16.</b> GC-FID chromatograms of non-volatile fractions from microwave-assisted heating of coal tar (A), coal tar with biochar (B), coal tar with activated carbon (C), and coal tar with TiO <sub>2</sub> (D) using the open microwave system at a set temperature of 300 °C. ....	117
<b>Figure 4.17.</b> GC-FID analysis of coal tar fraction that is dissolved in anhydrous EtOH (A) and volatile fraction from microwave-assisted heating of coal tar/EtOH (B), coal tar/EtOH with activated carbon (C), coal tar/EtOH with biochar (D), and coal tar/EtOH with TiO <sub>2</sub> (E). Microwave experiments were achieved using an open system at a set temperature of 300 °C. ....	118
<b>Figure 4.18.</b> GC-FID chromatograms of the non-volatile fraction from microwave-assisted heating of coal tar/EtOH (A), with biochar (B), with activated carbon (C), and with TiO <sub>2</sub> (D). Experiments were achieved using an open microwave system at a set temperature of 300 °C. ....	119
<b>Figure 4.19.</b> GC-FID analysis of coal tar/EtOH (A) and supernatants of coal tar/EtOH with TiO <sub>2</sub> (B), with activated carbon (C), and with biochar (D) after 24 h of absorption time. ....	120
<b>Figure 4.20.</b> Percentage of PAH sorption from coal tar soluble in anhydrous after mixing with biochar, activated carbon, and TiO <sub>2</sub> . ....	121
<b>Figure 4.21.</b> TGA analysis of coal tar with and without additives (biochar, AC, and TiO <sub>2</sub> ). ....	123
<b>Figure 5.1.</b> GC-FID analysis of pyrene before and after bromination reaction using H <sub>2</sub> O <sub>2</sub> -HBr. ....	134
<b>Figure 5.2.</b> Chemical structure of pyrene and the its active sites for electrophilic substitution reaction. Mono substitution at position 1 (A) and tetra substitution at positions 1,3,6, and 8 (B). ....	136

<b>Figure 5.3.</b> GC-FID chromatogram of coal tar extract in DCM (A) and bromination reaction products of coal tar (B-F). Peak numbers correspond to compounds listed in Table 5.1 and reaction conditions listed in Table 5.2. ....	138
<b>Figure 5.4.</b> Removal percentages of PAHs from coal tar after bromination reaction using 0.25-4.0 molar equivalents of HBr-H <sub>2</sub> O <sub>2</sub> . ....	139
<b>Figure S4.1.</b> FT-IR analysis of biochar (A), pyrene (E), pyrene with biochar (B), and residue from microwave-assisted heating of pyrene with biochar using an open (C) and a closed (D) microwave system. ....	165
<b>Figure S4.2.</b> SEM analysis of biochar (A), biochar with pyrene (B), and residue from microwave heating of pyrene with biochar, using the closed (C), and open (D) microwave systems. ....	166
<b>Figure S5.1.</b> The structure of pyrene with the atom labels shown in Tables S5.1. ....	168

## List of Tables

<b>Table 1.1.</b> Physical and chemical properties of PAHs. Reproduced with permission from reference [2]. .....	8
<b>Table 1.2.</b> Selected PAHs and their chemical formula, molecular weight, and toxic equivalency factor. Reproduced with permission from reference [3]. .....	9
<b>Table 1.3.</b> LD <sub>50</sub> of selected PAHs. Reproduced with permission from reference [4]. .....	9
<b>Table 1.4.</b> Types of AOPs and some examples. Reproduced with permission from reference [5]. .....	13
<b>Table 2.1.</b> Screening variables for four factors using only low and high levels for anthracene reduction. ....	42
<b>Table 2.2.</b> Analysis of variance of four factors (Mg, graphite, glacial acetic acid, and time), which were studied in the screening variables stage of the experimental design. ....	43
<b>Table 2.3.</b> Central composite design using the 3 significant factors at 3 levels for optimizing the anthracene reduction. ....	45
<b>Table 2.4.</b> ANOVA for response surface quadratic model of anthracene reduction. ....	46
<b>Table 2.5.</b> PAH compounds identified in anhydrous ethanol extract of coal tar before and after reduction. ....	51
<b>Table 2.6.</b> Reaction conditions used for PAHs reduction in coal tar. ....	52
<b>Table 3.1.</b> Screening experiments for four factors using only low and high levels for Fenton oxidation of anthracene. ....	69
<b>Table 3.2.</b> CCD using the 3 significant factors at 3 levels for optimizing the Fenton oxidation of anthracene. The Fe <sup>2+</sup> (0.50 mol/L) dosage is 250 µL. ....	72
<b>Table 3.3.</b> ANOVA for optimizing the Fenton oxidation of anthracene using CCD. ....	73
<b>Table 3.4.</b> CCD for optimizing the anthracene oxidation using peroxyacetic-acid catalyzed by sulfuric acid using two factors at 3 levels. ....	78
<b>Table 3.5.</b> ANOVA analysis of anthracene oxidation using peroxyacetic-acid catalyzed by sulfuric acid. The effect of temperature and time on removal % using CCD. ....	79
<b>Table 3.6.</b> PAH compounds identified in anhydrous ethanol extract of coal tar before and after oxidation. ....	83

<b>Table 3.7.</b> Experimental conditions for Fenton oxidation of coal tar. 2.0 mL aliquot of coal tar in anhydrous ethanol. ....	83
<b>Table 4.1.</b> PAH compounds identified in coal tar using GC-FID. ....	115
<b>Table 5.1.</b> PAH compounds identified in coal tar using GC-FID. ....	137
<b>Table 5.2.</b> Experimental conditions for PAH bromination in coal tar. ....	139
<b>Table S1.1.</b> Summary of recent research for PAH and PCB degradation using an acidified Mg/EtOH system. ....	151
<b>Table S1.2.</b> Brief summary of research using Fenton oxidation for PAH degradation. ....	153
<b>Table S1.3.</b> Brief summaries of work on PAH degradation using peroxyacetic acid. ...	160
<b>Table S1.4.</b> Some studies that have achieved thermal removal of PAHs from contaminated soils. ....	162
<b>Table S5.1.</b> Results of Hirshfeld population analysis: Fukui functions ( $f^+$ , $f^-$ , $f^o$ ) for pyrene. ....	168

## List of Schemes

<b>Scheme 1.1.</b> A proposed mechanism for the Fenton oxidation of anthracene. Reproduced with permission from reference [60]. .....	15
<b>Scheme 1.2.</b> A proposed mechanism of oxidation of some PAHs (e.g., phenanthrene, fluoranthene, and benzo[a]pyrene). Reproduced with permission from reference [61]. ..	16
<b>Scheme 1.3.</b> A proposed mechanism for peroxy-acid activation by sulfuric acid. Modified and reproduced with permission from reference [64]. .....	18
<b>Scheme 1.4.</b> Modified proposed mechanism for anthracene oxidation using peroxyacetic acid catalyzed by sulfuric acid Modified and reproduced with permission from reference [65]. .....	19
<b>Scheme 2.1.</b> A proposed mechanism for the anthracene reduction using the Mg catalyzed by glacial acetic acid, which is a modification of mechanism earlier proposed by Elie [28]. .....	40
<b>Scheme 5.1.</b> A modified mechanism for pyrene monobromination using H <sub>2</sub> O <sub>2</sub> -HBr [37]. .....	135
<b>Scheme 5.2.</b> Resonance structures of pyrene radical brominated at positions 1 ( <b>I</b> ) and 10 ( <b>VI</b> ). .....	135

## List of Abbreviations

- ACA: Acenaphthene
- ANT: Anthracene
- AOP: Advanced oxidation process
- BaA: Benzo[a]anthracene
- BAP: Benzo[a]pyrene
- BJK: Benzo[b,j,k]fluoranthene
- BPR: Benzo[ghi]perylene
- CAN: Acenaphthylene
- CCD: Central composite design
- CHR: Chrysene
- DAN: Dibenzo[a,h]anthracene
- DCM: Dichloromethane
- DBahA: Dibenz[a,h]anthracene
- EPA: Environmental protection agency
- EtOH: Ethanol
- FID: Flame ionization detector
- FLE: Fluoranthene
- FLU: Fluorene
- FTIR: Fourier transform infrared spectroscopy
- GC: Gas chromatography
- HMW: High molecular weight
- HOMO: Highest occupied molecular orbital

INP: Indeno[1,2,3-c,d]pyrene

$K_{ow}$ : Octanol-water partition coefficient

LMW: Low molecular weight

LUMO: Lowest unoccupied molecular orbital

MEN: 2-Methylnaphtalene

MS: Mass spectrometer

MWH: Microwave heating

NAP: Naphthalene

PAHs: Polycyclic aromatic hydrocarbons

PCB: Polychlorinated Biphenyls

PHE: Phenanthrene

ppm: Parts per million (mg/L)

PYR: Pyrene

SET: Single-electron transfer

SYSCO: Sydney Steel Corporation

TEF: Toxic equivalency factor

TGA: Thermogravimetric analysis

WHO: World Health Organization

# **Chapter 1**

## **Introduction**

## **1.1. Background and research question**

The US Environmental Protection Agency (EPA) and the World Health Organization (WHO) have listed 16 polycyclic aromatic hydrocarbons (PAHs) as priority environmental pollutants [1]. Furthermore, some PAHs, such as benzo[a]pyrene, are carcinogenic, teratogenic, and ecotoxic [2,3]; therefore, their degradation has received great attention [4]. Several methods have been used for PAH degradation which can be classified as physical, chemical, and biological methods [5]. Among these methods, physical and chemical remediations are the more efficient methods for degradation [6]. In contrast, biological methods (e.g., bioremediation and phytoremediation) have some drawbacks, such as slow remediation processes (days-year) and low removal efficiencies [7].

Coal tar is a by-product of incomplete combustion of coal and mainly consists of PAHs [8]. The Sydney Coal Tar Ponds in Nova Scotia, Canada are examples of PAH-contaminated sites, which were contaminated during the operation of the Sydney Steel Corporation (SYSCO) steel plant and coking production in the years from 1901 to 1988 [9]. As a result of this process, hazardous materials which are mainly coal tar were produced and transferred to the surrounding environment causing pollution of the air and soil [10]. In the work which forms a part of this thesis, a coal tar sample was collected from this site and used as a case study. Specifically, the research is focused on degradation of the PAH contaminants in the Sydney coal tar using chemical reactions. This study is also aimed at answering the following question: Can PAHs in coal tar be degraded using environmentally-friendly, effective, fast, and relatively low-cost methods?

## **1.2. Hypothesis**

The hypothesis of this research is that PAHs can be degraded into less or non-toxic compounds after their aromatic structures are altered through certain chemical reactions. There are numerous methods, such as reduction using acidified Mg/EtOH, oxidation using Fenton oxidation and peroxyacetic acid, microwave-assisted thermal removal, or bromination using H<sub>2</sub>O<sub>2</sub>/HBr, which can be developed to effectively degrade and/or remove PAHs from coal tar. These methods were used and optimized in the first step for the reaction with anthracene or pyrene as representative (model) compounds of PAHs in coal tar. The optimized degradation conditions for these model PAH were then applied to the degradation/removal of PAH in coal tar.

## **1.3. Objectives**

This dissertation mainly focuses on reductive, oxidative, bromination and thermal degradation of PAHs in coal tar. Sydney coal tar was chosen a real environmental sample for this project. The favoured methods for remediation of PAHs in coal tar or PAH-contaminated sites should have several advantages such as being relatively rapid, inexpensive, efficient, and environmentally-friendly.

In this thesis, experimental design was used to optimize the PAH degradation (Chapters 3 and 4), which in turn reduced the number of experiments and took into account the interactions among various experimental parameters. The main motivation behind this research is to find simple and effective approaches of environmental cleanup by removing the PAHs or reducing their risks from the environment. Briefly, the aims of this study are as follows:

- i. Optimize the degradation of PAHs in coal tar using Mg/EtOH in the presence of glacial acetic acid. The experimental design methodology was applied to achieve high removal efficiency.
- ii. Investigate degradation of PAHs in coal tar using Fenton oxidation and peroxyacetic acid and determine the optimum conditions using the experimental design methodology.
- iii. Remove PAHs from coal tar using microwave-assisted heating at low temperatures (< 300 °C) with and without additives (e.g. biochar, activated carbon, and TiO<sub>2</sub>).
- iv. Use hydrobromic acid/hydrogen peroxide for PAH bromination as a promising route to convert PAHs into value-added products useful in organic semiconductor industry.

#### **1.4. Literature review**

##### **1.4.1. Polycyclic aromatic hydrocarbons: chemical structures, sources, physical and chemical properties, and toxicity.**

###### *Chemical structures*

Polycyclic aromatic hydrocarbons (PAHs) are a class of organic compounds that consist of two or more benzene rings arranged in a linear, clustered, or angular alignment shape (Figure 1.1) [11]. Depending on the number of benzene rings, PAHs can be classified as: 1) low molecular weight (LMW) PAHs which have two or three fused benzene rings, such as naphthalene, 1-methylnaphthalene, 2-methylnaphthalene, anthracene, and phenanthrene; and 2) high molecular weight (HMW) PAHs which have four or more fused benzene rings, such as fluoranthene, pyrene, benzo[a]anthracene, chrysene, and benzo[a]pyrene [12].

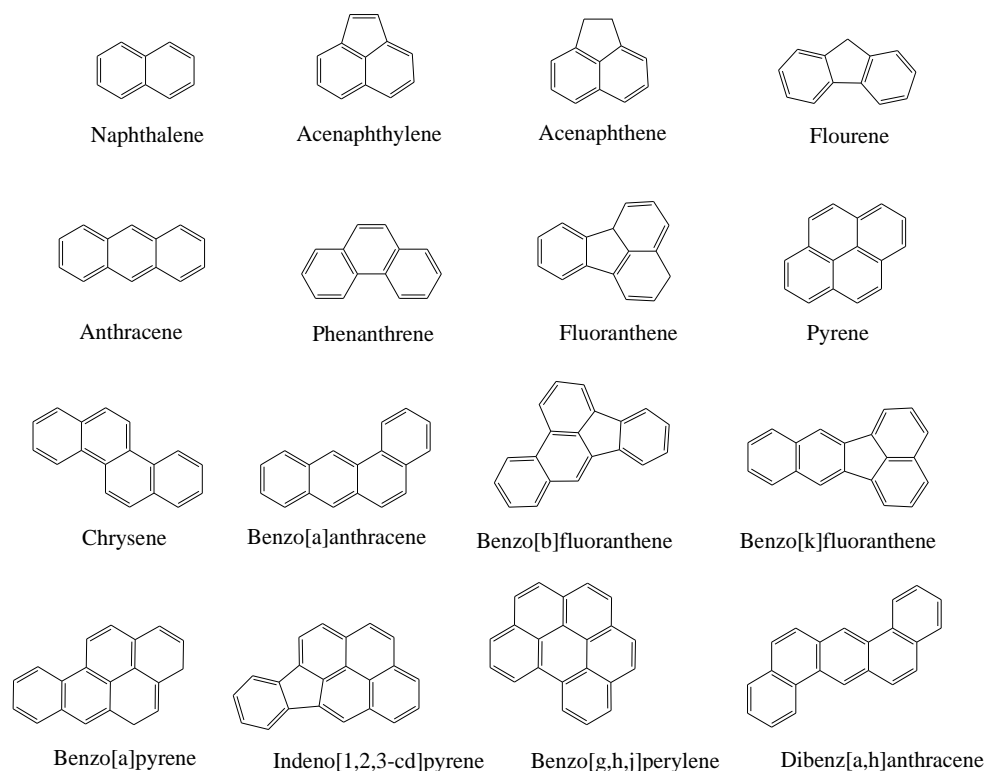


**Figure 1.1.** Chemical structures and nomenclatures of 16 selected PAHs [13].

### *Sources*

Several sources contribute to the production of PAHs, including vehicle emissions, incomplete combustion of fossil fuel (e.g., coal and oil), petroleum refining, straw and firewood burning, industrial processing, chemical manufacturing, oil spills, and coal tar [14]. PAHs are also produced from natural processes, such as volcanic eruptions and forest fires, which are then released into the ecosystem [15]. Temperature, biomass type, and residence time have clear effects on PAHs formation and distribution [16]. For example, increasing the temperature for combustion of municipal solid waste from 500 °C to 900 °C increases the PAH yield from 1132 µg/g to 3725 µg/g [17]. The residence time at the final temperature of the pyrolysis is an important factor, while increasing the residence time increases the PAHs yield [16]. In addition, LMW PAHs are formed at low temperatures

and HMW PAHs are formed at high temperatures. Petrogenic sources (e.g., petroleum) consist mainly of light PAHs (2-3 rings), while combustion of pyrogenic sources (e.g., wood, coal, and biomass) mainly form heavy PAHs ( $\geq 4$  rings) [13].

#### *Physical and chemical properties*

PAHs are colorless to pale yellow solids and have low solubility in water [18]. They are hydrophobic and persistent compounds; therefore, they have a high ability to be absorbed and accumulated in sediments, soil, and suspended particles in the air [3,19]. The distribution of PAHs and their behavior in the environment are mainly dependent on their chemical and physical properties, such as solubility in aqueous media, vapor pressure, octanol solubility, octanol-water partition coefficient, octanol-air partition coefficient, and air-water partition coefficient [20]. Table 1.1 lists some physical and chemical properties of PAHs, such as solubility, partition coefficient ( $\log K_{ow}$ ), and vapor pressure. PAHs are hydrophobic and soluble in organic solvents (e.g., DCM, hexane, and toluene). Their solubility in aqueous media decreases with increasing molecular weight [21].

#### *Toxicity*

Since PAHs are hydrophobic compounds and highly soluble in lipids, they are easily absorbed into the fat content of humans and animals [22]. In PAH-contaminated environments, PAHs accumulate in marine organisms (e.g., fish and cephalopods) and are transferred to humans through the food chain [23]. The chemical structures of individual PAHs are an important factor that has a clear effect on its toxicity: higher molecular weight PAHs, such as benzo[a]pyrene, are very toxic and carcinogenic. Toxic equivalency factor is the ratio between the toxicity of a specific PAH compound to a reference PAH (e.g. benzo[a]pyrene) [24]. The toxicity of other PAHs are compared to benzo[a]pyrene's

toxicity (Table 1.2) [25]. The term LD<sub>50</sub> has been used to refer to the relative toxicity of PAHs. This term is the abbreviation of lethal dose in 50% of cases and it is defined as the amount of toxic substrate (mg) per the subject's body weight (kg) required to kill 50% of the test population. LD<sub>50</sub> values of some PAHs are listed in Table 1.3 [22]. In addition, structural isomers of PAHs can have different toxicity, ranging from toxic to non-toxic [23]. The ability of PAHs to damage DNA is dependant on the strength of the DNA system; for example, biological studies have shown that fish have a weak DNA repair system, which makes fish more vulnerable through exposure to PAHs. The transfer of PAHs to humans by food can cause health risks (e.g., cancer), since PAHs accumulation can cause damage cell tissues.

**Table 1.1.** Physical and chemical properties of PAHs. Reproduced with permission from reference [26].

PAHs	Parameters						
	Abbreviation	Molecular structure	Number of aromatic rings	Molecular weight (g mol <sup>-1</sup> )	Aqueous solubility (25 °C, mg L <sup>-1</sup> )	Octanol/water partition coefficient (log K <sub>ow</sub> ), 25 °C	Vapour pressure (20-25 °C, mmHg)
Naphthalene	NAP	C <sub>10</sub> H <sub>8</sub>	2	128	31.700	3.37	8.7×10 <sup>-2</sup>
2-Methylnaphthalene	MEN	C <sub>11</sub> H <sub>10</sub>	2	142	24.600	3.87	6.8×10 <sup>-2</sup>
Acenaphthylene	ACN	C <sub>12</sub> H <sub>8</sub>	3	152	3.9300	4.07	2.9×10 <sup>-2</sup>
Acenaphthene	ACA	C <sub>12</sub> H <sub>10</sub>	3	154	1.9300	3.98	4.5×10 <sup>-3</sup>
Fluorene	FLU	C <sub>13</sub> H <sub>10</sub>	3	166	1.8300	4.18	3.2×10 <sup>-4</sup>
Phenanthrene	PHE	C <sub>14</sub> H <sub>10</sub>	3	178	1.2000	4.45	6.8×10 <sup>-4</sup>
Anthracene	ANT	C <sub>14</sub> H <sub>10</sub>	3	178	0.0760	4.45	1.7×10 <sup>-5</sup>
Fluoranthene	FLE	C <sub>16</sub> H <sub>10</sub>	4	202	0.2300	4.90	5.0×10 <sup>-6</sup>
Pyrene	PYR	C <sub>16</sub> H <sub>10</sub>	4	202	0.0770	4.88	6.8×10 <sup>-7</sup>
Benzo[a]anthracene	BAA	C <sub>18</sub> H <sub>12</sub>	4	228	0.0094	5.61	2.2×10 <sup>-8</sup>
Chrysene	CHR	C <sub>18</sub> H <sub>12</sub>	4	228	0.0018	5.63	6.3×10 <sup>-7</sup>
Benzo[b,j,k]fluoranthene	BJK	C <sub>20</sub> H <sub>12</sub>	5	252	0.0015	6.04	5.0×10 <sup>-7</sup>
Benzo[a]pyrene	BAP	C <sub>20</sub> H <sub>12</sub>	5	252	0.0016	6.06	5.6×10 <sup>-9</sup>
Dibenzo[a,h]anthracene	DAN	C <sub>22</sub> H <sub>14</sub>	5	278	0.0005	6.84	1.0×10 <sup>-10</sup>
Indeno[1,2,3-c,d]pyrene	INP	C <sub>20</sub> H <sub>12</sub>	6	276	0.0620	6.58	1.0×10 <sup>-10</sup>
Benzo[g,h,i]perylene	BPR	C <sub>20</sub> H <sub>12</sub>	6	276	0.0003	6.50	1.0×10 <sup>-10</sup>

**Table 1.2.** Selected PAHs and their chemical formula, molecular weight, and toxic equivalency factor. Reproduced with permission from reference [25].

Order	PAH	Abbreviation	Chemical formula	Molecular mass (g mol <sup>-1</sup> )	Toxic equivalency factor
1	Naphthalene	NAP	C <sub>10</sub> H <sub>8</sub>	128.17	0.001
2	Fluorene	FLR	C <sub>13</sub> H <sub>10</sub>	166.22	0.001
3	Anthracene	ANT	C <sub>14</sub> H <sub>10</sub>	178.23	0.010
4	Phenanthrene	PHN	C <sub>14</sub> H <sub>10</sub>	178.23	0.001
5	Fluoranthene	FLT	C <sub>16</sub> H <sub>10</sub>	202.26	0.001
6	Pyrene	PYR	C <sub>16</sub> H <sub>10</sub>	202.25	0.001
7	Benzo[a]anthracene	BAA	C <sub>18</sub> H <sub>12</sub>	228.00	0.100
8	Chrysene	CHY	C <sub>18</sub> H <sub>12</sub>	228.00	0.001
9	Benzo[a]pyrene	BAP	C <sub>20</sub> H <sub>12</sub>	252.00	1.000
10	Benzo[b]fluoranthene	BBF	C <sub>20</sub> H <sub>12</sub>	252.00	0.100
11	Benzo[e]pyrene	BEP	C <sub>20</sub> H <sub>12</sub>	252.31	–
12	Benzo[j]fluoranthene	BJF	C <sub>20</sub> H <sub>12</sub>	252.00	–
13	Benzo[k]fluoranthene	BKF	C <sub>20</sub> H <sub>12</sub>	252.00	0.010
14	Dibenzo[a,h]anthracene	DBA	C <sub>22</sub> H <sub>14</sub>	278.00	1.000
15	Indo[123-cd]pyrene	IP	C <sub>22</sub> H <sub>12</sub>	276.00	0.100
16	Dibenzo[aL]pyrene	DBP	C <sub>24</sub> H <sub>14</sub>	302.00	–

**Table 1.3.** LD<sub>50</sub> of selected PAHs. Reproduced with permission from reference [22].

Material	Number of carbon rings	LD <sub>50</sub> value (mg kg <sup>-1</sup> )	Test subject	Exposure route
Naphthalene	2	533-710	Male/Female mice respectively	Oral
Phenanthrene	3	750	Mice	Oral
Anthracene	3	> 430	Mice	Intraperitoneal
Fluoranthene	4	100	Mice	Intraperitoneal
Pyrene	4	514	Mice	Intraperitoneal
Benzo[a]pyrene	5	232	Mice	Intraperitoneal

#### 1.4.2. The Sydney Tar Ponds and Coke Ovens

Coal tar mainly consists of PAHs and it is formed as a by-product from pyrolysis of organic materials, such as coal or wood [13]. The weight percentage of PAHs in coal tar is up to 85% and the remaining 15% are phenols and heterocyclic compounds [27]. PAHs are

produced from pyrolysis of organic materials at temperatures in the range of 650-900 °C [19]. The Coal Tar in Sydney Nova Scotia was formed as a by-product from coking ovens in the SYSCO steel plant during its operation from 1901 to 1988 [28]. Drainage of this coal tar caused pollution of the nearby region, including Muggah Creek, which is located on the south arm of Sydney Harbour [29]. These leached pollutants were identified as PAHs (3500 tonnes), PCBs from the electrical equipment used in that project (3.6 tonnes), and heavy metals (e.g., arsenic, lead, copper, vanadium, and zinc) [30]. The concentration of these pollutants in Sydney Harbour was found to be decreasing toward the outer part of the harbour [31]. In addition, the first observation of contamination by PAHs was made in lobsters in the 1980s, after which the degradation of coal tar became a great concern [32]. Incineration using a fluid bed reactor was used, for the first time, to degrade this coal tar at the end of 1980s, but this process did not succeed because the temperature of the fluid bed reactor was not sufficient to break down PAHs and PCBs [33]. Another cleanup process started in 2009, which involved the stabilization and solidification of the coal tar using Portland cement as a hydraulic binder to convert it to “a durable, solid, low-hydraulic conductivity matrix to reduce contaminant leaching rates into the surrounding environment” [31].

#### **1.4.3. Approaches for PAH degradation**

The methods that have been used for the degradation of PAHs can be classified as biological such as bioremediation [34], physical (e.g., thermal desorption) [35], chemical reduction (e.g., H<sub>2</sub> with metal such as Pt, Pd, or Co or acidified Mg/ethanol) [36], chemical oxidation (e.g., Fenton’s reagent, ozone, and persulfate) [37], and C-H bond activation (e.g., PAH bromination) [38]. Bioremediation is safe, simple, and environmentally-friendly

process, however it is slow (weeks to years) and has a low degradation efficiency due to low bioavailability, where PAHs have low solubility in water and high sorption in the soil [39]. Therefore, chemical reduction and oxidation are widely reported in the literature due to their advantages, such as shorter reaction time and better degradation efficiency [40].

#### **1.4.3.1. Chemical reduction**

Converting toxic PAHs to less toxic compounds is a useful process to remediate polluted environments. Since hydrogenated PAHs are less toxic compounds compared to their parent PAHs, chemical reduction is a potentially effective method to mitigate PAHs [41]. Chemical reduction can be achieved by different reducing reagents such as hydrogen with metals (e.g., Pd, Pt, Co) and metal-free hydrogenation (e.g., H<sub>2</sub> with B(C<sub>6</sub>F<sub>5</sub>)<sub>3</sub>/Ph<sub>2</sub>PC<sub>6</sub>F<sub>5</sub>) [42]. These methods require high temperatures and significant hydrogen pressure. It would be more useful to find methods that can successfully work at ambient temperature using low-cost catalysts or metals. The use of zero-valent metals (ZVMs) such as iron and magnesium in hydrogenation reactions has been reported in the literature. They have several advantages such as availability, low cost, and high reduction efficiency [43]. ZVMs were used to remediate environmental pollutants such as PAHs and chlorinated hydrocarbons in contaminated soils [44]. Activated magnesium (Mg) together with an acid in anhydrous ethanol was successfully used in several studies and was described as an effective system for PAH and oxy-PAH degradation. The acidified Mg/EtOH system was successfully used in several studies, which are briefly summarized and listed in Table S1.1 of Appendix A.

### 1.4.3.2. Chemical oxidation

Chemical oxidation, also called advanced oxidation processes (AOPs), is a chemical technique that has been successfully used to degrade and enhance the bioremediation of pollutants in the environment [45]. AOPs can be classified into homogenous and heterogenous processes based on their  $\cdot\text{OH}$  radical source (see Table 1.4). Specifically, AOPs are described in the literature as promising methods for degrading toxic compounds such as PAHs [46]. Degradation of PAHs by AOPs can be achieved by different oxidizing reagents, such as permanganate, peroxy-acids, ozone, persulfate, and Fenton's reagent. Among these methods, the Fenton's reagent has a high efficiency for PAH degradation and it is a fast and inexpensive process [47].

#### *Fenton oxidation*

Fenton's reagent was developed by Henry John Horstman Fenton in the 1890s [48]. It consists of a solution of  $\text{Fe}^{2+}$  and  $\text{H}_2\text{O}_2$  to produce hydroxyl radicals ( $\cdot\text{OH}$ ) [7]. Fenton oxidation is widely used for degradation of organic wastes, including PAHs [49]. A summary of the studies achieved using Fenton oxidation for degradation or removal of PAHs from PAH-contaminated soils is listed in Table S1.2 of Appendix A. The reagent has several advantages such as being fast, effective, and relatively cheap [47]. Extraction of PAHs from real samples (e.g. PAH-contaminated soil and coal tar) is commonly done to make them available for oxidation using Fenton's reagent, a critical issue for the efficiency of the PAH degradation. Ethanol is a favoured solvent to extract PAHs from soil or coal tar due to its advantages such as being safe, cheap, and high PAH extraction efficiency, This approach has been used in several studies to extract and oxidize PAHs [50–52].

**Table 1.4.** Types of AOPs and some examples. Reproduced with permission from reference [53].

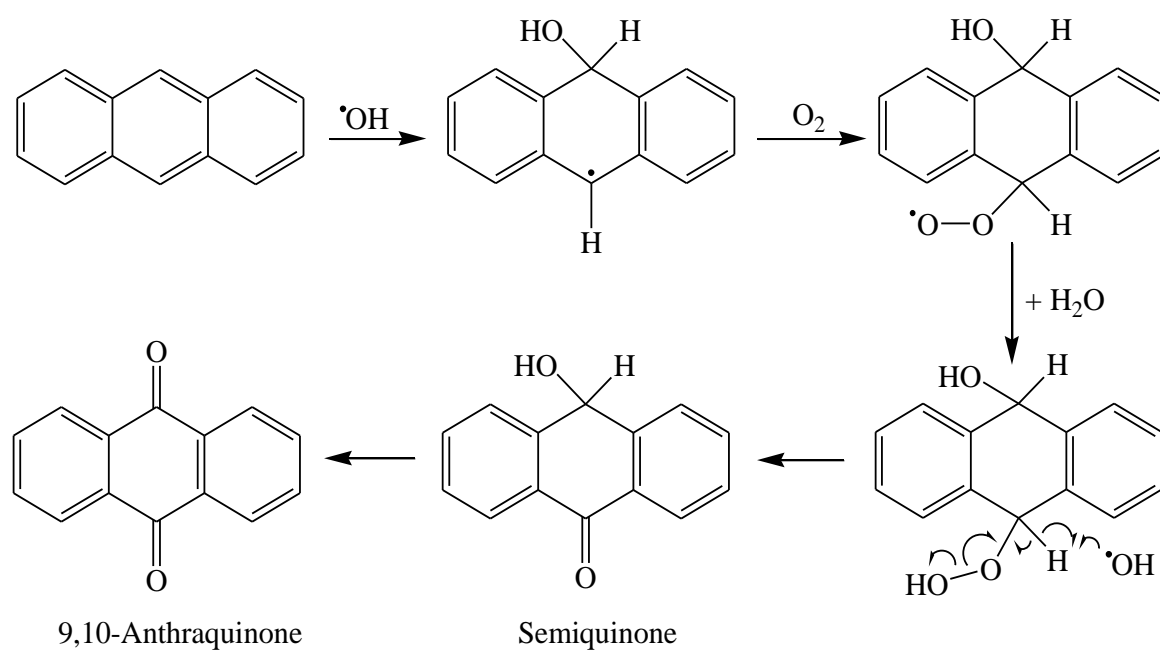
<b>Type of process</b>	<b>Examples</b>
Homogeneous	<i>Fenton-based processes</i> Fenton: $\text{H}_2\text{O}_2 + \text{Fe}^{2+}$ Fenton-like: $\text{H}_2\text{O}_2 + \text{Fe}^{3+}/\text{m}^{n+}$ Sono-Fenton: $\text{US}/\text{H}_2\text{O}_2 + \text{Fe}^{2+}$ Photo-Fenton: $\text{UV}/\text{H}_2\text{O}_2 + \text{Fe}^{2+}$ Electro-Fenton Sono-electro-Fenton Photo-electro-Fenton Sono-photo-Fenton <i>O<sub>3</sub> based processes</i> O <sub>3</sub> O <sub>3</sub> + UV O <sub>3</sub> + H <sub>2</sub> O <sub>2</sub> O <sub>3</sub> + UV + H <sub>2</sub> O <sub>2</sub>
Heterogeneous	$\text{H}_2\text{O}_2 + \text{Fe}^{2+}/\text{Fe}^{3+}/\text{m}^{n+}$ -solid TiO <sub>2</sub> /ZnO/CdS + UV $\text{H}_2\text{O}_2 + \text{Fe}^0 / \text{Fe}$ (nano-zero valent iron) $\text{H}_2\text{O}_2 +$ immobilized nano-zero valent iron

$\text{m}^{n+}$ :  $\text{Mn}^{2+}$ ,  $\text{Cu}^{2+}$ , and  $\text{Co}^{2+}$ .

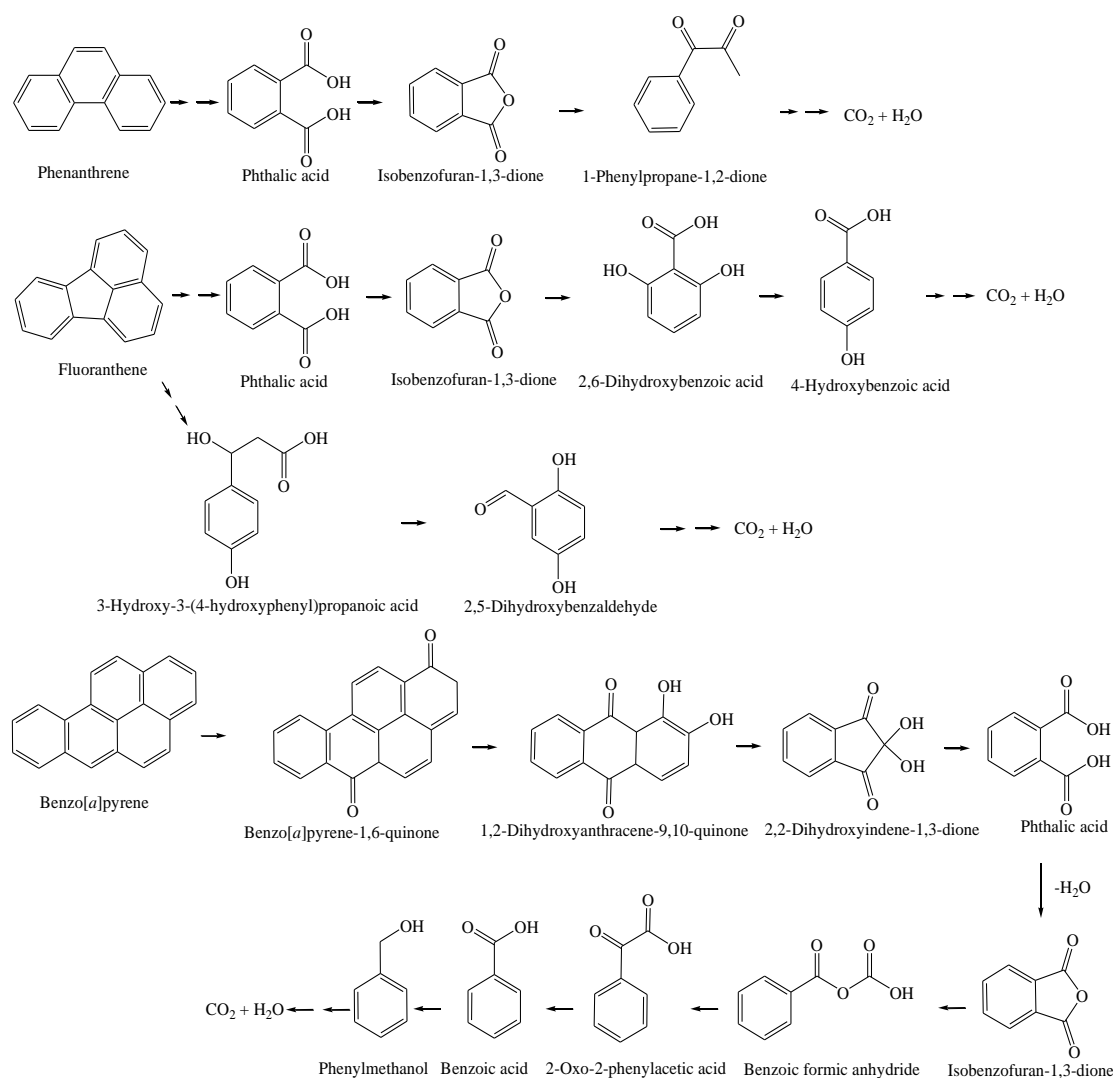
AOPs produce  $\cdot\text{OH}$  radicals, which are highly reactive species, whose standard reduction potential ( $E^\circ$ ) is +2.80 V which is just below that of fluorine ( $E^\circ = +3.03$ ) [54]. Therefore, AOPs can be successfully used for the degradation of pollutants that cannot be degraded by biological oxidation. If the starting hydrocarbon or organic substrate undergoes complete oxidation, it will convert to  $\text{CO}_2$  and water [55]. Consequently, the oxidation using  $\cdot\text{OH}$  radicals is not selective [56]. The Fenton reactions include some common reactions between  $\cdot\text{OH}$  radicals and aromatic compounds such as: 1) Hydrogen abstraction, where hydrogen atoms are abstracted from the aromatic molecules by  $\cdot\text{OH}$  radicals forming organic radicals ( $\text{R}\cdot$ ). The organic radicals can react with  $\text{H}_2\text{O}_2$  to form reactive  $\cdot\text{OH}$  radicals, initiating chain reactions (Equations 1.1-1.4); and 2) Addition of  $\cdot\text{OH}$  radicals to the double bond of aromatic molecules [57]. In addition to the radical initiation and radical

termination (Equations 1.1 and 1.2), the Fenton reaction includes some secondary reactions involved in oxygen production (Equations 1.5-1.8) [57,58]. Anthracene oxidation by the Fenton's reagent mainly produces 9,10-anthraquinone [52,59]. A proposed mechanism for the Fenton oxidation of anthracene is shown in Scheme 1.1 [60]. A complete conversion of the PAHs to H<sub>2</sub>O and CO<sub>2</sub> can occur in the case of using excess oxidizing reagents such as the Fenton's reagent shown in the proposed mechanism in Scheme 1.2.





**Scheme 1.1.** A proposed mechanism for the Fenton oxidation of anthracene. Reproduced with permission from reference [60].



**Scheme 1.2.** A proposed mechanism of the complete oxidation of some PAHs (e.g., phenanthrene, fluoranthene, and benzo[a]pyrene). Reproduced with permission from reference [61].

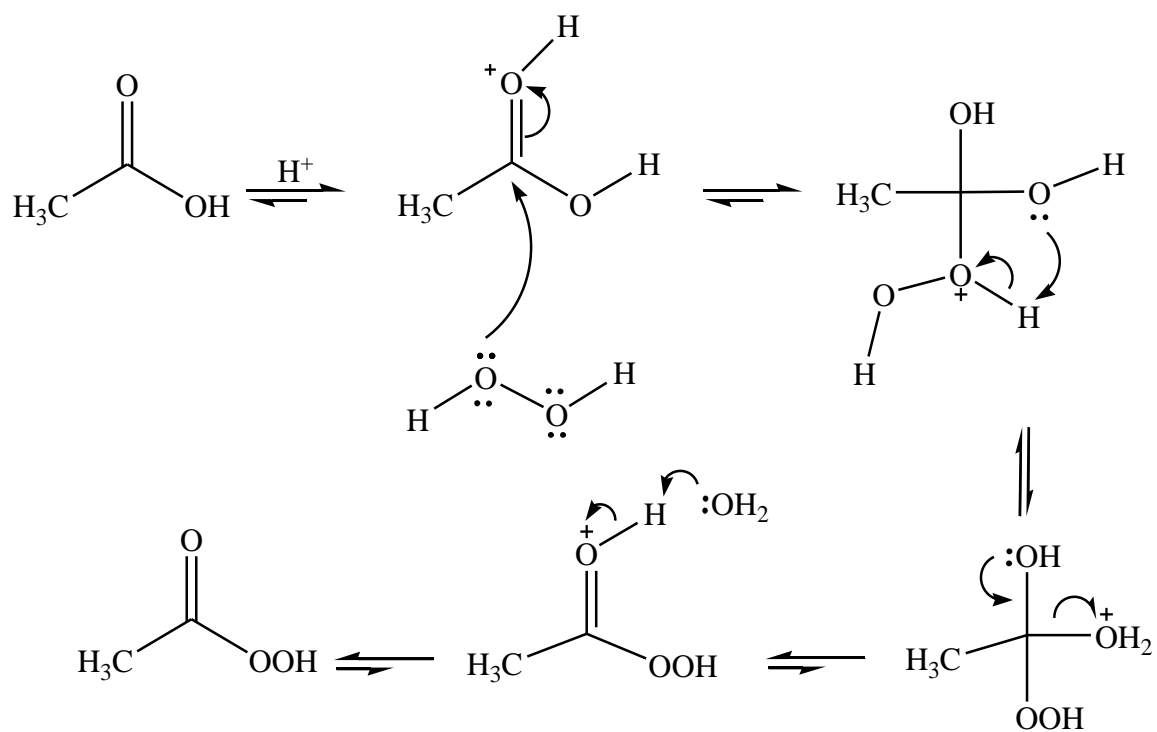
### *Peroxyacetic acid*

Peroxyacetic acid (PAA), also called peracetic acid, is an oxidant produced from the reaction between hydrogen peroxide and acetic acid as shown in Equation 1.9 [62].

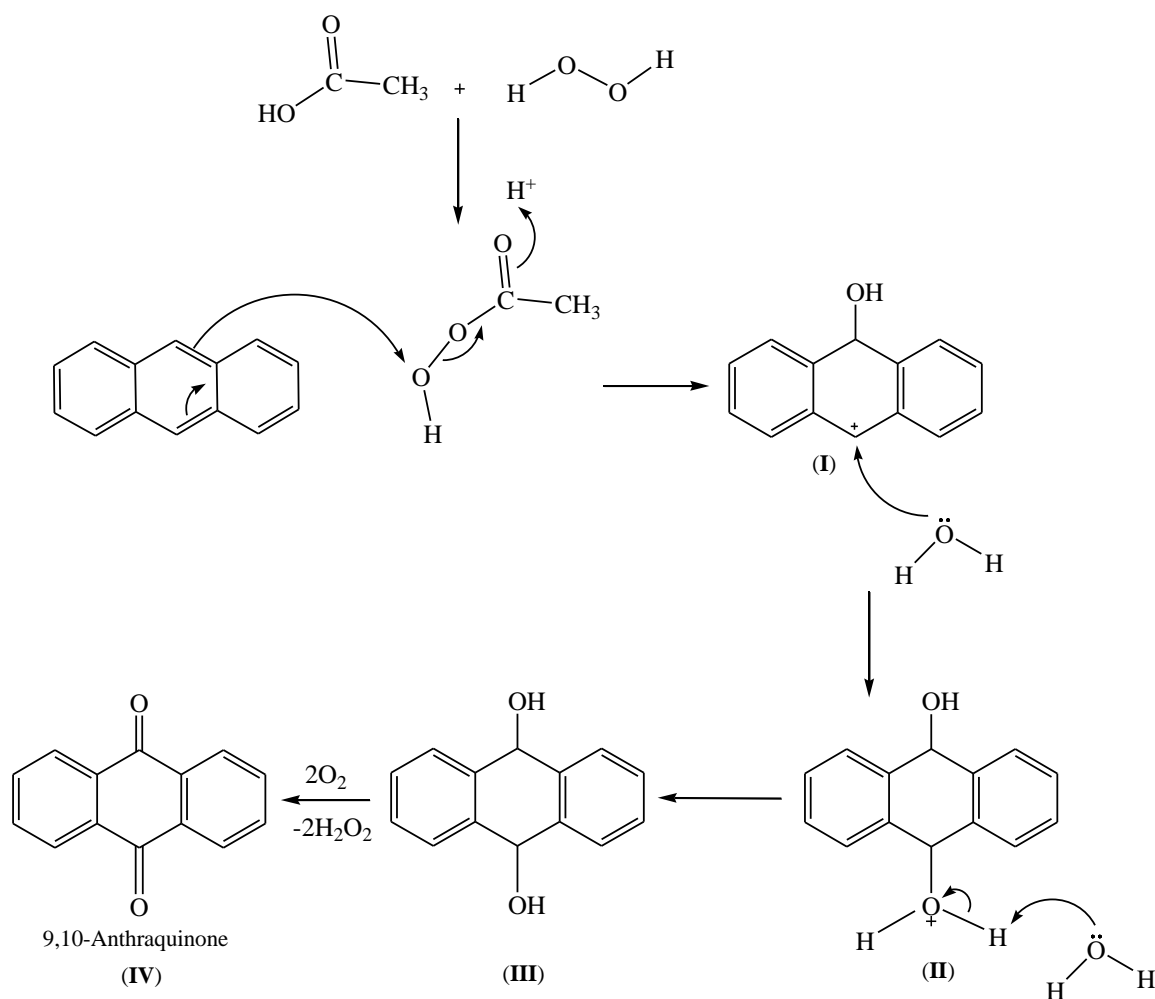


PAA is widely used in several applications such as the textile and paper industry (bleaching reagent), waste water treatment, disinfection and in the pharmaceutical, beverage, and food industries [63]. A summary of the studies that successfully achieved PAH degradation or removal in PAH-contaminated soil using PAA is listed in Table S1.3 of Appendix A. The reaction between acetic acid and hydrogen peroxide for peroxyacetic acid formation can be catalyzed using sulfuric acid as shown in Scheme 1.3. The reaction is reversible, and it was found that using 0-5% (v/v) sulfuric acid shifts the reaction forward to produce peroxyacetic acid. Increasing sulfuric acid percentage to >5% did not lead to any significant improvement of peroxyacid formation [64].

The proposed mechanism of the reaction between peroxyacetic acid and anthracene as a model compound of PAHs is shown in Scheme 1.4 [65]. Peroxyacetic acid is initially produced from the reaction between acetic acid and hydrogen peroxide, and then it reacts with anthracene in the presence of sulfuric acid to form a hydroxy anthracene cation (**I**). The latter reacts with a water molecule to produce intermediate (**II**), and then the dihydroxy anthracene (**III**). Compound (**III**) is oxidized to produce 9,10-anthraquinone (**IV**).



**Scheme 1.3.** A proposed mechanism for peroxyacetic acid activation by sulfuric acid. Modified and reproduced with permission from reference [64].



**Scheme 1.4.** Proposed mechanism for anthracene oxidation using peroxyacetic acid catalyzed by sulfuric acid. Modified from that of reference [65].

### 1.4.3.3. Thermal remediation

Thermal remediation is another method that has been successfully used for PAH degradation [66]. In general, thermal remediation can be classified as incineration (600-1200 °C) and thermal desorption (100-600 °C) [67]. The main drawbacks related to incineration of organic pollutants are: i) high energy cost for removing moisture from

pollutants and then their combustion, and ii) the resulting air pollution by some gases such as hydrogen chloride (HCl), sulphur oxides (SO<sub>x</sub>), nitrogen oxides (NO<sub>x</sub>), dioxins/furans, and metal emissions, thus requiring the use of control devices to monitor these produced gases [7].

Thermal remediation can be achieved by conventional or microwave-assisted heating (MAH). MAH has several advantages compared to conventional heating, such as faster heating rate, more energy efficiency, and selective and volumetric heating [68,69]. The heating mechanisms using microwaves are dipole polarization and ionic conduction while conventional heating is thermal conduction [70]. Microwave heating rate can be improved using microwave absorbers, such as biochar and activated carbon [71]. Thermal treatment has been successfully used in several studies of the removal of PAHs from contaminated sites or from soil spiked by PAHs. A summary of the studies conducted for PAH removal using thermal treatment is listed in Table S1.4 of Appendix A.

#### **1.4.3.4. PAH bromination**

Bromination is an effective method to convert PAHs into more useful chemicals. In general, the activation of the C-H bond in aromatic compounds is an important step in organic reactions [72]. This can be achieved by halogenation of the aromatic ring to produce halogenated derivatives. The halogenated aromatics are important intermediates for C-C bond formation and nucleophilic substitution reactions leading to other useful aromatics derivatives [73]. Brominated aromatics are widely used in industries for the production of flame retardants, herbicides, and biocides, and in general organic synthesis [74]. The conventional method for aromatic bromination uses bromine as the reagent, but this reaction has several disadvantages such as high cost and reaction stoichiometry (the

remaining 50% of bromine starting material becomes hydrobromic acid) as shown in equation 1.10 [75].



Oxidative bromination using a strong oxidant has been developed as a successful route to improve the reaction [76]. For example, several chemical reagents such as  $\text{NaBrO}_3/\text{NaHSO}_3/\text{HCl}$  [77],  $\text{NaBr}/\text{H}_2\text{O}_2/\text{H}_2\text{SO}_4$  [78],  $\text{H}_2\text{O}_2/\text{HBr}$  [79] have been used for the bromination of aromatic compounds. Furthermore, oxidation using  $\text{HBr}/\text{H}_2\text{O}_2$  was reported to be a faster oxidation reagent compared to other reagents such as  $\text{HCl}/\text{H}_2\text{O}_2$ . This is due to the lower oxidation potential of  $\text{HBr}$ , which can oxidize the targeted compound under milder conditions [80].  $\text{HBr}/\text{H}_2\text{O}_2$  has been reported in several studies as an effective reagent for PAHs bromination [38,81,82]. For example, the bromination yields of naphthalene, anthracene, and pyrene using  $\text{HBr}/\text{H}_2\text{O}_2$  in approximately 15 h are 60%, 84%, 95%, respectively [38].

### **1.5. Co-authorship statement**

The principal author of this work conducted all experiments except measuring the SEM for surface methodology (Section S4.3, Appendix B) which was done by David Grant, CREIAT Network at Memorial University of Newfoundland, and calculation of Fukui functions (Appendix C) which was done by Ibrahim Awad (PhD candidate, Chemistry Department, Memorial University).

The drafts of all chapters in this dissertation were prepared by the principal author in consultation and discussion with the supervisory committee.

## 1.6. References

- [1] Agudelo-Castañeda, D. M.; Teixeira, E. C.; Schneider, I. L.; Lara, S. R.; Silva, L. F. O. Exposure to Polycyclic Aromatic Hydrocarbons in Atmospheric PM 1.0 of Urban Environments: Carcinogenic and Mutagenic Respiratory Health Risk by Age Groups. *Environ. Pollut.* **2017**, *224*, 158–170.
- [2] Marques, M.; Mari, M.; Sierra, J.; Nadal, M.; Domingo, J. L. Solar Radiation as a Swift Pathway for PAH Photodegradation: A Field Study. *Sci. Total Environ.* **2017**, *581*, 530–540.
- [3] Niu, S.; Dong, L.; Zhang, L.; Zhu, C.; Hai, R. Temporal and Spatial Distribution, Sources, and Potential Health Risks of Ambient Polycyclic Aromatic Hydrocarbons in the Yangtze River Delta (YRD) of Eastern China. *Chemosphere* **2016**, *172*, 72–79.
- [4] Qi, Y.-B.; Wang, C.-Y.; Lv, C.-Y.; Lun, Z.-M.; Zheng, C.-G. Removal Capacities of Polycyclic Aromatic Hydrocarbons (PAHs) by a Newly Isolated Strain from Oilfield Produced Water. *Int. J. Environ. Res. Public Health* **2017**, *14*, 1-15.
- [5] Lamichhane, S.; Bal Krishna, K. C.; Sarukkalige, R. Surfactant-Enhanced Remediation of Polycyclic Aromatic Hydrocarbons: A Review. *J. Environ. Manage.* **2017**, *199*, 46–61.
- [6] Kuppusamy, S.; Thavamani, P.; Singh, S.; Naidu, R.; Megharaj, M. Polycyclic Aromatic Hydrocarbons (PAHs) Degradation Potential, Surfactant Production, Metal Resistance and Enzymatic Activity of Two Novel Cellulose-Degrading Bacteria Isolated from Koala Faeces. *Environ. Earth Sci.* **2017**, *76*, 1–12.
- [7] Gan, S.; Lau, E. V.; Ng, H. K. Remediation of Soils Contaminated with Polycyclic Aromatic Hydrocarbons (PAHs). *J. Hazard. Mater.* **2009**, *172*, 532–549.
- [8] Titaley, I. A.; Chlebowski, A.; Truong, L.; Tanguay, R. L.; Simonich, S. L. M. Identification and Toxicological Evaluation of Unsubstituted Pahs and Novel Pah Derivatives in Pavement Sealcoat Products. *Environ. Sci. Technol. Lett.* **2016**, *3*, 234–242.
- [9] Lambert, T. W.; Guyn, L.; Lane, S. E. Development of Local Knowledge of Environmental Contamination in Sydney, Nova Scotia: Environmental Health Practice from an Environmental Justice Perspective. *Sci. Total Environ.* **2006**, *368*, 471–484.
- [10] MacAskill, N. D.; Walker, T. R.; Oakes, K.; Walsh, M. Forensic Assessment of Polycyclic Aromatic Hydrocarbons at the Former Sydney Tar Ponds and Surrounding Environment Using Fingerprint Techniques. *Environ. Pollut.* **2016**, *212*, 166–177.
- [11] Yousefinejad, S.; Honarasa, F.; Nekoeinia, M.; Zangene, F. Investigation and Modeling of the Solubility of Anthracene in Organic Phases. *J. Solution Chem.* **2017**,

46, 352–373.

- [12] Nishimura, C.; Horii, Y.; Tanaka, S.; Asante, K. A.; Ballesteros, F.; Viet, P. H.; Itai, T.; Takigami, H.; Tanabe, S.; Fujimori, T. Occurrence, Profiles, and Toxic Equivalents of Chlorinated and Brominated Polycyclic Aromatic Hydrocarbons in E-Waste Open Burning Soils. *Environ. Pollut.* **2017**, *252*, 252–260.
- [13] Wang, C.; Wu, S.; Zhou, S.; Shi, Y.; Song, J. Characteristics and Source Identification of Polycyclic Aromatic Hydrocarbons (PAHs) in Urban Soils: A Review. *Pedosphere* **2017**, *27*, 17–26.
- [14] Kang, F.; Mao, X.; Wang, X.; Wang, J.; Yang, B.; Gao, Y. Sources and Health Risks of Polycyclic Aromatic Hydrocarbons during Haze Days in Eastern China: A 1-Year Case Study in Nanjing City. *Ecotoxicol. Environ. Saf.* **2017**, *140*, 76–83.
- [15] Malakahmad, A.; Law, M. X.; Ng, K.-W.; Manan, T. S. A. The Fate and Toxicity Assessment of Polycyclic Aromatic Hydrocarbons (PAHs) in Water Streams of Malaysia. *Procedia Eng.* **2016**, *148*, 806–811.
- [16] McGrath, T.; Sharma, R.; Hajaligol, M. An Experimental Investigation into the Formation of Polycyclic-Aromatic Hydrocarbons (PAH) from Pyrolysis of Biomass Materials. *Fuel* **2001**, *80*, 1787–1797.
- [17] Peng, N.; Liu, Z.; Liu, T.; Gai, C. Emissions of Polycyclic Aromatic Hydrocarbons (PAHs) during Hydrothermally Treated Municipal Solid Waste Combustion for Energy Generation. *Appl. Energy* **2016**, *184*, 396–403.
- [18] Haritash, a. K.; Kaushik, C. P. Biodegradation Aspects of Polycyclic Aromatic Hydrocarbons (PAHs): A Review. *J. Hazard. Mater.* **2009**, *169*, 1–15.
- [19] Vikas, P.; Sharma, R.; Kumar, V. Sources, Properties and Health Risks of Carcinogenic Polycyclic Aromatic Hydrocarbons. *Pelagia Res. Libr. Adv. Appl. Sci. Res.* **2016**, *7*, 144–149.
- [20] Ma, Y. G.; Lei, Y. D.; Xiao, H.; Wania, F.; Wang, W. H. Critical Review and Recommended Values for the Physical-Chemical Property Data of 15 Polycyclic Aromatic Hydrocarbons at 25 °C. *J. Chem. Eng. Data* **2010**, *55*, 819–825.
- [21] Kim, K.-H.; Jahan, S. A.; Kabir, E.; Brown, R. J. C. A Review of Airborne Polycyclic Aromatic Hydrocarbons (PAHs) and Their Human Health Effects. *Environ. Int.* **2013**, *60*, 71–80.
- [22] Bamforth, S. M.; Singleton, I. Bioremediation of Polycyclic Aromatic Hydrocarbons: Current Knowledge and Future Directions. *J. Chem. Technol. Biotechnol.* **2005**, *80*, 723–736.
- [23] Ke, C. L.; Gu, Y. G.; Liu, Q.; Li, L. D.; Huang, H. H.; Cai, N.; Sun, Z. W. Polycyclic Aromatic Hydrocarbons (PAHs) in Wild Marine Organisms from South China Sea: Occurrence, Sources, and Human Health Implications. *Mar. Pollut. Bull.* **2017**, *117*, 507–511.

- [24] Samburova, V.; Zielinska, B.; Khlystov, A. Do 16 Polycyclic Aromatic Hydrocarbons Represent PAH Air Toxicity? *Toxics* **2017**, *5*, 1-17.
- [25] Bansal, V.; Kim, K. H. Review of PAH Contamination in Food Products and Their Health Hazards. *Environ. Int.* **2015**, *84*, 26–38.
- [26] Tran, L. H.; Drogui, P.; Mercier, G.; Blais, J. F. Electrochemical Degradation of Polycyclic Aromatic Hydrocarbons in Creosote Solution Using Ruthenium Oxide on Titanium Expanded Mesh Anode. *J. Hazard. Mater.* **2009**, *164*, 1118–1129.
- [27] Forsey, S. P.; Thomson, N. R.; Barker, J. F. Oxidation Kinetics of Polycyclic Aromatic Hydrocarbons by Permanganate. *Chemosphere* **2010**, *79*, 628–636.
- [28] Walker, T. R.; MacAskill, D. Monitoring Water Quality in Sydney Harbour Using Blue Mussels during Remediation of the Sydney Tar Ponds, Nova Scotia, Canada. *Environ. Monit. Assess.* **2014**, *186*, 1623–1638.
- [29] Lambert, T. W.; Lane, S. Lead, Arsenic and Polycyclic Aromatic Hydrocarbons in Soil and House Dust in the Communities Surrounding the Sydney, Nova Scotia, Tar Ponds. *Environ. Health Perspect.* **2004**, *112*, 35–41.
- [30] Smith, J. N.; Lee, K.; Gobeil, C.; Macdonald, R. W. Natural Rates of Sediment Containment of PAH, PCB and Metal Inventories in Sydney Harbour, Nova Scotia. *Sci. Total Environ.* **2009**, *407*, 4858–4869.
- [31] Walker, T. R.; MacAskill, D.; Rushton, T.; Thalheimer, A.; Weaver, P. Monitoring Effects of Remediation on Natural Sediment Recovery in Sydney Harbour, Nova Scotia. *Environ. Monit. Assess.* **2013**, *185*, 8089–8107.
- [32] King, T. L.; Uthe, J. F.; Musial, C. J. Polycyclic Aromatic Hydrocarbons in the Digestive Glands of the American Lobster, *Homarus Americanus*, Captured in the Proximity of a Coal-Coking Plant. *Bull. Environ. Contain. Toxicol.* **1993**, *50*, 907–914.
- [33] Furimsky, E. Sydney Tar Ponds: Some Problems in Quantifying Toxic Waste. *Environ. Manage.* **2002**, *30*, 872–879.
- [34] Biswas, B.; Sarkar, B.; Rusmin, R.; Naidu, R. Mild Acid and Alkali Treated Clay Minerals Enhance Bioremediation of Polycyclic Aromatic Hydrocarbons in Long-Term Contaminated Soil: A <sup>14</sup>C-Tracer Study. *Environ. Pollut.* **2017**, *223*, 255–265.
- [35] Zhang, H.; Ma, D.; Qiu, R.; Tang, Y.; Du, C. Non-Thermal Plasma Technology for Organic Contaminated Soil Remediation: A Review. *Chem. Eng. J.* **2017**, *313*, 157–170.
- [36] Elie, M. R.; Clausen, C. A.; Geiger, C. L. Reduction of Benzo[a]pyrene with Acid-Activated Magnesium Metal in Ethanol: A Possible Application for Environmental Remediation. *J. Hazard. Mater.* **2012**, *203*, 77–85.
- [37] Rubio-Clemente, A.; Torres-Palma, R. A.; Penuela, G. A. Removal of Polycyclic

- Aromatic Hydrocarbons in Aqueous Environment by Chemical Treatments: A Review. *Sci. Total Environ.* **2014**, *478*, 201–225.
- [38] Vyas, P. V.; Bhatt, A. K.; Ramachandraiah, G.; Bedekar, A. V. Environmentally Benign Chlorination and Bromination of Aromatic Amines, Hydrocarbons and Naphthols. *Tetrahedron Lett.* **2003**, *44*, 4085–4088.
- [39] Kuppusamy, S.; Thavamani, P.; Megharaj, M.; Naidu, R. Bioaugmentation with Novel Microbial Formula vs. Natural Attenuation of a Long-Term Mixed Contaminated Soil-Treatability Studies in Solid- and Slurry-Phase Microcosms. *Water. Air. Soil Pollut.* **2016**, *227*, 1-15.
- [40] Ferrarese, E.; Andreottola, G.; Oprea, I. A. Remediation of PAH-Contaminated Sediments by Chemical Oxidation. *J. Hazard. Mater.* **2008**, *152*, 128–139.
- [41] Nelkenbaum, E.; Dror, I.; Berkowitz, B. Reductive Hydrogenation of Polycyclic Aromatic Hydrocarbons Catalyzed by Metalloporphyrins. *Chemosphere* **2007**, *68*, 210–217.
- [42] Segawa, Y.; Stephan, D. W. Metal-Free Hydrogenation Catalysis of Polycyclic Aromatic Hydrocarbons. *Chem. Commun.* **2012**, *48*, 11963.
- [43] Alias, S.; Omar, M.; Hussain, N.-H.; Abdul-Talib, S. Zero Valent Iron Particles for the Degradation of Polycyclic Aromatic Hydrocarbons in Contaminated Soil. *Adv. Mater. Res.* **2012**, *587*, 111–115.
- [44] Chang, M.-C.; Shu, H.-Y.; Hsieh, W.-P.; Wang, M.-C. Using Nanoscale Zero-Valent Iron for the Remediation of Polycyclic Aromatic Hydrocarbons Contaminated Soil. *J. Air Waste Manage. Assoc.* **2005**, *55*, 1200–1207.
- [45] Dewil, R.; Mantzavinos, D.; Poulios, I.; Rodrigo, M. A. New Perspectives for Advanced Oxidation Processes. *J. Environ. Manage.* **2017**, *195*, 93–99.
- [46] Muranaka, C. T.; Julcour, C.; Wilhelm, A. M.; Delmas, H.; Nascimento, C. A. O. Regeneration of Activated Carbon by (Photo)-Fenton Oxidation. *Ind. Eng. Chem. Res.* **2010**, *49*, 989–995.
- [47] Mirzaei, A.; Chen, Z.; Haghghat, F.; Yerushalmi, L. Removal of Pharmaceuticals from Water by Homo/heterogenous Fenton-Type Processes- a Review. *Chemosphere* **2017**, *174*, 665–688.
- [48] Fenton, H. J. Oxidation of Tartaric Acid in Presence of Iron. *J. Chem. Soc.* **1894**, *65*, 899–910.
- [49] Bello, M. M.; Abdul Raman, A. A. Trend and Current Practices of Palm Oil Mill Effluent Polishing: Application of Advanced Oxidation Processes and Their Future Perspectives. *J. Environ. Manage.* **2017**, *198*, 170–182.
- [50] Lee, B. D.; Hosomi, M. A Hybrid Fenton Oxidation-Microbial Treatment for Soil Highly Contaminated with Benz[a]anthracene. *Chemosphere* **2001**, *43*, 1127–1132.

- [51] Lee, B.-D.; Hosomi, M. Ethanol Washing of PAH-Contaminated Soil and Fenton Oxidation of Washing Solution. *J. Mater.* **2000**, *2*, 24–30.
- [52] Lundstedt, S.; Persson, Y.; Öberg, L. Transformation of PAHs during Ethanol-Fenton Treatment of an Aged Gasworks' Soil. *Chemosphere* **2006**, *65*, 1288–1294.
- [53] Babuponnusami, A.; Muthukumar, K. A Review on Fenton and Improvements to the Fenton Process for Wastewater Treatment. *J. Environ. Chem. Eng.* **2014**, *2*, 557–572.
- [54] Pereira, M. C.; Oliveira, L. C. a.; Murad, E. Iron Oxide Catalysts: Fenton and Fentonlike Reactions – a Review. *Clay Miner.* **2012**, *47*, 285–302.
- [55] Bokare, A. D.; Choi, W. Review of Iron-Free Fenton-like Systems for Activating H<sub>2</sub>O<sub>2</sub> in Advanced Oxidation Processes. *J. Hazard. Mater.* **2014**, *275*, 121–135.
- [56] Garcia-Segura, S.; Bellotindos, L. M.; Huang, Y. H.; Brillas, E.; Lu, M. C. Fluidized-Bed Fenton Process as Alternative Wastewater Treatment technology??A Review. *J. Taiwan Inst. Chem. Eng.* **2016**, *67*, 211–225.
- [57] Yap, C. L.; Gan, S.; Ng, H. K. Fenton Based Remediation of Polycyclic Aromatic Hydrocarbons-Contaminated Soils. *Chemosphere* **2011**, *83*, 1414–1430.
- [58] Neyens, E.; Baeyens, J. A Review of Classic Fenton's Peroxidation as an Advanced Oxidation Technique. *J. Hazard. Mater.* **2003**, *98*, 33–50.
- [59] Lee, B. D.; Hosomi, M.; Murakami, A. Fenton Oxidation with Ethanol to Degrade Anthracene into Biodegradable 9,10-Anthraquinone: A Pretreatment Method for Anthracene-Contaminated Soil. *Water Sci. Technol.* **1998**, *38*, 91–97.
- [60] Cordeiro, D. S.; Corio, P. Electrochemical and Photocatalytic Reactions of Polycyclic Aromatic Hydrocarbons Investigated by Raman Spectroscopy. *J. Braz. Chem. Soc.* **2009**, *20*, 80–87.
- [61] Bendouz, M.; Tran, L. H.; Coudert, L.; Mercier, G.; Blais, J.-F. Degradation of Polycyclic Aromatic Hydrocarbons in Different Synthetic Solutions by Fenton's Oxidation. *Environ. Technol.* **2016**, *38*, 1–12.
- [62] Kitis, M. Disinfection of Wastewater with Peracetic Acid: A Review. *Environ. Int.* **2004**, *30*, 47–55.
- [63] Vandekinderen, I.; Devlieghere, F.; De Meulenaer, B.; Ragaert, P.; Van Camp, J. Optimization and Evaluation of a Decontamination Step with Peroxyacetic Acid for Fresh-Cut Produce. *Food Microbiol.* **2009**, *26*, 882–888.
- [64] Dul'neva, L. V.; Moskvina, A. V. Kinetics of Formation of Peroxyacetic Acid. *Russ. J. Gen. Chem.* **2005**, *75*, 1125–1130.
- [65] N'Guessan, A. L.; Levitt, J. S.; Nyman, M. C. Remediation of Benzo(a)pyrene in Contaminated Sediments Using Peroxy-Acid. *Chemosphere* **2004**, *55*, 1413–1420.

- [66] Chawla, R. C. Contaminant Removal from Dry and Wet Sands by Thermal Desorption Ali Pourhashemi. *Int. J. Environ. Waste Manag.* **2006**, *1*, 39–48.
- [67] Vidonish, J. E.; Zygourakis, K.; Masiello, C. A.; Gao, X.; Mathieu, J.; Alvarez, P. J. J. Pyrolytic Treatment and Fertility Enhancement of Soils Contaminated with Heavy Hydrocarbons. *Environ. Sci. Technol.* **2016**, *50*, 2498–2506.
- [68] Li, D.; Zhang, Y.; Quan, X.; Zhao, Y. Microwave Thermal Remediation of Crude Oil Contaminated Soil Enhanced by Carbon Fiber. *J. Environ. Sci.* **2009**, *21*, 1290–1295.
- [79] Zhang, Y.; Chen, P.; Liu, S.; Peng, P.; Min, M.; Cheng, Y.; Anderson, E.; Zhou, N.; Fan, L.; Liu, C.; Chen, G.; Liu, Y.; Lei, H.; Li, B.; Ruan, R. Effects of Feedstock Characteristics on Microwave-Assisted Pyrolysis – a Review. *Bioresour. Technol.* **2017**, *230*, 143–151.
- [70] Yunpu, W.; Leilei, D.; Liangliang, F.; Shaoqi, S.; Yuhuan, L.; Roger, R. Review of Microwave-Assisted Lignin Conversion for Renewable Fuels and Chemicals. *J. Anal. Appl. Pyrolysis* **2016**, *119*, 104–113.
- [71] Martín, M. T.; Sanz, A. B.; Nozal, L.; Castro, F.; Alonso, R.; Aguirre, J. L.; González, S. D.; Matía, M. P.; Novella, J. L.; Peinado, M.; Vaquero, J. J. Microwave-Assisted Pyrolysis of Mediterranean Forest Biomass Waste: Bioproduct Characterization. *J. Anal. Appl. Pyrolysis* **2017**, *127*, 278–285.
- [72] Jia, C.; Piao, D.; Oyadama, J.; Lu, W.; Tsugio, K.; Fujiwara, Y. Efficient Activation of Aromatic C-H Bonds for Addition to C-C Multiple Bonds. *Science* **2000**, *287*, 1992–1995.
- [73] Gavara, L.; Boisse, T.; Rigo, B.; Hénichart, J. P. A New Method of Bromination of Aromatic Rings by an Iso-Amyl nitrite/HBr System. *Tetrahedron* **2008**, *64*, 4999–5004.
- [74] Kumar, L.; Mahajan, T.; Agarwal, D. D. Bromination of Deactivated Aromatic Compounds with Sodium Bromide/sodium Periodate under Mild Acidic Conditions. *Ind. Eng. Chem. Res.* **2012**, *51*, 11593–11597.
- [75] Choudary, B. M.; Someshwar, T.; Venkat Reddy, C.; Lakshmi Kantam, M.; Jeeva Ratnam, K.; Sivaji, L. V. The First Example of Bromination of Aromatic Compounds with Unprecedented Atom Economy Using Molecular Bromine. *Appl. Catal. A Gen.* **2003**, *251*, 397–409.
- [76] Joshi, A. V.; Baidossi, M.; Mukhopadhyay, S.; Sasson, Y. Oxidative Bromination of Activated Aromatic Compounds Using Aqueous Nitric Acid as an Oxidant. *Org. Process Res. Dev.* **2004**, *8*, 568–570.
- [77] Kikuchi, D.; Sakaguchi, S.; Ishii, Y. An Alternative Method for the Selective Bromination of Alkylbenzenes Using NaBrO<sub>3</sub> /NaHSO<sub>3</sub> Reagent. *J. Org. Chem.* **1998**, *63*, 6023–6026.

- [78] Mestres, R.; Palenzuela, J. High Atomic Yield Bromine-Less Benzylic Bromination. *Green Chem.* **2002**, *4*, 314–316.
- [79] Podgoršek, A.; Stavber, S.; Zupan, M.; Iskra, J. Free Radical Bromination by the H<sub>2</sub>O<sub>2</sub>-HBr System on Water. *Tetrahedron Lett.* **2006**, *47*, 7245–7247.
- [80] Podgoršek, A.; Zupan, M.; Iskra, J. Oxidative Halogenation With “green” oxidants: Oxygen and Hydrogen Peroxide. *Angew. Chemie - Int. Ed.* **2009**, *48*, 8424–8450.
- [81] Chidirala, S.; Ulla, H.; Valaboju, A.; Kiran, M. R.; Mohanty, M. E.; Satyanarayan, M. N.; Umesh, G.; Bhanuprakash, K.; Rao, V. J. Pyrene-Oxadiazoles for Organic Light-Emitting Diodes: Triplet to Singlet Energy Transfer and Role of Hole-Injection/Hole-Blocking Materials. *J. Org. Chem.* **2016**, *81*, 603–614.
- [82] Schulze, M. Synthesis of 1-Bromopyrene and 1-Pyrenecarbaldehyde. *Org. Synth.* **2016**, *93*, 100–114.

## Chapter 2

### **Optimizing reductive degradation of PAHs using anhydrous ethanol with magnesium catalyzed by glacial acetic acid<sup>1</sup>**

---

<sup>1</sup> This chapter was submitted to *Environmental Science & Technology*.

## **Abstract**

Targeted degradation of individual polycyclic aromatic hydrocarbon (PAH) constituents like anthracene, may offer cost-effective and efficient cleaning of coal tar-contaminated sites. Consequently, a reductive degradation procedure of anthracene using activated magnesium with anhydrous ethanol at room temperature was developed and optimized. The effects of magnesium concentrations, glacial acetic acid volumes, and exposure time on the anthracene reduction were studied. An experimental design was adopted to minimize the number of experiments and to determine the optimum conditions for anthracene reduction. This happens in two stages: screening for variables, and optimization using a response surface method based on central composite design. The main product from anthracene reduction is 9,10-dihydroanthracene. Optimum conditions for 98% degradation capacity of anthracene ( $2.80 \times 10^{-3}$  mmol) were 30 mg of Mg powder (1.20 mmol), 60  $\mu$ L of glacial acetic acid (1.05 mmol), and 30 min exposure time. When the optimized method was tested on the coal tar specimen, twice as many reagents (i.e. Mg and glacial acetic acid) were required to obtain a 90% degradation of anthracene and fluoranthene from the coal tar. This method of using activated Mg and anhydrous ethanol selectively reduces PAHs in coal tar; in particular anthracene and fluoranthene are most efficiently removed.

## 2.1. Introduction

Polycyclic aromatic hydrocarbons (PAHs) are a class of organic compounds that consist of two or more fused benzene rings. PAHs are lipophilic and have high desorption activation energy from PAH-contaminated soil [1]. They are colorless to pale solids and have low solubility in water, high melting and boiling points, and low vapor pressures [2]. PAHs are mainly produced from the incomplete combustion of fossil fuel and organic materials, and the evaporation of petroleum derivatives [3]. Most PAHs do not easily degrade in the environment and are classified as persistent organic pollutants. They are considered as carcinogenic, teratogenic and mutagenic [4]. The United States Environmental Protection Agency (EPA) has listed 16 PAHs as priority pollutants [5]. Seven of these PAHs, namely benz[a]anthracene, chrysene, benzo[b]fluoranthene, benzo[k]fluoranthene, benzo[a]pyrene, indo[1,2,2-cd]pyrene, and dibenzo[a,h]anthracene, are considered to be carcinogenic compounds [6]. Therefore, conversion of PAHs into less toxic products is one of the strategies in the remediation of PAHs contaminated sites [7].

Catalytic reduction is one of the methods used for PAH degradation [8,9]. For example, transition metals (e.g., rhodium, ruthenium, palladium, etc.) have been successfully used as catalysts in degrading PAHs through hydrogenation [10–18], but the procedure requires high temperatures and pressure of hydrogen to obtain relatively small non-toxic products. Thus, it is a relatively expensive procedure for PAH reduction [19]. Birch reduction has also been used for PAH reduction, which involves the use of ammonia and alkali metals such as sodium or lithium [20]. However, the Birch reduction has disadvantages, such as the toxicity of ammonia, difficulty in handling reactive metals and scaling up [21,22].

Therefore, it is necessary to find an alternative metal/solvent system effective for PAH reduction, which is cheap, easily handled, and environmentally friendly. Magnesium with methanol can be such a system, because it is widely used in several organic synthetic procedures [23]. Magnesium with acidified ethanol was successfully used to remove polychlorinated biphenyls (PCBs) from painted surfaces [24,25]. In addition, magnesium with a combined solvent of ethanol and ethyl lactate (1:1, v/v) was used to remove some PAHs such as dibenzo[a,l]pyrene, fluoranthene, benzo[a]pyrene, fluorene, benz[a]anthracene, 9-fluorenone, 7*H*-benz[de]anthracene-7-one, benz[a]anthracene-7,12-dione and 9-fluorenol, from spiked soil. The degradation was 79-88% of oxygenated PAHs and 66-87% of PAHs after 24 h of reaction and room temperature. To effectively apply such a method in contaminated sites, like the coal tar-contaminant of the defunct Steel Mill processing plant in Sydney Nova Scotia, the degradation of PAHs needs to be fast, so that turnover can be multifold within a day.

In view of this, the PAH reduction procedure was modified by using activated Mg as the catalyst in order to increase degradation turnover. The Mg was activated by glacial acetic acid with anhydrous ethanol as a co-solvent to enhance the PAH degradation in coal tar. Therefore, the objectives of this work were to investigate the ability of Mg powder activated by glacial acetic acid with anhydrous ethanol to effect reduction of PAHs in coal tar at room temperature and to determine the optimum conditions for PAH reduction in coal tar.

## **2.2. Materials and method**

### **2.2.1. Chemicals**

Anthracene (>90%) was purchased from Alfa Aesar (US) and used as received. Nitrobenzene (99%) as an internal standard was purchased from Fisher Scientific (New

Jersey, USA), toluene (99.5%) was purchased from Caledon Laboratories Ltd. (Georgetown, ON, Canada), acetonitrile (HPLC grade, 99.9%) was purchased from ACP Chemicals (Montreal, Canada), and anhydrous ethanol was purchased from Commercial Alcohols (Brampton, ON, Canada). All of these chemicals were used without further purification except acetonitrile, which was dried over molecular sieves for 2 weeks. Glacial acetic acid (> 99.85%), magnesium powder ( $\leq 150 \mu\text{m}$ , 98% purity), magnesium turnings ( $\sim 4000 \mu\text{m}$ , 98% purity), and graphite (99.99%) were purchased from Sigma-Aldrich, Canada. Coal tar samples were collected from Sydney Tar Ponds, Nova Scotia, Canada, according to coal tar sampling methodology [26].

### **2.2.2. Anthracene and coal tar reduction experiments**

Initially, anthracene was used as a representative model compound of PAHs and subjected to reductive degradation with Mg powder in anhydrous ethanol. Then, the optimum conditions were used for reduction of PAHs in coal tar. The method used in this study is based on a procedure used in a previous study [27]. Briefly, a 2.0 mL of solution of anthracene (250 ppm) in anhydrous ethanol, in a 20 mL PTFE vial was added with a desirable amount (10-30 mg) of Mg powder, which was previously well-ground using an agate mortar and pestle. The reaction started by adding a desirable volume of glacial acetic acid (10-60  $\mu\text{L}$ ), which was used as an activator, and the reaction mixture was rapidly stirred for various time intervals (0.5-3.0 h) at room temperature (21.5 °C). The reaction was quenched by adding 2.0 mL of toluene, then the mixture was sonicated for 15 min, and filtered using nylon micro filter paper. For product separation, 4.0 mL of deionized water was added, and then the mixture was centrifuged (3000 rpm) for 20 min. The toluene extracts were stored at 4 °C in 5 mL-sealed glass vials with PTFE lined caps. The toluene

extracts as well as reductive degradation on the PAHs were confirmed using gas chromatography mass spectrometry (GC-MS) and a gas chromatography flame ionization detector (GC-FID). For coal tar degradation, 0.400 g of coal tar was dissolved in 60.0 mL of anhydrous ethanol, sonicated then filtered using nylon 0.45  $\mu\text{m}$  PTFE CHROMIC. Approximately 66% of the coal tar dissolved. A solution of 2.0 mL of coal tar in anhydrous ethanol was added to 30 mg of Mg and 60  $\mu\text{L}$  of glacial acetic acid. The reaction mixture in a sealed vial was stirred rapidly for 30 min. Then, the reaction was stopped and the product was separated using the same steps used for anthracene reduction.

### **2.2.3. Experimental Design**

The experimental design for the anthracene reduction was achieved using the Design-Expert 9.0.0 software. This experimental design was carried out through two stages: screening of variables, and optimization using central composite design. In the stage of variables screening, a half factorial design ( $2^{4-1}$ ) for four factors (magnesium dosage, glacial acetic acid dosage, graphite dosage, and time) were investigated to determine the importance of these factors. The factor that has a less significant effect can be ignored to reduce the number of experiments. The stage of screening variables includes the eight runs listed in Table 2.1. In the screening of variables, each factor has two levels: low and high, which were coded by -1 for low and +1 for high levels. The minimum and maximum values of each factor were chosen according to the preliminary experiments and literature [28]. The second stage is optimization using the response surface methodology (RSM) based on the central composite design (CCD). RSM is a mathematical and statistical technique used for modelling and analysis of experimental data via study of the relation between the response (e.g., removal (%)) and the variables (factors) to obtain the optimum response

[29]. In addition, CCD is a kind of RSM including central points with factorial or fractional factorial design and it is widely used for second-order modeling [30]. For optimizing the anthracene reduction, three significant factors (i.e. Mg dosage (10-30 mg), glacial acetic acid volume (10-60  $\mu$ L), and exposure time (0.5-3.0 h)) were investigated. Each factor has three levels: low (-1), medium (0), and high (+1). The experiments were 17 runs and conducted in triplicates (Table 2.2).

#### **2.2.4. Samples analysis**

To confirm degradation of the PAHs, the samples were analyzed on a GC-MS (Agilent 7683 series II, Wilmington, USA) and GC-FID (Trace Ultra Thermo Scientific, USA). The GC-MS is equipped with an Agilent 5973 Mass Selective Detector (MSD), which was used at the operation conditions of 70 eV electron ionization energy, 40–550 m/z scan range, and 250 °C mass interface temperature. The GC column is a DB-5 capillary column (30 m x 0.25 mm i.d. x 0.25  $\mu$ m film thickness) with a helium flow rate of 1.5 mL/min. The temperature of the GC oven was programmed at the initial temperature of 80 °C for 1 min then was increased to 300 °C with a heating rate of 10 °C/min and held for 2 min at the final temperature. The injection volume and the injector temperature were 2  $\mu$ L and 300 °C, respectively. The analysis was achieved in splitless mode. For quantitative analysis, calibration curves of PAHs were achieved in triplicates with good linearity ( $R^2 > 0.97$ ). The compounds were identified by GC-MS through matching the spectrum obtained with the reference spectra in the NIST library. GC-FID equipped with the same column type of GC-MS mentioned above. The detector and the injector temperature were 300 °C. The GC-FID oven temperature was programmed to be the same as of GC-MS. The hydrogen and air flow rates were 40 mL/min and 300 mL/min, respectively.

## 2.3. Results and discussion

### 2.3.1. Effect of magnesium activation

Using a commercial Mg powder without activation was found to be ineffective for the anthracene reduction as shown in Figure 2.1 (bar A). In addition, particle size has a clear effect on the removal efficiency of anthracene, where small-size Mg particles ( $\leq 150 \mu\text{m}$ ) are more efficient for anthracene reduction ( $> 90\%$  removal efficiency) than Mg turnings ( $\sim 50\%$  removal efficiency) as shown in Figure 2.1 (bars B and C). This is due to the large surface area of Mg powder that is available for reaction with anthracene molecules [31]. Activation of Mg powder using glacial acetic acid is a necessary process to remove the formed layers of magnesium oxide (MgO) and magnesium hydroxide (Mg(OH)<sub>2</sub>) from the Mg surface. These layers prevent the interaction between Mg and the substrate (e.g. anthracene) [27]. Mg activation can be achieved by using methyl iodide or ethyl bromide, but this method is not favored since a side reaction with the Mg can occur through the Grignard reagent formation [32]. Mercury chloride also can be used, but it is highly toxic [33]. Stirring of Mg during the reaction is an important process and helps to remove the oxide layers and reduces the reaction time ( $< 1 \text{ h}$ ), but it is not favored for large scale reduction using Mg turnings since the glass reactor can be damaged by abrasion, whereas slower stirring is not effective with large-scale reductions [34]. Acid treatment is another method to remove the oxidized layers from the Mg surface [35] by which Mg is activated through increasing the active sites on the Mg surface [34]. In this work, glacial acetic acid was used as the activator because it is water-free, which improves the reaction efficiency, and is easy to handle and environmentally friendly.

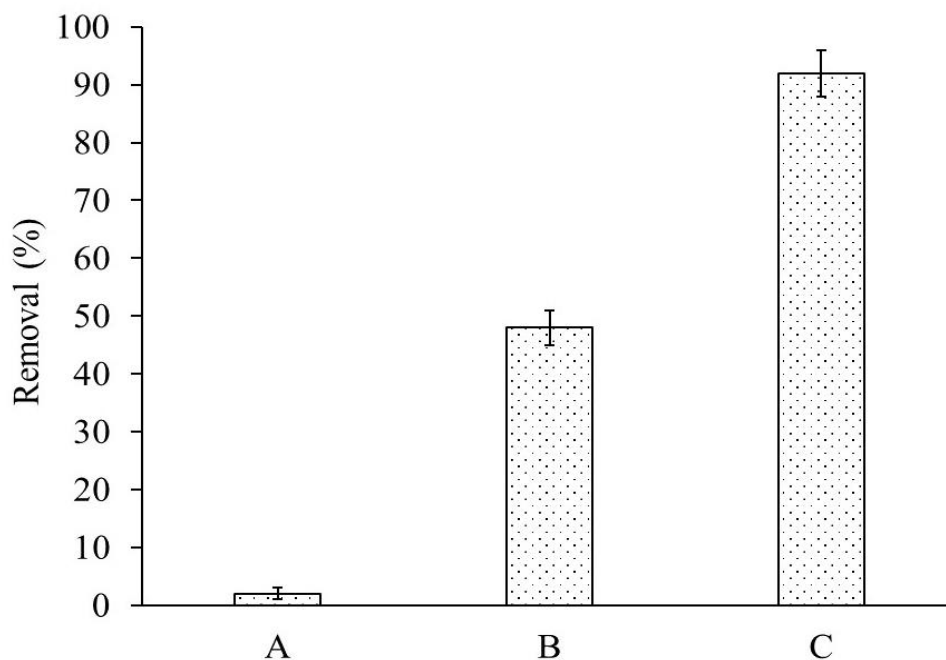
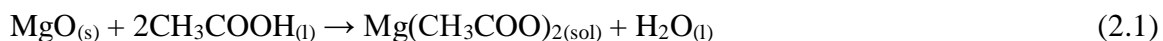


**Figure 2.1.** Effect of Mg activation and Mg particle size on reduction of anthracene in anhydrous ethanol at room temperature. A) Non-catalyzed Mg powder, B) catalyzed Mg turnings, and C) catalyzed Mg powder. The reaction conditions are 250 ppm anthracene (Ci), 30 mg Mg, glacial acetic acid (30  $\mu$ L), and 3 h reaction time. Error bars represent the RSD%, n=3.

The Mg cleaning using glacial acetic acid includes the reaction between the acid and the oxide layers (MgO and Mg(OH)<sub>2</sub>) as shown in Equations 2.1 and 2.2 [27].



### 2.3.2. Effect of magnesium with ethanol

An aprotic solvent (dried acetonitrile) was used with Mg catalyzed by glacial acetic acid for anthracene reduction to understand the role of co-solvent in anthracene reduction, and to compare with anhydrous ethanol (Figure 3.2). The results indicate ethanol is an essential co-solvent with catalyzed Mg for anthracene reduction, while dry acetonitrile did not show any efficiency in anthracene reduction. Anhydrous ethanol works as a proton source as

shown in the reaction mechanism (Scheme 2.1). In addition, using anhydrous ethanol as a co-solvent has several advantages, such as being non-toxic, cheap, and it has a high ability to extract PAHs. Mg reacts with anhydrous ethanol to produce hydrogen gas and magnesium ethoxide as shown in Equation 2.3. Anthracene degradation increases with increasing reaction time, where a high conversion of anthracene (>90%) occurs at time ~ 3 h (see inset plot in Figure 2.2).

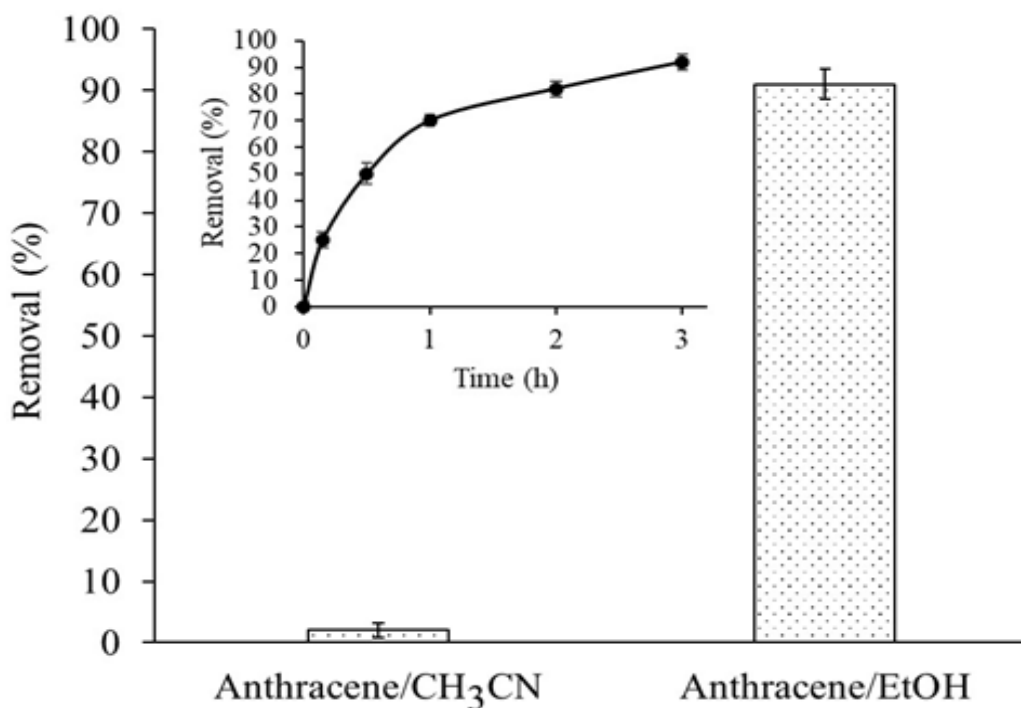
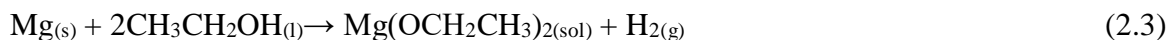


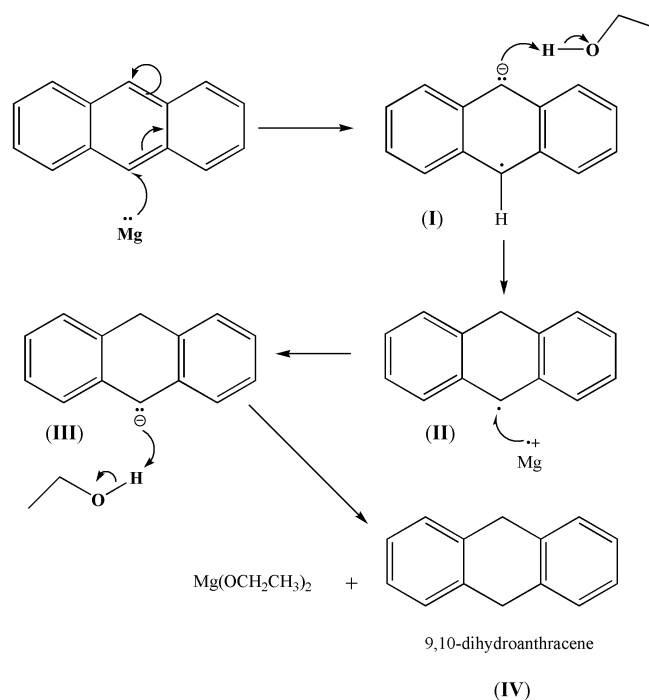
**Figure 2.2.** Effect of co-solvent on anthracene reduction using Mg catalyzed by glacial acetic acid (30  $\mu$ L). The inset plot represents the anthracene degradation using Mg/EtOH as a function of time. The reaction conditions are 250 ppm anthracene ( $C_i$ ), 30 mg of Mg powder, and 3 h reaction time. Error bars represent the RSD%,  $n=3$ .



Due to these side reactions shown in Equations 2.1-2.3, the amount of Mg powder (1.20 mmol) and glacial acetic acid (1.05 mmol) are in excess compared to the amount of anthracene used ( $2.80 \times 10^{-3}$  mmol). Therefore, the reaction is not stoichiometric.

### 2.3.3. Anthracene reduction mechanism

Reduction of anthracene using activated Mg with anhydrous ethanol gives 9,10-dihydroanthracene as the main product. A proposed modified mechanism of this reaction based upon that described in [28] is shown in Scheme 2.1. A single electron-transfer (SET) is the first step in the mechanism, where a single electron transfers from Mg (The electron donor) to anthracene (The electron acceptor) to form a radical anion (I) at position 9 or 10 of the anthracene molecule. Then, (I) is protonated to form the protonated radical (II). The second electron transfers from Mg to (II) to form anion (III), which in turn is protonated by ethanol molecules to produce 9,10-dihydroanthracene (IV).



**Scheme 2.1.** A proposed mechanism for the anthracene reduction using the Mg catalyzed by glacial acetic acid, which is a modification of mechanism earlier proposed by Elie [28].

### **2.3.4. Optimization of anthracene reduction**

The single-factor-at-a-time approach is widely reported in the literature, in which a single factor is studied and other factors remain constant [36]. Nevertheless, that approach is not fully successful because it ignores the interactions between the factors and requires many experiments. However, the experimental design methodology reduces the number of experiments and takes into the account the interactions between the factors [37].

#### **2.3.4.1. Screening of variables**

The screening of variables of anthracene reduction using the Mg catalyzed by glacial acetic acid was achieved using four factors, namely Mg powder dosage, volume of glacial acetic acid, mass of graphite, and time. Graphite was introduced as a possible factor since Elie [27] reported a catalytic function for graphite in his experiments. Using the data shown in Table 1, the significance of each factor was then determined by a Pareto chart (Figure 2.3) in which the significance of each factor is shown to be proportional to the length of the corresponding line bar. For example, glacial acetic acid and Mg have a significant effect ( $p \leq 0.05$  at 95% confidence level), having values of 12.12 and 11.00, respectively. However, graphite has an insignificant effect ( $p = 0.2199$ ) as shown in Table 2.2. This result was proven by other experiments designed to study the effect of the added graphite. For example, experiment #4 in Table 2.1 was repeated with graphite (30 mg), and experiment #8 was also repeated, but without graphite. There is no apparent effect on reduction of anthracene in both cases. Therefore, the three factors that have a clear effect on removal % of anthracene reduction are Mg dosage, volume of glacial acetic acid, and time. Among them, glacial acetic acid has the highest effect followed by Mg and time, respectively.

**Table 2.1.** Screening variables for four factors using only low and high levels for anthracene reduction.

		Factor		Level	
				Low (-1)	High (+1)
		Graphite (mg)	0	30	
		Mg (mg)	10	30	
		Glacial acetic acid ( $\mu\text{L}$ )	10	60	
		Time (min)	30	180	
#	Mg	Graphite	Glacial acetic acid	Time	Removal (%) <sup>a</sup>
1	-1	-1	+1	+1	78.7
2	+1	-1	+1	-1	98.0
3	+1	-1	-1	+1	74.4
4	-1	-1	-1	-1	48.3
5	-1	+1	+1	-1	60.0
6	+1	+1	+1	+1	98.5
7	+1	+1	-1	-1	59.8
8	-1	+1	-1	+1	50.0

<sup>a</sup> The mean of three experiments, RSD% < 3.6%.

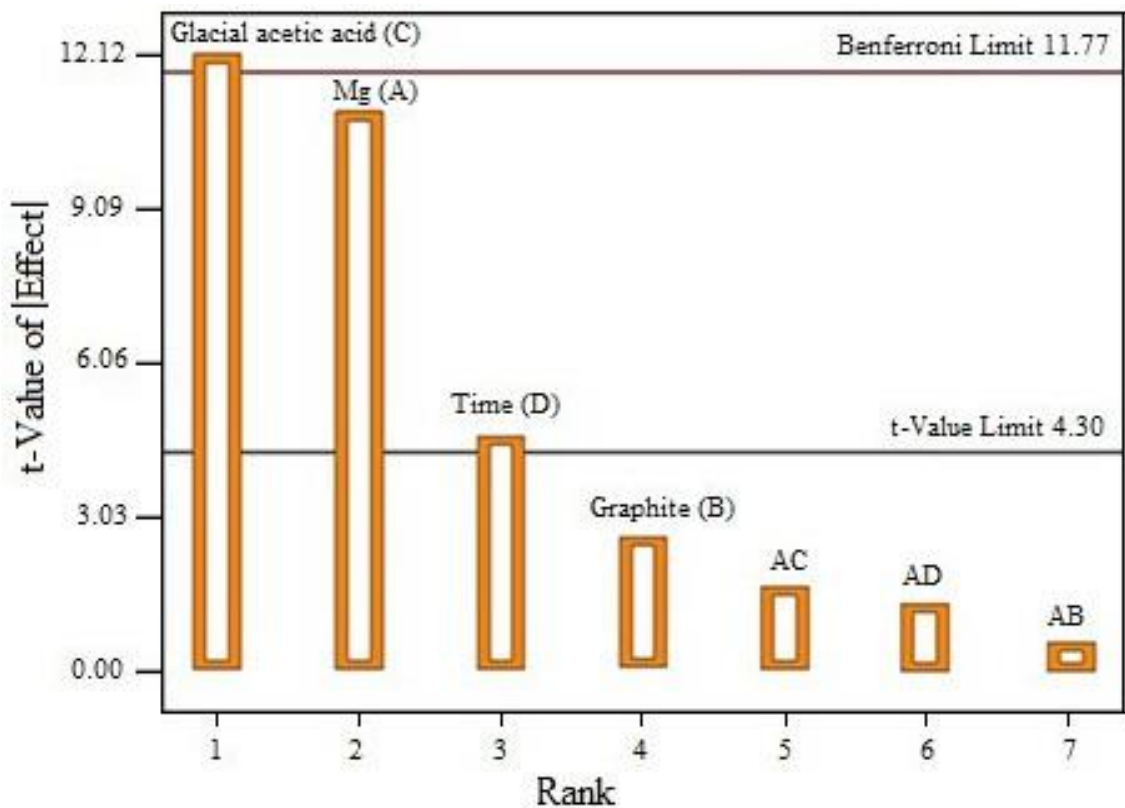


**Figure 2.3.** Pareto chart for four factors (Table 2.1) effecting on anthracene reduction using magnesium activated by glacial acetic acid with anhydrous ethanol as co-solvent.

**Table 2.2.** Analysis of variance of four factors (Mg, graphite, glacial acetic acid, and time), which were studied in the screening variables stage of the experimental design.

<b>Source</b>	<b>Sum of squares</b>	<b>df</b>	<b>Mean Square</b>	<b>F Value</b>	<b>p-value Prob &gt; F</b>	
Model	3005.71	5	601.14	26.41	0.0369	Significant
Mg	1225.13	1	1225.13	53.82	0.0181	
Graphite	70.81	1	70.81	3.11	0.2199	
Glacial acetic acid	1490.58	1	1490.58	65.48	0.0149	
Time	216.32	1	216.32	9.50	0.0911	
Residual	45.53	2	22.76			
Cor Total	3051.24	7				

#### **2.3.4.2. Optimization using central composite design (CCD)**

The use of RSM based on CCD is widely reported in the literature because it is simple and easy to use, minimizes the number of experiments, and provides a useful information on the effects of the factors studied and their interactions [38]. The experiments completed for the optimization of anthracene reduction using activated Mg with anhydrous ethanol are listed in Table 2.3. Three factors (i.e., Mg powder, glacial acetic acid, and time) were studied and each factor has three levels: low (-1), medium (0), and high (+1). Increasing the Mg dosage increases the removal % of anthracene. The same trend can be observed when the glacial acetic acid volume increases. Using the highest Mg dosage and high glacial acetic acid dosage resulted in high removal % of anthracene during a relatively short time (30 min). The results of analysis of variance (ANOVA) of the CCD model are listed in Table 2.4, where the p-values of the three factors (Mg powder, glacial acetic acid, and time) are less than 0.05, which indicate that they have a clear significant influence on anthracene reduction. In addition, F-values are large and the lack of fit is insignificant, which leads us to conclude that the model is in a good agreement with the data used [39].

Depending on the ANOVA analysis, the final mathematical equation, in terms of actual factors, for removal calculation is as follows (Equation 2.4):

$$\text{Removal} = +71.86 + 11.90*A + 12.80*B + 6.68*C + 1.95*AB - 1.45*AC - 0.43*BC - 8.451E-003 A^2 - 4.01* B^2 + 2.99 *C^2 \text{ (Where, A: Mg, B: Glacial acetic acid, and C: Time)} \quad (2.4)$$

The model validity was evaluated by ANOVA analysis, where the correlation coefficient ( $R^2$ ) is 0.91 and the adjusted  $R^2$  is 0.89 at a confidence level of 95%. In addition, the standard deviation is 7.1% and the lack of fit is not significant. The model accuracy can be evaluated through the homogenous distribution of externally studentized residuals and predicted probability values around the straight line (Figure 2.4-A). In addition, Figure 2.4-B shows the distribution of the real values obtained from experiments and the predicted values from the model around the straight line ( $y = x$ ), which explains a good agreement between the actual and predicted values [40]. Therefore, this model can be used for optimizing the PAHs reduction using Mg/ethanol system. Depending on Figure 2.5, the optimum conditions for anthracene reduction are 30 mg of Mg, 60  $\mu$ L of glacial acetic acid and a reaction time of 30 min. The result of the GC-FID analysis of the anthracene before and after the reaction using Mg catalyzed by glacial acetic acid at the optimum conditions mentioned above is shown in Figure 2.6. Clearly, the anthracene reduction using Mg catalyzed by glacial acetic acid gives the 9,10-dydranthracene as the main product, which is also reported in the literature [28].

**Table 2.3.** Central composite design using the 3 significant factors at 3 levels for optimizing the anthracene reduction.

<b>Factor</b>		<b>Level</b>		
		Low (-1)	Medium (0)	High (+1)
Mg (mg)		10	20	30
Glacial acetic acid (μL)		10	35	60
Time (min)		30	105	180
#	Mg	Glacial acetic acid	Time	Removal (%) <sup>b</sup>
1	0	0	0	78.0
2	-1	+1	-1	60.0
3	0	0	0	75.0
4	0	0	-1	65.1
5	+1	+1	+1	98.5
6	0	0	0	65.0
7	0	-1	0	61.0
8	-1	-1	-1	42.0
9	-1	+1	+1	78.7
10	-1	-1	+1	50.0
11	0	+1	0	80.0
12	+1	0	0	84.0
13	0	0	+1	90.0
14	-1	0	0	65.0
15	+1	+1	-1	98.0
16	+1	-1	+1	74.4
17	+1	-1	-1	59.8

<sup>b</sup> The mean of three experiments, RSD% < 3.0%.

**Table 2.4.** ANOVA for response surface quadratic model of anthracene reduction.

<b>Source</b>	<b>Sum of Squares</b>	<b>df</b>	<b>Mean Square</b>	<b>F Value</b>	<b>p-value Prob &gt; F</b>	
Model	3601.67	9	400.19	7.94	0.0061	significant
Mg (A)	1416.10	1	1416.10	28.10	0.0011	
Glacial acetic acid (B)	1638.40	1	1638.40	32.51	0.0007	
Time (C)	446.22	1	446.22	8.86	0.0206	
AB	30.42	1	30.42	0.60	0.4626	
AC	16.82	1	16.82	0.33	0.5815	
BC	1.45	1	1.45	0.029	0.8703	
A <sup>2</sup>	1.913E-004	1	1.913E-004	3.797E-006	0.9985	
B <sup>2</sup>	43.05	1	43.05	0.85	0.3861	
C <sup>2</sup>	23.98	1	23.98	0.48	0.5125	
Residual	352.73	7	50.39			
Lack of Fit	286.06	5	57.21	1.72	0.4077	not significant
Pure Error	66.67	2	33.33			
Cor Total	3954.40	16				

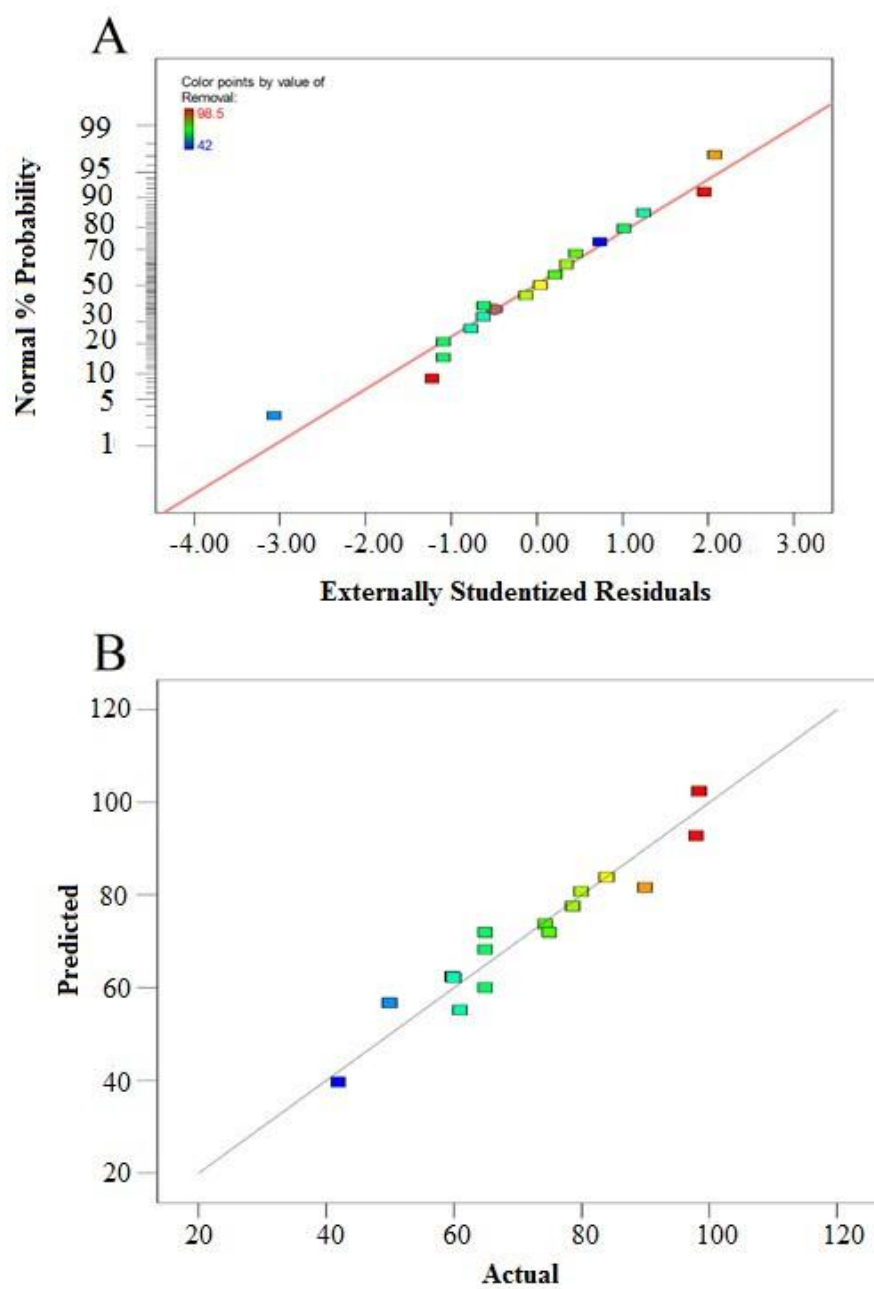


**Figure 2.4.** Normal plot of residuals (A) and predicted vs. actual values (B) of anthracene reduction in the optimization stage of the designed experiment.

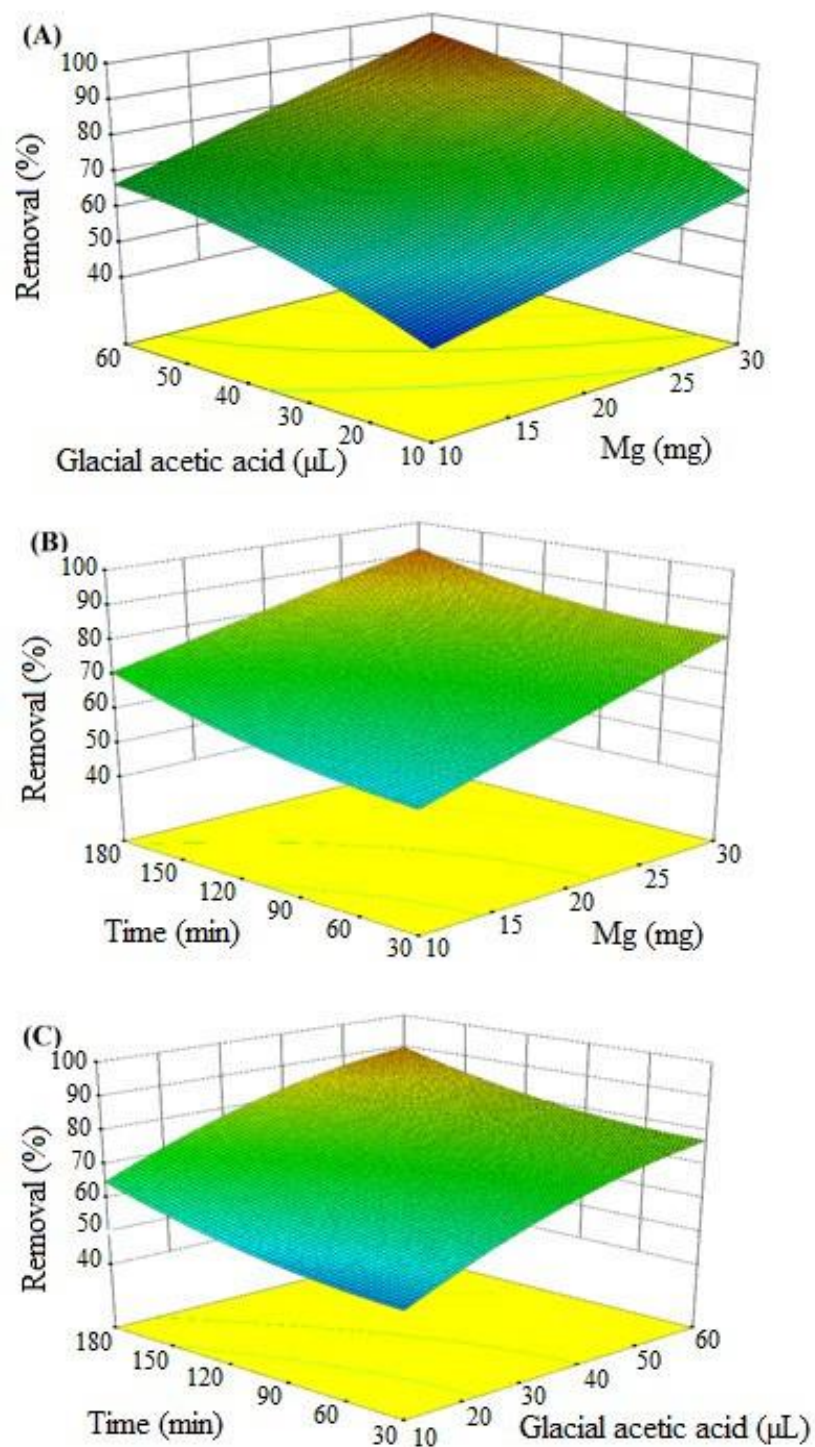


**Figure 2.5.** (A) Effect of glacial acetic acid and magnesium (Mg), at constant reaction time (105 min), (B) time and Mg at constant volume of glacial acetic acid (35  $\mu\text{L}$ ), and (C) time and glacial acetic acid at constant amount of Mg (20 mg) on anthracene reduction.

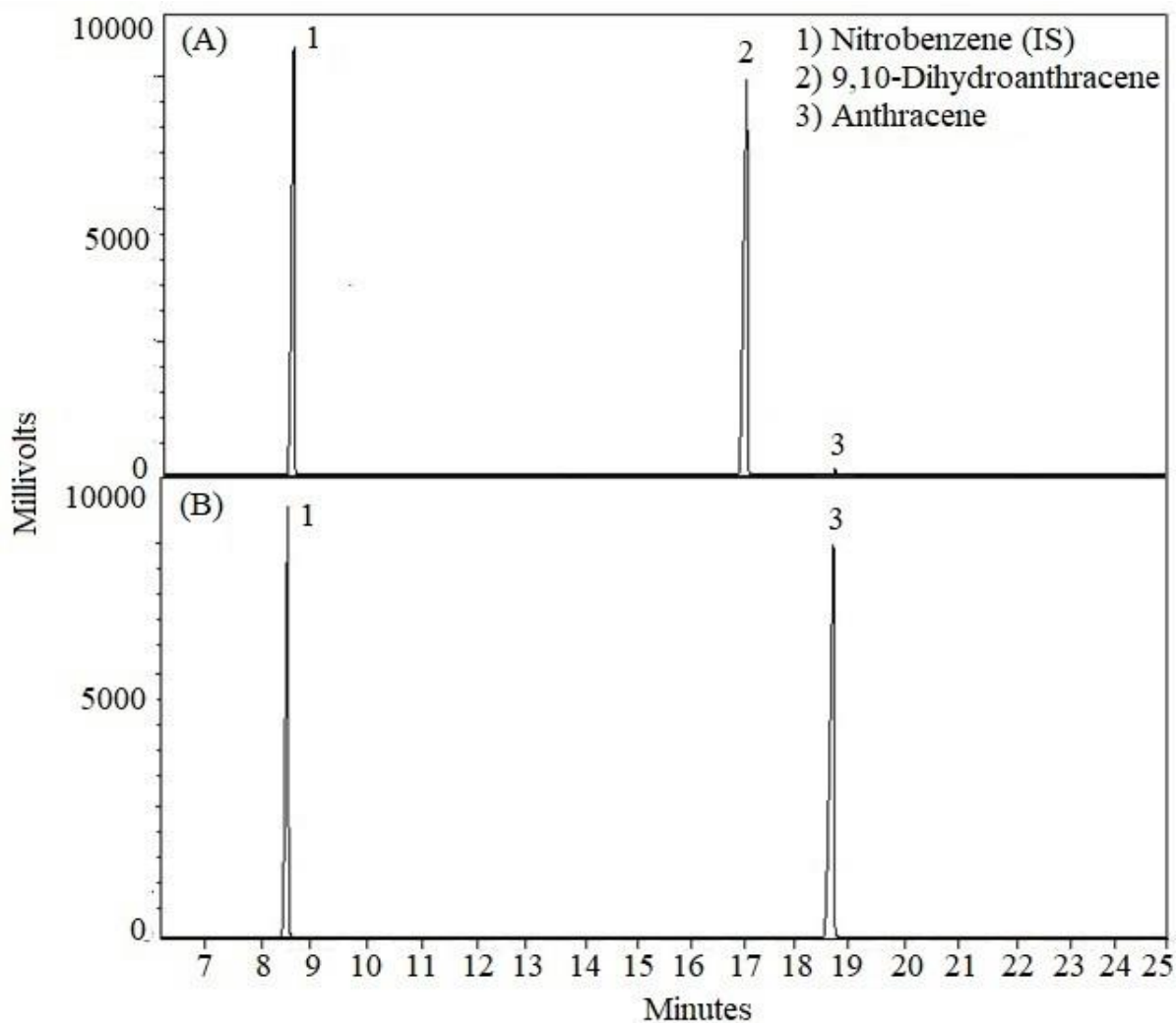


**Figure 2.6.** GC-FID analysis of anthracene (A) and the reaction product of anthracene reduction using Mg/EtOH system (B). The reaction conditions: 30 mg Mg concentration, 60  $\mu$ L glacial acetic acid volume, 30 min exposure time, and  $C_i$  of anthracene is 250 ppm.

### 2.3.5. Optimization of coal tar reduction

The coal tar used in this study consists mainly of light PAHs such as naphthalene, phenanthrene, fluoranthene, and pyrene (Figure 2.7 and Table 2.5). The concentration of these PAHs extracted from the coal tar using anhydrous ethanol was determined using standard calibration curves and their concentrations are listed in Table 2.3.

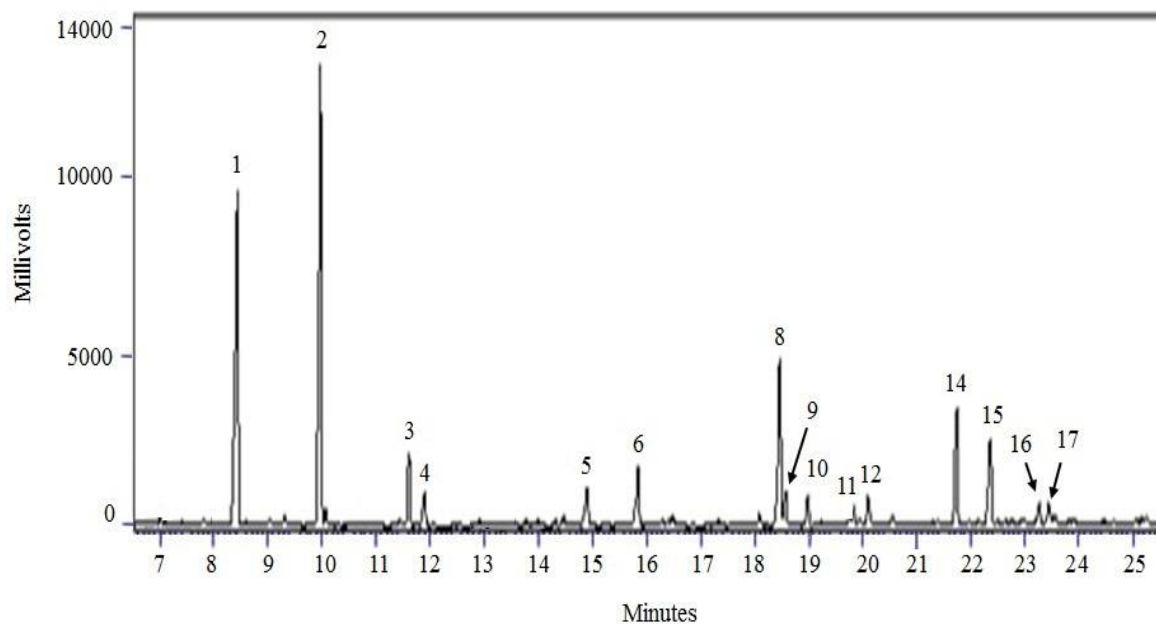


**Figure 2.7.** Chromatogram of GC-FID analysis of coal tar soluble in anhydrous ethanol. 0.400 g coal tar dissolved in 60 mL of anhydrous ethanol. Approximately, 66% of coal tar dissolved. Peak numbers correspond to compounds listed in Table 5.

**Table 2.5.** PAH compounds identified in anhydrous ethanol extract of coal tar before and after reduction.

Peak no. <sup>c</sup>	Compound name	Conc. in coal tar (ppm) <sup>d</sup>
1	Nitrobenzene (Internal standard)	NA
2	Naphthalene	1823
3	2-Methylnaphthalene	120
4	1-Methylnaphthalene	113
5	Acenaphthene	160
6	Fluorene	192
7	9,10-Dihydroanthracene	NA
8	Phenanthrene	631
9	Anthracene	130
10	Carbazole	110
11	9-Methylanthracene	102
12	4H-cyclopenta[def]phenanthrene	115
13	3,10b-dihydrofluoranthene	NA
14	Fluoranthene	370
15	Pyrene	300
16	Benz[a]anthracene	130
17	Chrysene	110

<sup>c</sup> Peak numbers refer to peaks in chromatograms in Figures 2.7 and 2.8.

<sup>d</sup> RSD% < 5%, n=3.

The use of the optimum conditions from the anthracene reduction experiments was found to be insufficient for obtaining high removal of some of PAHs in the coal tar because it includes multiple PAHs. Using 30 mg of Mg and 60  $\mu$ L of glacial acetic acid gave 56% removal of anthracene and 89% removal of fluoranthene. The sum of the concentrations of anthracene and fluoranthene in coal tar is close to 500 ppm. Therefore, a double dosage of reagents (Mg powder + glacial acetic acid) was added to the anhydrous ethanol extract of

coal tar to increase the PAH removal. Thus, increasing the dosage to 60 mg of Mg powder and to 120  $\mu\text{L}$  of glacial acetic acid increases the anthracene removal to 89% and fluoranthene to 90%. Triple dosage (90 mg of Mg powder + 180  $\mu\text{L}$  glacial acetic acid) did not show any improvement of PAH degradation (Figures 2.8 and 2.9).

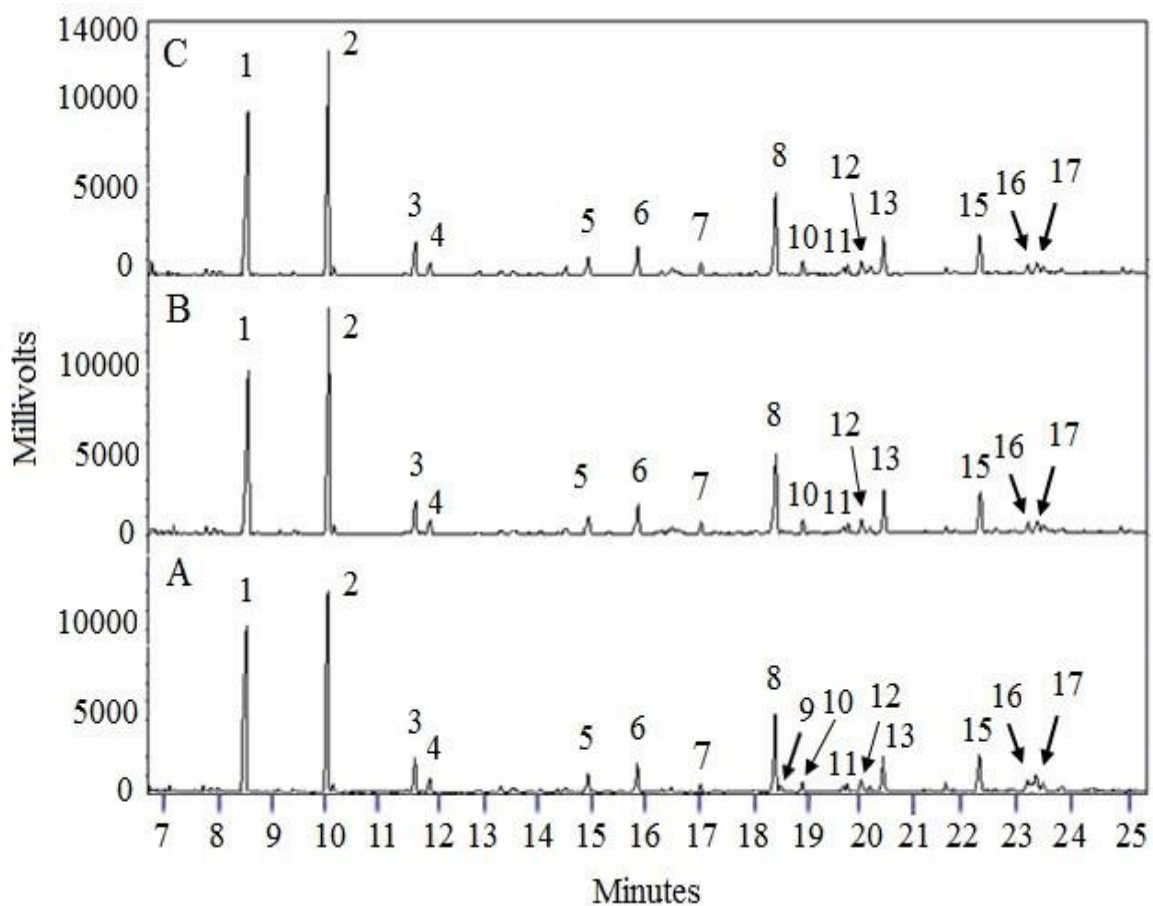


**Figure 2.8.** Chromatogram of GC-FID analysis of reduction of coal tar soluble in anhydrous ethanol using Mg catalyzed by glacial acetic acid under the conditions (A, B, and C) listed in Table 2.6. Peak numbers correspond to compounds listed in Table 2.5.

**Table 2.6.** Reaction conditions used for PAHs reduction in coal tar.

Condition	Mg powder (mg)	Glacial acetic acid ( $\mu\text{L}$ )	Time (h)
A	30	60	0.5
B	60	120	0.5
C	90	180	0.5

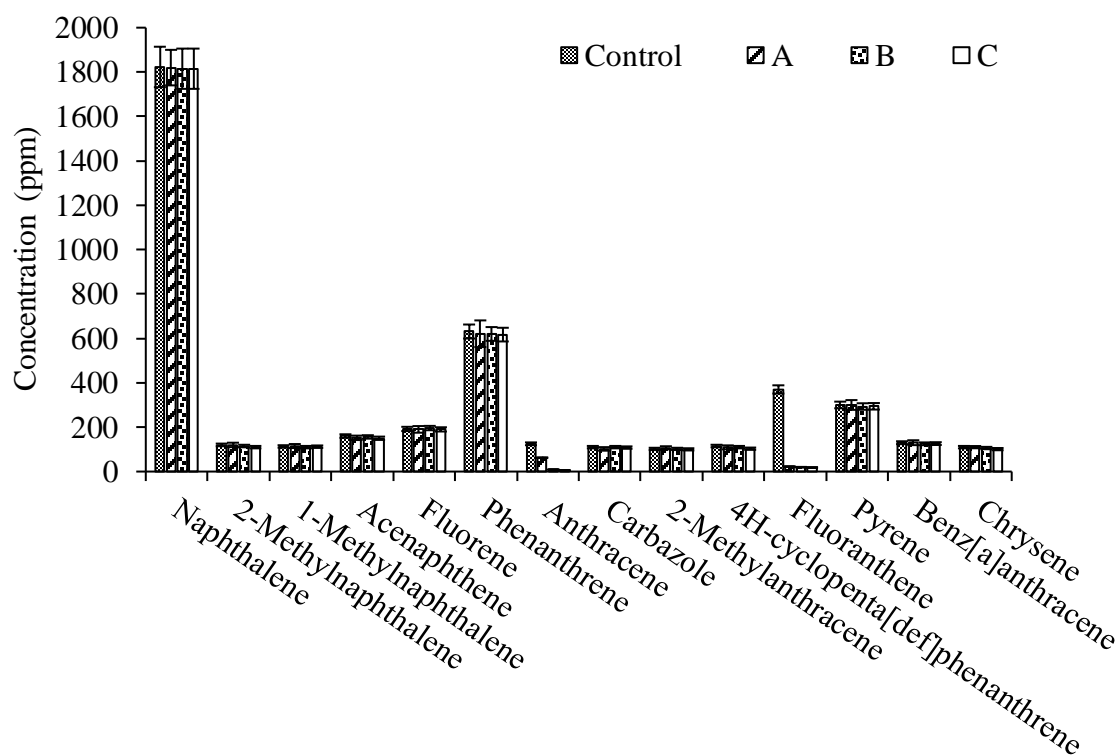


**Figure 2.9.** Evaluation of Mg powder catalyzed by glacial acetic acid in anhydrous ethanol for PAHs reduction in coal tar at room temperature. Reaction conditions (A, B, and C) are listed in Table 2.6. Error bars represents RSD%, n=3.

The reduction of PAHs using activated Mg and anhydrous ethanol is selective, since only anthracene (9) and fluoranthene (14) in the coal tar were reduced with high removal %. The main product from anthracene and fluoranthene are 9,10-dihydroanthracene and 2,3-dihydrofluoranthene, respectively. The light PAHs such as naphthalene, 2-methylnaphthalene, 1-methylnaphthalene, phenanthrene, and pyrene were not reduced by the anhydrous ethanol with Mg catalyzed by glacial acetic acid under the conditions used. The current reaction conditions can be described as being mild conditions, therefore reduction of the light PAHs (naphthalene, 2-methylnaphthalene, and 1-methylnaphthalene) requires harsher conditions, or coordination of these PAHs with iron cyclopentadienyl cation to be reduced [41].

## 2.4. Conclusions

Activated Mg with anhydrous ethanol is an effective system to convert some of the PAHs (e.g., anthracene and fluoranthene) to hydrogenated PAHs with high removal (~ 90%) during a relatively short time (30 min). The experimental design approach is a useful methodology that can be used to optimize the PAH reduction using activated Mg and anhydrous ethanol. The PAH reduction is mainly affected by three factors: Mg powder dosage, glacial acetic acid volume, and reaction time. The order of these factors from the highest to the lowest significant effect is as follows: Mg powder dosage > glacial acetic acid volume > time. The products from PAH reduction are less toxic compared to their parent compounds. Therefore, Mg activated by glacial acetic acid with anhydrous ethanol can be considered as a promising route for environmental remediation for the removal of PAHs from PAH contaminated coal tar.

## 2.5. References

- [1] Lamichhane, S.; Bal Krishna, K. C.; Sarukkalige, R. Polycyclic Aromatic Hydrocarbons (PAHs) Removal by Sorption: A Review. *Chemosphere* **2016**, *148*, 336–353.
- [2] Bautista, L. F.; Morales, G.; Sanz, R. Biodegradation of Polycyclic Aromatic Hydrocarbons (PAHs) by Laccase from *Trametes Versicolor* Covalently Immobilized on Amino-Functionalized SBA-15. *Chemosphere* **2015**, *136*, 273–280.
- [3] Loppi, S.; Pozo, K.; Estellano, V. H.; Corsolini, S.; Sardella, G.; Paoli, L. Accumulation of Polycyclic Aromatic Hydrocarbons by Lichen Transplants: Comparison with Gas-Phase Passive Air Samplers. *Chemosphere* **2015**, *134*, 39–43.
- [4] Zhao, O.; Zhang, X.; Feng, S.-D.; Zhang, L.-X.; Shi, W.; Yang, Z.; Chena, M.-M.; Fanga, X.-D. Starch-Enhanced Degradation of HMW PAHs by *Fusarium* Sp. in an Aged Polluted Soil from a Coal Mining Area. *Chemosphere* **2017**, *174*, 774–780.
- [5] Xu, J.; Wang, H.; Sheng, L.; Liu, X.; Zheng, X. Distribution Characteristics and Risk Assessment of Polycyclic Aromatic Hydrocarbons in the Momoge Wetland, China. *Int. J. Environ. Res. Public Health* **2017**, *14*, 85.
- [6] Zheng, B.; Wang, L.; Lei, K.; Nan, B. Distribution and Ecological Risk Assessment of Polycyclic Aromatic Hydrocarbons in Water, Suspended Particulate Matter and Sediment from Daliao River Estuary and the Adjacent Area, China. *Chemosphere* **2016**, *149*, 91–100.
- [7] Bezza, F. A.; Chirwa, E. M. N. The Role of Lipopeptide Biosurfactant on Microbial Remediation of Aged Polycyclic Aromatic Hydrocarbons (PAHs)-Contaminated Soil. *Chem. Eng. J.* **2017**, *309*, 563–576.
- [8] Nelkenbaum, E.; Dror, I.; Berkowitz, B. Reductive Hydrogenation of Polycyclic Aromatic Hydrocarbons Catalyzed by Metalloporphyrins. *Chemosphere* **2007**, *68*, 210–217.
- [9] Yuan, T.; Fournier, A. R.; Proudlock, R.; Marshall, W. D. Continuous Catalytic Hydrogenation of Polyaromatic Hydrocarbon Compounds in Hydrogen-Supercritical Carbon Dioxide. *Environ. Sci. Technol.* **2007**, *41*, 1983–1988.
- [10] Hiyoshi, N.; Osada, M.; Rode, C. V.; Sato, O.; Shirai, M. Hydrogenation of Benzothiophene-Free Naphthalene over Charcoal-Supported Metal Catalysts in Supercritical Carbon Dioxide Solvent. *Appl. Catal. A Gen.* **2007**, *331*, 1–7.
- [11] Abu-Reziq, R.; Avnir, D.; Miloslavski, I.; Schumann, H.; Blum, J. Entrapment of Metallic Palladium and a rhodium(I) Complex in a Silica Sol-Gel Matrix: Formation of a Highly Active Recyclable Arene Hydrogenation Catalyst. *J. Mol. Catal. A Chem.* **2002**, *185*, 179–185.
- [12] Yuan, T.; Marshall, W. D. Catalytic Hydrogenation of Polycyclic Aromatic

- Hydrocarbons over Palladium-Al<sub>2</sub>O<sub>3</sub> under Mild Conditions. *J. Hazard. Mater.* **2005**, *126*, 149–157.
- [13] Jacinto, M. J.; Santos, O. H. C. F.; Landers, R.; Kiyohara, P. K.; Rossi, L. M. On the Catalytic Hydrogenation of Polycyclic Aromatic Hydrocarbons into Less Toxic Compounds by a Facile Recoverable Catalyst. *Appl. Catal. B Environ.* **2009**, *90*, 688–692.
- [14] Segawa, Y.; Stephan, D. W. Metal-Free Hydrogenation Catalysis of Polycyclic Aromatic Hydrocarbons. *Chem. Commun.* **2012**, *48*, 11963–11965.
- [15] Bresó-Femenia, E.; Chaudret, B.; Castillon, S. Selective Catalytic Hydrogenation of Polycyclic Aromatic Hydrocarbons Promoted by Ruthenium Nanoparticles. *Catal. Sci. Technol.* **2015**, *5*, 2741–2751.
- [16] Nador, F.; Moglie, Y.; Vitale, C.; Yus, M.; Alonso, F.; Radivoy, G. Reduction of Polycyclic Aromatic Hydrocarbons Promoted by Cobalt or Manganese Nanoparticles. *Tetrahedron* **2010**, *66*, 4318–4325.
- [17] Baikenov, M. I.; Baikenova, G. G.; Sarsembayev, B. S.; Tateeva, A. B.; Tusipkhan, A.; Matayeva, A. Z. Influence of Catalytic Systems on Process of Model Object Hydrogenation. *Int. J. Coal Sci. Technol.* **2014**, *1*, 88–92.
- [18] Schüth, C.; Reinhard, M. Hydrodechlorination and Hydrogenation of Aromatic Compounds over Palladium on Alumina in Hydrogen-Saturated Water. *Appl. Catal. B Environ.* **1998**, *18*, 215–221.
- [19] Zhang, D.; Zhao, J.; Zhang, Y.; Lu, X. Catalytic Hydrogenation of Phenanthrene over NiMo/Al<sub>2</sub>O<sub>3</sub> Catalysts as Hydrogen Storage Intermediate. *Int. J. Hydrogen Energy* **2016**, *41*, 11675–11681.
- [20] Birch, A. J. Reduction by Dissolving Metals. *J. Chem. Soc.* **1942**, 430, 430–436.
- [21] Donohoe, T. J.; Garg, R.; Stevenson, C. A. Prospects for Stereocontrol in the Reduction of Aromatic Compounds. *Tetrahedron Asymmetry* **1996**, *7*, 317–344.
- [22] Costanzo, M. J.; Patel, M. N.; Petersen, K. A.; Vogt, P. F. Ammonia-Free Birch Reductions with Sodium Stabilized in Silica Gel, Na-SG(I). *Tetrahedron Lett.* **2009**, *50*, 5463–5466.
- [23] Lee, G.; Youn, I.; Choi, E.; Lee, H.; Yon, G.; Yang, H.; Pak, C. Magnesium in Methanol (Mg/MeOH) in Organic Syntheses. *Curr. Org. Chem.* **2004**, *8*, 1263–1287.
- [24] Saitta, E. K. H.; Gittings, M. J.; Clausen, C.; Quinn, J.; Yestrebky, C. L. Laboratory Evaluation of a Prospective Remediation Method for PCB-Contaminated Paint. *J. Environ. Heal. Sci. Eng.* **2014**, *12*, 1–5.
- [25] Maloney, P.; DeVor, R.; Novaes-Card, S.; Saitta, E.; Quinn, J.; Clausen, C. A.; Geiger, C. L. Dechlorination of Polychlorinated Biphenyls Using Magnesium and

Acidified Alcohols. *J. Hazard. Mater.* **2011**, *187*, 235–240.

- [26] Brinckerhoff, P.; Grid, N.; Holdings, P. Method statement: Coal tar sampling [https://www.academia.edu/7404269/Coal\\_Tar\\_Sampling\\_Methodology](https://www.academia.edu/7404269/Coal_Tar_Sampling_Methodology) (accessed July 20, 2017).
- [27] Elie, M. R.; Clausen, C. A.; Geiger, C. L. Reduction of Benzo[a]pyrene with Acid-Activated Magnesium Metal in Ethanol: A Possible Application for Environmental Remediation. *J. Hazard. Mater.* **2012**, *203*, 77–85.
- [28] Elie, M. R. G. Use of Anactivated Magnesium/cosolvent System for the Desorption and Degradation of Polycyclic Aromatic Hydrocarbons and Thier Oxygenated, Ph.D. Dissertation, University of Central Florida, Gainesville, FL, 2012.
- [29] Gan, G.; Liu, J.; Zhu, Z.; Yang, Z.; Zhang, C.; Hou, X. A Novel Magnetic Nanoscaled Fe<sub>3</sub>O<sub>4</sub>/CeO<sub>2</sub> Composite Prepared by Oxidation-Precipitation Process and Its Application for Degradation of Orange G in Aqueous Solution as Fenton-like Heterogeneous Catalyst. *Chemosphere* **2017**, *168*, 254–263.
- [30] Montgomery, D. C. *D Esign and Analysis of Experiments*, 8th Ed.; John Wiley and Sons Inc.: Arizona, USA, 2013.
- [31] Bartley, J. K.; Xu, C.; Lloyd, R.; Enache, D. I.; Knight, D. W.; Hutchings, G. J. Simple Method to Synthesize High Surface Area Magnesium Oxide and Its Use as a Heterogeneous Base Catalyst. *Appl. Catal. B Environ.* **2012**, *128*, 31–38.
- [32] Herman G. Rechy. *Grignard Reagents New Developments*, 1st ed.; John Wiely and Sons Inc.: New York, USA, 2000.
- [33] Lee, Ge Hyeong; Choi, Eun Bok; Lee, Eun; Pack, C. S. An Efficient Desulfonylation Method Mediated by Magnesium in Ethanol. *Tetrahedron Lett.* **1993**, *34*, 4541–4542.
- [34] Tilstam, U.; Weinmann, H. Activation of Mg Metal for Safe Formation of Grignard Reagents on Plant Scale. *Org. Process Res. Dev.* **2002**, *6*, 906–910.
- [35] Zhang, X.; Zhang, Y.; Ma, Q. Y.; Dai, Y.; Hu, F. P.; Wei, G. B.; Xu, T. C.; Zeng, Q. W.; Wang, S. Z.; Xie, W. D. Effect of Surface Treatment on the Corrosion Properties of Magnesium-Based Fibre Metal Laminate. *Appl. Surf. Sci.* **2017**, *396*, 1264–1272.
- [36] Wittayarak, I.; Imyim, A.; Wongravee, K. Simultaneous Removal of As(III) and As(V) from Wastewater by Co-Precipitation Using an Experimental Design Approach. *Desalin. Water Treat.* **2016**, *57*, 16571–16582.
- [37] Muangthai, I.; Ratanatamsakul, C.; Lu, M. Removal of 2,4-Dichlorophenol By Fluidized-Bed Fenton Process. *Sustain. Environ. Res.* **2010**, *20*, 325–331.
- [38] Venny; Gan, S.; Ng, H. K. Modified Fenton Oxidation of Polycyclic Aromatic Hydrocarbon (PAH)-Contaminated Soils and the Potential of Bioremediation as Post-Treatment. *Sci. Total Environ.* **2012**, *419*, 240–249.

- [39] Draper, N. R.; Smith, H. *Applied Regression Analysis*, 1st ed.; John Wiley & Sons Inc: Hoboken, 1966.
- [40] Fan, M.; Li, T.; Hu, J.; Cao, R.; Wu, Q.; Wei, X.; Li, L.; Shi, X.; Ruan, W. Synthesis and Characterization of Reduced Graphene Oxide-Supported Nanoscale Zero-Valent Iron (nZVI/rGO) Composites Used for Pb (II) Removal. *Materials Basel*. **2016**, *9* (8).
- [41] Masterson, D. S.; Tratz, C. M.; Behrens, B. A.; Glatzhofer, D. T. Hydrogenation of Iron (II) Cationic Complexes of Naphthalene and Methyl-Substituted Naphthalenes. *Organometallics* **2000**, *19*, 244–249.

## Chapter 3

### Oxidation of coal tar: Fenton's reagent vs. peroxyacetic acid/H<sub>2</sub>SO<sub>4</sub><sup>2</sup>

---

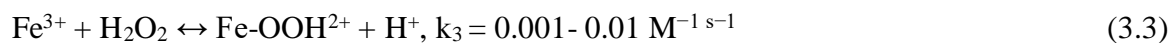
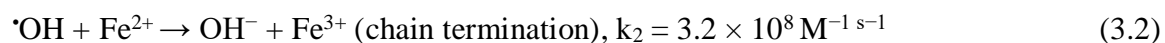
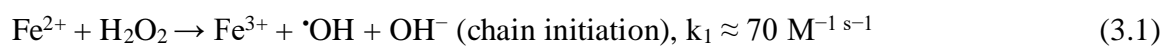
<sup>2</sup> This chapter was submitted to *Environmental Pollution*.

## Abstract

Coal tar ponds containing large amounts of polycyclic aromatic hydrocarbons (PAHs) are major environmental hazards. The study investigated, for the first time, the removal of PAH constituents of coal tar by chemical oxidation, thus anthracene was used as a model compound to optimize the reaction conditions for Fenton chemistry and in situ-generated peroxyacetic acid before applying the optimized conditions to real coal tar samples. The effects of H<sub>2</sub>O<sub>2</sub> dosage, Fe<sup>2+</sup> dosage, temperature, and time on the Fenton oxidation of anthracene in ethanol (250 ppm) were investigated using an experimental design methodology. The results indicate that the optimum conditions for anthracene oxidation are 45 °C, 0.5 h reaction time, 350 µL of 30% H<sub>2</sub>O<sub>2</sub> (~6.0 % w/w), and 250 µL of 0.50 mol/L Fe<sup>2+</sup> (~0.4 % w/w). In addition, oxidation of anthracene using peroxyacetic acid/H<sub>2</sub>SO<sub>4</sub> was achieved using a 5:5:5:1 (v/v/v/v) solution of H<sub>2</sub>O<sub>2</sub>, glacial acetic acid (CH<sub>3</sub>COOH)/deionized water (DI)/sulfuric acid (H<sub>2</sub>SO<sub>4</sub>). The effects of temperature (20-60 °C) and time (0.5-4.0 h) on anthracene oxidation using peroxyacetic acid/H<sub>2</sub>SO<sub>4</sub> was studied using a central composite design. The optimized conditions for anthracene oxidation using Fenton's reagent, and with that of peroxyacetic acid were then employed with coal tar (ΣPAHs = 4,400 ppm). It was found that double dosages of Fenton's reagent or peroxyacetic acid were required to observe any removal of PAHs from the coal tar. Anthracene, pyrene, and carbazole were highly oxidized while the lighter PAHs such as naphthalene, 2-methylnaphthalene, 1-methylnaphthalene, and phenanthrene showed less removal.

### 3.1. Introduction

Polycyclic aromatic hydrocarbons (PAHs) are environmental pollutants produced from the incomplete combustion of fossil fuels, e.g., coal and oil [1]. PAHs are the main components of coal tar, which is a by-product from the pyrolysis of coal to form coke for steelmaking, and in past practices, the hot tar would be disposed of in landfills and ponds [2]. PAHs are hydrophobic, highly stable in the environment, and many are toxic, carcinogenic, cytotoxic, teratogenic and mutagenic [3]. Degradation of PAHs has become an environmental concern [4] and advanced oxidation processes (AOPs), which produce hydroxyl radicals ( $\cdot\text{OH}$ ) [5], are useful methods to degrade most organic pollutants without producing significant amount of hazardous wastes or transferring pollutants from one phase to another (e.g., precipitation and adsorption) [6]. Furthermore, AOPs are effective for the decarcinogenation of some PAHs, such as pyrene by converting them into different products (e.g.,  $\text{CO}_2$ , monohydroxypyrene, and 1,2-, 1,6-, or 1,8-pyrenedione) [7]. Ferrarese et al. [8] have demonstrated that chemical oxidation combined with bioremediation greatly enhances the biodegradability of PAHs. Several reagents, such as potassium permanganate ( $\text{KMnO}_4$ ), hydrogen peroxide ( $\text{H}_2\text{O}_2$ ), ferrous ( $\text{Fe}^{2+}$ )-activated persulfate, and peroxy-acids can be used to achieve chemical oxidation of PAHs [9]. Compared to other AOPs (e.g., ozonation, photocatalysis, and plasma oxidation) [6], Fenton oxidation has clear advantages, such as low cost, relatively fast reaction times, and safe and simple operating principles [10,11]. The initial step in classical Fenton oxidation is the reaction between  $\text{Fe}^{2+}$  and  $\text{H}_2\text{O}_2$  to produce  $\cdot\text{OH}$ , and the terminal step is the reaction between  $\cdot\text{OH}$  and  $\text{Fe}^{2+}$  (Equations 1 and 2). Other reactions also occur, such as the reaction between  $\text{Fe}^{3+}$  and  $\text{H}_2\text{O}_2$  (Equation 3.3) and the dissociation of  $\text{Fe-OOH}^{2+}$  to re-generate  $\text{Fe}^{2+}$  (Equation 3.4) [12].



Rivas [13] showed that the low cost, relatively fast Fenton reaction ( $\text{Fe}^{2+}$  and  $\text{H}_2\text{O}_2$ ) with ethanol used as a co-solvent greatly enhanced the effect of the reaction. Lee et al. [14] showed that anthracene-contaminated soil which was treated using Fenton oxidation using ethanol as a solvent reduced the total amount of anthracene by 97% after 24 h at room temperature. Lee and Hosomi [15,16] oxidized many PAHs (e.g., anthracene, benzo[a]pyrene, pyrene, acenaphthylene, acenaphthene, benz[a]anthracene, benzo[j]fluoranthene, and indeno[1,2,3-cd]pyrene) in ethanol using Fenton oxidation, which gave high removal efficacy (73-99%). However, smaller PAHs (e.g., naphthalene, fluorene, fluoranthene, phenanthrene, and benzo[b]fluoranthene in ethanol) resulted in less efficient removal (10-28%) [15]. Peroxyacetic acid formed from the reaction of acetic acid (AcOH) with hydrogen peroxide ( $\text{H}_2\text{O}_2$ ) is another promising oxidizing agent for PAH degradation. Alderman et al. (2007) used ratios of 3:5:7 (v/v/v) and 3:3:9 (v/v/v) of  $\text{H}_2\text{O}_2$ , acetic acid, and deionized water (DI), respectively, for PAH removal from PAH-contaminated soil, which approximately gave 30-50% removal efficiency of PAHs within 24 h at room temperature. Alderman and Nyman [18] also used different ratios of hydrogen peroxide to acetic acid with a catalytic amount of sulfuric acid was found to be beneficial for benzo[a]pyrene oxidation on glass beads, with 60% removal of benzo[a]pyrene within 24 h.

The current study reported herein evaluates both the use of Fenton's reagent and the use of peroxyacetic acid/H<sub>2</sub>SO<sub>4</sub> for anthracene oxidation as a surrogate for PAHs. Optimization of both methods for anthracene oxidation was determined using experimental design, for the first time, and the optimized conditions were employed for coal tar oxidation. This is the first study on the potential application of coal tar oxidation using Fenton chemistry and peroxyacetic acid/H<sub>2</sub>SO<sub>4</sub> to mitigate the environmental hazards of PAHs.

### **3.2. Materials and Methods**

#### **3.2.1. Chemicals**

Anthracene (>90%) was purchased from Alfa Aesar (USA) and was used as received. Hydrogen peroxide (30% w/v) and dichloromethane were purchased from ACP Chemicals Inc. (Montreal, Quebec, Canada). Iron(II) sulfate heptahydrate (FeSO<sub>4</sub>·7H<sub>2</sub>O) was purchased from J. T. Baker Chemical Co. (Phillipsburg, NJ, USA). Acetone and sulfuric acid were purchased from Fisher Scientific (Pittsburgh, PA, USA). Glacial acetic acid was purchased from Sigma-Aldrich (Oakville, ON, Canada). Sodium sulfite (≥ 99%) was purchased from Sigma Aldrich (St. Louis, MO, USA). Nitrobenzene (99%) used as an internal standard was purchased from Fisher Scientific (Bridgewater, NJ, USA). Anhydrous ethanol was purchased from Commercial Alcohols (Brampton, ON, Canada). All reagents and solvents were of ACS grade unless otherwise stated. Coal tar samples were collected from the Sydney Tar Ponds, Nova Scotia, Canada.

#### **3.2.2. Fenton oxidation**

In a typical experiment, a 2.0 mL aliquot of anthracene in anhydrous ethanol (250 ppm) was loaded into a 20-mL vial, and 0.15-0.25 mL of aqueous Fe<sup>2+</sup> (0.5 mol/L) was added. The Fenton oxidation of anthracene started when a suitable dosage (0.30-0.40 mL) of H<sub>2</sub>O<sub>2</sub>

(aqueous 30%) was added. The reaction vial was tightly closed and the reaction mixture was vigorously stirred in a dark place, at 20-60 °C for 0.5-3.0 h. The reaction was quenched by adding five drops of concentrated sulfuric acid. The oxidation product was extracted with 2.0 mL of dichloromethane (DCM) and 4.0 mL of deionized water. The reaction mixture was vigorously shaken for 0.5 min then left for 10 min to separate. For the Fenton oxidation of coal tar, 2.0 mL aliquots of coal tar solution and the same procedure was used. The coal tar stock solution was prepared by treating 0.400 g of coal tar in 60.0 mL anhydrous ethanol followed by sonication and filtration. Only about 66% of coal tar dissolved. The total PAH concentration in coal tar is ~4,400 ppm, which was determined using standard calibration curves using GC-FID.

### **3.2.3. Peroxyacetic acid/H<sub>2</sub>SO<sub>4</sub> oxidation**

The procedure used in the current work was based on a modified procedure from a previous study [18]. Briefly, 200 µL of anthracene stock solution in acetone (5.00 g/L) was loaded into a 25.0 mL vial. The acetone was evaporated and then 5.0 mL each of deionized water, H<sub>2</sub>O<sub>2</sub>, and glacial acetic acid, and 1.0 mL of sulfuric acid were added, respectively. The reaction vial was closed tightly, and the reaction mixture was vigorously stirred in the dark for selected time intervals (0.5-4.0 h). The reaction was quenched by adding 3.0 mL of aqueous 1.0 mol/L sodium sulfite. The reaction products were extracted by adding 4.0 mL of DCM. The mixture was vigorously shaken by hand for 0.5 min then left for 10 min to phase separate. The same procedure was used for the coal tar oxidation. The coal tar stock solution was prepared by treating 1.200 g of coal tar in 10.0 mL acetone followed by sonication and filtration. Note that only ~73% of the coal tar dissolved.

The DCM extracts of reaction solutions were analyzed using GC-FID (quantitative analysis) and GC-MS to identify the PAHs in coal tar extract. Nitrobenzene was used as an internal standard. The removal (%) was calculated using Equation 3.5 where  $C_i$  is the initial concentration and  $C_f$  is the final concentration of the PAH compound:

$$\text{Removal (\%)} = \left(1 - \frac{C_f}{C_i}\right) \times 100\% \quad (3.5)$$

### 3.2.4. GC analyses

#### *GC-MS*

An Agilent 7683 Series II instrument coupled with an Agilent 5973 mass selective detector (MSD) was used. The operational conditions of MSD were 70 eV electron ionization energy, 40-550 m/z scan range, and 250 °C mass interface temperature. The GC was equipped with a DB-5 capillary column (30 m × 0.25 mm i.d. × 0.25 μm film thickness). The carrier gas was helium with a column flow rate of 1 mL min<sup>-1</sup>. The GC oven temperature was programmed from 80 °C (1 min) to 300 °C (2 min) at a heating rate of 10 °C/min. The injection volume was 2 μL in splitless mode. Both injection port and detector temperatures were 300 °C. The mass spectra were compared with reference spectra in the NIST library.

#### *GC-FID*

Quantitative analysis was achieved using a ThermoFisher Scientific GC equipped by flame ionization (FID). The GC column and oven temperature program were the same as the GC-MS method described above; the helium pressure was 14 psi, and the sample injection volume was 2.0 μL using splitless injection mode. The inlet and the detector were at 300 °C. Calibration curve of PAHs was achieved with good linearity ( $R^2 > 0.9985$ ). Nitrobenzene was also used as an internal standard.

### 3.2.5. Experimental design

This is the first study of the application of experimental design methodology for anthracene oxidation using Fenton's reagent and peroxyacetic acid. In the case of Fenton oxidation of anthracene, this process was achieved through two sequential stages, namely screening the factors and optimization using central composite design (CCD). While in the case of anthracene oxidation using peroxyacetic acid, optimization process was achieved in one stage using CCD.

#### 3.2.5.1. Fenton oxidation of anthracene

##### *Screening variables*

As an initial stage in the experimental design for the Fenton oxidation of anthracene in anhydrous ethanol, screening of the relevant experimental factors was achieved to determine the significance level for each factor. Initially, a fractional factorial design of ( $2^{4-1}$ ) was used to investigate the effects of four factors (temperature, time, H<sub>2</sub>O<sub>2</sub> dosage, and Fe<sup>2+</sup> dosage) on the anthracene oxidation. Each factor has two levels: *low* coded by -1 and *high* coded by +1, as shown in Table 3.1. The level of each factor was chosen based on preliminary experiments and previous studies [14,19].

##### *Optimization using central composite design*

A response surface methodology (RSM) based on CCD was used to study the effect of the more significant factors on the Fenton oxidation of anthracene. The CCD introduced by Box and Wilson [20] is widely used for fitting a quadratic response surface model [21]. CCD consists of three groups of points; cube (derived from factorial design), axial, and centre points. The total number of the experiments ( $N$ ) of CCD is calculated using the

following equation (Equation 3.7), where  $k$  is the number of factors and  $C_o$  is the center points. Furthermore, the cubic and axial runs are  $2^k$  and  $2k$ , respectively [22]:

$$N=2^k + 2k + C_o \quad (3.7)$$

Table 2 shows the actual and coded values of three factors in optimization stage, where each factor has three levels; low (-1), medium (0), and high (+1).

### **3.2.5.2. Peroxyacetic acid oxidation of anthracene**

#### *Optimization using central composite design*

Based on Alderman and Nyman's work [18], a 5:5:5:1 (v/v/v/v) ratio of hydrogen peroxide, acetic acid, deionized water, and sulfuric acid, was the optimum ratio to obtain a high removal (>80%) of benzo[a]pyrene as a model compound of PAHs. Therefore, this ratio was used in the current work and further optimized by studying the effect of temperature (20-60 °C) and time (0.5-4.0 h) on PAH removal. The temperature and time ranges were selected based on preliminary experiments and a previous study [19]. The RSM based on CCD was used to study the effects of temperature and time on anthracene oxidation using peroxyacetic acid/H<sub>2</sub>SO<sub>4</sub>. The total volume of the oxidizing agent mixture (H<sub>2</sub>O<sub>2</sub>, CH<sub>3</sub>COOH, DI, and H<sub>2</sub>SO<sub>4</sub>) was 16.0 mL in a ratio of 5:5:5:1. The required experiments are listed in Table 3.4.

## **3.3. Results and discussion**

### **3.3.1. Operational conditions for Fenton oxidation**

According to preliminary experiments, the main factors that impact the Fenton oxidation of anthracene in ethanol are H<sub>2</sub>O<sub>2</sub> dosage, Fe<sup>2+</sup> dosage, temperature, and time. In addition, pH can be an important factor, as the Fenton reaction works effectively when the pH of reaction media is in the range of 2 to 4 [23]. In the current work, the pH of the reaction

mixture was 2.9, which is close to the optimum pH (~3) for Fenton oxidation, before the start of Fe<sup>3+</sup> (as Fe(OH)<sub>3</sub>) precipitation can occur [24]. Increasing the H<sub>2</sub>O<sub>2</sub> dosage increases the % removal of the starting substrate reaching the maximum because of the increase of reactive •OH radicals available in the reaction media. Thus, excess H<sub>2</sub>O<sub>2</sub> decreases the removal % due to the reaction between the reactive •OH radicals and H<sub>2</sub>O<sub>2</sub>, which produces the less reactive species (HO<sub>2</sub>•) as shown in Equation 3.8 [25,26]. The same behaviour can be observed when an excess of Fe<sup>2+</sup> is used, where Fe<sup>2+</sup> reacts with •OH radicals (Equation 3.9) [27]. The reaction between Fe<sup>2+</sup> and the hydroperoxyl radical (HO<sub>2</sub>•) involves in scavenging the HO<sub>2</sub>• radicals (Equation 3.10) [28]. Therefore, an optimum dosage of H<sub>2</sub>O<sub>2</sub> and Fe<sup>2+</sup> should be used to obtain a maximum removal % of PAHs.



Temperature is also an important factor, where increasing the temperature increases the reaction rate of the Fenton oxidation. The rate constants of •OH production and Fe<sup>2+</sup> regeneration are exponentially correlated to the reaction temperature according to the Arrhenius law [29].

### 3.3.2. Experimental design

#### 3.3.2.1. Fenton oxidation of anthracene: Screening variables

The results of the screening variables stage indicate that Fe<sup>2+</sup> has a less significant effect on the removal % of anthracene compared to the other factors studied (Table 3.1). Figure 3.1 shows the Pareto chart of the contribution of the factors on the Fenton oxidation. The bar lengths are proportional to the significance levels of each factor. Temperature, time, and

H<sub>2</sub>O<sub>2</sub> have the highest t-values, 16.75, 8.30, and 4.50, respectively. Therefore, these three factors were used in the optimization of the Fenton oxidation of anthracene conditions. Because of the presence of a significant interaction between H<sub>2</sub>O<sub>2</sub> and Fe<sup>2+</sup> (bar AB in Figure 3.1), the Fe<sup>2+</sup> dosage (250 μL) was used and kept constant in all the experiments at the optimization stage. Consequently, the order of these factors from high to low effects is as follows: temperature > time > H<sub>2</sub>O<sub>2</sub> > Fe<sup>2+</sup>.

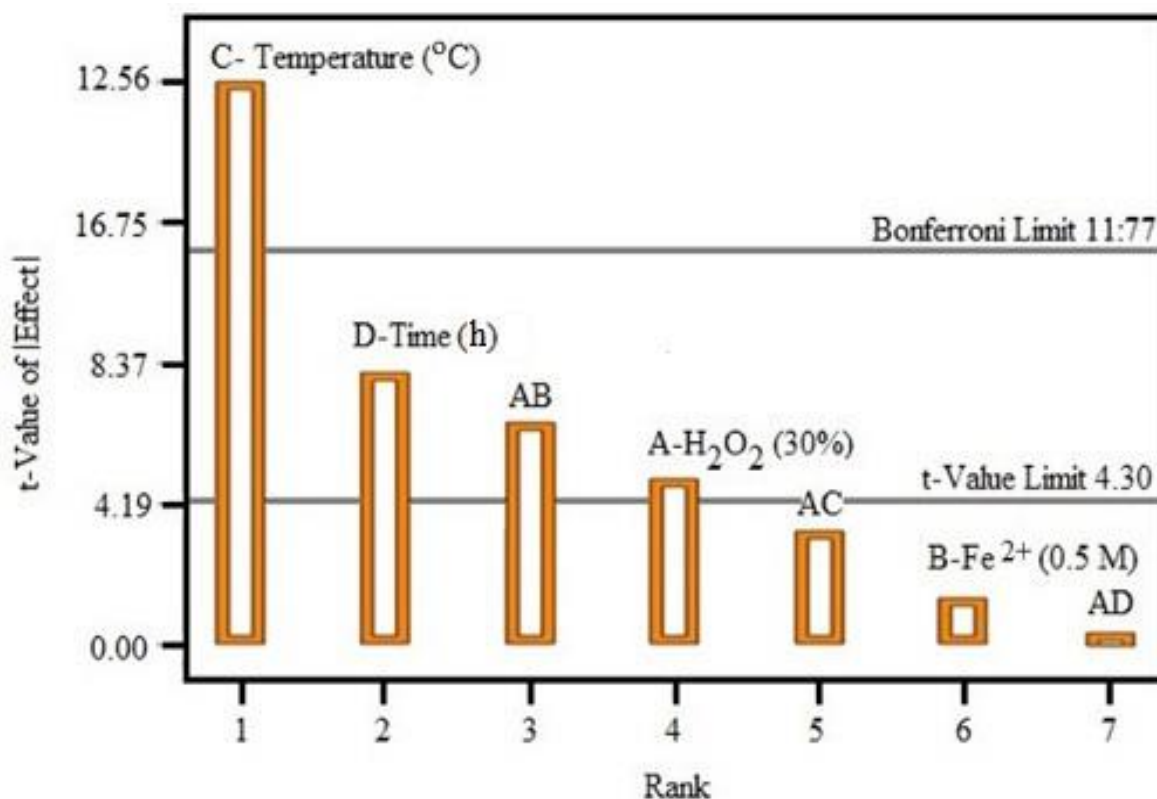
**Table 3.1.** Screening experiments for four factors using only low and high levels for Fenton oxidation of anthracene

Factor	Level	
	Low (-1)	High (+1)
H <sub>2</sub> O <sub>2</sub> (30%), (μL)	300	400
Fe <sup>2+</sup> (0.5 mol/L), (μL)	150	250
Temperature (°C)	20	60
Time (h)	0.5	3.0

Exp. #	H <sub>2</sub> O <sub>2</sub>	Fe <sup>2+</sup>	Temp	Time	Removal (%)*
1	+1	+1	-1	-1	55.8
2	+1	-1	+1	-1	93.0
3	-1	+1	+1	-1	92.1
4	+1	-1	-1	+1	81.9
5	-1	-1	+1	+1	93.0
6	-1	+1	-1	+1	68.0
7	+1	+1	+1	+1	98.0
8	-1	-1	-1	-1	35.5

\* n=3, RSD% < 2.8%.



**Figure 3.1.** Pareto chart of the four factors (from Table 3.1) affecting anthracene oxidation with Fenton's reagent.

### 3.3.2.2. Fenton oxidation of anthracene: Optimization using central composite design

The analysis of variance (ANOVA) results of the factors affecting Fenton oxidation of anthracene in anhydrous ethanol at the optimization stage (using results in Table 3.2) are shown in Table 3.3 using the quadratic model. The p-values are small ( $p < 0.05$ ) and F-values are large, indicating that these factors (temperature, time, and H<sub>2</sub>O<sub>2</sub>) are significant. In addition, the adjusted regression coefficient (Adj R<sup>2</sup>) and the prediction regression coefficient (Pred R<sup>2</sup>) are 0.9855 and 0.9465, respectively. The predicted and the actual values of the removal % (Figure 3.2-A) and the normal % probability versus the externally studentized residuals (Figure 3.2-B) distribute around the straight line. Therefore, the used model is valid and agrees well with the experimental data. The removal % of anthracene

using Fenton oxidation can be calculated using Equation 3.11, where, A: Volume of 30 % H<sub>2</sub>O<sub>2</sub> (μL) B: Temperature (°C) and C: Time (h):

$$\text{Removal \%} = 95.81 + 3.08A + 16.49B + 6.28C - 2.19AB - 0.86AC - 5.39BC - 0.99A^2 - 13.04B^2 - 2.29C^2 \quad (3.11)$$

Figure 3.3 shows the 3D-plots of the three important factors. Increasing the temperature from room temperature to 40 °C increases the removal % of anthracene from 44% to 90%. Only a slight increase in removal % can be observed when the temperature is increased to 60 °C (Figure 3.3A). The interaction between temperature with time and temperature with H<sub>2</sub>O<sub>2</sub> are significant while the interaction between time and H<sub>2</sub>O<sub>2</sub> is found to be insignificant (Table 3.3). Therefore, the temperature has the highest influence on the Fenton oxidation. Thus, the optimum conditions for obtaining a high removal % of anthracene using Fenton's reagent during a short 0.5 h reaction time are 250 μL of 0.5 mol/L Fe<sup>2+</sup> (~ 0.4 % w/w), 350 μL of 30% H<sub>2</sub>O<sub>2</sub> (~ 6.0 % w/w) at 45 °C. The oxidation products are 9,10-anthraquinone (major product) and anthrone (minor product) (Figure 3.4). 9,10-Anthraquinone has been reported in several studies as a main product from Fenton oxidation of anthracene [14,15,30].

**Table 3.2.** CCD using the 3 significant factors at 3 levels for optimizing the Fenton oxidation of anthracene. The Fe<sup>2+</sup> (0.50 mol/L) dosage is 250 μL.

	<b>Factor</b>	<b>Level</b>		
		Low (-1)	Medium (0)	High (+1)
	H <sub>2</sub> O <sub>2</sub> (30%), (μL)	300	350	400
	Temperature (°C)	20	40	60
	Time (h)	0.50	1.75	3.00
Exp. #	H <sub>2</sub> O <sub>2</sub>	Temp	Time	Removal (%)*
1	-1	-1	-1	44.2
2	+1	-1	+1	80.0
3	0	0	-1	90.0
4	-1	+1	+1	97.9
5	0	0	+1	97.1
6	+1	+1	-1	97.1
7	+1	+1	+1	97.9
8	-1	+1	-1	92.4
9	0	+1	0	97.9
10	0	0	0	96.3
11	-1	0	0	92.9
12	+1	-1	-1	56.4
13	-1	-1	+1	70.0
14	+1	0	0	96.8
15	0	0	0	95.8
16	0	-1	0	67.7
17	0	0	0	95.2

\* n=3, RSD% < 3%.

**Table 3.3.** ANOVA for optimizing the Fenton oxidation of anthracene using CCD.

<b>Source</b>	<b>Sum of Squares</b>	<b>df</b>	<b>Mean Square</b>	<b>F Value</b>	<b>p-value Prob &gt; F</b>	
Model	4400.70	9	488.97	122.01	< 0.0001	significant
(A) H <sub>2</sub> O <sub>2</sub> (μL)	94.86	1	94.86	23.67	0.0018	
(B) Temperature (°C)	2719.20	1	2719.20	678.50	< 0.0001	
(C) Time (h)	394.38	1	394.38	98.41	< 0.0001	
AB	38.28	1	38.28	9.55	0.0176	
AC	5.95	1	5.95	1.48	0.2625	
BC	232.20	1	232.20	57.94	0.0001	
A <sup>2</sup>	2.61	1	2.61	0.65	0.4461	
B <sup>2</sup>	455.40	1	455.40	113.63	< 0.0001	
C <sup>2</sup>	14.02	1	14.02	3.50	0.1036	
Residual	28.05	7	4.01			
Lack of Fit	27.45	5	5.49	18.10	0.0532	not significant
Pure Error	0.61	2	0.30			
Cor Total	4428.76	16				

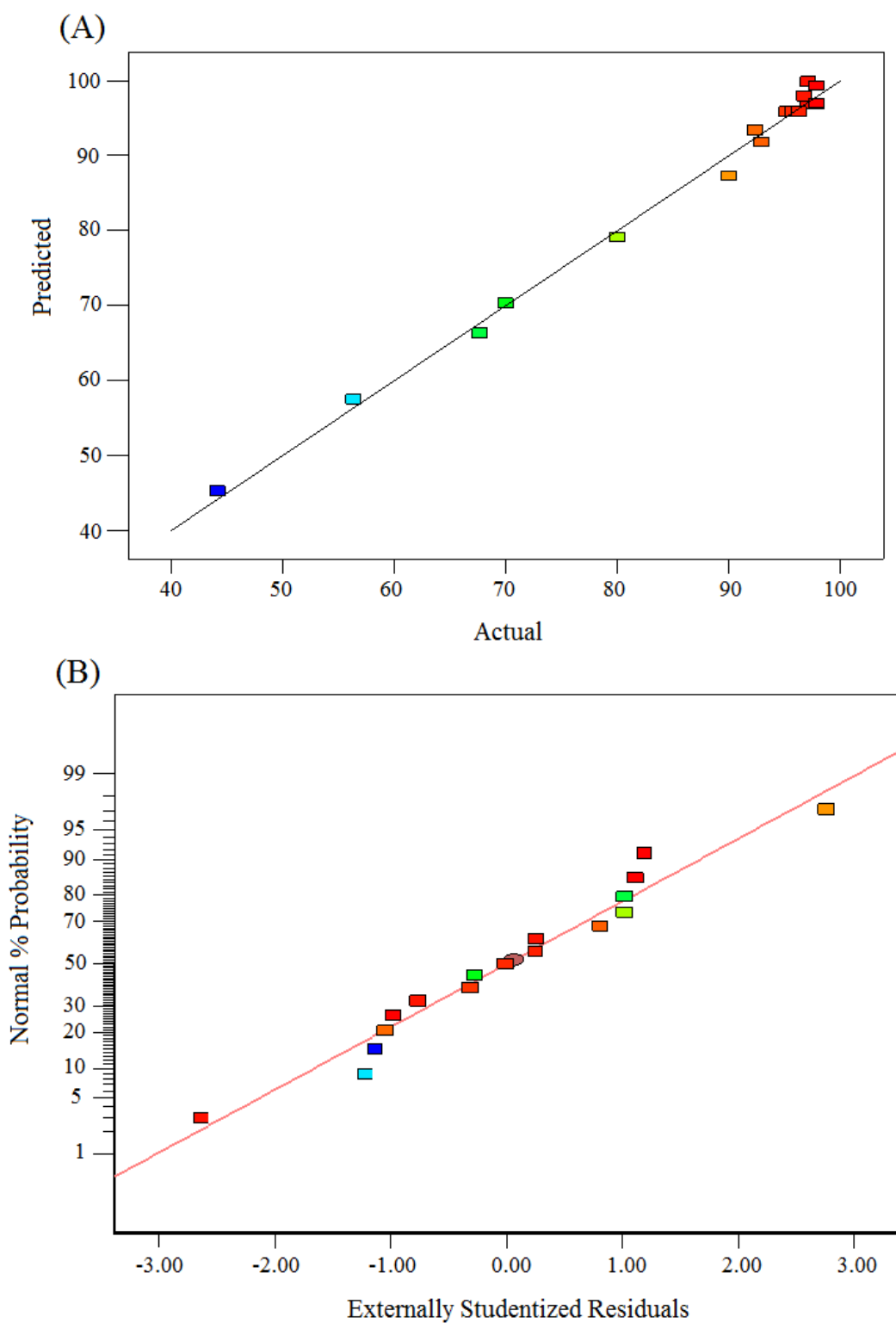


**Figure 3.2.** Predicted and actual values of anthracene removal (%) (A), and normal % probability vs. externally studentized residuals using CCD for optimizing the Fenton oxidation of anthracene in anhydrous ethanol (B).

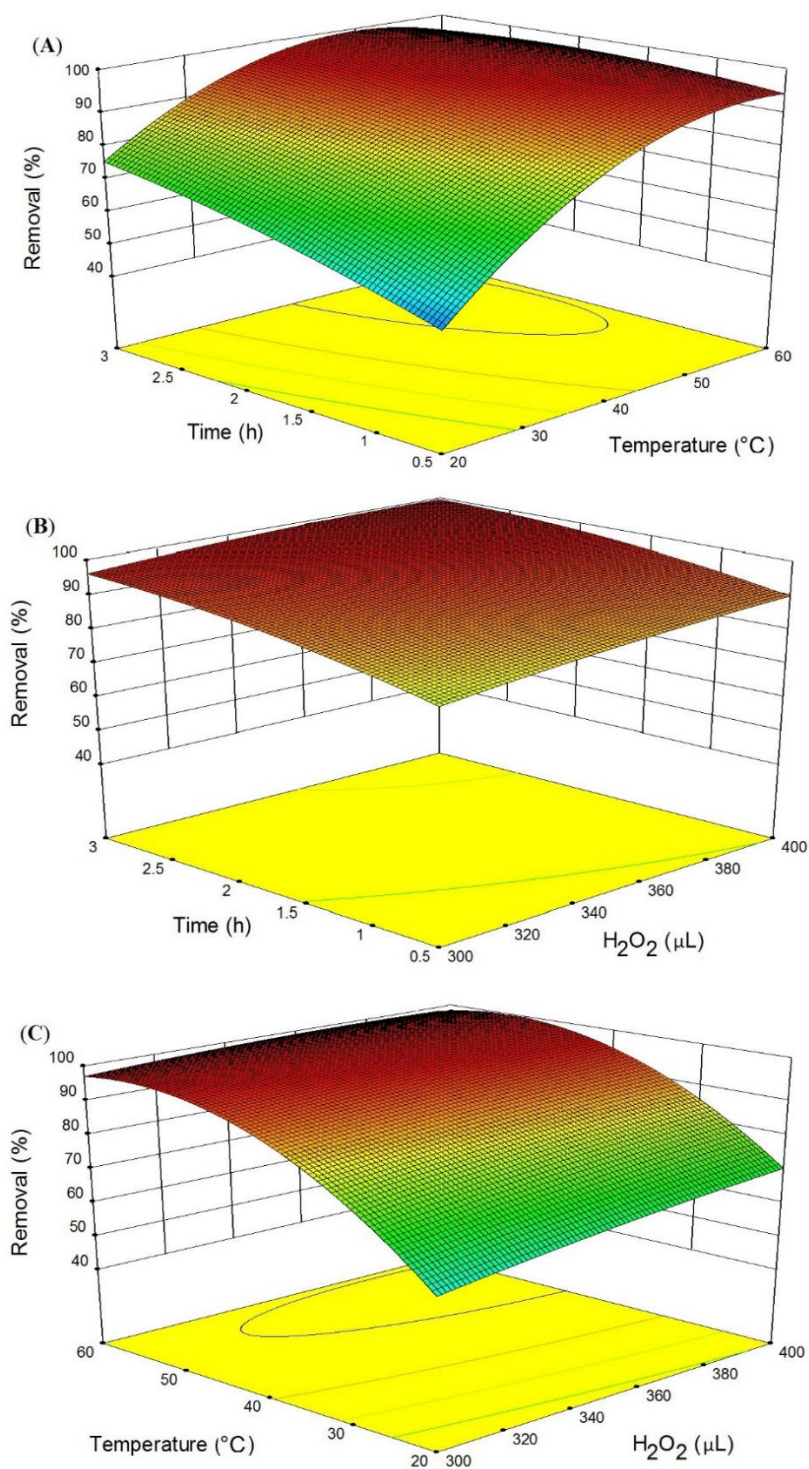


**Figure 3.3.** 3D-plots of the effect of (A) time and temperature at the constant H<sub>2</sub>O<sub>2</sub> dosage (350 μL), (B) H<sub>2</sub>O<sub>2</sub> dosage and time at constant temperature (40 °C), and (C) H<sub>2</sub>O<sub>2</sub> dosage and temperature at constant time (0.5 h) on removal % of anthracene. A constant dosage (250 μL) of Fe<sup>2+</sup> (0.50 M) was used in all experiments.

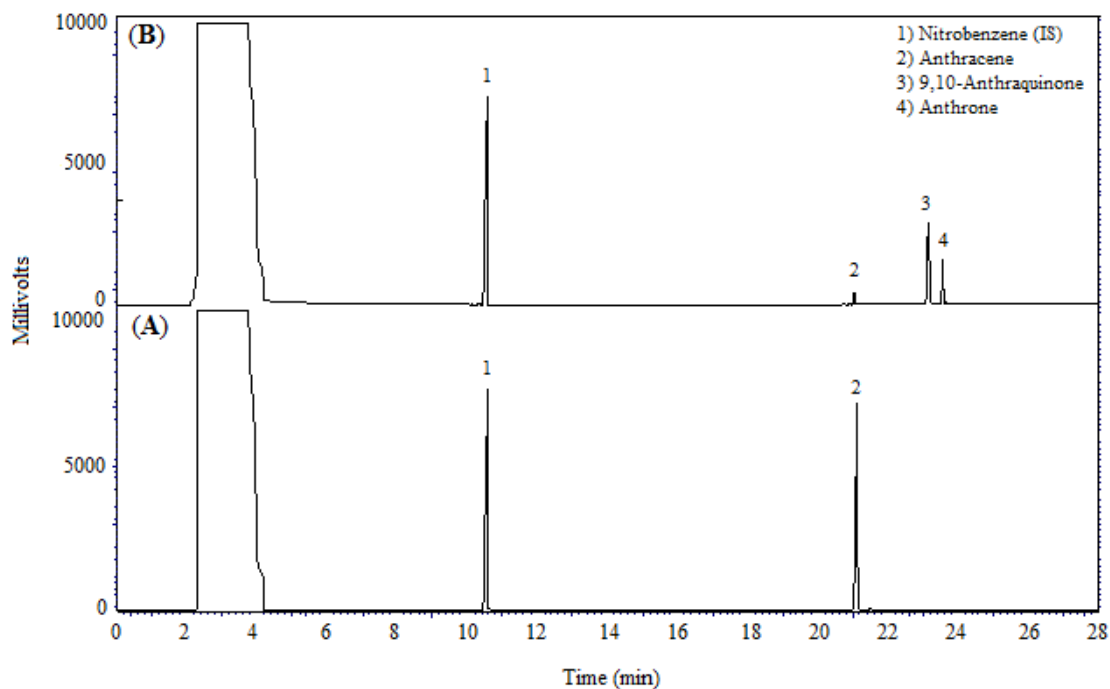


**Figure 3.4.** GC-FID chromatogram of anthracene (A), and the reaction products of Fenton oxidation of anthracene (B). Reaction conditions: 250  $\mu\text{L}$  of  $\text{Fe}^{2+}$ , 350  $\mu\text{L}$  of  $\text{H}_2\text{O}_2$ , 45  $^\circ\text{C}$ , 0.5 h, and 2.0 mL of 250 ppm of anthracene.

### 3.3.2.3. Oxidation of anthracene with peroxyacetic acid: Optimization using central composite design

The reaction of  $\text{H}_2\text{O}_2$  with  $\text{CH}_3\text{COOH}$  produces peroxyacetic acid. The rate of reaction can be accelerated using a strong acid such as sulfuric acid [31]. The proposed mechanism of the peroxyacetic acid formation in the presence of acid is described in a previous study [32]. Figure 3.5 shows the 3D-plot of anthracene oxidation using peroxyacetic acid/ $\text{H}_2\text{SO}_4$  with two variables, temperature and time. Clearly, increasing the temperature from 20 to 40  $^\circ\text{C}$  increases the removal % from 54% to 90%. Only a slight increase in removal % is observed when the temperature increases to 60  $^\circ\text{C}$ . The results of the ANOVA analysis (Table 3.5) of the experiments listed in Table 3.4 indicate that both temperature and time

have a clear effect on the removal % of anthracene, where p-values are significant ( $p < 0.05$ ). Compared to time, temperature has the highest effect ( $p < 0.0001$ ) that is due to an increase in the reaction rate [33]. The pred  $R^2$  and the adj  $R^2$  are 0.9923 and 0.9525, respectively. Therefore, the model is valid and in a good agreement with experimental data [34]. The predicted value of removal % can be calculated using Eq. 12, where A is time (h) and B is temperature ( $^{\circ}\text{C}$ ):

$$\text{Removal (\%)} = 94.7 + 7.53A + 13.53B - 8.35AB + 0.34A^2 - 9.86B^2 \quad (3.12)$$

Anthracene oxidation using peroxyacetic acid produces 9,10-anthraquinone as the major product, and 9-hydroxyanthracene as a minor product as shown in chromatogram (Figure 3.6). A proposed mechanism of this reaction is shown in Chapter 1 (Scheme 1.4). Clearly, Figure 3.5 indicates that the optimum conditions for anthracene oxidation using peroxyacetic acid are 5.0 mL of deionized water, 5.0 mL of  $\text{H}_2\text{O}_2$ , 5.0 mL of glacial acetic acid, 1.0 mL of sulfuric acid,  $45\text{ }^{\circ}\text{C}$ , and 0.5 h.

**Table 3.4.** CCD for optimizing the anthracene oxidation using peroxyacetic-acid catalyzed by sulfuric acid using two factors at 3 levels.

	Factor		Level		
	Time (h)	Temperature (°C)	Low (-1)	Medium (0)	High (+1)
			0.50	2.25	4.00
			20	40	60
Exp. #	Time	Temp.	Removal (%) <sup>a</sup>		
1	0	0	95.1		
2	0	0	94.0		
3	-1	0	90.2		
4	+1	0	98.0		
5	0	0	93.3		
6	-1	+1	98.0		
7	0	0	98.0		
8	+1	-1	90.0		
9	+1	+1	100.0		
10	-1	-1	54.6		
11	0	-1	70.0		
12	0	0	95.0		
13	0	+1	97.8		

<sup>a</sup> n=3, RSD% < 2%.

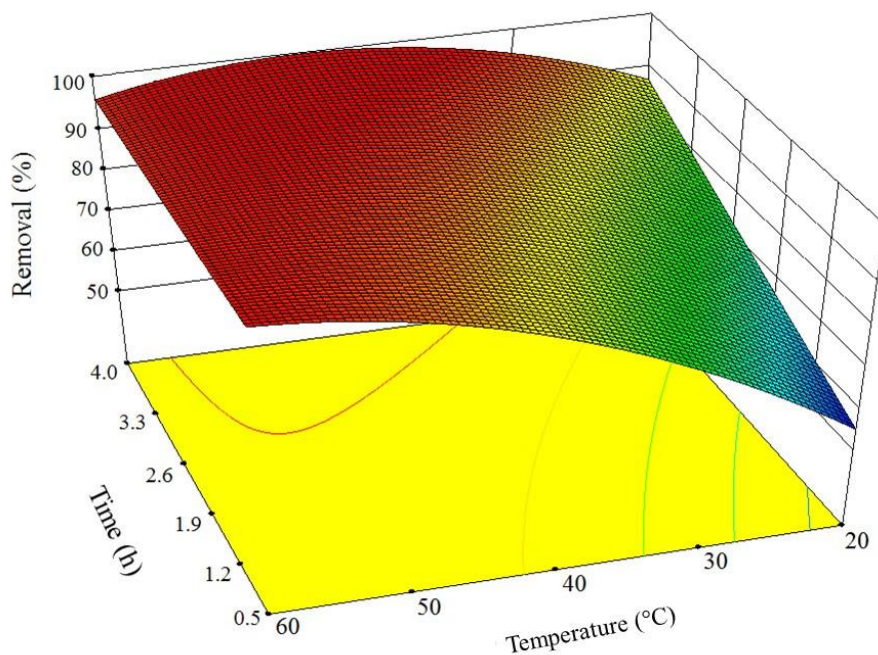


**Figure 3.5.** 3D-plots of the effect of time and temperature on anthracene oxidation using peroxyacetic acid/H<sub>2</sub>SO<sub>4</sub>.

**Table 3.5.** ANOVA analysis of anthracene oxidation using peroxyacetic-acid catalyzed by sulfuric acid. The effect of temperature and time on removal % using CCD.

Source	Sum of Squares	df	Mean Square	F Value	P-value Prob > F	
Model	2024.69	5	404.94	48.86	< 0.0001	significant
A) Time (h)	340.51	1	340.51	41.09	0.0004	
B) Temperature (°C)	1098.91	1	1098.91	132.59	< 0.0001	
AB	278.89	1	278.89	33.65	0.0007	
A <sup>2</sup>	0.32	1	0.32	0.038	0.8509	
B <sup>2</sup>	268.62	1	268.62	32.41	0.0007	
Residual	58.01	7	8.29			
Lack of Fit	45.15	3	15.05	4.68	0.0851	not significant
Pure Error	12.87	4	3.22			
Cor Total	2082.71	12				

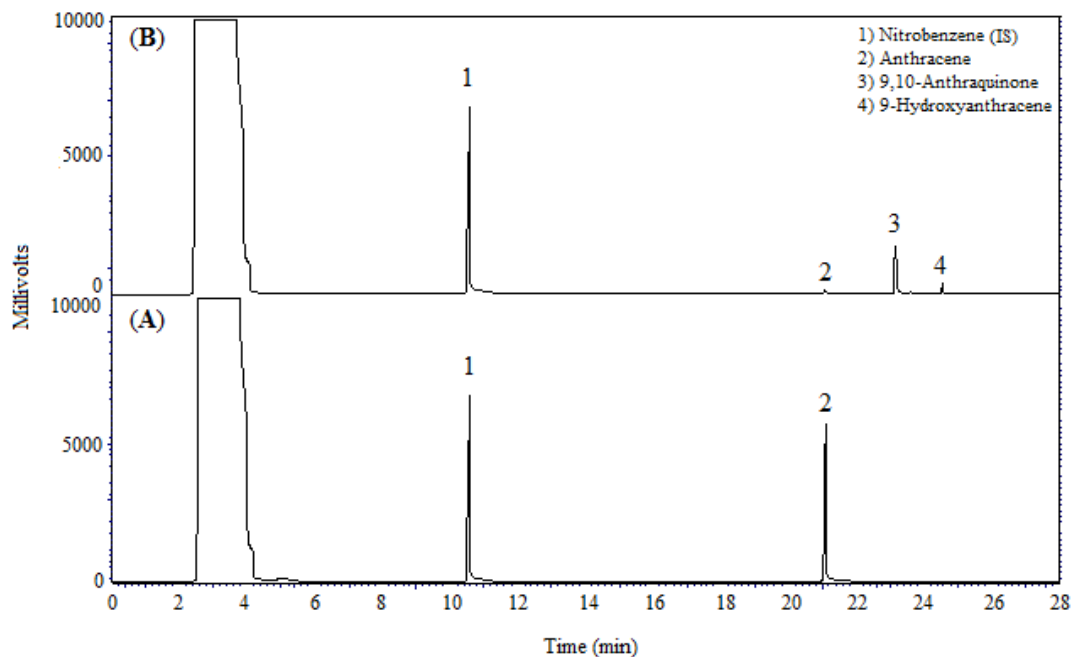


**Figure 3.6.** GC-FID analysis of anthracene (A), and the reaction product of anthracene oxidation using peroxyacetic acid catalyzed by sulfuric acid (B). Reaction conditions: 5.0 mL of deionized water, 5.0 mL of H<sub>2</sub>O<sub>2</sub>, 5.0 mL of glacial acetic acid, 1.0 mL of sulfuric acid, 45 °C, 0.5 h, and 200 µL of anthracene (5.00 g/L).

### 3.3.3. Optimization of coal tar oxidation

The coal tar sample used in the current work (i.e. the portion soluble in anhydrous ethanol) consists mainly of PAHs with two fused benzene or aromatic rings (e.g., naphthalene, 1-methylnaphthalene, and 2-methylnaphthalene), three fused aromatic rings (e.g., anthracene and phenanthrene), and four fused aromatic rings (e.g., fluoranthene, pyrene, chrysene, and benzo[a]anthracene) as shown in its chromatogram (Figure 3.7-A), and listed in Table 3.6.

#### 3.3.3.1. The effect of Fenton's reagent

Using the optimum amounts of reagent calculated from the experiments of the Fenton oxidation of anthracene is insufficient to cause a significant removal of PAHs in coal tar (Figure 4.7-B). This is due to the total concentration of PAHs in coal tar is ~4,400 ppm and the reaction is not stoichiometric because of possible further oxidation reaction pathways of various PAHs [19]. Therefore, increased dosages of Fenton's reagent (i.e. multiples of optimum conditions) were used (Table 3.7), resulting in higher removal as seen in Figure 3.7, and the results are more clearly graphed in Figure 3.8. Using these optimized conditions, it was found that some PAHs have a greater susceptibility to oxidization; the removal % using five times the dose of Fenton reagent (condition F) of anthracene (**8**), carbazole (**9**), and pyrene (**14**) is ~90%, followed by acenaphthene (**5**), and fluorene (**6**) at ~70%, while other PAHs in coal tar such as naphthalene (**1**), phenanthrene (**7**), and chrysene (**16**) have lower removal % (<50%). This variance in PAHs removal is due to their structure and reactivity [35]. In general, the PAHs' reactivity towards oxidation increases as the number of the fused benzene rings increases. As such the oxidation can occur on one of the rings and the other aromatic rings remain intact, making the required energy for breaking the aromaticity of one ring in PAHs less than that of benzene. Other

factors such as steric interactions, reaction conditions, and the connectivity of the aromatic rings can influence the reaction rate [36]. Clar's rule explains the PAHs aromaticity using the Kekulé resonance structures, where the preferred Kekulé resonance structure has the largest number of disjoint aromatic  $\pi$ -sextets, i.e., benzene-like moieties [37]. Thus, Clar's rule can be used to predict the most reactive sites in PAHs [38]. For example, the 9 and 10 positions in anthracene are more reactive than the 1 and 2 positions due to formation of a stable intermediate which includes two  $6\pi$ -electron benzenoid rings in case of reaction on positions 9 and 10, while reaction on either of the terminal rings a less stable intermediate and product having only a single  $6\pi$ -electron benzenoid ring [36].

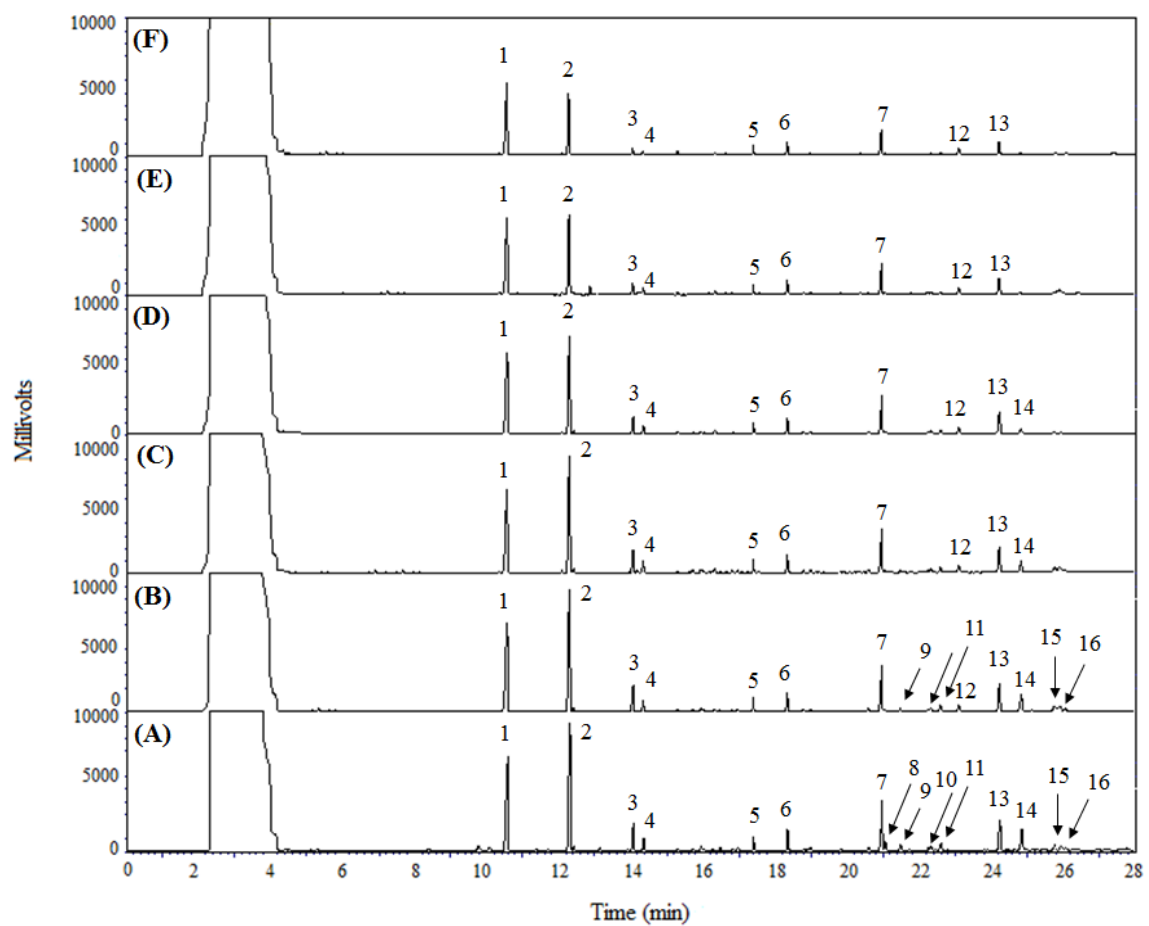


**Figure 3.7.** GC-FID chromatogram of coal tar soluble in anhydrous ethanol (A) and oxidation of coal tar in anhydrous ethanol (B-F). Peak numbers correspond to compounds listed in Table 3.6 and reaction conditions listed in Table 3.7.

**Table 3.6.** PAH compounds identified in anhydrous ethanol extract of coal tar before and after oxidation.

Peak # <sup>a</sup>	Compound name	Conc. in coal tar (ppm) <sup>b</sup>
1	Nitrobenzene (Internal standard)	NA
2	Naphthalene	1823
3	2-Methylnaphthalene	120
4	1-Methylnaphthalene	113
5	Acenaphthylene	160
6	9H-fluorene	192
7	Phenanthrene	631
8	Anthracene	130
9	Carbazole	110
10	9-Methylanthracene	102
11	4H-cyclopenta[def]phenanthrene	115
12	9,10-Anthraquinone	NA
13	Fluoranthene	370
14	Pyrene	300
15	Benz[a]anthracene	130
16	Chrysene	110

<sup>a</sup> Numbers refer to GC peaks in Figures 3.7 and 3.9.

<sup>b</sup> Concentrations of PAHs in ethanol extract of coal tar before oxidation. RSD% < 5%, n=3.

**Table 3.7.** Experimental conditions for Fenton oxidation of coal tar. 2.0 mL aliquot of coal tar in anhydrous ethanol.

Condition	H <sub>2</sub> O <sub>2</sub> (μL)	Fe <sup>+2</sup> (μL)	Temperature (°C)	Time (h)
B	350	250	45	0.5
C	700	500	45	0.5
D	1050	750	45	0.5
E	1400	1000	45	0.5
F	1750	1250	45	0.5

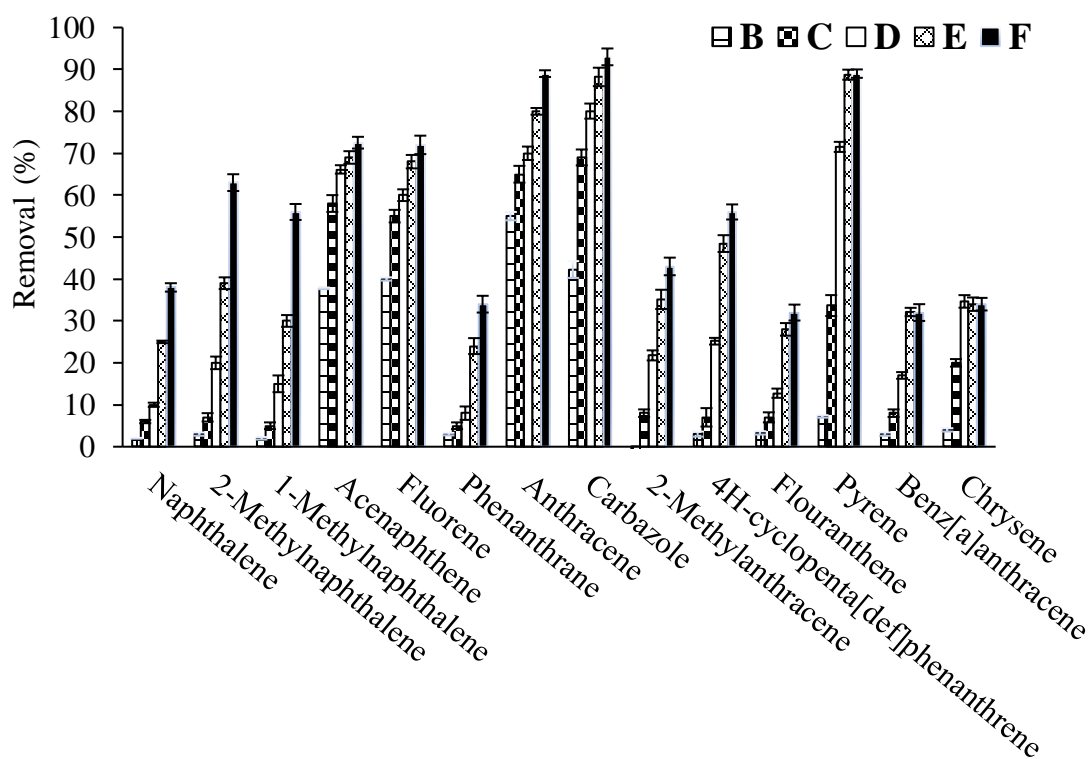


**Figure 3.8.** Removal % of coal tar PAHs using Fenton oxidation under the conditions (B-F) listed in Table 3.7. Error bars represent RSD < 5%, n = 3.

### 3.3.3.2. The effect of peroxyacetic acid/H<sub>2</sub>SO<sub>4</sub>

Doubling the dosage of the catalyzed peroxyacetic acid/H<sub>2</sub>SO<sub>4</sub> is necessary to observe a significant removal of PAHs from coal tar (Figures 3.9 and 3.10). The PAHs that are most oxidizable are anthracene (8) and carbazole (9), followed by pyrene (14), benz[a]anthracene (15), and chrysene (16), while other PAHs such as naphthalene (2), 2-methylnaphthalene (3), 1-methylnaphthalene (4), acenaphthene (5) and fluorene (6), phenanthrene (7) are poorly oxidizable.

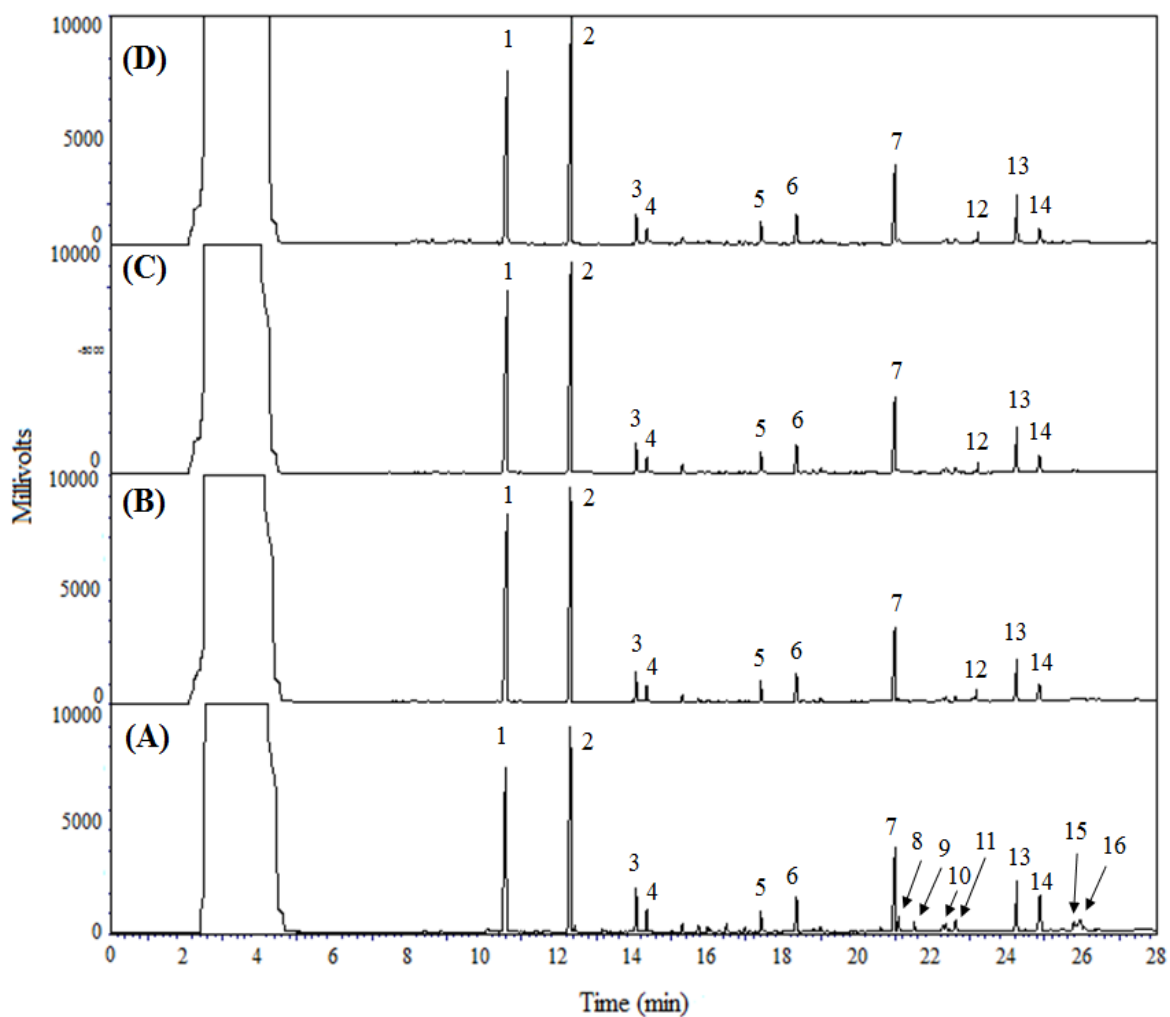


**Figure 3.9.** GC-FID chromatogram of DCM extracts of coal tar **A)** and oxidation of coal tar using different dosages of  $\text{H}_2\text{O}_2$ : $\text{CH}_3\text{COOH}$ : $\text{DI}$ : $\text{H}_2\text{SO}_4$  (v/v/v/v); **B)** (5:5:5:1) mL, **C)** 2 x (5:5:5:1) mL, and **D)** 3 x (5:5:5:1) mL. Peak numbers correspond to compounds listed in Table 3.4. The temperature of the reaction was adjusted to be 45 °C and the time was 0.5 h.

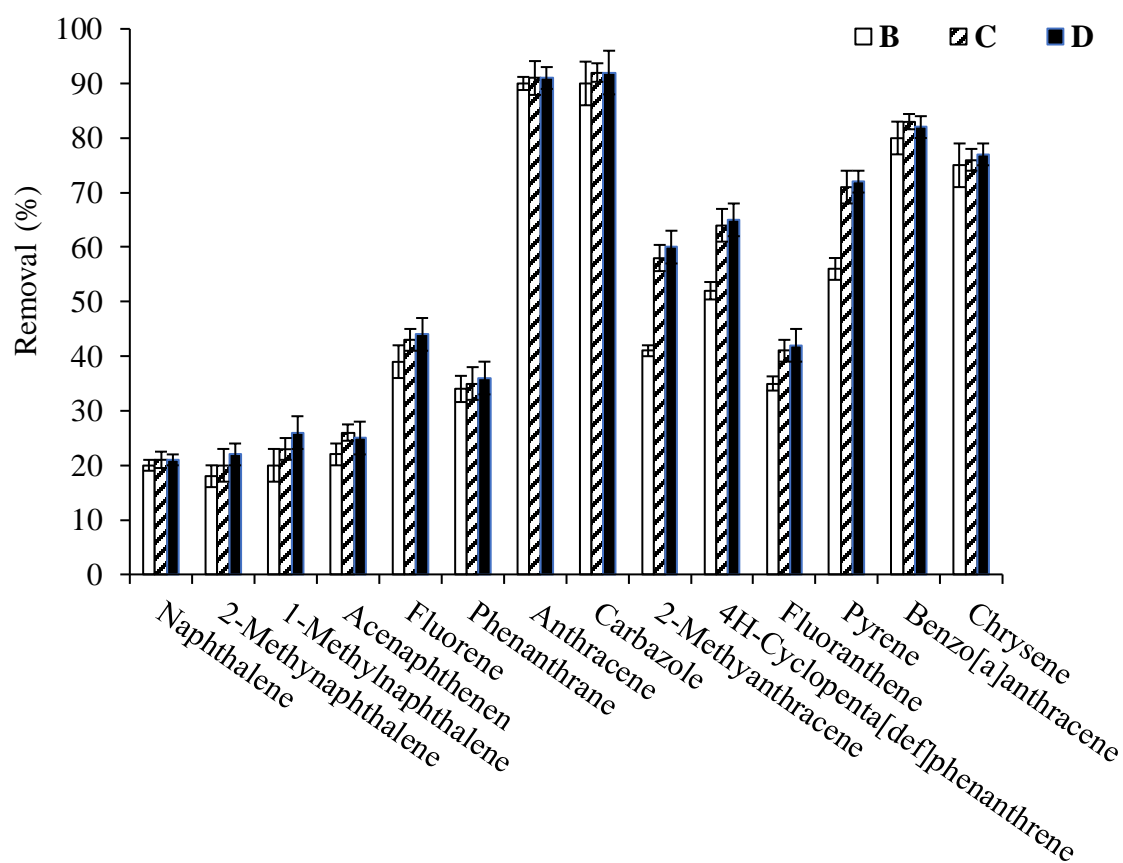


**Figure 3.10.** Removal % of coal tar PAHs using different dosages of  $\text{H}_2\text{O}_2:\text{CH}_3\text{COOH}:\text{DI}:\text{H}_2\text{SO}_4$  (5:5:5:1 v/v/v/v); **B**) 16.0 mL, **C**) 32.0 mL, and **D**) 48.0 mL. Reaction conditions: 45 °C and 0.5 h. Error bars represent RSD < 6%, n = 3.

### 3.3.3.3. Fenton's reagent vs. peroxyacetic acid

Oxidation of PAHs requires a higher dosage of peroxyacetic acid (10.0 mL) vs. 0.60 mL of Fenton's reagent because of the efficiency of the Fenton reagent's ability to produce highly reactive  $\cdot\text{OH}$  radicals [39]. In general, both Fenton's reagent and the peroxyacetic acid/ $\text{H}_2\text{SO}_4$  conditions show the ability to degrade some of the coal tar PAHs, but Fenton's reagent appears superior. There is observed product (9,10-Anthraquinone) from anthracene oxidation, but other oxidation products for PAHs in coal tar were not observed under these conditions (Figures 3.7 and 3.9). This is possibly due to complete oxidation of PAHs to

produce CO<sub>2</sub> and H<sub>2</sub>O [19]. In addition, analytical artifacts during GC injection of thermally unstable and high molecular weight oxygenated PAHs are reported in the literature [40]. For example, underestimation of phenanthrene-9,10-dione was observed when it was analyzed by GC. Only one CO molecule was eliminated from phenanthrene-9,10-dione during injection in GC, producing 9H-fluorene-9-one as product [41]. Furthermore, high molecular weight PAHs, such as benzo[a]pyrene isomers have low volatility and hence result in poor detection limits (ng range) when they are analyzed by GC [42]. The removal of PAHs from PAH-contaminated soil was also reported in other studies using Fenton oxidation without observing or identifying chromatographic peaks of reaction products [15,43]. Coal tar is a complex and enriched mixture of PAHs and its oxidation is much harder than PAH-contaminated soil, where native iron in soil can also enhance PAHs oxidation (Fenton-like oxidation) and the sorption sites of PAHs in soil increases the availability of the PAHs for chemical degradation [23].

### 3.4. Conclusion

Fenton's reagent was found to be a more effective agent than peroxyacetic acid/H<sub>2</sub>SO<sub>4</sub> for coal tar oxidation. Based on optimization conditions with anthracene temperature and time, had a most significant influence on coal tar PAH oxidation followed by H<sub>2</sub>O<sub>2</sub> and Fe<sup>2+</sup>. Experimental design has been successfully used for optimizing the conditions or protocols of Fenton or peroxyacetic acid/H<sub>2</sub>SO<sub>4</sub> induced oxidation of coal tar. By this approach, the number of experiments were reduced and the optimum conditions could be determined by taking into the account the interactions between the relevant factors. Fenton oxidation was found to be faster than peroxyacetic-acid at room temperature due to the ease of Fe<sup>2+</sup> oxidation and a high production of <sup>•</sup>OH radicals. Furthermore, Fenton oxidation requires less dosage and is easier to handle, compared to peroxyacetic acid/H<sub>2</sub>SO<sub>4</sub> dosage. In general, Fenton oxidation has been demonstrated as a promising route for degradation of PAHs in coal tar and shows advantages, such as low cost, simplicity, speed, and effectiveness.

### 3.5. References

- [1] Chen, Y.; Du, W.; Shen, G.; Zhuo, S.; Zhu, X.; Shen, H.; Huang, Y.; Su, S.; Lin, N.; Pei, L.; Zheng, X.; Wu, J.; Duan, Y.; Wang, X.; Liu, W.; Wong, M.; Tao, S. Household Air Pollution and Personal Exposure to Nitrated and Oxygenated Polycyclic Aromatics (PAHs) in Rural Households: Influence of Household Cooking Energies. *Indoor Air* **2017**, *27*, 169–178.
- [2] MacAskill, N. D.; Walker, T. R.; Oakes, K.; Walsh, M. Forensic Assessment of Polycyclic Aromatic Hydrocarbons at the Former Sydney Tar Ponds and Surrounding Environment Using Fingerprint Techniques. *Environ. Pollut.* **2016**, *212*, 166–177.
- [3] Hernández-Vega, J. C.; Cady, B.; Kayanja, G.; Mauriello, A.; Cervantes, N.; Gillespie, A.; Lavia, L.; Trujillo, J.; Alkio, M.; Colón-Carmona, A. Detoxification of Polycyclic Aromatic Hydrocarbons (PAHs) in *Arabidopsis Thaliana* Involves a Putative Flavonol Synthase. *J. Hazard. Mater.* **2017**, *321*, 268–280.
- [4] Qin, W.; Zhu, Y.; Fan, F.; Wang, Y.; Liu, X.; Ding, A.; Dou, J. Biodegradation of Benzo[a]pyrene by *Microbacterium* Sp. Strain under Denitrification: Degradation Pathway and Effects of Limiting Electron Acceptors or Carbon Source. *Biochem. Eng. J.* **2017**, *121*, 131–138.
- [5] Hassan M. A. Advanced Oxidation Processes for Textile Wastewater Treatment. *Int. J. Photochem. Photobiol.* **2017**, *2*, 85–93.
- [6] Cheng, M.; Zeng, G.; Huang, D.; Lai, C.; Xu, P.; Zhang, C.; Liu, Y. Hydroxyl Radicals Based Advanced Oxidation Processes (AOPs) for Remediation of Soils Contaminated with Organic Compounds: A Review. *Chem. Eng. J.* **2016**, *284*, 582–598.
- [7] Barathi, P.; Kumar, A. S. Electrochemical Conversion of Unreactive Pyrene to Highly Redox-Active 1,2-Quinone Derivatives on a Carbon Nanotube-Modified Gold Electrode Surface and Its Selective Hydrogen Peroxide Sensing. *Langmuir* **2013**, *29*, 10617–10623.
- [8] Ferrarese, E.; Andreottola, G.; Oprea, I. A. Remediation of PAH-Contaminated Sediments by Chemical Oxidation. *J. Hazard. Mater.* **2008**, *152*, 128–139.
- [9] Kuppusamy, S.; Thavamani, P.; Venkateswarlu, K.; Lee, Y. B.; Naidu, R.; Megharaj, M. Remediation Approaches for Polycyclic Aromatic Hydrocarbons (PAHs) Contaminated Soils: Technological Constraints, Emerging Trends and Future Directions. *Chemosphere* **2016**, *168*, 944–968.
- [10] Pawar, V.; Gawande, S. An Overview of the Fenton Process for Industrial Wastewater. *J. Mech. Civ. Eng.* **2015**, 127–136.
- [11] Mirzaei, A.; Chen, Z.; Haghghat, F.; Yerushalmi, L. Removal of Pharmaceuticals

- from Water by Homo/heterogeneous Fenton-Type Processes-A Review. *Chemosphere* **2017**, *174*, 665–688.
- [12] Neyens, E.; Baeyens, J. A Review of Classic Fenton's Peroxidation as an Advanced Oxidation Technique. *J. Hazard. Mater.* **2003**, *98*, 33–50.
- [13] Rivas, F. J. Polycyclic Aromatic Hydrocarbons Sorbed on Soils: A Short Review of Chemical Oxidation Based Treatments. *J. Hazard. Mater.* **2006**, *138*, 234–251.
- [14] Lee, B. D.; Hosomi, M.; Murakami, A. Fenton Oxidation with Ethanol to Degrade Anthracene into Biodegradable 9, 10-Anthraquinone: A Pretreatment Method for Anthracene-Contaminated Soil. *Water Sci. Technol.* **1998**, *38*, 91–97.
- [15] Lee, B.-D.; Hosomi, M. Ethanol Washing of PAH-Contaminated Soil and Fenton Oxidation of Washing Solution. *J. Mater.* **2000**, *2*, 24–30.
- [16] Lee, B.; Hosomi, M. Research Note Fenton Oxidation of Ethanol-Washed Distillation-Concentrated Benzo[a]pyrene: Reaction Product Identification and Biodegradability. *Science* **2001**, *35*, 2314–2319.
- [17] Scott Alderman, N.; N'Guessan, A. L.; Nyman, M. C. Effective Treatment of PAH Contaminated Superfund Site Soil with the Peroxy-Acid Process. *J. Hazard. Mater.* **2007**, *146*, 652–660.
- [18] Alderman, N. S.; Nyman, M. C. Oxidation of PAHs in a Simplified System Using Peroxy-Acid and Glass Beads: Identification of Oxidizing Species. *J. Environ. Sci. Health. A. Tox. Hazard. Subst. Environ. Eng.* **2009**, *44*, 1077–1087.
- [19] Bendouz, M.; Tran, L. H.; Coudert, L.; Mercier, G.; Blais, J.-F. Degradation of Polycyclic Aromatic Hydrocarbons in Different Synthetic Solutions by Fenton's Oxidation. *Environ. Technol.* **2016**, *38*, 1–12.
- [20] Box, G. E. P.; Wilson, K. B. On the Experimental Attainment of Optimum Conditions. *J. R. Stat. Soc.* **1951**, *13*, 1–45.
- [21] Sharifpour, E.; Ghaedi, M.; Haddadi, H. Optimization of Simultaneous Ultrasound Assisted Toxic Dyes Adsorption Conditions from Single and Multi-Components Using Central Composite Design: Application of Derivative Spectrophotometry and Evaluation of the Kinetics and Isotherms. *Ultrason. Sonochem.* **2016**, *36*, 236–245.
- [22] Sakkas, V. A.; Islam, M. A.; Stalikas, C.; Albanis, T. A. Photocatalytic Degradation Using Design of Experiments: A Review and Example of the Congo Red Degradation. *J. Hazard. Mater.* **2010**, *175*, 33–44.
- [23] Yap, C. L.; Gan, S.; Ng, H. K. Fenton Based Remediation of Polycyclic Aromatic Hydrocarbons-Contaminated Soils. *Chemosphere* **2011**, *83*, 1414–1430.
- [24] Usman, M.; Faure, P.; Ruby, C.; Hanna, K. Remediation of PAH-Contaminated Soils by Magnetite Catalyzed Fenton-like Oxidation. *Appl. Catal. B Environ.* **2012**, *117*, 10–17.

- [25] Chu, W. Modeling the Quantum Yields of Herbicide 2,4-D Decay in UV/H<sub>2</sub>O<sub>2</sub> Process. *Chemosphere* **2001**, *44*, 935–941.
- [26] Tony, M. a.; Bedri, Z. Experimental Design of Photo-Fenton Reactions for the Treatment of Car Wash Wastewater Effluents by Response Surface Methodological Analysis. *Adv. Environ. Chem.* **2014**, *2014*, 1–8.
- [27] Akbari, S.; Ghanbari, F.; Moradi, M. Bisphenol A Degradation in Aqueous Solutions by Electrogenerated Ferrous Ion Activated Ozone, Hydrogen Peroxide and Persulfate: Applying Low Current Density for Oxidation Mechanism. *Chem. Eng. J.* **2016**, *294*, 298–307.
- [28] Torrades, F.; García-Montaña, J. Using Central Composite Experimental Design to Optimize the Degradation of Real Dye Wastewater by Fenton and Photo-Fenton Reactions. *Dye. Pigment.* **2014**, *100*, 184–189.
- [29] Herney-Ramirez, J.; Lampinen, M.; Vicente, M. A.; Costa, C. A.; Madeira, L. M. Experimental Design to Optimize the Oxidation of Orange II Dye Solution Using a Clay-Based Fenton-like Catalyst. *Ind. Eng. Chem. Res.* **2008**, *47*, 284–294.
- [30] Lundstedt, S.; Persson, Y.; Öberg, L. Transformation of PAHs during Ethanol-Fenton Treatment of an Aged Gasworks' Soil. *Chemosphere* **2006**, *65*, 1288–1294.
- [31] Dul'neva, L. V.; Moskvina, A. V. Kinetics of Formation of Peroxyacetic Acid. *Russ. J. Gen. Chem.* **2005**, *75*, 1125–1130.
- [32] Zhao, X.; Zhang, T.; Zhou, Y.; Liu, D. Preparation of Peracetic Acid from Hydrogen Peroxide. Part I: Kinetics for Peracetic Acid Synthesis and Hydrolysis. *J. Mol. Catal. A Chem.* **2007**, *271*, 246–252.
- [33] Abdulmalek, E.; Arumugam, M.; Basri, M.; Rahman, M. B. A. Optimization of Lipase-Mediated Synthesis of 1-Nonene Oxide Using Phenylacetic Acid and Hydrogen Peroxide. *Int. J. Mol. Sci.* **2012**, *13*, 13140–13149.
- [34] Draper, N. R.; Smith, H. *Applied Regression Analysis*, 1st ed.; John Wiley and Sons Inc.: Hoboken, 1966.
- [35] Jonsson, S.; Persson, Y.; Frankki, S.; van Bavel, B.; Lundstedt, S.; Haglund, P.; Tysklind, M. Degradation of Polycyclic Aromatic Hydrocarbons (PAHs) in Contaminated Soils by Fenton's Reagent: A Multivariate Evaluation of the Importance of Soil Characteristics and PAH Properties. *J. Hazard. Mater.* **2007**, *149*, 86–96.
- [36] Forsey, S. P.; Thomson, N. R.; Barker, J. F. Oxidation Kinetics of Polycyclic Aromatic Hydrocarbons by Permanganate. *Chemosphere* **2010**, *79*, 628–636.
- [37] Solà, M. Forty Years of Clar's Aromatic  $\pi$ -Sextet Rule. *Front. Chem.* **2013**, *1*, 4–11.
- [38] Clar, E. *The Aromatic Sextet* John, 1st ed.; John Wiley and Sons Inc.: New York, 1972.

- [39] Gligorovski, S.; Streckowski, R.; Barbati, S.; Vione, D. Environmental Implications of Hydroxyl Radicals ( $\cdot\text{OH}$ ). *Chem. Rev.* **2015**, *115*, 13051–13092.
- [40] Walgraeve, C.; Demeestere, K.; De Wispelaere, P.; Dewulf, J.; Lintelmann, J.; Fischer, K.; Van Langenhove, H. Selective Accurate-Mass-Based Analysis of 11 Oxy-PAHs on Atmospheric Particulate Matter by Pressurized Liquid Extraction Followed by High-Performance Liquid Chromatography and Magnetic Sector Mass Spectrometry. *Anal. Bioanal. Chem.* **2012**, *402*, 1697–1711.
- [41] Liu, Y.; Yu, S.; Zhou, J. Adaptive Segment-Based Patching Scheme for Video Streaming Delivery System. *Comput. Commun.* **2006**, *29*, 1889–1895.
- [42] Koeber, R.; Bayona, J. M.; Niessner, R. Determination of Benzo[*a*]Pyrene Diones in Air Particulate Matter with Liquid Chromatography Mass Spectrometry. *Environ. Sci. Technol.* **1999**, *33*, 1552–1558.
- [43] Forsey, S. P. In Situ Chemical Oxidation of Creosote/Coal Tar Residuals: Experimental and Numerical Investigation, Ph.D. Dissertation, University of Waterloo, Waterloo, ON, 2004.

## **Chapter 4**

### **Microwave-assisted thermal removal of PAHs from coal tar**

## **Abstract**

In this study, microwave-assisted heating (MAH) of pyrene as a model PAH and coal tar was investigated at relatively low temperatures ( $T \leq 300$  °C) and low microwave power (300 W). Small-scale samples (0.025 g) were tested on a commercial microwave apparatus. The effect of addition (20%) of biochar, activated carbon (AC), and  $\text{TiO}_2$  as microwave absorbers for the microwave-assisted thermal removal of PAHs from coal tar was investigated. It was observed that ~95% removal efficiency of pyrene was obtained using an open microwave system. The gaseous products from coal tar increased when using biochar and AC (i.e., 8% yield, coal tar only, 18% with biochar, and 16% with AC) using a closed microwave system at only 190 °C. In addition, using microwave absorbers (biochar and AC) and closed microwave system shortened the time required to reach the set temperature and thereby reducing the microwave power consumption. Both volatile and non-volatile fractions from the MAH of coal tar with and without microwave absorbers were analyzed by gas chromatography-mass spectrometry (GC-MS) and gas chromatography-flame ionization detector (GC-FID). The results indicate that MAH of coal tar with biochar and AC at low temperature is an effective route for removing PAHs from coal tar. Thermogravimetric analysis (TGA) on coal tar with and without biochar, AC, and  $\text{TiO}_2$  was conducted in order to understand the influence of these factors on coal tar under conventional heating. TGA results showed that using biochar and AC with coal tar increased the percentage of volatile fraction from coal tar.

#### **4.1. Introduction**

Coal tar is a black liquid with an extremely high viscosity [1]. It is a by-product from coal carbonization/gasification and consists of different classes of organic compounds such as polycyclic aromatic hydrocarbons (PAHs), phenols, and heterocyclic aromatic compounds [2]. The coal tar composition is mainly dependent on the reaction temperature and the coal type [3]. Coal tar can be described as a non-aqueous phase liquid (NAPL) and is considered as a human carcinogen or procarcinogen [4]. Therefore, efforts have been made to remove the PAHs present in the coal tar [5]. Thermal treatment, which can be achieved by microwave-assisted or conventional heating, has been used for removal of PAHs from PAH-contaminated soils [6,7]. Microwave-assisted heating (MAH) has several advantages compared to conventional heating, in particular more rapid and effective heating [8].

The ability of a material to absorb microwave irradiation is highly dependent on its dielectric properties [9]. The relative dielectric loss factor represents the efficiency of a material to convert electromagnetic energy into heat [10]. A material that has a high dielectric constant and a high dielectric loss factor heats faster under microwave irradiation [11]. The MWH mechanisms are dipole rotation and ionic conduction [12]. In dipolar rotation, dipolar molecules such as water are agitated by an oscillating electric field and reoriented to adopt the same phase of the oscillating electric field. The motion of dipolar molecules is resisted by inertial, elastic, frictional, and inter-molecular forces by which the kinetic energy increases to generate heat [13]. In ionic conduction, ions in the sample interact with the electric field of microwaves, oscillating up and down. An electric current is produced through the movement of ions. The collisions between ions, neighboring molecules and atoms resist the created current. As a result of this process, the microwave

irradiated material heats up [14]. Furthermore, hot spots are overheated spots in the target material that are created during MAH; the temperatures of these spots are higher than that of other regions [15]. The creation of a hot spot is due to the inhomogeneous nature of the applied microwave field [16]. For example, hot spots can be created on an activated carbon (AC) surface during microwave heating (800 W) and the measured temperature can be higher than 1000 °C within 20 sec [17,18].

MAH has been used in the remediation of sites contaminated by organic pollutants such as PAHs and polychlorinated biphenols (PCBs) [19]. For example, 2,4,5-trichlorobiphenyl was successfully removed from 2,4,5-trichlorobiphenyl-contaminated soil (>90% removal efficiency). In that study, AC was used as a microwave absorber and its amount had a clear influence on the temperature profile and removal kinetics of 2,4,5-trichlorobiphenyl [20]. Furthermore, MAH was used to remove hexachlorobenzene (HCB) from HCB-contaminated soils where MnO<sub>2</sub> was added to HCB-contaminated soil samples as a microwave absorber. The results of that work indicate that 100% removal of HCB was achieved within 10 min [21].

The aim of the current work was to evaluate the capability of MAH to remove PAHs from coal tar at relatively low temperatures ( $T \leq 300$  °C) and to investigate the effectiveness of some microwave absorbers such as biochar, AC, and TiO<sub>2</sub> on MAH of coal tar. TGA analysis of coal tar with the same microwave absorbers were conducted to understand the influence of these materials on PAH removal from coal tar using a conventional heating source.

## 4.2. Materials and methods

### 4.2.1. Materials

Pyrene (>98%) was purchased from Alfa Aesar (Ward Hill, MA, USA). The coal tar sample used in this work was collected from the Sydney Tar Ponds in Nova Scotia, Canada. Activated carbon (Fisher Scientific, 50-200 mesh) and titanium (IV) oxide (Anatase, 99.8% trace metals basis) were purchased from Sigma-Aldrich, Canada. Fly ash biochar (364 cm<sup>2</sup>/g BET surface area, 0.145 cm<sup>3</sup>/g pore volume, and 23.2 Å pore width) was obtained from Nova Scotia Power Inc. All of these materials were used as received without any further treatment. C<sub>18</sub> cartridges (Supelco Envi-18, 3 mL tube; used to trap the volatiles) anhydrous ethanol (Sigma-Aldrich), and dichloromethane (Sigma-Aldrich, high-purity grade, ≥ 99.8%) were also used as received.

### 4.2.2. Experimental methods

#### *Microwave system*

The CEM Discover Microwave Synthesis System (Figure 4.1A) was used for the microwave-assisted heating of the coal tar. The experiments were carried out using both closed and open microwave systems (Figures 4.1C and 4.1D). In the closed microwave system, 0.025 g of pyrene or coal tar was carefully weighed and loaded into a small 2 mL vial and then was inserted into a 10 mL microwave tube (Figure 4.1C). Before closing the microwave tube, the sample was purged by nitrogen gas with a flow rate of 40 mL/min for 2 min. The closed microwave tube was then loaded into the microwave cavity and heated to 190 °C. The effects of biochar on pyrene, and of biochar, AC, and TiO<sub>2</sub> on coal tar, were investigated using the two systems. The ratio of catalyst to pyrene, or coal tar, was 1:5 wt/wt (0.005 g of appropriate catalyst was added to 0.025 g of pyrene or coal tar). Then,

the mixture was heated carefully at 80 °C for 10 min using a heating block (Corning, PC-420D) to reduce the viscosity of coal tar to facilitate the mixing of coal tar with the catalyst. The mixing was done with a small paper clip. In the case of pyrene, biochar was also mixed well with pyrene using a mortar and pestle. The weights of samples were precisely measured before and after microwave heating. The gas % was calculated using the following equation:

$$\text{Gas\%} = 100\% - \text{Non-volatile\%} - \text{Volatile\%}$$

In the open microwave system (Figure 4.1D), the C<sub>18</sub> cartridge was coupled to the head of the 10 mL microwave tube to trap the volatile fraction. A 40 mL/min nitrogen flow was used to keep the heating process under an inert atmosphere, and the set temperature for the open microwave system was 300 °C. In both the open and closed microwave systems, the volatile and non-volatile fractions were collected separately using 2.0 mL of dichloromethane (DCM) for each, and then the DCM solutions were analyzed by GC-MS and GC-FID. In addition, 0.005 g of AC, 0.005 g of biochar, or 0.005 g of TiO<sub>2</sub> were individually added to 250 µL of coal tar dissolved in anhydrous ethanol (0.400 g of coal tar was dissolved in 60.0 mL anhydrous ethanol and the measurement of coal tar solubility in anhydrous ethanol is explained in Appendix B (Section S4.1)) and kept in a small sealed glass vial (2.0 mL) on a lab bench at room temperature for 24 h. The small vial containing the sample and microwave absorber was then loaded into a 10 mL microwave tube using the open microwave system under the same experimental conditions used for the open microwave system mentioned above. Both volatile and non-volatile fractions were collected separately using 2.0 mL of DCM for each and the resulting DCM solution were then analyzed by GC-FID.

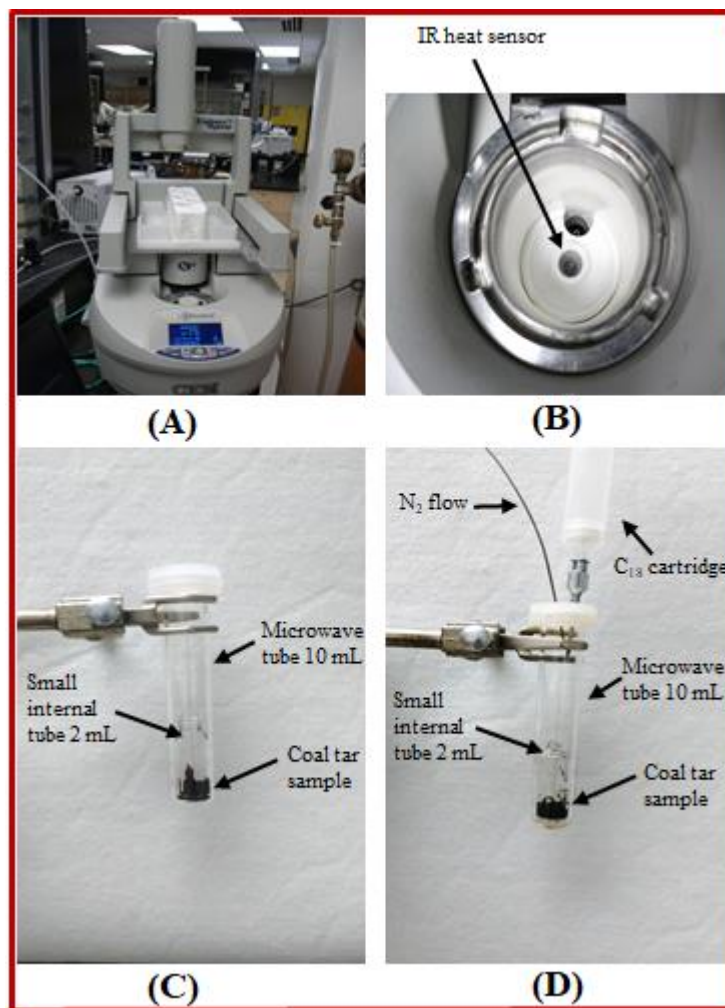


**Figure 4.1.** (A) CEM Discover microwave synthesis system, (B) inside microwave cavity, (C) closed microwave system, and (D) open microwave system. The clamp is used for illustration purposes only.

#### 4.2.3. GC Analysis

The pyrene, coal tar, and both volatile and non-volatile fractions from the microwave heating of pyrene and coal tar were analyzed using gas chromatography mass spectrometry (GC-MS) in full scan mode and a gas chromatography-flame ionization detector (GC-FID).

##### *GC-MS*

An Agilent Technologies 6890 gas chromatograph coupled to an Agilent 7683 Series Injector and an Agilent 5973 inert Mass Selective Detector (MSD) was used. The GC

capillary column is DB-5 (30 m x 0.25 mm i.d. x 0.25  $\mu$ m film thickness). Compounds were ionized by electron ionization at 70 eV with a scan range of  $m/z$  40-550, and mass spectra were matched with the NIST library data base. Furthermore, retention time data from references [22–24] was used for compound identification and model compound analysis. The temperature program for the GC-MS oven was 80 °C for 1 min then gradually increased to 300 °C at a heating rate of 10 °C/min and held for 2 min at the final temperature. 2  $\mu$ L of the sample was injected in splitless injection mode. The injector, interface, and detector temperatures were 300, 250, and 280 °C, respectively.

#### *GC-FID*

The GC-FID (Thermo Fisher Ultra Trace) was equipped with the same column type as the GC-MS setup. The temperature programming of the GC-FID oven was the same used in the GC-MS analysis mentioned above. The injector and flame temperatures were both set at 300 °C and the sample (2  $\mu$ L) was introduced in splitless injection mode.

#### **4.2.4. Thermogravimetric analysis (TGA)**

A sample of approximately 0.015 g of coal tar was loaded on the Pt-sample pan of the TGA (TA Instruments Q500, USA) then inserted into the TGA oven. The sample was heated from room temperature to 800 °C with a constant heating rate of 5 °C/min under an inert environment of N<sub>2</sub> gas (40 mL/min flow rate). In addition, 0.003 g of each AC, biochar, and TiO<sub>2</sub> was individually added to 0.015 g of coal tar and heated at 80 °C using a heating block for 10 min, mixed well, and then analyzed by TGA.

### **4.3. Results and discussion**

#### **4.3.1. Operating conditioning of the microwave with carbon materials**

The CEM Discover microwave used in this work has a maximum power of 300 W and a maximum temperature of 300 °C. The set microwave power used for all the microwave experiments was 300 W. Temperature is an important factor that affects the amount of volatile fraction from MAH of pyrene and coal tar. Different temperatures in the range of 150-190 °C were investigated in the preliminary experiments using a closed microwave system. Among these temperatures, 190 °C was the best for producing enough volatile fraction that could be analyzed by GC-MS and GC-FID without any damage to the microwave tube. The highest amount of sample that could be loaded was 0.025 g. Increasing the temperature above 190 °C increases the pressure inside the microwave tube, which damages the microwave tube.

The open microwave system affords the ability to increase the set temperature up to 300 °C because of the absence of the build-up of pressure effect in the system.

#### **4.3.2. Effect of microwave absorber**

Microwave absorbers such as AC, biochar, and TiO<sub>2</sub> were used to enhance the heating rate and to increase removal efficiency of PAHs from coal tar. Carbon materials are good microwave absorbers and their loss tangent (the ratio of the dielectric loss factor to the dielectric constant) values are located in the range of 0.35 to 0.8 [25], and TiO<sub>2</sub> anatase has a loss tangent of 0.13 at 2.45 GHz at room temperature (~25 °C) [26].

##### *Pyrene*

Mixing biochar with pyrene increases the microwave heating rate, as shown in Figure 4.2.

In the closed microwave system, the time required to reach the set temperature (190 °C) is

1.5 min for pyrene with biochar, and 2.5 min for pyrene without biochar. Furthermore, the recorded pressure is 2 psi (for pyrene) vs. 32 psi (for pyrene + biochar). Using biochar with pyrene in the open microwave system did not show any improvement in microwave heating rate that could be due to the absence of built-up pressure, but there was a slight reduction in energy consumption (Figure 4.3). The percentages of volatile, non-volatile, and gas fractions from MAH of pyrene and pyrene with biochar using the open and closed microwave systems are shown in Figure 4.4. Clearly, the open microwave system is the best to transfer pyrene to be in the volatile fraction due to the high set temperature used (300 °C), but using biochar with pyrene reduces the volatile fraction (42%). In the case of using the closed system, pyrene remains in the small vial. This may be due to the low set temperature used (190 °C). Figure 4.5 shows the pyrene recovery, which was calculated according to the difference in the weights before and after MAH and according to the GC-analysis of volatile and non-volatile fractions. A high recovery of pyrene (> 92%) after MAH of pyrene was observed, while mixing biochar with pyrene reduced the recovery to ~40%. This may be due to the interactions between pyrene and biochar and/or possible degradation of pyrene at 300 °C. The image of the pyrene + biochar before and after the MAH is shown in Figure 4.6. Further discussion of non-volatile fraction from MAH of pyrene with biochar including FT-IR and SEM analyses is made in Appendix B (Sections S4.2 and S4.3).

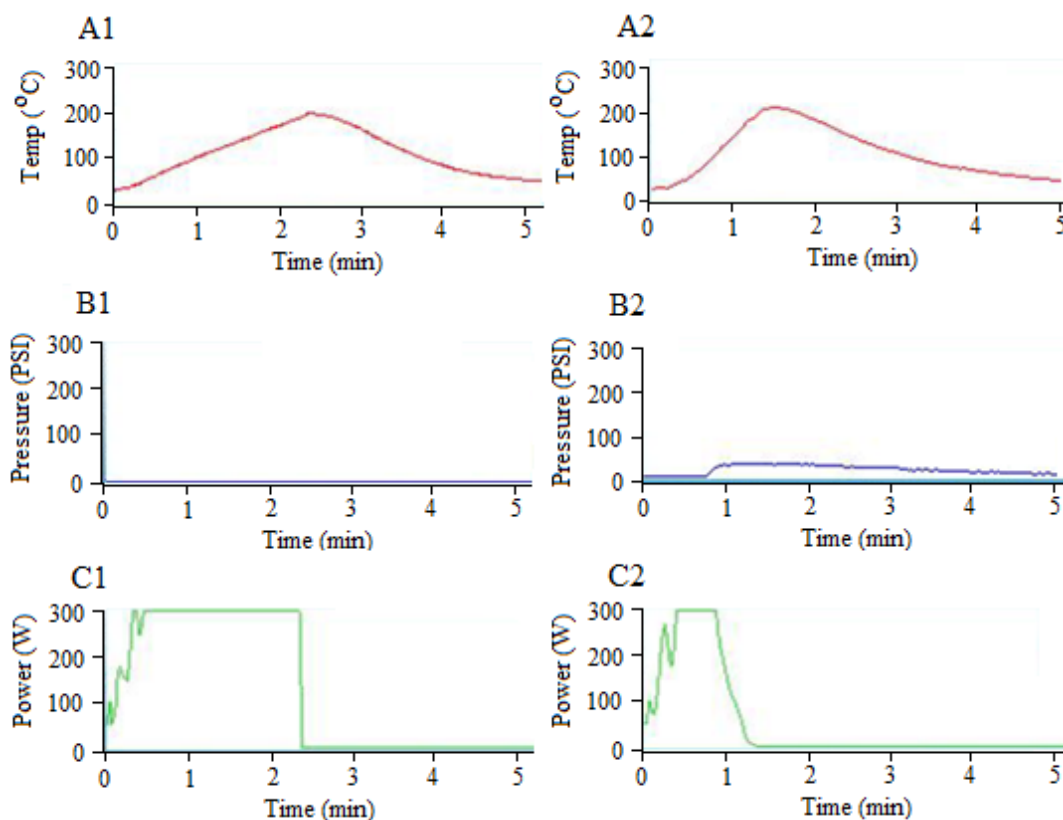


**Figure 4.2.** Temperature, pressure, and microwave power profile of microwave heating of pyrene (A1-C1) and pyrene with biochar (A2-C2) using a closed microwave system.

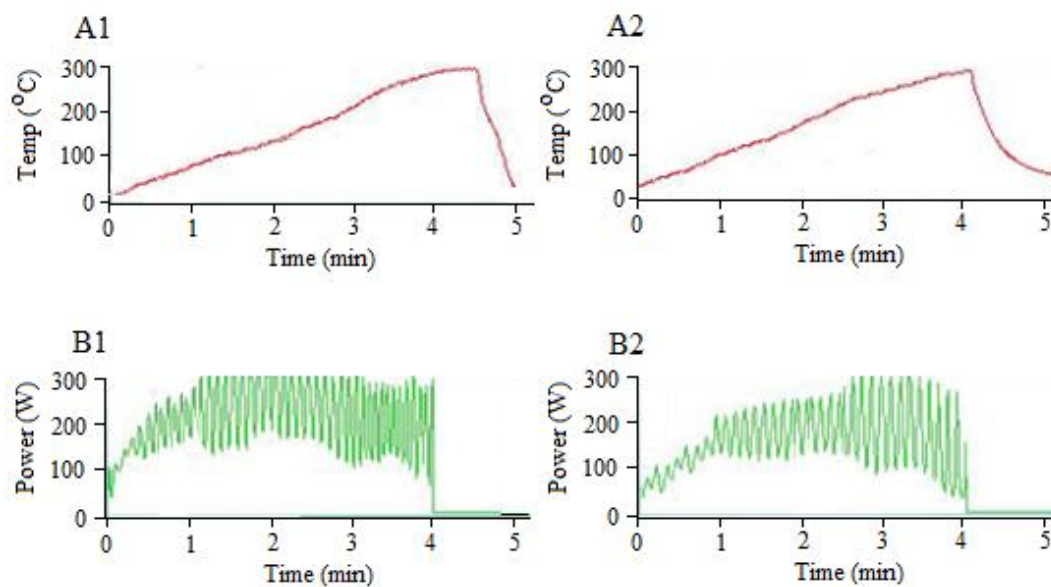


**Figure 4.3.** Temperature and microwave power profile of microwave-assisted heating of pyrene (A1 and B1) and pyrene with biochar (A2 and B2) using an open microwave system.

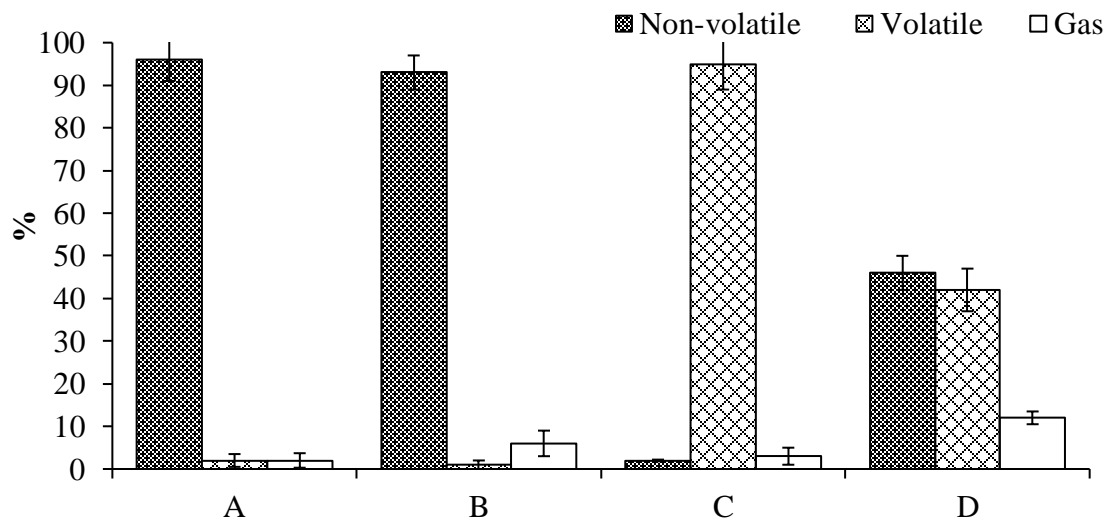


**Figure 4.4.** Percentages of volatile, non-volatile, and gas fractions from microwave-assisted heating of pyrene/closed system (A), pyrene + biochar/closed system (B), pyrene/open system (C), and pyrene + biochar/ open system (D). Error bars represent RSD ( $n = 3$ ).

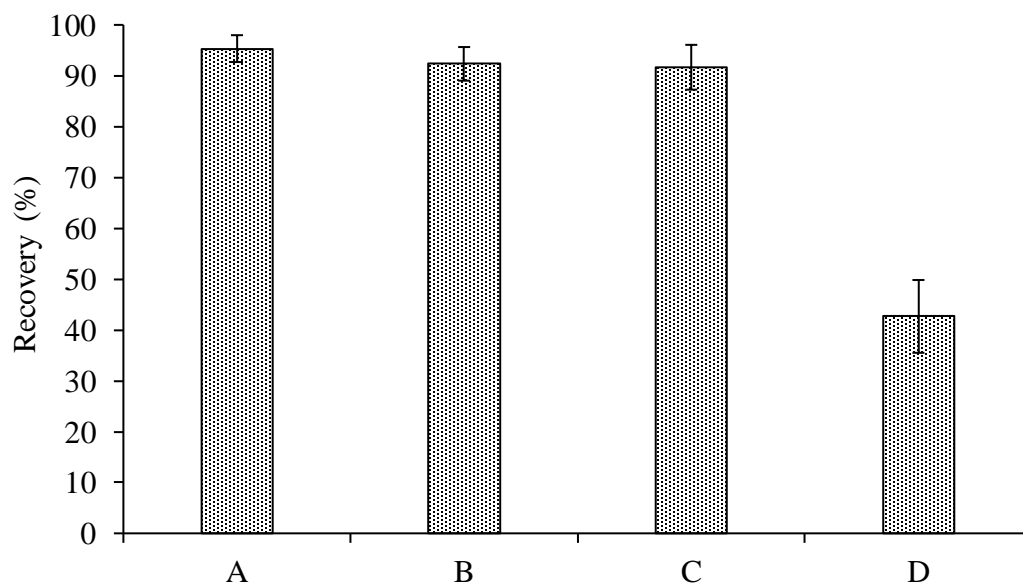


**Figure 4.5.** Pyrene recovery after microwave-assisted heating of pyrene/closed system (A), pyrene + biochar/closed system (B), pyrene/open system (C), and pyrene + biochar/ open system (D). Error bars represent RSD ( $n = 3$ ).

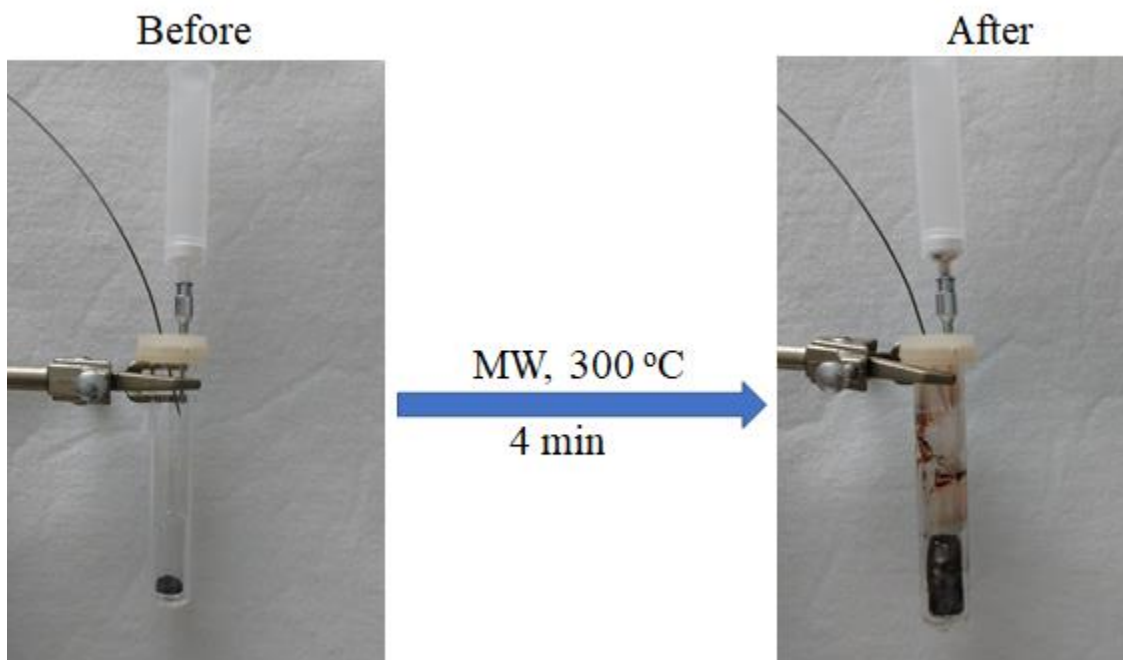


**Figure 4.6.** Pyrene with biochar before and after microwave-assisted heating using open system.

#### *Coal tar*

Using the closed microwave system, the addition of AC and biochar to coal tar accelerated the heating rate by reducing the required time to reach the set temperature: 90 sec for MAH of coal tar with AC and 45 sec for MAH of coal tar with biochar, versus 120 sec for MAH of coal tar without a microwave absorber (Figures 4.7A1, 4.7B1, and 4.7C1). The  $\text{TiO}_2$  addition did not cause any acceleration in the heating rate (Figure 4.7D1). This is due to its low loss tangent compared to that of AC and biochar. In addition, the use of AC and biochar as microwave absorbers reduced the microwave power consumption as noted by the reduction of the areas under the curves in the microwave power profiles (Figures 4.7 (B3 and C3) and 4.8 (B2 and C2)). The recorded pressure values of coal tar, coal tar with biochar, coal tar with AC, and coal tar with  $\text{TiO}_2$  were 22, 32, 26, and 14 psi, respectively.

The distribution of volatile, non-volatile, and gas fractions from the MAH of coal tar with and without the microwave absorbers using the closed microwave system are shown in Figures 4.9 and 4.10. The gas yield from coal tar using the open microwave system is higher than that measured using the closed microwave system. This may be due to the high set temperature used (300 °C). In the closed microwave system, the pressure effect may involve re-condensation of some molecules from the gas fraction, which in turn reduces the total yield of the gas fraction.

Ethanol has been reported to be an environmentally friendly solvent for extracting PAHs from real samples such as PAH-contaminated soil or coal tar [27]. In the current work, ethanol was used to extract the PAHs from coal tar and to facilitate mixing of the coal tar with the microwave absorbers (e.g., biochar, AC, TiO<sub>2</sub>). Figure 4.11 shows the temperature and microwave power profiles of the coal tar extracts in anhydrous ethanol with, or without, microwave absorbers using an open microwave system. The addition of biochar and AC reduces the microwave power required to reach the set temperature, but there is no reduction in the time required to reach the set temperature. This may be due to the absence of any internal pressure buildup because the system is open and the volatile compounds transfer directly to the low temperature region into the microwave cavity (upper part of microwave tube).

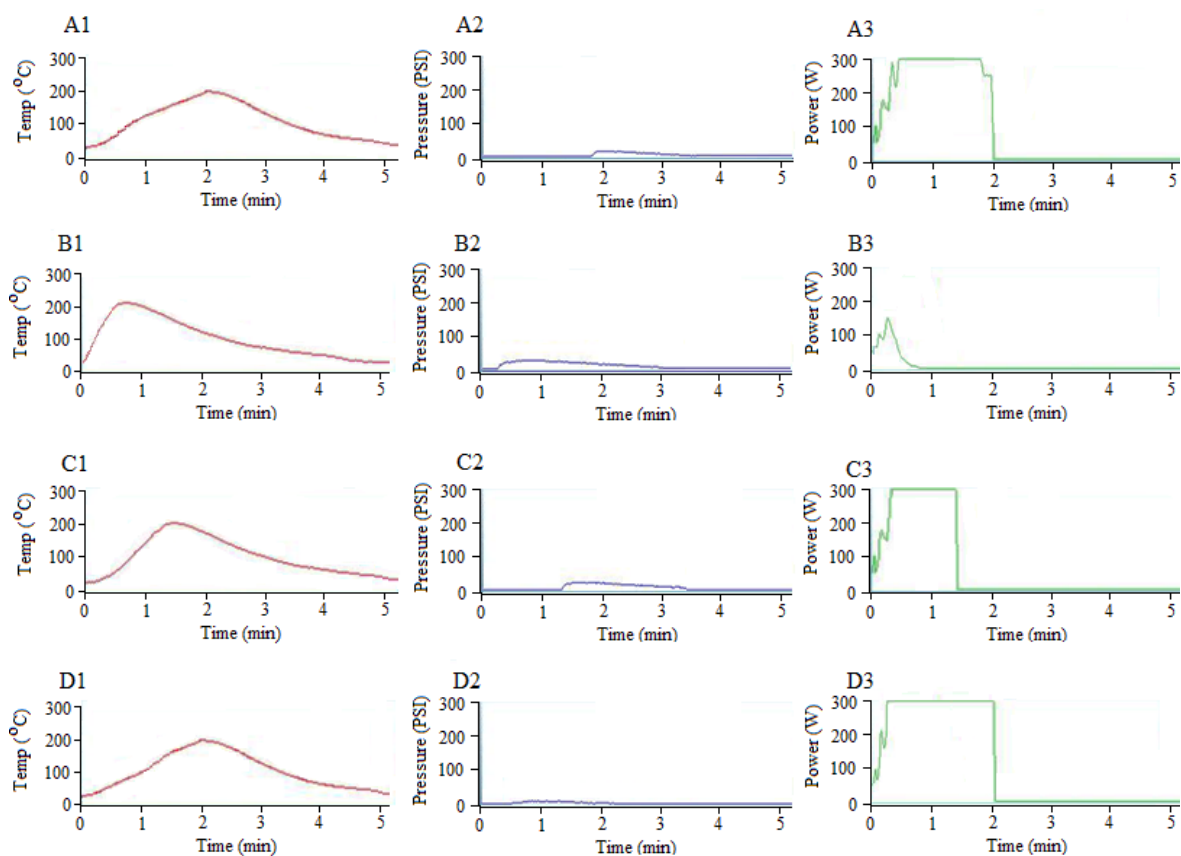


**Figure 4.7.** Temperature, pressure, and microwave power profiles of coal tar (A1-A3), coal tar with biochar (B1-B3), coal tar with activated carbon (C1-C3), and coal tar with TiO<sub>2</sub> (D1-D3). All experiments were conducted in a closed microwave system at a set temperature of 190 °C.

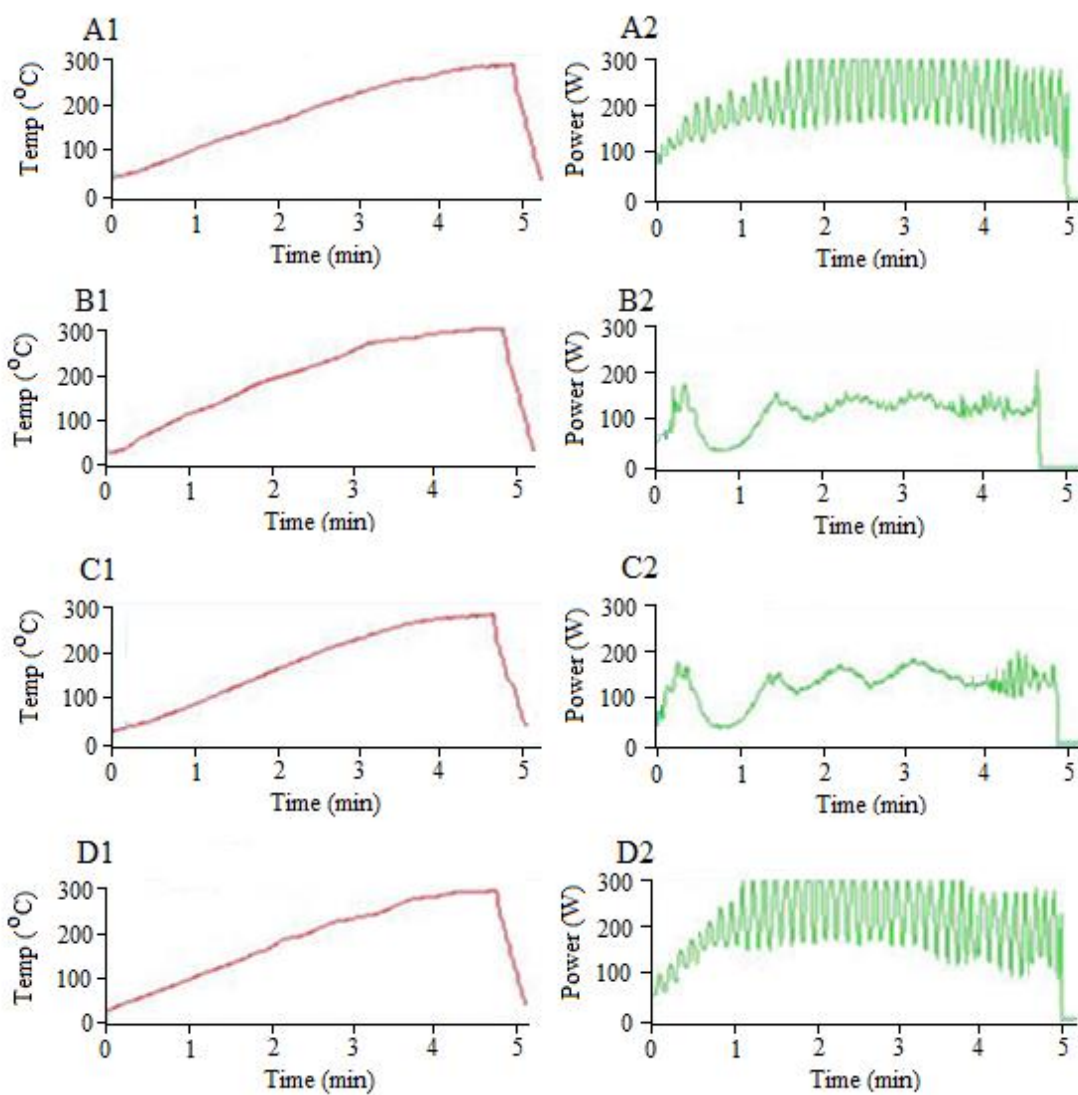


**Figure 4.8.** Temperature, pressure, and microwave power profiles of coal tar (A1 and A2), coal tar with activated carbon (B1, B2), coal tar with biochar (C1 and C2) and coal tar with TiO<sub>2</sub> (D1 and D2). All experiments were conducted in an open microwave system at a set temperature of 300 °C.

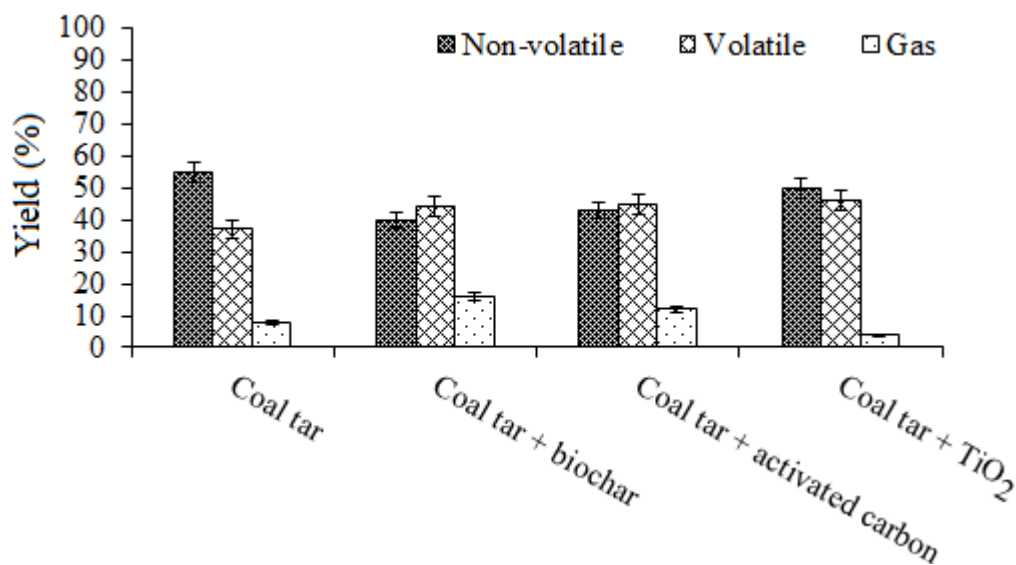


**Figure 4.9.** Non-volatile, volatile, and gas yield (%) from microwave of coal tar and coal tar with microwave absorbers (biochar, activated carbon, and TiO<sub>2</sub>) using closed microwave system. The set temperature is 190 °C. Error bars represent RSD ( $n = 3$ ).

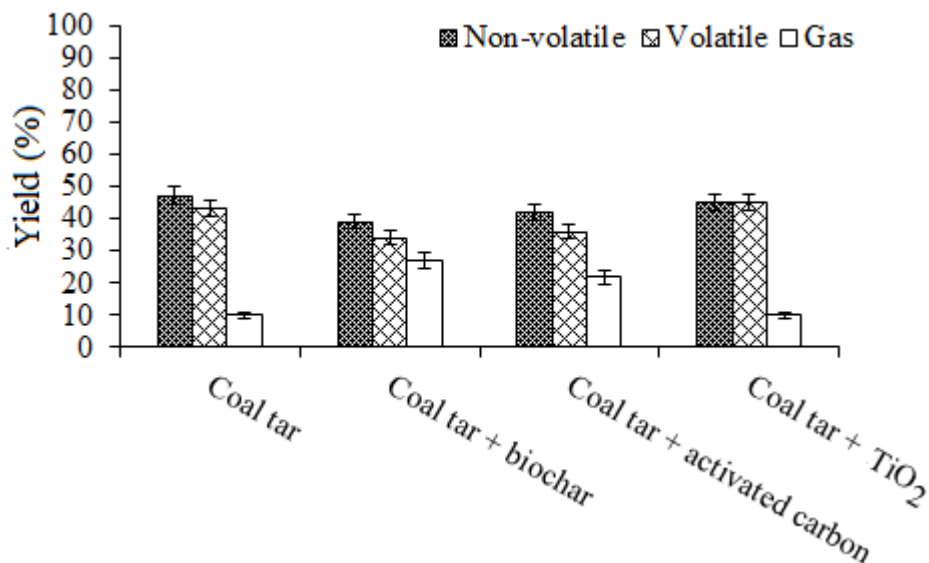


**Figure 4.10.** Non-volatile, volatile, and gas yield (%) from microwave-assisted heating of coal tar and coal tar with microwave absorbers (biochar, activated carbon, and TiO<sub>2</sub>) using open microwave system. The set temperature is 300 °C. Error bars represent the RSD ( $n = 3$ ).

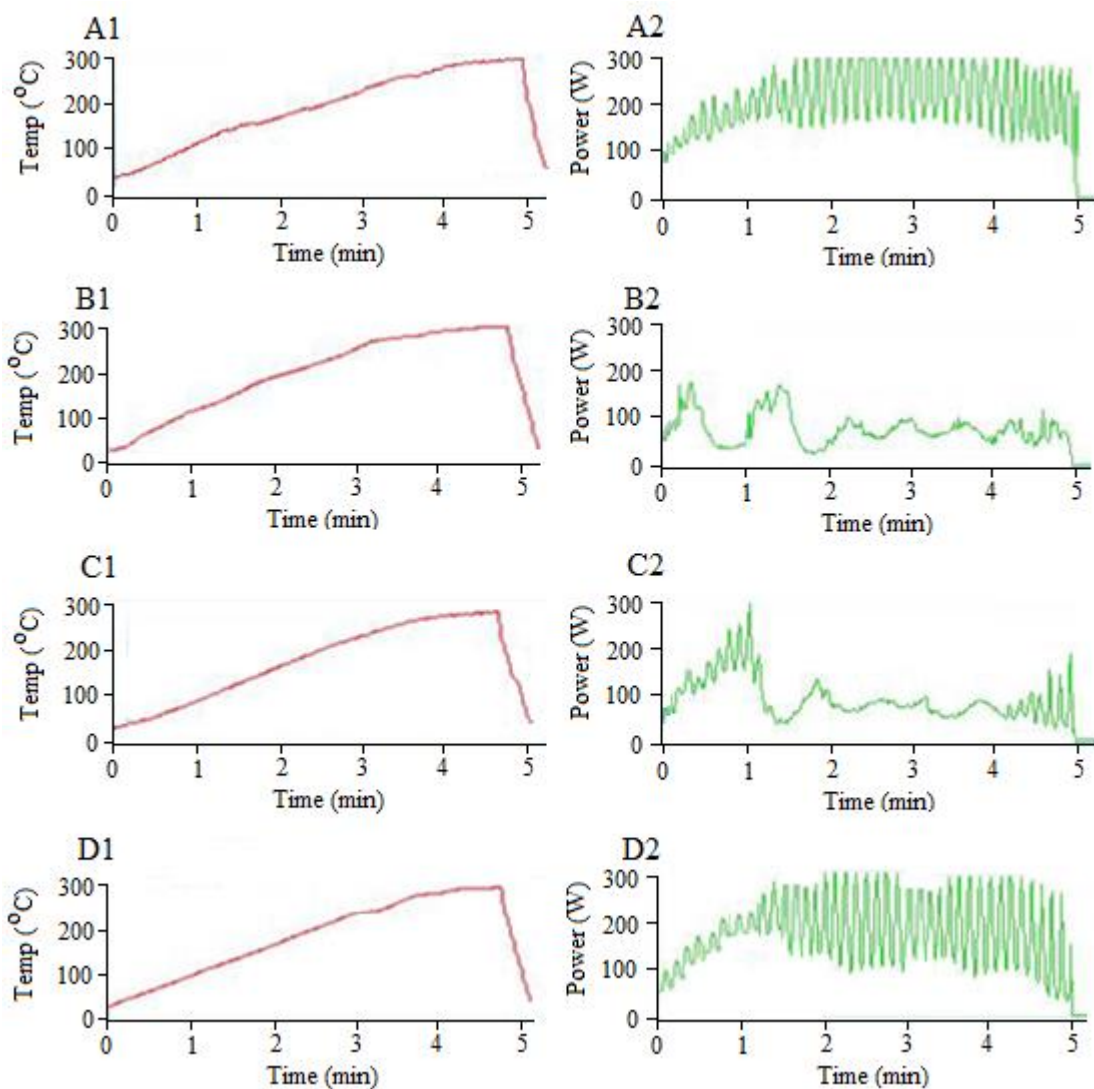


**Figure 4.11.** Temperature and microwave power profiles of microwave-assisted heating of coal tar dissolved in anhydrous ethanol (A1 and A2), coal tar with biochar in anhydrous ethanol (B1 and B2), coal tar with activated carbon in anhydrous ethanol (C1 and C2), and coal tar with  $\text{TiO}_2$  in anhydrous ethanol (D1 and D2)). Experiments were conducted using an open microwave system at a set temperature of 300 °C.

### 4.3.3. GC analyses

#### *Pyrene*

Figure 4.12 shows the GC-FID analysis of pyrene with biochar after MAH using the open and closed microwave systems. In the open microwave system, pyrene was observed in the volatile fraction due to the high temperature used (300 °C) without any pressure buildup. In contrast, in the case of the closed microwave system, pyrene mainly remains in the non-volatile fraction. This result may be due to the low set temperature used (190 °C) and the possibility that pressure may be a factor in the re-condensation of volatiles.

#### *Coal tar*

The PAHs in coal tar that were dissolved in DCM were identified using GC-MS and the chromatograph is shown in Figure 4.13. The ion count percentages of these compounds in coal tar are listed in Table 4.1. Naphthalene (**1**), phenanthrene (**6**), fluoranthene (**11**), and pyrene (**12**) are the predominant compounds in the coal tar and constitute ~76% of the total ion peak areas. Preliminary analysis of the volatile and non-volatile fractions from the closed system MAH of coal tar with and without microwave absorbers did not show any significant differences in PAH composition (PAHs were detected in both volatile and non-volatile fractions). Therefore, both volatile and non-volatile fractions were collected as a single fraction, using 4.0 mL of DCM, and were then analyzed by GC-FID (see Figure 4.14). In the case of using the open microwave system, most PAHs are transferred to the volatile fraction (Figures 4.15 and 4.16).

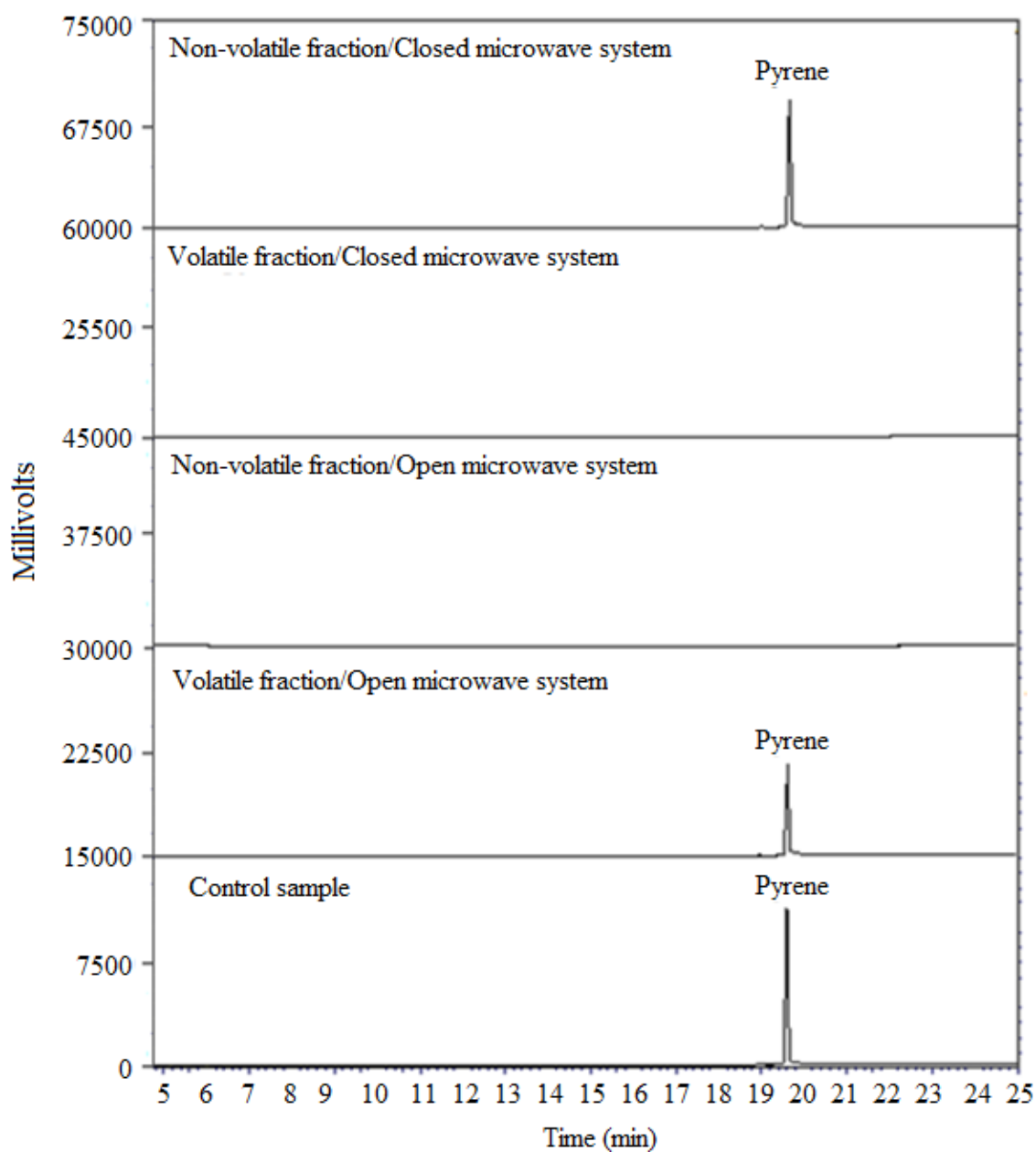


**Figure 4.12.** GC-FID analysis of pyrene (control sample), volatile and non-volatile fractions from microwave-assisted heating of pyrene with biochar using open and closed microwave systems.

PAHs identified were phenanthrene (**6**), anthracene (**7**), 2-methyanthracene (**8**), carbazole (**9**), 4*H*-cyclopenta[def]phenanthrene (**10**), fluoranthene (**11**), pyrene (**12**), chrysene (**13**), and benz[a]anthracene (**14**). They appear in both the volatile and non-volatile fractions when the coal tar and the coal tar with TiO<sub>2</sub> were exposed to microwave radiation. This behaviour may be due to the lack of enough energy to completely vaporize these compounds to the volatile fraction. Using carbon microwave absorbers such as biochar and AC with the coal tar in the open microwave system can enhance hot spot formation [28], which in turn may enhance removal of PAHs at relatively low temperatures. Interestingly all PAHs in the coal tar were only observed in the volatile fraction when microwave absorbers (biochar and AC) were added (Figure 4.15). Using a C<sub>18</sub> cartridge in the open microwave system (Figure 4.1D) helps to trap some of the volatile fraction (10-30%). The remaining part of the volatile fraction had condensed in the upper part of the microwave tube. The percentages of the volatile fractions, from the MAH of the coal tar with, and without, microwave absorbers (biochar, AC and TiO<sub>2</sub>), are in the range of 30-45 % (Figure 4.10). Figures 4.17 and 4.18 show the GC analysis of volatile and non-volatile fractions from MAH of coal tar/EtOH with and without microwave absorbers. Clearly, microwave absorbers enhance the removal of PAHs from coal tar/EtOH, and lead to significant removal of compounds **6-14** from coal tar. When microwave absorbers (biochar and AC) are added to coal tar/EtOH for 24 h, PAHs are absorbed on their surfaces. The sorption efficiencies were calculated based on the decrease in the peak areas of the PAHs in coal tar/EtOH (Figures 4.19 and 4.20). Among the microwave absorbers used, biochar shows high sorption efficiency (72-98%). This high sorption of PAHs by carbon additives (biochar and AC) is due to their porous structures and high surface area [29]. As a result, the sorption

of PAHs on carbon microwave absorbers may enhance PAH removal from coal tar when the absorbent particles with adsorbed PAHs are exposed to microwave irradiation.

Removal of PAHs is highly dependent on the PAH chemical structure, temperature, and time. For example, thermal treatment of benzo[a]pyrene (BaP), benzo[a]anthracene (BaA) and dibenz[a,h]anthracene (DBahA) in the solid state or when dissolved in hexane using a sealed vial at 100 °C or 200 °C, showed a high removal rate at a higher temperature (200 °C) with BaA having the highest removal rate [30]. Under thermal treatment of PAHs using the closed or open systems at a low temperature (300 °C), some of the PAHs convert to non-volatile products (charring) [31]. In addition, soot (i.e. amorphous carbon) can form during the thermal degradation of coal tar at high temperatures (>700 °C) using a conventional heating source such as a Fluidized-Bed Reactor [32].

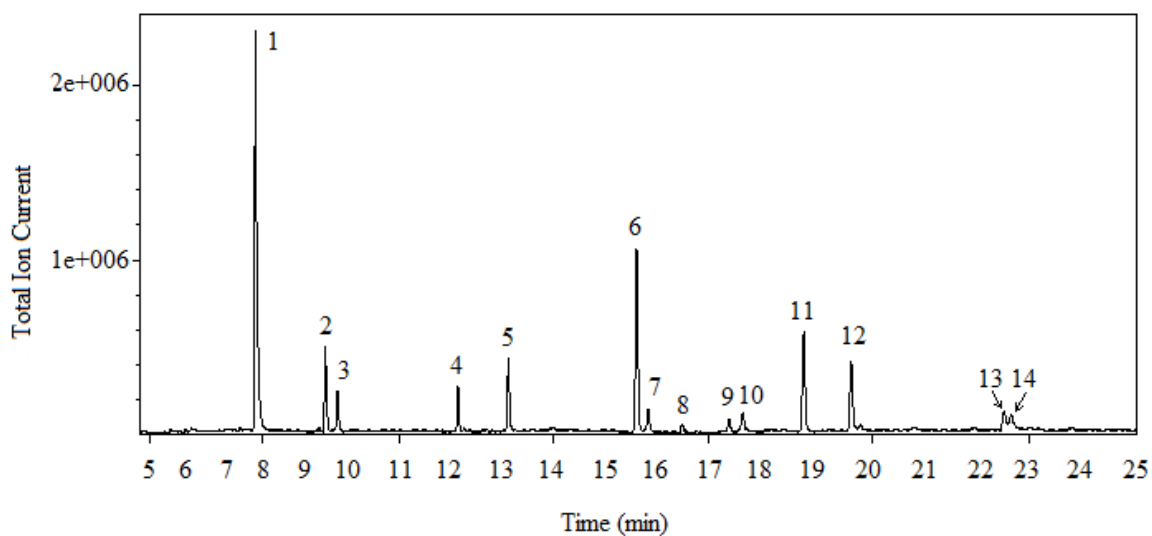


**Figure 4.13.** GC-MS TIC of coal tar dissolved in DCM. Compound were identified and listed in Table 4.1.

**Table 4.1.** PAH compounds identified in coal tar using GC-FID.

<b>Peak #</b>	<b>Compound name</b>	<b>Time (min)</b>	<b>Area (%)</b>
1	Naphthalene	7.8	39.9
2	2-Methylnaphthalene	9.5	3.3
3	1-Methylnaphthalene	9.8	1.3
4	Acenaphthene	12.2	3.5
5	Fluorene	13.18	6.5
6	Phenanthrene	15.8	18.7
7	Anthracene	15.9	2.2
8	Carbazole	16.6	0.7
9	9-Methylanthracene	17.3	1.7
10	4 <i>H</i> -Cyclopenta[def]phenanthrene	17.5	2.0
11	Fluoranthene	18.8	11.0
12	Pyrene	19.8	6.3
13	Benz[a]anthracene	22.6	1.7
14	Chrysene	22.7	1.2

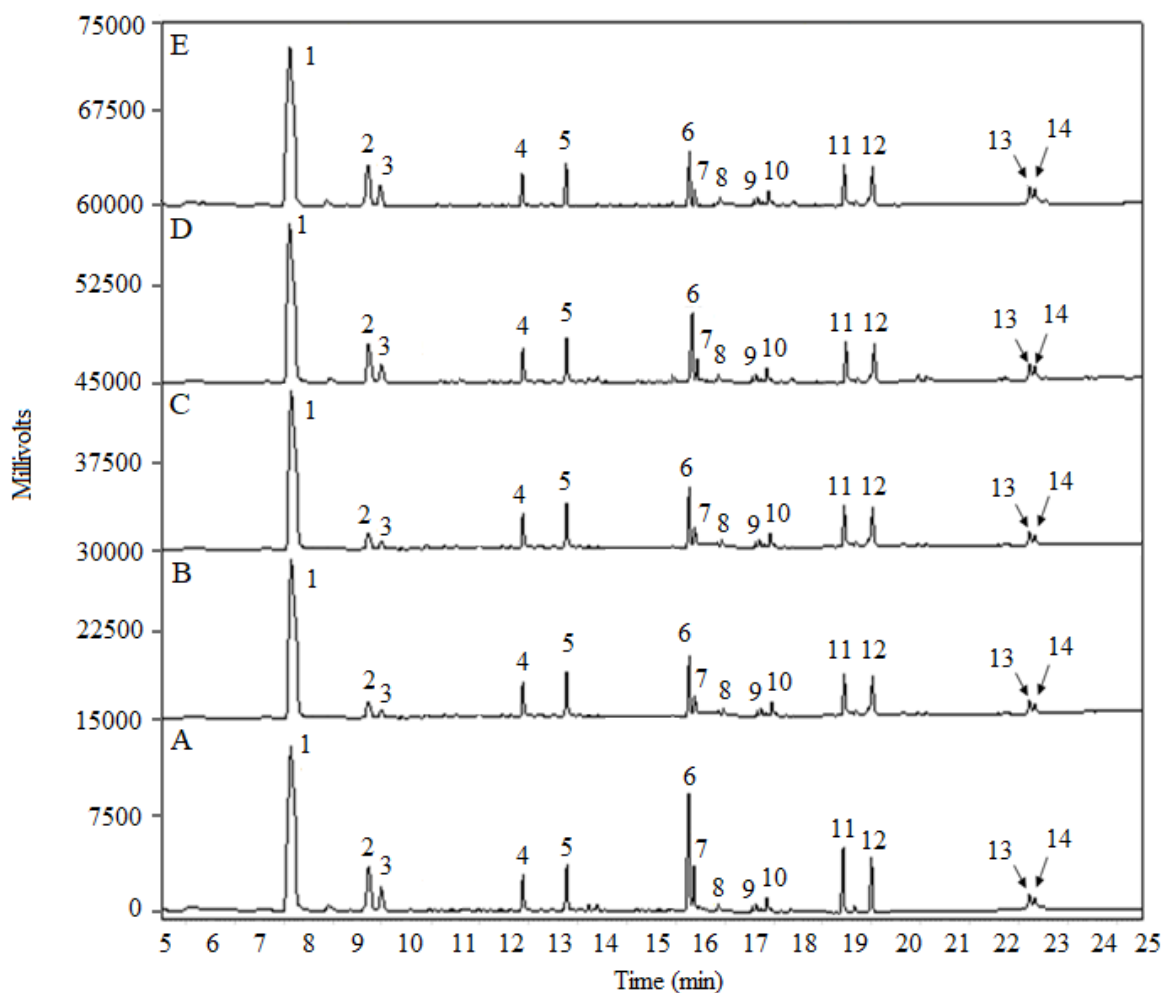


**Figure 4.14.** GC-FID chromatograms of the combined fractions (volatile + non-volatile) from coal tar after microwave-assisted heating of coal tar (A), coal tar with biochar (B), coal tar with activated carbon (C), and coal tar with  $\text{TiO}_2$  (D) using the closed microwave system at a set temperature of 190 °C.

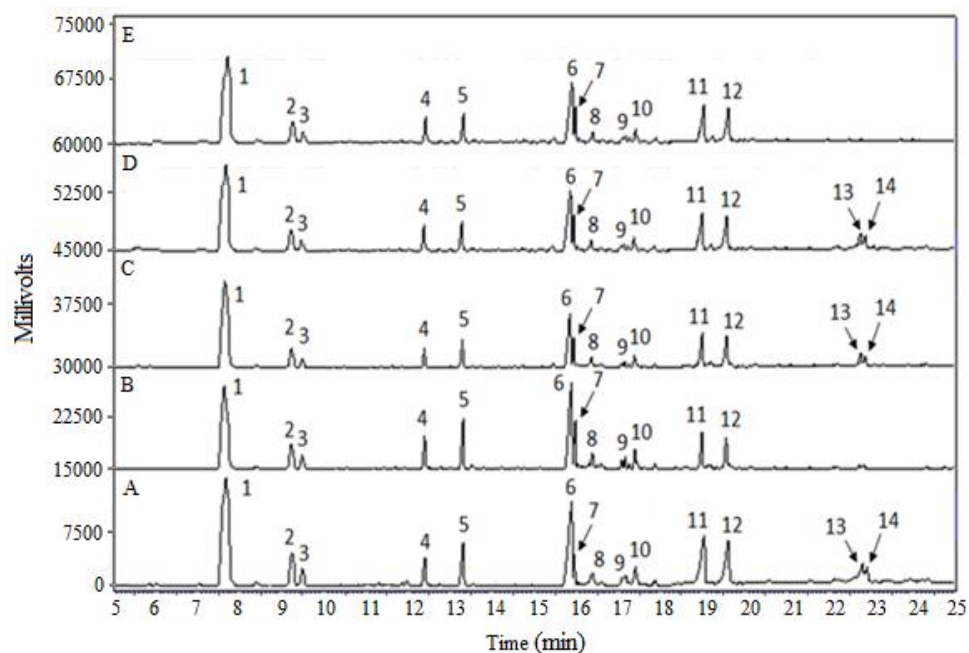


**Figure 4.15.** GC-FID chromatograms of coal tar (A) and volatile fractions from microwave-assisted heating of coal tar (B), coal tar with biochar (C), coal tar with activated carbon (D), and coal tar with TiO<sub>2</sub> (E) using the open microwave system at a set temperature of 300 °C.

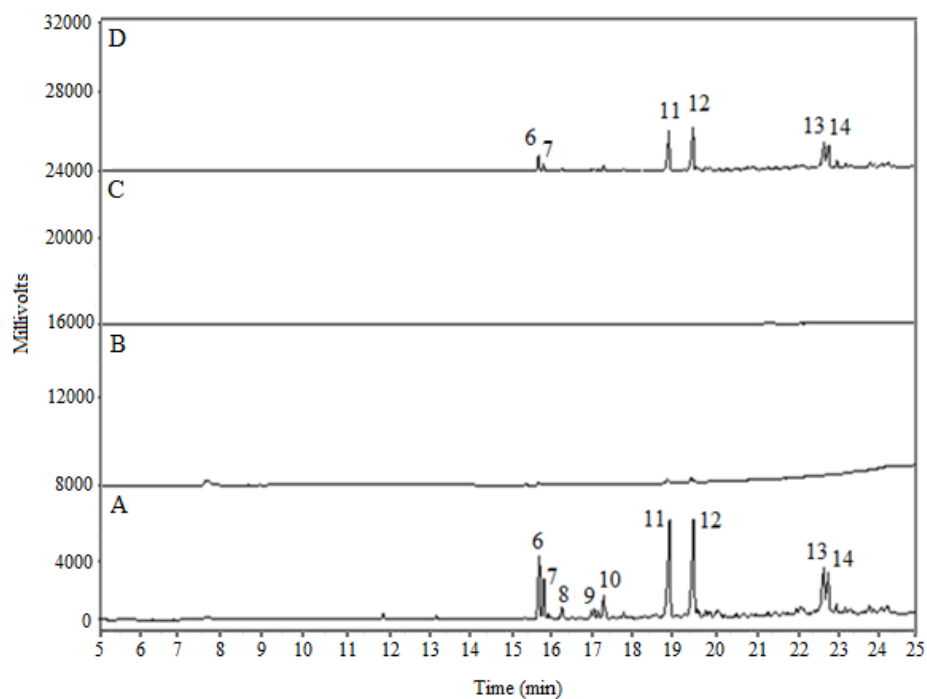


**Figure 4.16.** GC-FID chromatograms of non-volatile fractions from microwave-assisted heating of coal tar (A), coal tar with biochar (B), coal tar with activated carbon (C), and coal tar with TiO<sub>2</sub> (D) using the open microwave system at a set temperature of 300 °C.

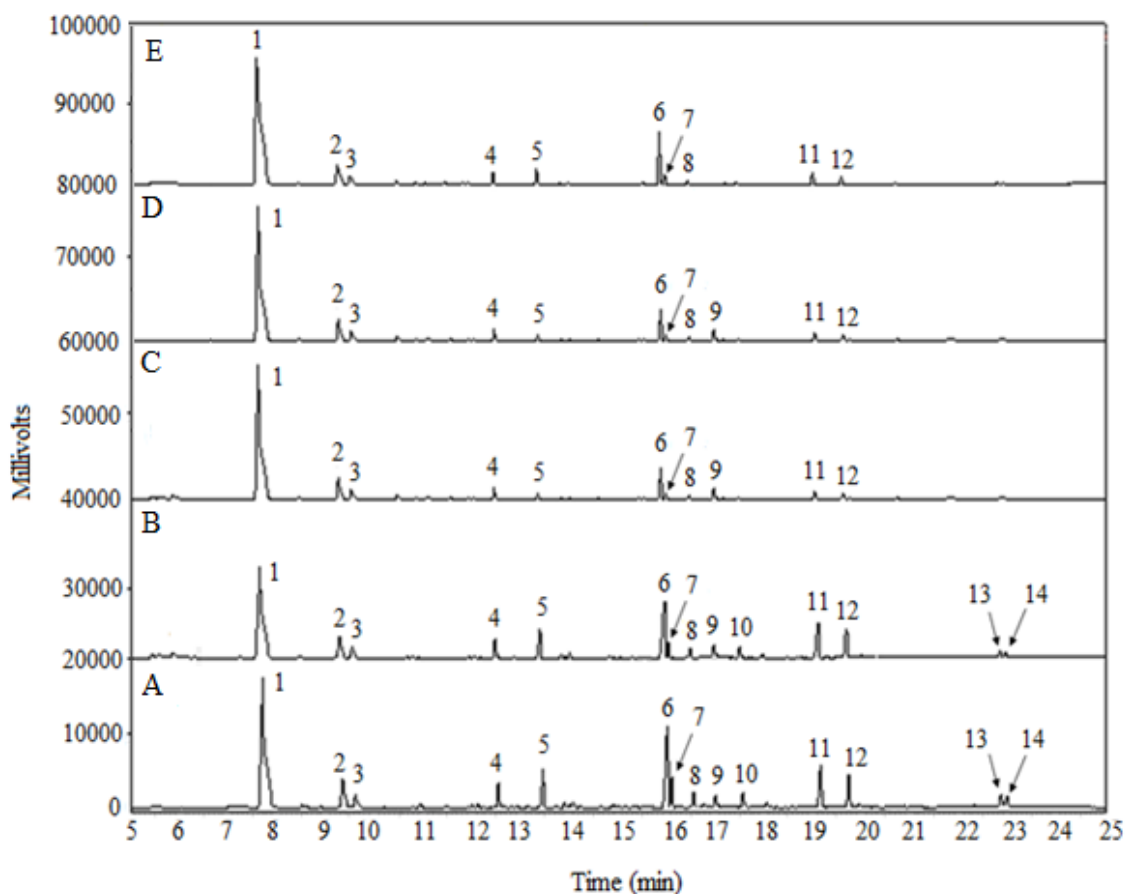


**Figure 4.17.** GC-FID analysis of coal tar fraction that is dissolved in anhydrous EtOH (A) and volatile fraction from microwave-assisted heating of coal tar/EtOH (B), coal tar/EtOH with activated carbon (C), coal tar/EtOH with biochar (D), and coal tar/EtOH with TiO<sub>2</sub> (E). Microwave experiments were achieved using an open system at a set temperature of 300 °C.

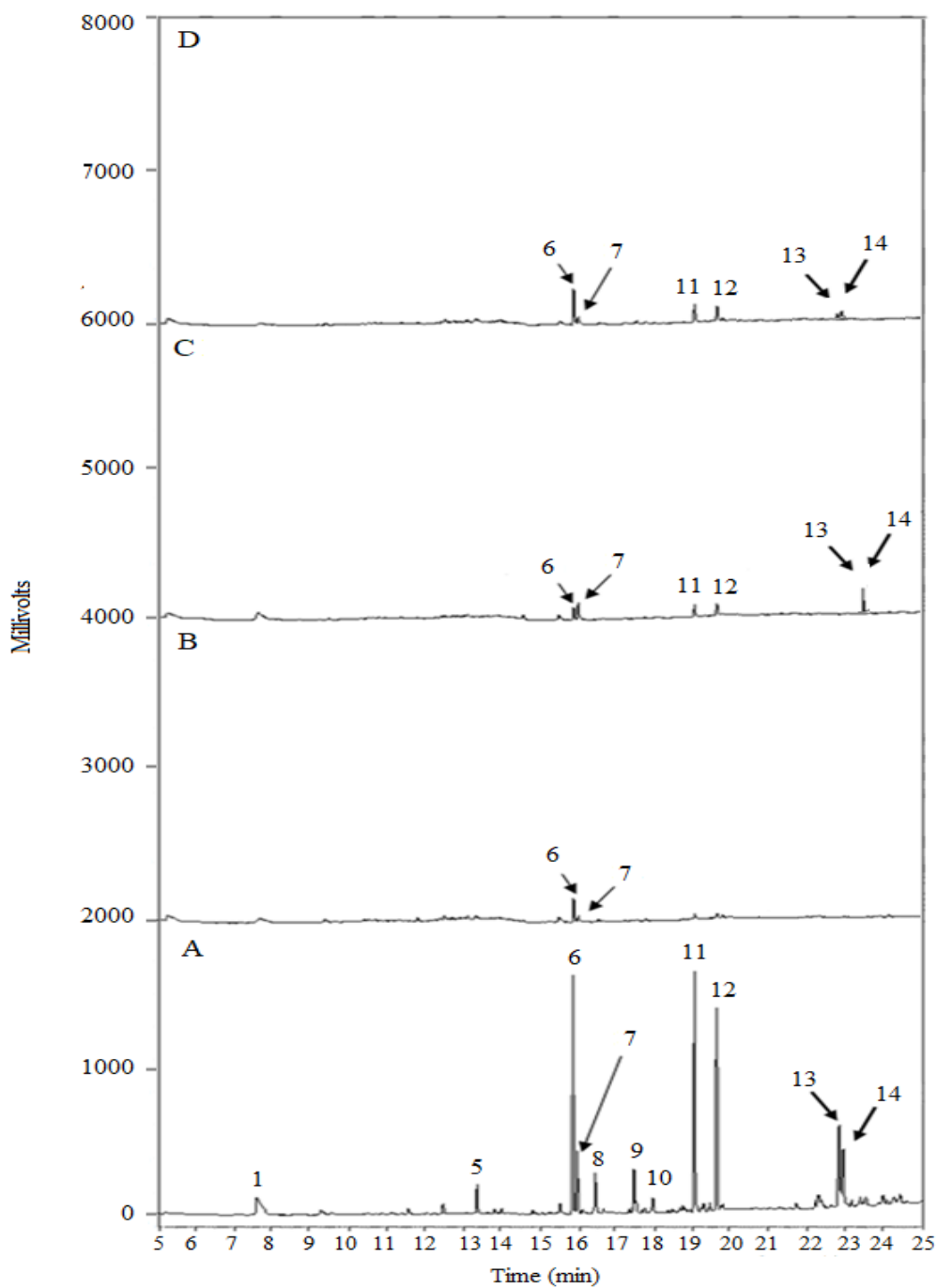


**Figure 4.18.** GC-FID chromatograms of the non-volatile fraction from microwave-assisted heating of coal tar/EtOH (A), with biochar (B), with activated carbon (C), and with TiO<sub>2</sub> (D). Experiments were achieved using an open microwave system at a set temperature of 300 °C.

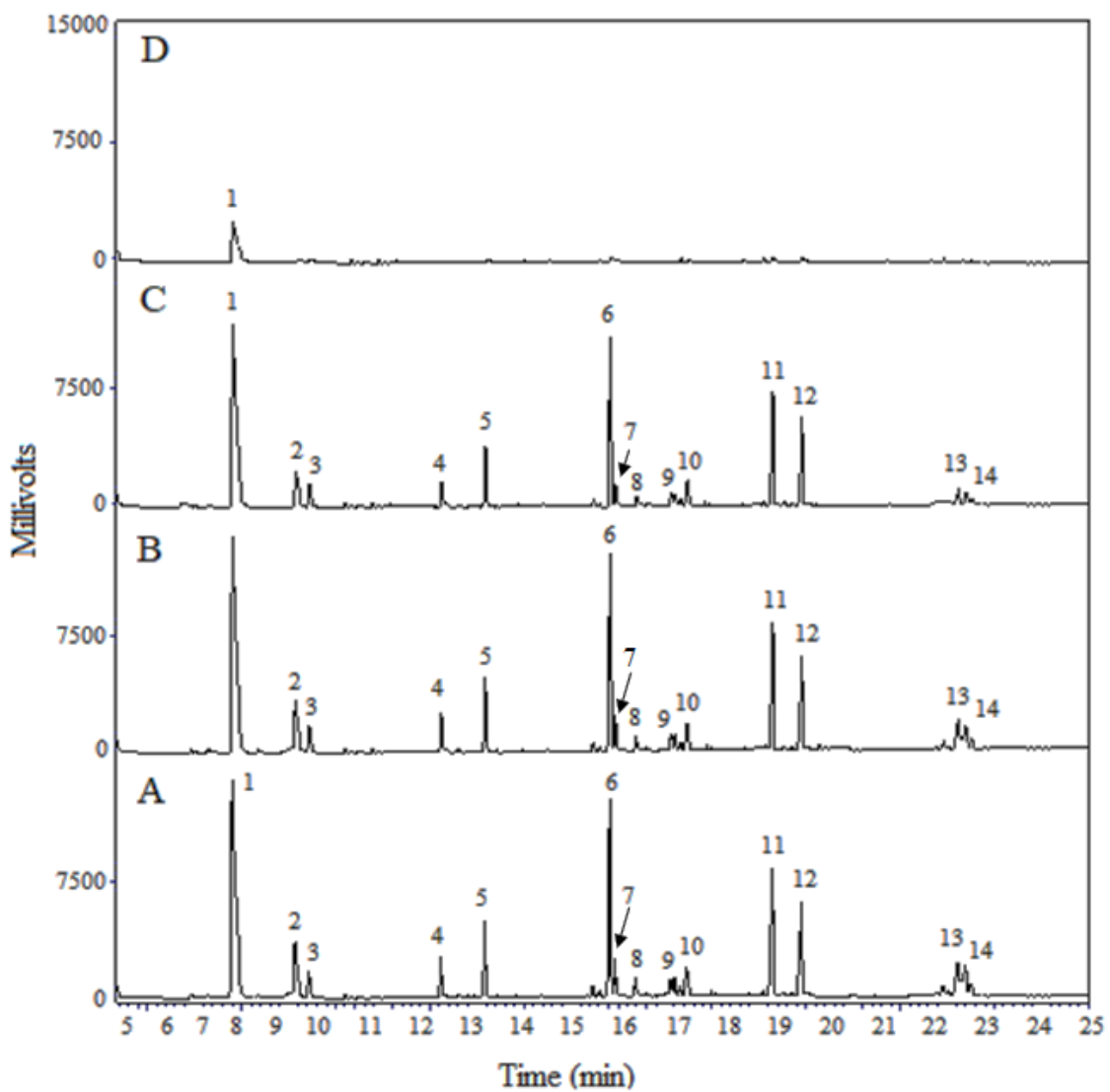


**Figure 4.19.** GC-FID analysis of coal tar/EtOH (A) and supernatants of coal tar/EtOH with  $\text{TiO}_2$  (B), with activated carbon (C), and with biochar (D) after 24 h of absorption time.

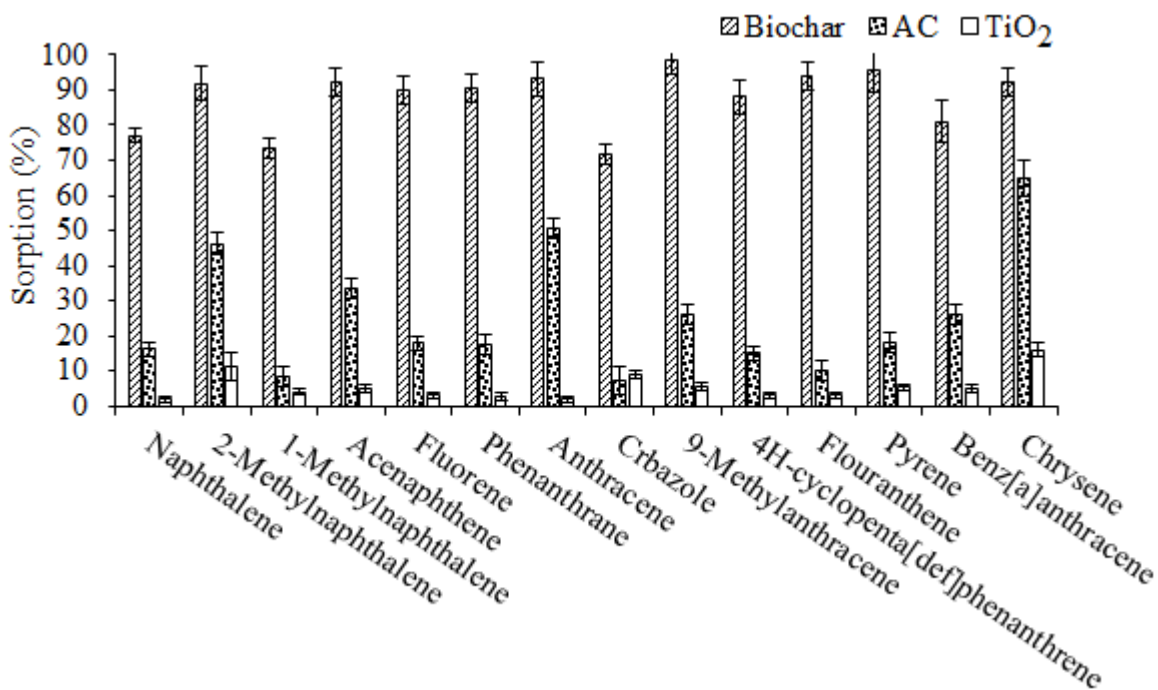


**Figure 4.20.** Percentage of PAH sorption from coal tar soluble in anhydrous after mixing with biochar, activated carbon (AC), and TiO<sub>2</sub>. Error bars represent the RSD%, n=3

#### 4.3.4. TGA analysis

TGA is an effective analytical technique measuring the change in sample weight as a function of temperature and time [26]. Figure 4.21 shows the TGA analysis of the coal tar, with and without biochar, AC, and TiO<sub>2</sub>. The coal tar sample used in the current work is mostly free of water content (< 1%, calculated by the Karl Fischer Method). The light volatile contents were removed from the coal tar at 150 °C. The percentages of these fractions from the coal tar, coal tar + biochar, coal tar + AC, and coal tar + TiO<sub>2</sub> samples were 5%, 21%, 13%, and 1%, respectively. The volatile fractions were completely removed at ~500 °C and the percentage of these volatile fractions from the coal tar, coal tar + biochar, coal tar + AC, and coal tar + TiO<sub>2</sub> samples were 67%, 85%, 73%, and 50%, respectively. Consequently, biochar and AC increase the percentage of volatile fraction from coal tar,

while  $\text{TiO}_2$  decreases it. This may be due to a potential interaction between  $\text{TiO}_2$  and PAHs in coal tar [34–36], which could reduce the PAH volatility. The water content and the light volatile components from biochar and AC itself can be ignored, since homogenous mixing of the additive with coal tar was achieved at 80 °C for 10 min, which in turn reduces the coal tar viscosity. The volatile fraction from the TGA of the coal tar is 54% at 300 °C, which is the same as the final temperature of the GC column oven and the injector temperature. This result confirms that GC is a reliable analytical technique for coal tar analysis [37]. In addition, TGA analysis of coal tar at 300 °C approximately shows similar results (39-60%, non-volatile fraction) as the open microwave system, but MAH is faster and offers the ability to separate the volatile and non-volatile fractions.

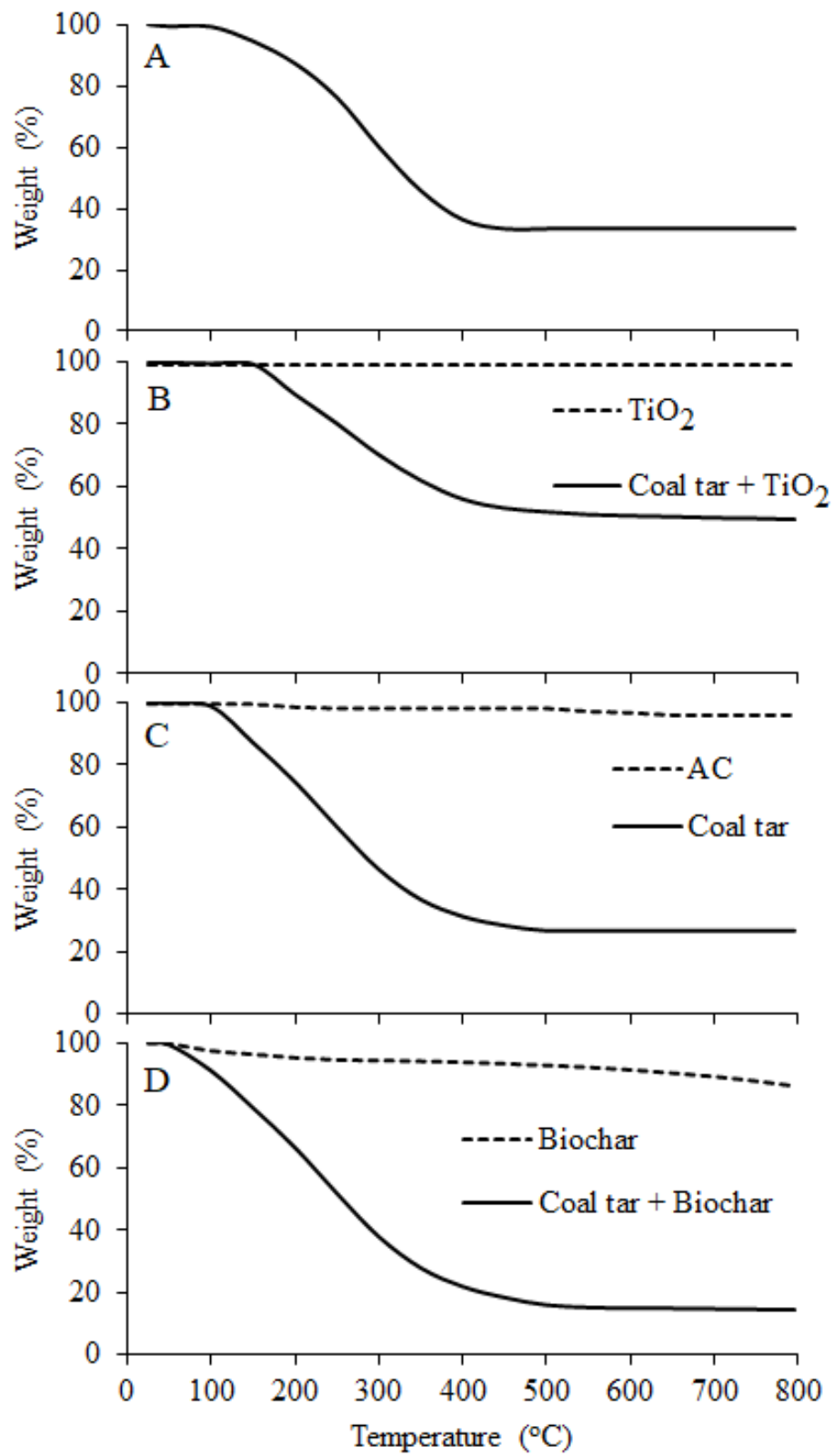


**Figure 4.21.** TGA analysis of coal tar with and without additive (biochar, AC, and  $\text{TiO}_2$ ).

#### **4.4. Conclusions**

MAH of coal tar at low temperatures ( $T \leq 300$  °C) is an effective and rapid method for removing PAHs from coal tar. When using a closed microwave system, the heating rate of the microwave can be increased by adding microwave absorbers such as AC and biochar. In addition, microwave absorbers reduce energy consumption. Anhydrous ethanol is a suitable solvent for extracting coal tar components and it assists the mixing of coal tar with microwave absorbers such as AC, biochar, and TiO<sub>2</sub>. The use of carbon microwave absorbers with coal tar enhances removal of PAHs from coal tar. Conventional pyrolysis of coal tar usually requires a high temperature (500 °C) to remove of the all volatile content, while the use of carbon materials (e.g., AC and biochar) with coal tar increases the percentage of the volatile fraction at the expense of the non-volatile fraction (residue).

#### 4.5. References

- [1] Sun, X.; Yin, S.; Wang, H.; Li, C.; Zhang, S. Effect of the Addition of Cornstalk to Coal Powder/coal Tar Combustion. *J. Therm. Anal. Calorim.* **2012**, *109*, 817–823.
- [2] Fardhyanti, D. S.; Damayanti, A. Analysis of Coal Tar Compositions Produced from Sub-Bituminous Kalimantan Coal Tar. **2015**, *9*, 1022–1025.
- [3] Zhu, J. L.; Fan, X.; Wei, X. Y.; Wang, S. Z.; Zhu, T. G.; Zhou, C. C.; Zhao, Y. P.; Wang, R. Y.; Lu, Y.; Chen, L.; You, C. Y. Molecular Characterization of Heteroatomic Compounds in a High-Temperature Coal Tar Using Three Mass Spectrometers. *Fuel Process. Technol.* **2015**, *138*, 65–73.
- [4] Scholes, G. C.; Gerhard, J. I.; Grant, G. P.; Major, D. W.; Vidumsky, J. E.; Switzer, C.; Torero, J. L. Smoldering Remediation of Coal-Tar-Contaminated Soil: Pilot Field Tests of STAR. *Environ. Sci. Technol.* **2015**, *49*, 14334–14342.
- [5] Ukiwe, L. N.; Egereonu, U. U.; Njoku, P. C.; Nwoko, C. I. a.; Allinor, J. I. Polycyclic Aromatic Hydrocarbons Degradation Techniques: A Review. *Int. J. Chem.* **2013**, *5*, 43–55.
- [6] Lau, E. V.; Gan, S.; Ng, H. K. Extraction Techniques for Polycyclic Aromatic Hydrocarbons in Soils. *Int. J. Anal. Chem.* **2010**, *2010*, 1–9.
- [7] Falciglia, P. P.; De Guidi, G.; Catalfo, A.; Vagliasindi, F. G. A. Remediation of Soils Contaminated with PAHs and Nitro-PAHs Using Microwave Irradiation. *Chem. Eng. J.* **2016**, *296*, 162–172.
- [8] Ahmed, M. J. Application of Agricultural Based Activated Carbons by Microwave and Conventional Activations for Basic Dye Adsorption: Review. *J. Environ. Chem. Eng.* **2016**, *4*, 89–99.
- [9] Lam, S. S.; Wan Mahari, W. A.; Jusoh, A.; Chong, C. T.; Lee, C. L.; Chase, H. A. Pyrolysis Using Microwave Absorbents as Reaction Bed: An Improved Approach to Transform Used Frying Oil into Biofuel Product with Desirable Properties. *J. Clean. Prod.* **2017**, *147*, 263–272.
- [10] Liu, H. P.; Chen, T. P.; Li, Y.; Song, Z. Y.; Wang, S. W.; Wu, S. H. Temperature Rise Characteristics of ZhunDong Coal during Microwave Pyrolysis. *Fuel Process. Technol.* **2016**, *148*, 317–323.
- [11] Ganesapillai, M.; Manara, P.; Zabaniotou, A. Effect of Microwave Pretreatment on Pyrolysis of Crude Glycerol-Olive Kernel Alternative Fuels. *Energy Convers. Manag.* **2016**, *110*, 287–295.
- [12] Yunpu, W.; Leilei, D.; Liangliang, F.; Shaoqi, S.; Yuhuan, L.; Roger, R. Review of Microwave-Assisted Lignin Conversion for Renewable Fuels and Chemicals. *J. Anal. Appl. Pyrolysis* **2016**, *119*, 104–113.
- [13] Mishra, R. R.; Sharma, A. K. Microwave-Material Interaction Phenomena: Heating Mechanisms, Challenges and Opportunities in Material Processing. *Compos. Part A Appl. Sci. Manuf.* **2016**, *81*, 78–97.

- [14] Anwar, J.; Shafique, U.; Waheed-uz-Zaman; Rehman, R.; Salman, M.; Dar, A.; Anzano, J. M.; Ashraf, U.; Ashraf, S. Microwave Chemistry: Effect of Ions on Dielectric Heating in Microwave Ovens. *Arab. J. Chem.* **2015**, *8*, 100–104.
- [15] Wang, N.; Wang, P. Study and Application Status of Microwave in Organic Wastewater Treatment - A Review. *Chem. Eng. J.* **2016**, *283*, 193–214.
- [16] De, A.; Díaz-Ortiz, Á.; Moreno, A. Microwaves in Organic Synthesis. Thermal and Non-Thermal Microwave Effects. *Chem. Soc. Rev.* **2005**, *34*, 164–178.
- [17] Bo, L. L.; Zhang, Y. B.; Quan, X.; Zhao, B. Microwave Assisted Catalytic Oxidation of P-Nitrophenol in Aqueous Solution Using Carbon-Supported Copper Catalyst. *J. Hazard. Mater.* **2008**, *153*, 1201–1206.
- [18] Fu, J.; Wen, T.; Wang, Q.; Zhang, X. W.; Zeng, Q. F.; An, S. Q.; Zhu, H. L. Degradation of Active Brilliant Red X-3B by a Microwave Discharge Electrodeless Lamp in the Presence of Activated Carbon. *Environ. Technol.* **2010**, *31*, 771–779.
- [19] Jones, D. a.; Lelyveld, T. P.; Mavrofidis, S. D.; Kingman, S. W.; Miles, N. J. Microwave Heating Applications in Environmental Engineering— a Review. *Resour. Conserv. Recycl.* **2002**, *34*, 75–90.
- [20] Liu, X.; Yu, G. Combined Effect of Microwave and Activated Carbon on the Remediation of Polychlorinated Biphenyl-Contaminated Soil. *Chemosphere* **2006**, *63*, 228–235.
- [21] Yuan, S.; Tian, M.; Lu, X. Microwave Remediation of Soil Contaminated with Hexachlorobenzene. *J. Hazard. Mater.* **2006**, *137*, 878–885.
- [22] Domínguez, A.; Blanco, C.; Santamaría, R.; Granda, M.; Blanco, C. G.; Menéndez, R. Monitoring Coal-Tar Pitch Composition Changes during Air-Blowing by Gas Chromatography. *J. Chromatogr. A* **2004**, *1026*, 231–238.
- [23] Fan, X.; Fei, Y.; Chen, L.; Li, W. Distribution and Structural Analysis of Polycyclic Aromatic Hydrocarbons Abundant in Coal Tar Pitch. *Energy and Fuel* **2017**, *31*, 4694–4704
- [24] Morgan, T. J.; George, A.; Álvarez, P.; Millan, M.; Herod, A. A.; Kandiyoti, R. Characterization of Molecular Mass Ranges of Two Coal Tar Distillate Fractions (Creosote and Anthracene Oils) and Aromatic Standards by LD-MS, GC-MS, Probe-MS and Size-Exclusion Chromatography. *Energy and Fuels* **2008**, *22*, 3275–3292.
- [25] Mushtaq, F.; Mat, R.; Ani, F. N. A Review on Microwave Assisted Pyrolysis of Coal and Biomass for Fuel Production. *Renew. Sustain. Energy Rev.* **2014**, *39*, 555–574.
- [26] Horikoshi, S.; Sakai, F.; Kajitani, M.; Abe, M.; Emeline, A. V.; Serpone, N. Microwave-Specific Effects in Various TiO<sub>2</sub> Specimens. Dielectric Properties and Degradation of 4-Chlorophenol. *J. Phys. Chem. C* **2009**, *113*, 5649–5657.
- [27] Lundstedt, S.; Persson, Y.; Öberg, L. Transformation of PAHs during Ethanol-Fenton Treatment of an Aged Gasworks' Soil. *Chemosphere* **2006**, *65*, 1288–1294.
- [28] Luo, H.; Bao, L.; Kong, L.; Sun, Y. Low Temperature Microwave-Assisted

- Pyrolysis of Wood Sawdust for Phenolic Rich Compounds: Kinetics and Dielectric Properties Analysis. *Bioresour. Technol.* **2017**, *238*, 109–115.
- [29] Lamichhane, S.; Bal Krishna, K. C.; Sarukkalige, R. Polycyclic Aromatic Hydrocarbons (PAHs) Removal by Sorption: A Review. *Chemosphere* **2016**, *148*, 336–353.
- [30] Chen, Y. C.; Chen, B. H. Stability of Polycyclic Aromatic Hydrocarbons during Heating. *J. Food Drug Anal.* **2001**, *9*, 33–39.
- [31] Kopinke, F. D.; Remmler, M. Reactions of Hydrocarbons during Thermodesorption from Sediments. *Thermochim. Acta* **1995**, *263*, 123–139.
- [32] Li, C.; Nelson, P. F. Fate of Aromatic Ring Systems during Thermal Cracking of Tars in a Fluidized-Bed Reactor. *Energy* **1996**, *12*, 1083–1090.
- [33] Jain, A. A.; Mehra, A.; Ranade, V. V. Processing of TGA Data: Analysis of Isoconversional and Model Fitting Methods. *Fuel* **2016**, *165*, 490–498.
- [34] Dhasmana, A.; Mohd. Sajid Jamal, Q.; Mir, S. S.; Lal Bramha Bhatt, M.; Rahman, Q.; Gupta, R.; Siddiqui, M. H.; Lohani, M. Titanium Dioxide Nanoparticles as Guardian against Environmental Carcinogen Benzo[alpha]pyrene. *PLoS One* **2014**, *9*, 1–9.
- [35] Benjalak Karnchanaset, O. S. A Preliminary Study for Removing Phenanthrene and Benzo(a) Pyrene from Soil by Nanoparticles. *J. Appl. Sci.* **2007**, *7*, 3317–3321.
- [36] Jin, X.; Kusumoto, Y. Spectroscopic Studies of Pyrene Adsorbed to Titanium Dioxide. *Chem. Phys. Lett.* **2003**, *378*, 192–194.
- [37] Wu, Y. Y.; Li, J. J.; Xu, J.; Jiao, C. J.; Wang, D. Q.; Ding, W. Z. Determination of the Volatile Fraction of Coal Tar. *J. Shanghai Univ.* **2010**, *14*, 313–321.

## **Chapter 5**

### **A preliminary study for PAH bromination in coal tar using HBr-H<sub>2</sub>O<sub>2</sub>**

## **Abstract**

In this study, hydrogen peroxide was combined with hydrobromic acid to brominate pyrene, a representative model PAH. The results indicate that pyrene was converted to 1-bromopyrene in high yield (96%) within 12 h. The same method was also used for PAH bromination in coal tar. Bromination of PAHs in coal tar, however, is more complicated. It was found that the removal percentages of PAHs increase with increasing amount of brominating reagent. Identification of any simple brominated products from the bromination experiments of coal tar by GC-MS and GC-FID was attempted but failed to give meaningful results.

## 5.1. Introduction

Polycyclic aromatic hydrocarbons (PAHs) have received a great attention due to their negative impact on environment and human health [1]. Several methods have been used to degrade PAHs, such as thermal, physical, chemical, and biological remediation [2]. Bromination is widely used to activate many organic compounds including PAHs to produce useful brominated derivatives and intermediates which can be further used in industrial applications including pharmaceuticals, fine chemicals, agrochemicals, fire retardants, pesticides, and herbicides [3]. Some pyrene derivatives (e.g., 1,3,6,8-tetrabromopyrene) have been used as organic chromophores and as light emitting materials in organic field effect transistors [4]. Bromination can be achieved using different reagents, such as *N*-bromosuccinimide (NBS) [5], 3-methylimidazolium tribromide [6], DMSO-HBr [7],  $\text{NH}_4\text{VO}_3\text{-H}_2\text{O}_2\text{-HBr/KBr}$  [8],  $\text{Bu}_4\text{NBr-V}_2\text{O}_5\text{-H}_2\text{O}_2$  [9], poly(diallyldimethylammonium tribromide) [10], KBr-benzyltriphenylphosphonium peroxymonosulfate [11], bromodichloroisocyanuric acid [12], *N,N,N,N*-tetrabromobenzene-1,3-disulfonylamide [13], NBS- $\text{CCl}_4$  [14], NBS- $\text{H}_2\text{SO}_4$  [15],  $\text{Br}_2\text{-SO}_2\text{Cl}_2$  [16],  $\text{Br}_2\text{-hexamethylenetetramine}$  [17], KBr- $\text{NaBO}_3\cdot 4\text{H}_2\text{O}$  [18], NBS-Amberlyst [19], *tert*-BuOOH- or  $\text{H}_2\text{O}_2\text{-HBr}$  [20], NBS- $\text{ZrCl}_4$  [21], NBS-Tetrabutylammonium bromide [22], NBS- $\text{Pd}(\text{OAc})_2$  [23], NBS/*p*-toluenesulfonic acid [24],  $\text{Br}_2\text{-(1-butyl-3-methylimidazolium nitrate)}$  [25], NBS- $\text{NH}_4\text{OAc}$  [26], NaBr-oxone [27], NBS- $\text{SiO}_2$  [28], NBS- $\text{Al}_2\text{O}_3$  [29], NBS-THF [30], and microporous organic polymers-HBr- $\text{O}_2$  [31]. The use of molecular bromine, however, has several disadvantages since it is toxic, corrosive, not easily-handled, and non-selective [32]. Therefore, it was of interest to find an alternative method for PAH bromination, which is environmentally friendly, relatively cheap, and can produce a high yield of desired products. HBr- $\text{H}_2\text{O}_2$  was

used in this study. A brief description of the advantages of this reagent can be found in Chapter 1, Section 1.4.3.4.

The objective of this study was to undertake a preliminary evaluation of the ability of HBr-H<sub>2</sub>O<sub>2</sub> as a reagent for the monobromination of pyrene in methanol/diethylether solvent, and to investigate the potential of this reagent for brominating PAHs in coal tar.

## **5.2. Experimental**

### **5.2.1. Chemicals**

Pyrene (>98%) was purchased from Alfa Aesar (USA) and used as received. Hydrobromic acid (47%) and H<sub>2</sub>O<sub>2</sub> (30%, w/v) were purchased from ACP Chemicals Inc. (Montreal, QC, Canada). Nitrobenzene (99%) used as an internal standard was purchased from Fisher Scientific (Bridgewater, NJ, USA). Dichloromethane (DCM), diethyl ether, and methanol were purchased from Sigma Aldrich and used without further purification. Coal tar samples were collected from Sydney Tar Ponds, Nova Scotia, Canada.

### **5.2.2. Method**

#### **5.2.2.1. Pyrene bromination**

The procedure used in this study for pyrene bromination was based on the optimum conditions reported in a previous study [33]. Pyrene (0.202 g, 1.00 mmol) was placed in a 50 mL round-bottom flask, then 15 mL of methanol/diethyl (1:1, v:v) was added. Hydrobromic acid (123 µL of 48% aqueous solution, 1.10 mmol) was then added, followed by slow addition of hydrogen peroxide (104 µL of 30% aqueous solution, 1.00 mmol) in three portions over 15 min at low temperature (5-10 °C). The reaction mixture was vigorously stirred and left at room temperature for 12 h in the dark. The reaction progress was monitored by TLC. The reaction was quenched by adding 15.0 mL of water and 15.0

mL of DCM. The mixture was vigorously shaken by hand for 0.5 min and then left for 10 min to separate. The DCM extracts were analyzed by GC-MS and GC-FID.

#### **5.2.2.2. Coal tar bromination**

Coal tar largely consists of PAHs and the concentrations of pyrene and other major PAHs in coal tar (Table 5.1) were determined using the calibration curves of standard PAHs, which were carried out in triplicate with good linearity ( $R^2 > 0.98$ ). The same procedure used above for the pyrene bromination was also used for the PAH bromination in coal tar. The coal tar extract solution was prepared by mixing 8.30 g of coal tar with 15.0 mL of methanol/diethyl ether (1:1, v:v) and sonicated for 1.0 h. Filtration was done using a 0.45  $\mu\text{m}$  PTFE filter. It was found that only 58% of the coal tar was dissolved.

#### **5.2.2.3. GC analysis**

##### *GC-MS*

An Agilent Technologies 6890 gas chromatograph equipped with an Agilent 7683 Series Injector and Agilent 5973 inert Mass Selective Detector (MSD) was used for GC-MS. The GC capillary used was a DB-5 column (30 m x 0.25 mm i.d. x 0.25  $\mu\text{m}$  film thickness). The analytes were ionized by electron ionization at 70 eV with a scan range of m/z 40-550, and their mass spectra were matched with the NIST library database. Furthermore, retention time data from references [34–36] was used for compound identification and model compound analysis. The temperature program for the GC-MS oven was 50 °C for 1 min then gradually increased to 300 °C at a heating rate of 10 °C/min and held for 2 min at the final temperature. 2  $\mu\text{L}$  of the sample was injected in splitless injection mode. The injector, interface, and detector temperatures were 300, 250, 280 °C, respectively.

### *GC-FID*

The GC-FID (Thermo Fisher Ultra Trace) was equipped with the same type of column as the one used in the GC-MS. The temperature programming of the GC-FID oven was the same used in the GC-MS analysis mentioned above. The injector and flame temperatures were 300 °C and the sample (2 µL) was introduced in splitless injection mode.

## **5.3. Results and discussion**

### **5.3.1. Pyrene bromination**

Pyrene is one of the main coal tar components and its concentration in the coal tar samples used in the present study was 42 g/kg. Therefore, pyrene was chosen to be a representative model compound for the PAHs in coal tar. The bromination of pyrene using H<sub>2</sub>O<sub>2</sub>-HBr gives a high conversion (96%) to product within 12 h. The results of GC analysis of pyrene before and after the bromination reaction are shown in Figure 5.1. The reaction produces mainly 1-bromopyrene. A proposed mechanism of this reaction is shown in Scheme 5.1 [37]. Clearly, the proposed reaction mechanism includes two steps: 1) formation of the hydroxyl and bromo free radicals, and 2) production of 1-bromopyrene from the reaction between pyrene and the bromo radical in the presence of hydroxyl radical which removes a hydrogen atom to bring about the re-aromatization of the ring. The attack of the bromo radical at the pyrene at C1 is favored because it presumably forms a tertiary radical (**I**) (Scheme 5.2) [38]. Radical (**I**) can be stabilized forming several resonance structures such as structures (**I-V**). Reaction at C10 however would form the less favored secondary radical.

Quantum chemical computations on pyrene were performed using density functional theory (DFT) [39]. The method and results are attached as Appendix C. According to these

computational results, monobromination of pyrene at C1 is more favored than the bromination at C10. The active sites in pyrene for the free radical and electrophilic substitution reaction have been described in a previous study [40]. The active sites of pyrene (Figure 5.2) were therefore determined based on both experimental results and theoretical calculations of the molecular orbitals of pyrene. Obviously, monosubstitution occurs at position 1 and tetrasubstitution occurs at positions 1,3,6, and 8.

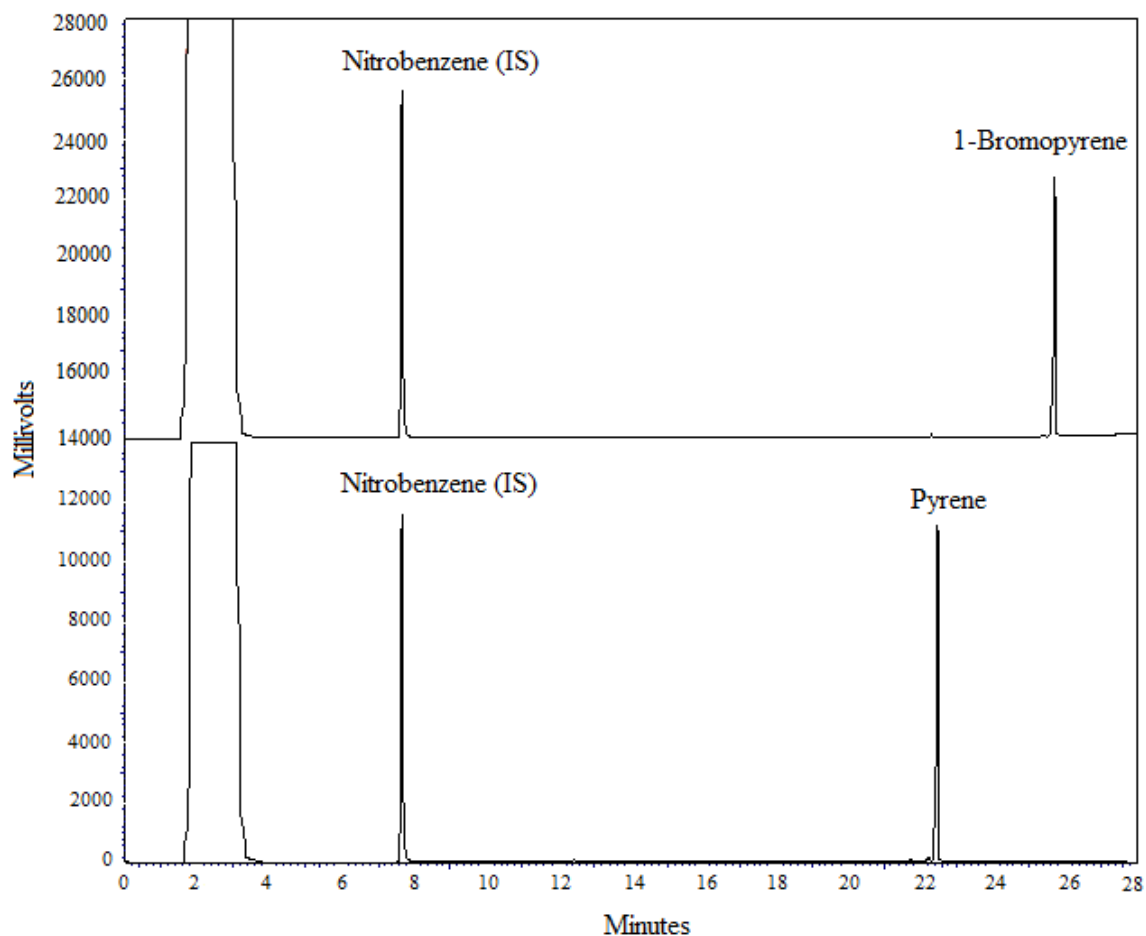
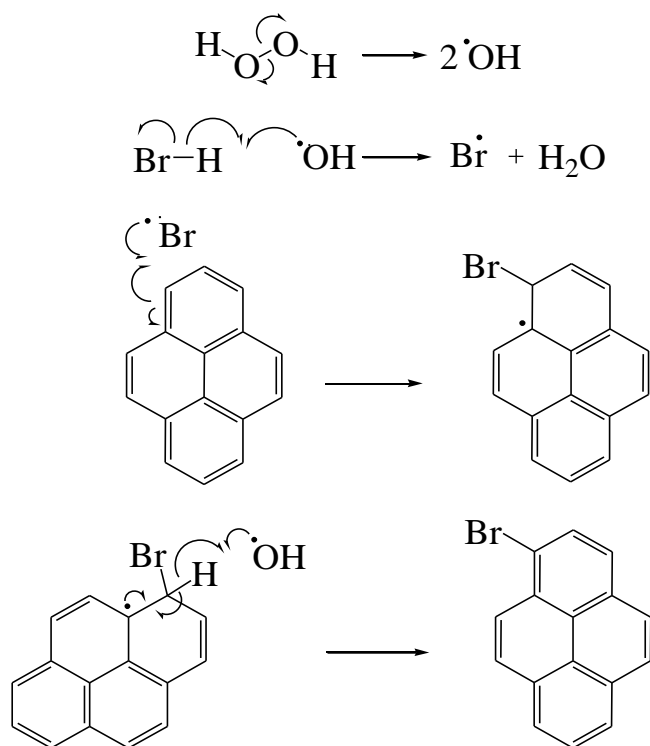
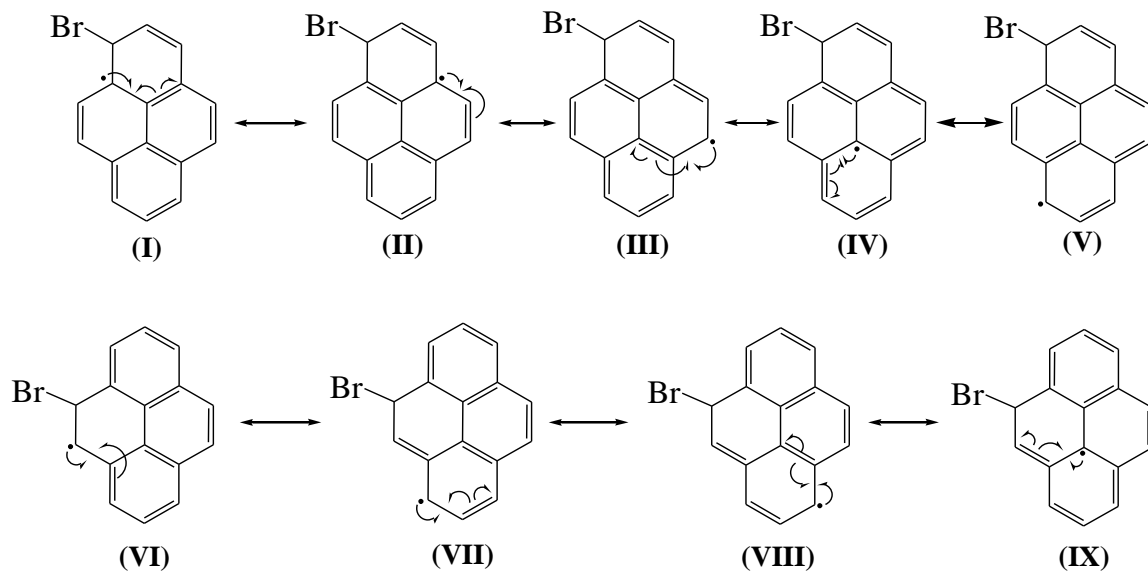


**Figure 5.1.** GC-FID analysis of pyrene before and after bromination reaction using  $\text{H}_2\text{O}_2$ -HBr.



**Scheme 5.1.** A modified mechanism for pyrene monobromination using  $\text{H}_2\text{O}_2\text{-HBr}$  [37].



**Scheme 5.2.** Resonance structures of pyrene radical brominated at positions 1 (I) and 10 (VI).

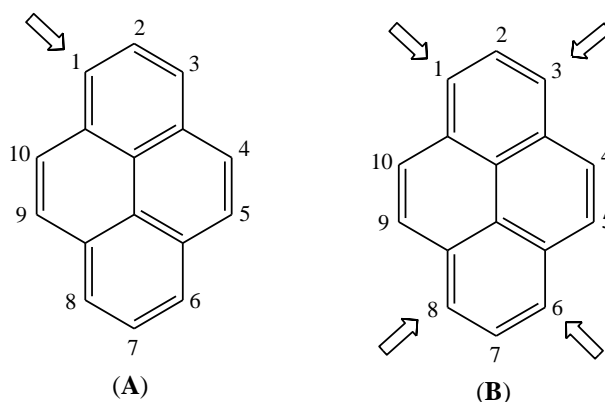


**Figure 5.2.** Chemical structure of pyrene and the its active sites for electrophilic substitution reaction. Mono substitution at position 1 (**A**) and tetra substitution at positions 1,3,6, and 8 (**B**).

### 5.3.2. PAH bromination in coal tar

Because coal tar includes a number of PAHs (Table 5.1) with  $\sum \text{PAHs} = 608 \text{ g/Kg}$ , it was therefore necessary to use several molar equivalents of  $\text{HBr-H}_2\text{O}_2$  to effect PAH brominations in coal tar. The results indicate that increasing the number of molar equivalents of  $\text{HBr-H}_2\text{O}_2$  for PAH bromination in coal tar increases the removal percentages of PAHs, but there were no brominated products that can be detected by GC-MS and GC-FID (Figures 5.3 and 5.4). This may likely be due to side reactions between the products in the coal tar, which would lead to the formation of high molecular weight products that cannot be detected by GC-MS and GC-FID. The conditions which were employed are summarized in Table 5.2 and the apparent resulting removal percentages are shown in Figure 5.4. These preliminary investigations clearly indicate that PAH bromination in coal tar is a complex task and further research will be required to evaluate its potential.

**Table 5.1.** PAH compounds identified in coal tar using GC-FID.

<b>Peak #</b>	<b>Compound name</b>	<b>g/Kg*</b>
1	Nitrobenzene (IS)	-
2	Naphthalene	251
3	2-Methylnaphthalene	17
4	1-Methylnaphthalene	15
5	Acenaphthene	23
6	Fluorene	26
7	Phenanthrene	87
8	Anthracene	15
9	Carbazole	16
10	9-Methylanthracene	16
11	4H-Cyclopenta[def]phenanthrene	14
12	Fluoranthene	52
13	Pyrene	42
14	Benz[a]anthracene	18
15	Chrysene	16

\* n= 3, RSD <6%

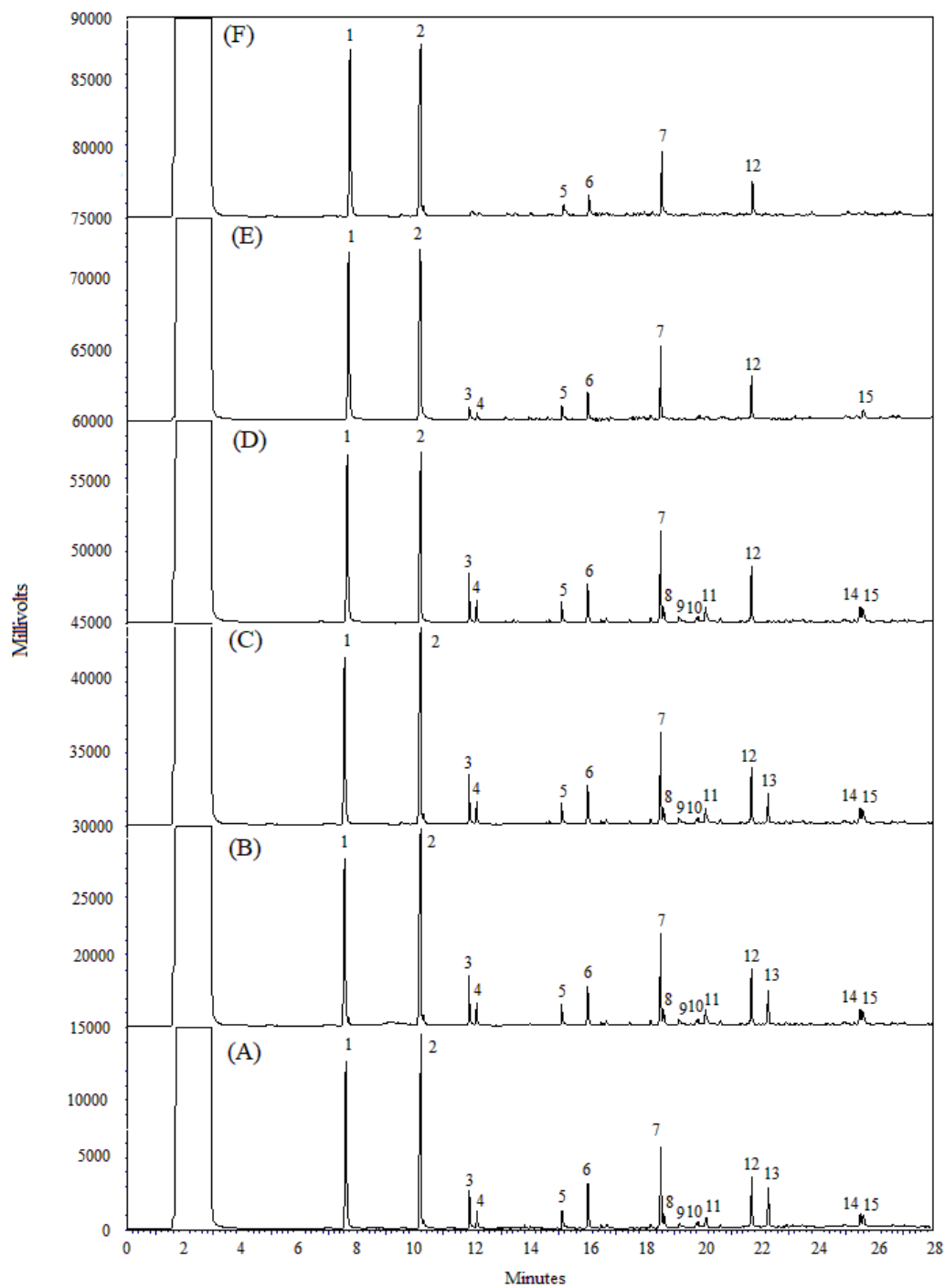


**Figure 5.3.** GC-FID chromatogram of coal tar extract in DCM (A) and bromination reaction products of coal tar (B-F). Peak numbers correspond to compounds listed in Table 5.1 and reaction conditions listed in Table 5.2.

**Table 5.2.** Experimental conditions for PAH bromination in coal tar

Condition	Equiv. #	HBr ( $\mu\text{L}$ )	H <sub>2</sub> O <sub>2</sub> ( $\mu\text{L}$ )	Time (h)
A (Control)	-	-	-	-
B	0.25	30.8	26.0	12
C	0.50	61.5	52.0	12
D	1.00	123.0	104.0	12
E	2.00	246.0	208.0	12
F	4.00	492.0	416.0	12

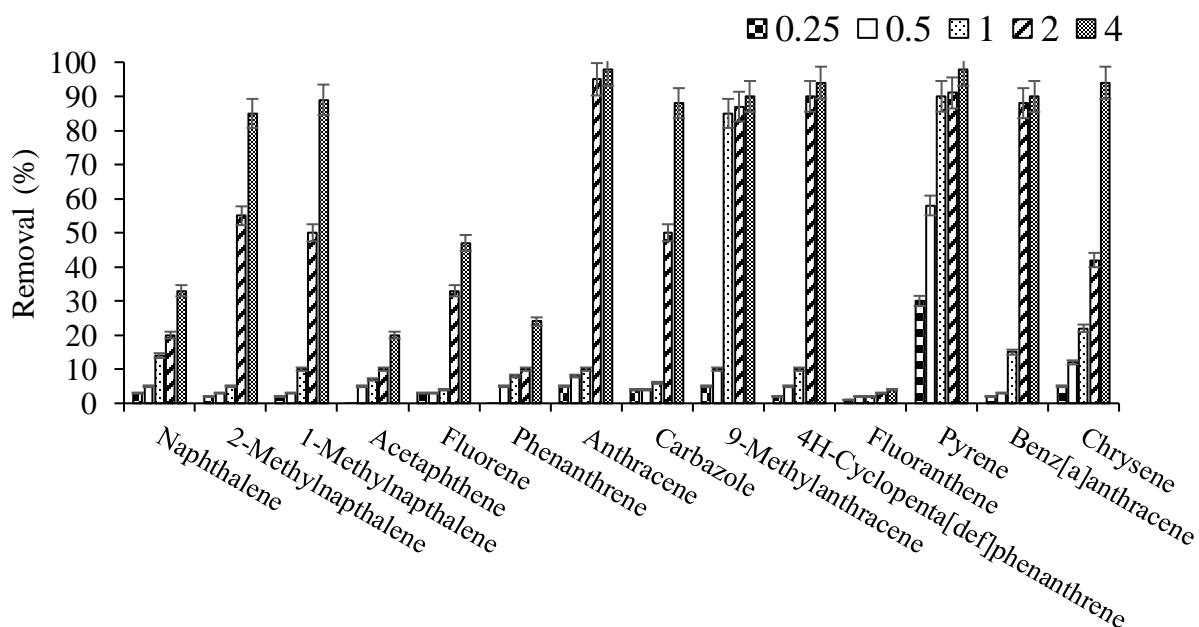


**Figure 5.4.** Removal percentages of PAHs from coal tar after bromination reaction using 0.25-4.0 molar equivalents of HBr-H<sub>2</sub>O<sub>2</sub>.

#### **5.4. Conclusions**

The use of hydrobromic acid with hydrogen peroxide is found to be a selective reagent for producing 1-bromopyrene from pyrene. Furthermore, this reaction has the advantages of being relatively environmentally-friendly, and is effective to produce a high yield of 1-bromopyrene. Bromination of PAHs in coal tar using H<sub>2</sub>O<sub>2</sub>-HBr however is a complicated process and it needs further optimization. Whereas increasing the number of molar equivalents of H<sub>2</sub>O<sub>2</sub>-HBr reagent increases the removal percentages of PAHs, no detectable products could be detected by GC-MS and GC-FID. Optimizing the PAH bromination conditions for coal tar will be a future work for this study.

## 5.5. References

- [1] Neira, C.; Cossaboon, J.; Mendoza, G.; Hoh, E.; Levin, L. A. Occurrence and Distribution of Polycyclic Aromatic Hydrocarbons in Surface Sediments of San Diego Bay Marinas. *Mar. Pollut. Bull.* **2017**, *114*, 466–479.
- [2] Kuppusamy, S.; Thavamani, P.; Venkateswarlu, K.; Lee, Y. B.; Naidu, R.; Megharaj, M. Remediation Approaches for Polycyclic Aromatic Hydrocarbons (PAHs) Contaminated Soils: Technological Constraints, Emerging Trends and Future Directions. *Chemosphere* **2017**, *168*, 944–968.
- [3] Kumar, L.; Mahajan, T.; Agarwal, D. D. An Instant and Facile Bromination of Industrially-Important Aromatic Compounds in Water Using Recyclable  $\text{CaBr}_2\text{-Br}_2$  System. *Green Chem.* **2011**, *13*, 2187.
- [4] Zöphel, L.; Beckmann, D.; Enkelmann, V.; Chercka, D.; Rieger, R.; Müllen, K. Asymmetric Pyrene Derivatives for Organic Field-Effect Transistors. *Chem. Commun.* **2011**, *47*, 6960–6962.
- [5] Lambert, F. L.; Ellis, W. D.; Parry, R. J. Halogenation of Aromatic Compounds by N-Bromo- and N-Chlorosuccinimide under Ionic Conditions. *J. Org. Chem.* **1965**, *30*, 304–306.
- [6] Chiappe, C.; Leandri, E.; Pieraccini, D. Highly Efficient Bromination of Aromatic Compounds Using 3-Methylimidazolium Tribromide as Reagent/solvent. *Chem. Commun.* **2004**, *1*, 2536–2537.
- [7] Song, S.; Sun, X.; Li, X.; Yuan, Y.; Jiao, N. Efficient and Practical Oxidative Bromination and Iodination of Arenes and Heteroarenes with DMSO and Hydrogen Halide: A Mild Protocol for Late-Stage Functionalization. *Org. Lett.* **2015**, *17*, 2886–2889.
- [8] Moriuchi, T.; Yamaguchi, M.; Kikushima, K.; Hirao, T. An Efficient Vanadium-Catalyzed Bromination Reaction. *Tetrahedron Lett.* **2007**, *48*, 2667–2670.
- [9] Bora, U.; Bose, G.; Chaudhuri, M. K.; Dhar, S. S.; Gopinath, R.; Khan, A. T.; Patel, B. K. Regioselective Bromination of Organic Substrates by Tetrabutylammonium Bromide Promoted by  $\text{V}_2\text{O}_5\text{-H}_2\text{O}_2$ : An Environmentally Favorable Synthetic Protocol. *Org. Lett.* **2000**, *2*, 247–249.
- [10] Hossein, Mahdavi; Zahra, K. Synthesis and Application of Poly(Diallyldimethylammonium Tribromide) as a Novel Polymeric Brominating Agent. *chin. j. chem.* **2010**, *28*, 2221–2225.
- [11] Adibi, H.; Hajipour, A. R.; Hashemi, M. A Convenient and Regioselective Oxidative Bromination of Electron-Rich Aromatic Rings Using Potassium Bromide and Benzyltriphenylphosphonium Peroxymonosulfate under Nearly Neutral Reaction Conditions. *Tetrahedron Lett.* **2007**, *48*, 1255–1259.

- [12] De Almeida, L. S.; Esteves, P. M.; De Mattos, M. C. S. Efficient Electrophilic Cobromination of Alkenes and Bromination of Activated Arenes with Bromodichloroisocyanuric Acid under Mild Conditions. *Synlett* **2007**, 11, 1687–1690.
- [13] Ghorbani-Vaghei, R.; Jalili, H. Mild and Regioselective Bromination of Aromatic Compounds with *N,N,N,N*-Tetrabromobenzene-1,3-Disulfonylamide and poly(*N*-Bromobenzene-1,3-Disulfonylamide). *Synthesis* **2005**, 7, 1099–1102.
- [14] Cheng, Ming; Qiu, Ya; Liu, Hongshan; Xia, Peng; Chen, Y. Bromination of 7-O-Substituted-8-Methyl-Coumarins and 4*H*-Chromen-4-Ones with *N*-Bromosuccinimide in CCl<sub>4</sub>. *Chinese J. Org. Chem.* **2010**, 30, 1737–1741.
- [15] Rajesh, K.; Somasundaram, M.; Saiganesh, R.; Balasubramanian, K. K. Bromination of Deactivated Aromatics: A Simple and Efficient Method. *J. Org. Chem.* **2007**, 72, 5867–5869.
- [16] Gnaim, J. M.; Sheldon, R. A. Regioselective Bromination of Aromatic Compounds with Br<sub>2</sub>/SO<sub>2</sub>Cl<sub>2</sub> over Microporous Catalysts. *Tetrahedron Lett.* **2005**, 46, 4465–4468.
- [17] Heravi, M. M.; Abdolhosseini, N.; Oskooie, H. A. Regioselective and High-Yielding Bromination of Aromatic Compounds Using Hexamethylenetetramine-Bromine. *Tetrahedron Lett.* **2005**, 46, 8959–8963.
- [18] Roche, D.; Prasad, K.; Repic, O.; Blacklock, T. J. Mild and Regioselective Oxidative Bromination of Anilines Using Potassium Bromide and Sodium Perborate. *Tetrahedron Lett.* **2000**, 41, 2083–2085.
- [19] Meshram, H. M.; Reddy, P. N.; Sadashiv, K.; Yadav, J. S. Amberlyst-15-Promoted Efficient 2-Halogenation of 1,3-Keto-Esters and Cyclic Ketones Using *N*-Halosuccinimides. *Tetrahedron Lett.* **2005**, 46, 623–626.
- [20] Barhate, N. B.; Gajare, A. S.; Wakharkar, R. D.; Bedekar, A. V. Simple and Efficient Chlorination and Bromination of Aromatic Compounds with Aqueous TBHP (or H<sub>2</sub>O<sub>2</sub>) and a Hydrohalic Acid. *Tetrahedron Lett.* **1998**, 39, 6349–6350.
- [21] Zhang, Y.; Shibatomi, K.; Yamamoto, H. Lewis Acid Catalyzed Highly Selective Halogenation of Aromatic Compounds. *Synlett* **2005**, 18, 2837–2842.
- [22] Ganguly, N. C.; De, P.; Dutta, S. Mild Regioselective Monobromination of Activated Aromatics and Heteroaromatics with *N*-Bromosuccinimide in Tetrabutylammonium Bromide. *Synthesis* **2005**, 7, 1103–1108.
- [23] John, A.; Nicholas, K. M. Palladium Catalyzed C-H Functionalization of *O*-Arylcarbamates: Selective Ortho -Bromination Using NBS. *J. Org. Chem.* **2012**, 77, 5600–5605.
- [24] Guan, X. Y.; Al-Misba'a, Z.; Huang, K. W. Efficient and Selective  $\alpha$ -Bromination of Carbonyl Compounds with *N*-Bromosuccinimide under Microwave. *Arab. J.*

*Chem.* **2015**, *8*, 892–896.

- [25] Ren, Y. L.; Wang, B.; Tian, X. Z.; Zhao, S.; Wang, J. Aerobic Oxidative Bromination of Arenes Using an Ionic Liquid as Both the Catalyst and the Solvent. *Tetrahedron Lett.* **2015**, *56*, 6452–6455.
- [26] Das, B.; Venkateswarlu, K.; Majhi, A.; Siddaiah, V.; Reddy, K. R. A Facile Nuclear Bromination of Phenols and Anilines Using NBS in the Presence of Ammonium Acetate as a Catalyst. *J. Mol. Catal. A Chem.* **2007**, *267*, 30–33.
- [27] Lee, K. J.; Cho, H. K.; Song, C. E. Bromination of Activated Arenes by Oxone and Sodium Bromide. *Bull. Korean Chem. Soc.* **2002**, *23*, 773–775.
- [28] Ghiaci, M.; Asghari, J. Increasing the Selectivity of Bromination of Aromatic Compounds Using Br<sub>2</sub>/SiO<sub>2</sub>. *Bull. Chem. Soc. Jpn.* **2001**, *74*, 1151–1152.
- [29] Mohan, R. B.; Reddy, G. T.; Gangi Reddy, N. C. Substrate Directed Regioselective Monobromination of Aralkyl Ketones Using N-Bromosuccinimide Catalysed by Active Aluminium Oxide:  $\alpha$ -Bromination versus Ring Bromination. *ISRN Org. Chem.* **2014**, *2014*, 1–11.
- [30] Voskressensky, L. G.; Golantsov, N. E.; Maharramov, A. M. Recent Advances in Bromination of Aromatic and Heteroaromatic Compounds. *Synth.* **2016**, *48*, 615–643.
- [31] Li, R.; Wang, Z. J.; Wang, L.; Ma, B. C.; Ghasimi, S.; Lu, H.; Landfester, K.; Zhang, K. A. I. Photocatalytic Selective Bromination of Electron-Rich Aromatic Compounds Using Microporous Organic Polymers with Visible Light. *ACS Catal.* **2016**, *6*, 1113–1121.
- [32] Podgoršek, A.; Stavber, S.; Zupan, M.; Iskra, J. Environmentally Benign Electrophilic and Radical Bromination “on Water”: H<sub>2</sub>O<sub>2</sub>-HBr System versus N-Bromosuccinimide. *Tetrahedron* **2009**, *65*, 4429–4439.
- [33] Vyas, P. V.; Bhatt, A. K.; Ramachandraiah, G.; Bedekar, A. V. Environmentally Benign Chlorination and Bromination of Aromatic Amines, Hydrocarbons and Naphthols. *Tetrahedron Lett.* **2003**, *44*, 4085–4088.
- [34] Domínguez, A.; Blanco, C.; Santamaría, R.; Granda, M.; Blanco, C. G.; Menéndez, R. Monitoring Coal-Tar Pitch Composition Changes during Air-Blowing by Gas Chromatography. *J. Chromatogr. A* **2004**, *1026*, 231–238.
- [35] Fan, X.; Fei, Y.; Chen, L.; Li, W. Distribution and Structural Analysis of Polycyclic Aromatic Hydrocarbons Abundant in Coal Tar Pitch. *Energy and Fuel* **2017**, *31*, 4694–4704
- [36] Morgan, T. J.; George, A.; Álvarez, P.; Millan, M.; Herod, A. A.; Kandiyoti, R. Characterization of Molecular Mass Ranges of Two Coal Tar Distillate Fractions (Creosote and Anthracene Oils) and Aromatic Standards by LD-MS, GC-MS, Probe-MS and Size-Exclusion Chromatography. *Energy and Fuels* **2008**, *22*, 3275–3292.

- [37] Bruce, P. Y. *Organic Chemistry*. Pearson education Inc., Upper Saddle River: NJ 2014, p 559.
- [38] Schwarz, J.; König, B. Metal-Free, Visible-Light-Mediated, Decarboxylative Alkylation of Biomass-Derived Compounds. *Green Chem.* **2016**, *18*, 4743–4749.
- [39] Geerlings, P.; De Proft, F.; Langenaeker, W. Conceptual Density Functional Theory. *Chem. Rev.* **2003**, *103*, 1793–1874.
- [40] Figueira-Duarte, T. M.; Klaus, M. Pyrene-Based Materials for Organic Electronics. *Chem. Rev.* **2011**, *111*, 7260–7314.

## 6. Conclusions and future work

### 6.1. Conclusions

Based upon the results presented in this dissertation, four promising routes have been explored for the degradation/removal of PAHs from coal tar. These routes are chemical reduction using acidified Mg/EtOH, chemical oxidation using Fenton's reagent and peroxyacetic acid, microwave-assisted heating, and bromination using H<sub>2</sub>O<sub>2</sub>/HBr. The order of these methods in term of high to low efficiency for removal/degradation of PAHs in coal tar is as follows: Fenton oxidation > peroxyacetic acid > acidified Mg/EtOH > bromination > microwave-assisted heating.

In the first approach, reductive degradation of PAHs in coal tar using an acidified Mg/EtOH system was investigated and optimized based on the effects of Mg activation and co-solvent. In addition, experimental design was used to investigate the effects of Mg concentration, time, glacial acetic acid, and graphite on the removal efficiency of PAHs. As result, this approach has been streamlined as a promising route to convert some PAHs to less toxic compounds (hydrogenated PAHs) at room temperature within a short reaction time (30 min). Furthermore, this method is selective for reduction of some PAHs such as anthracene and fluoranthene resulting in a high removal efficiency (> 90%) as confirmed by GC/MS analysis. Determination of the significant factors (glacial acetic acid, Mg concentration, and time) and the optimum conditions for the effective removal of PAHs has been achieved using experimental design methodology.

In the second approach, a comparison between Fenton's reagent and peroxyacetic acid was established for the first time. Briefly, oxidative degradation of PAHs in coal tar using Fenton's reagent (Fe<sup>2+</sup> + H<sub>2</sub>O<sub>2</sub>) was achieved within a short time (30 min) with high

removal efficiency (> 90%) of some PAHs. Compared to peroxyacetic acid, Fenton's reagent showed a higher efficiency in removing PAHs. In addition, a lesser amount of Fenton's reagent (0.6 mL) was required, as compared to the case using peroxyacetic acid (16 mL).

In the third approach, PAHs in coal tar can be thermally desorbed using microwave-assisted heating at low temperatures (< 300 °C). This method was improved using microwave absorbers such as biochar and activated carbon to achieve fast heating rate and low energy cost. In addition, the volatile fraction was easily separated using an open and closed microwave system. The extraction of PAHs from coal tar using ethanol was conducted and the resulting ethanol extracts were subjected to microwave-assisted heating. The ethanol extracts mixed with microwave absorbers (biochar, activated carbon, TiO<sub>2</sub>) gave enhanced MAH since ethanol is a polar solvent. However, an open microwave system is required to avoid damaging the microwave tube. Conventional heating using TGA showed that high temperatures (> 300 °C) are necessary to obtain a volatile fraction ~50% of coal tar sample. In the last approach, bromination of the PAHs in coal tar has been studied as another route for PAH chemical alteration and possible activation. The main result of this work is the selective formation of 1-bromopyrene from pyrene in high yield (> 95%). 1-Bromopyrene can be considered as a useful starting compound for various organic syntheses, which in turn can lead to applications in the semiconductors industry. However, quantification of brominated products obtained directly from PAH present in the coal tar has not yet been accomplished.

## 6.2. Future work

The following proposed studies can be considered for expanding the current work for a more comprehensive study of PAH degradation. These topics are as follows:

a) Using a mixture of authentic commercially-available PAHs as a simulation method for coal tar composition. The simulation mixture could consist of some of the typical components of coal tar, such as naphthalene, phenanthrene, fluoranthene, and pyrene, versus the whole coal tar, which is a highly complex mixture. This mixture can be prepared in the solid state, or dissolved in ethanol and then subjected to microwave-assisted thermal removal or to chemical oxidation or chemical reduction using methodology described in this thesis. This study may shed light on the effectiveness of the PAH degradation in coal tar because it deals with a simple mixture of the PAHs.

b) PAH-contaminated soil: A commercial soil sample can be spiked with a known amount of coal tar or with a mixture of standard PAHs dissolved in acetone. These could serve as samples for the study simulation of coal tar-contaminated soil in the environment. After evaporation of the acetone, the methods described in this dissertation (e.g., microwave-assisted thermal removal, Fenton oxidation, peroxyacetic acid, acidified Mg/EtOH, and bromination) can be evaluated for PAH degradation. In addition, the effect of PAH aging in soil can also be studied. For example, the aging of PAHs or the coal tar in soil for different time periods (e.g., week, month, and year) can be investigated. The expected result is that by increasing the PAH aging in soil, the PAH bioavailability decreases, which has been known to reduce the remediation efficiency in environmental samples [1].

c) A study of the microwave-assisted thermal removal of PAHs at high temperatures (> 300 °C) using higher powered microwave instruments (e.g., 1600 W) can be undertaken. Thus,

the effect of microwave absorbers such as carbon materials (biochar and activated carbon), temperature, and residence time can be investigated. Experimental design was in this study to determine the optimum conditions for high removal efficiency of PAHs. Furthermore, catalytic pyrolysis of these PAHs in coal tar can be investigated using a conventional heating source such as a tube furnace at high temperatures ( $> 300\text{ }^{\circ}\text{C}$ ). As a result of this study, a comparison between PAH degradation using microwave and conventional-assisted heating at low and high temperature can be evaluated.

d) For the reduction of PAHs using acidified Mg/EtOH, surface analysis of Mg before and after activation using glacial acetic acid will be a useful method to characterize the MgO and Mg(OH)<sub>2</sub> layers formed. X-ray photoelectron spectroscopy (XPS) can be used for achieving this goal [2]. XPS will provide more information about these surface layers that hinder the interactions between the active sites of Mg surface and the target PAH.

e) The effect of pH and temperature on the reductive degradation of PAHs using Mg/EtOH system should be investigated. Temperature may be an important factor as it increases the reaction rate as well as pH especially in aqueous media. These two factors can be studied in greater detail.

f) Integrated remediation processes. Integrated remediation processes have been shown to improve the removal efficiency of PAHs [3]. For example, using Fenton oxidation in the first step for PAH oxidation enhances the bioavailability of PAHs [4]. Bioremediation using bacteria or enzymes can be used to complete the PAHs degradation, where potential toxic intermediates (oxy-PAHs) can be degraded.

g) Photo-Fenton oxidation of PAHs. This approach can be used for degradation of PAHs in coal tar, where the role of UV radiation is to improve the production of hydroxyl radicals.

This process can be optimized through an experimental design approach to determine the optimum conditions for the highest removal efficiency of PAHs in coal tar. Several factors such as hydrogen peroxide, and  $\text{Fe}^{2+}$  concentrations, UV radiation, and irradiation time have been investigated in soils [5], but their application to coal tar has not been studied.

h) Cyclodextrin-Fenton oxidation of PAHs. One of the main problems related to PAH degradation in contaminated soils is their availability. The absorbed PAHs which penetrate the soil particles are unavailable for the reaction with reactive  $\cdot\text{OH}$  radicals. The centre cavity of cyclodextrins are hydrophobic and the outer surface is hydrophilic. They can be used as a as a solubilizing agent for desorbing PAHs from contaminated soils [6].

i) Bioremediation [7]. One of the drawbacks for PAH degradation in real samples such as coal tar and PAH-contaminated soil is their bioavailability, which reduces the removal efficiency of the PAHs. Therefore, biosurfactants or salicylic acid can be used to enhance bioavailability of PAHs. In addition, increasing the bio-organic matter content by adding organic wastes could be an effective method to enhance the PAH bioavailability.

### 6.3. References

- [1] Luo, L.; Lin, S.; Huang, H.; Zhang, S. Relationships between Aging of PAHs and Soil Properties. *Environ. Pollut.* **2012**, *170*, 177–182.
- [2] Yao, H. B.; Li, Y.; Wee, A. T. S. XPS Investigation of the Oxidation/corrosion of Melt-Spun Mg. *Appl. Surf. Sci.* **2000**, *158*, 112–119.
- [3] Luki, B.; Panico, A.; Huguenot, D.; Fabbicino, M.; van Hullebusch, E. D.; Esposito, G. A Review on the Efficiency of Landfarming Integrated with Composting as a Soil Remediation Treatment. *Environ. Technol. Rev.* **2017**, *6*, 94–116.
- [4] Lee, B. D.; Hosomi, M.; Murakami, A. Fenton Oxidation with Ethanol to Degrade Anthracene into Biodegradable 9, 10-Anthraquinone: A Pretreatment Method for Anthracene-Contaminated Soil. *Water Sci. Technol.* **1998**, *38*, 91–97.
- [5] Silva, P. T. de S. e.; Silva, V. L. da; Neto, B. de B.; Simonnot, M. O. Phenanthrene and Pyrene Oxidation in Contaminated Soils Using Fenton's Reagent. *J. Hazard. Mater.* **2009**, *161*, 967–973.
- [6] Yap, C. L.; Gan, S.; Ng, H. K. Fenton Based Remediation of Polycyclic Aromatic Hydrocarbons-Contaminated Soils. *Chemosphere* **2011**, *83*, 1414–1430.
- [7] Ghosal, D.; Ghosh, S.; Dutta, T. K.; Ahn, Y. Current State of Knowledge in Microbial Degradation of Polycyclic Aromatic Hydrocarbons (PAHs): A Review. *Front. Microbiol.* **2016**, *7*, 1-12.

## Appendices

### Appendix A. Supporting information for Chapter 1.

**Table S1.1.** Summary of recent research for PAH and PCB degradation using an acidified Mg/EtOH system.

Study	Experimental conditions	Results	Ref.
Oxy-PAH reduction using activated Mg/EtOH.	0.05 g of Mg powder, 250 ppm of each 9-fluorenone, 9,10-anthraquinone, 7,12-benz[a]anthraquinone, and 7H-benz[de]anthracene-7-one in 1:1 ethanol/ethyl acetate. 60 $\mu$ L of glacial acetic acid. Reaction was conducted at room temperature ( $\sim$ 27 $^{\circ}$ C) for 24 h.	86% removal efficiency. Activation of Mg is an necessary process.	[1]
PAH reduction using activated Mg/EtOH.	0.05-0.1 g of Mg powder, 200-270 ppm of Pyrene (PYR), benzo[k]fluoranthene (BkF) and benzo[g,h,i]perylene (B[ghi]P) in 1:1 ethanol/ethyl acetate. 20-60 $\mu$ L of glacial acetic acid. Reaction was conducted at room temperature ( $\sim$ 27 $^{\circ}$ C) for 24 h.	93% removal efficiency. This method is environmentally friendly process for PAHs remediation.	[2]
Pentachlorophenol degradation using activated Mg/EtOH.	0.02 of each Ball-milled zero-valent Mg (ZVMg), ball-milled zero-valent Mg carbon (ZVMg/C), and ball-milled zero-valent Mg with Pd (ZVMg/Pd) in 10 $\mu$ L acetic acid/ mL ethanol. Pentachlorophenol concentration is 20 ng/mL.	Dechlorination of pentachlorophenol to chlorophenols within $\sim$ 15 min 100% dichlorination was achieved within 6 days. The degradation reaction of PCP follows pseudo-first order kinetics.	[3]

**Table S1.1. (continued)**

Dechlorination of PCBs using activated Mg and activated Mg with activated carbon.	Hydrodehalogenation of polychlorinated biphenyls (PCBs) using Mg and activated carbon. 10.28 mmoles of ball milled Mg or ball milled Mg with activated carbon. $1.4 \times 10^{-7}$ - $2.7 \times 10^{-7}$ mmoles total PCB in 9:1 v/v ethanol:ethyl lactate. 50.0 $\mu$ L glacial acetic acid. Reaction mixture was shaken (200 rpm) until desirable time in range of 0-72 h. Reaction was quenched by adding 5.0 mL toluene, then 5.0 mL deionized water. Toluene extracts were analyzed by GC-MS.	38-98% removal efficiency of hexa-chlorinated PCB. Degradation of PCBs follows a pseudo first order kinetics.	[4]
Degradation of PAHs and oxy-PAHs in spiked soil.	Concentrations of PAHs and oxy-PAHs in the range of 90-100 mg kg <sup>-1</sup> . 1.0 or 5.0 g of contaminated soil. 0.05 g of Mg/C. 2.0 mL of ethanol: ethyl lactate (1:1 v/v). 60 $\mu$ L of glacial acetic acid (3 vol%). After a desirable time in range of 0-24 h. Reaction was quenched by adding 2.0 mL toluene, then 4.0 mL deionized water. Toluene extracts were analyzed by GC-MS.	Removal efficiency is 79%-88% of oxy-PAHs, and 66%-87% of PAHs. Degradation reaction of these compounds follows pseudo-first-order kinetics.	[5]
Benzo[a]pyrene Degradation using acid-activated Mg in ethanol.	Benzo[a]pyrene concentration is 250 ppm in anhydrous ethanol. 1.0-5.0 g of contaminated soil and 0.05 g of Mg/C. 2.0 mL of benzo[a]pyrene. 20 $\mu$ L of glacial acetic acid (1 vol.%). After a desirable time in (0-24 h), reaction was quenched by adding 2.0 mL toluene, then 4.0 mL deionized water. Toluene extracts were analyzed by GC-MS.	94% removal efficiency. Activated Mg/EtOH system is effective method for PAH hydrogenation.	[6]

**Table S1.2.** Summary of research using Fenton oxidation for PAH degradation.

<b>Goal of study</b>	<b>Reaction conditions</b>	<b>Results</b>	<b>Ref.</b>
Degradation of PAHs in contaminated soil using Fenton oxidation	Field soil includes 14 PAHs Sample dosage: 10 g. 30 mL of water, 20 mL of 30% H <sub>2</sub> O <sub>2</sub> (~9.4% w/v), 20 mL of 8.84 mmol/L Fe <sup>2+</sup> were added, respectively. The pH is 7. The reaction was left at room temperature in dark place for 24 h.	Twelve of 14 PAHs were removed from soil (13-56%) after 1 h. Fenton oxidation is an efficient method for removing PAHs from soil (72-93%) 24 h.	[7]
To study the effect of total organic carbon (TOC) and soil porosity on PAH degradation using Fenton oxidation	120 g of each soil spiked by coal tar including 12 PAHs (3-6 rings) with 1000 mg/Kg final concentration. 5.0 g of spiked soil, 25 mL deionized water, 100 mg of HgCl <sub>2</sub> (for inhibition the microbial activity), 1.0% w/v H <sub>2</sub> O <sub>2</sub> , Fe <sup>2+</sup> 10 mmol/L, pH 3.0, 14 days. Products were analyzed by HPLC.	15-80 % recovery. PAH degradation using Fenton oxidation was affected by total organic carbon (TOC) (> 5% TOC had a clear effect), and porosity-mediated sequestration over time.	[8]
Removal of PAHs from PAH-contaminated soil: Fenton treatment vs. ozonation	Soil (peat or sand) spiked with 11 PAHs. 5 g peat or 15 g sand:100 mL water, H <sub>2</sub> O <sub>2</sub> :soil:Fe <sup>2+</sup> 0.0087:1:0.0014 (w/w/w), 3 steps/days addition of H <sub>2</sub> O <sub>2</sub> (~0.015-0.04% w/v), pH 3, 24 h. Three-phase ozonation was used.	Degradation efficiency is dependent on H <sub>2</sub> O <sub>2</sub> /soil/Fe <sup>2+</sup> ratio and the time. 92% removal efficiency. Pre-treatment PAH-contaminated soil by Fenton oxidation improves PAH biodegradability.	[9]

**Table S1.2. (continued)**

PAH removal from soil, sludge and sediment using Fenton oxidation	2.0 g soil (spiked and non-spiked by FLR, BBF, and BAP). 10 mL water, 4.9 mol/L H <sub>2</sub> O <sub>2</sub> (~16.7% w/v), 0.01 mol/L Fe <sup>2+</sup> , 24 h, no pH adjustment.	PAH removal is dependant on type of matrix (e.g., soil, sludge and sediment). Removal efficiencies of PAHs are as follows: Native PAHs: Soil: 0-8% Sludge: 36.2-48.1% Sediment: 9.7-85% Native + spiked PAHs: Soil: 85.7-88.6% Sludge: 38-67 % Sediment: 97.6-99.1% Oxidation of a single compound is faster than of a mixture of PAHs. Oxidation was successfully achieved at room temperature without pH adjustment.	[10]
PAHs degradation in aged contaminated Soils: Fenton treatment versus ozonation	20 g soil (Field soil 24 PAHs) 10 mL water, 40 mL of 30% H <sub>2</sub> O <sub>2</sub> (~26.4% w/v), 4 mmol/L Fe <sup>2+</sup> , pH 3, 70 °C. The reaction was quenched after 2 h by adding five drops of conc. H <sub>2</sub> SO <sub>4</sub> (pH < 1). The extracted products were analyzed by GC-MS.	Removal efficiencies are 40-86% (Fenton) and 10-70% (ozone).	[11]

**Table S1.2. (continued)**

Effect of soil characteristics and PAH properties on PAH removal using Fenton oxidation	20 g soil (6 field soils including 24 PAHs). 30 mL of deionized water, 20 ml of 15% (w/v) H <sub>2</sub> O <sub>2</sub> , 10 mL of 10 mmol/L Fe <sup>2+</sup> , 1 h, 25 °C, pH 3.	8.8–43% removal efficiencies of PAHs are: 0-38% of 4-6 rings and 59-89% of 2 and 3 rings. PAHs removal was influenced by PAH properties (molecular weight) and soil characteristics such as organic matter and specific surface area.	[12]
Influence of Fenton oxidation on soil organic matter (SOM) and its sorption and desorption of pyrene (PYR)	1.0 g of soil was mixed with 10 mL of PYR solution. Pyrene concentration: 3-1.8 ppm for Soil 1, 4.6-2.2 ppm for Soil 2, and 16-12 ppm for Soil 3. 1:1 soil:water, 2.5 mol/L H <sub>2</sub> O <sub>2</sub> (~ 8.5% w/v), 0.2 mol/L Fe <sup>2+</sup> , 12 h, without adjustment of pH.	The SOM content of soil was changed by Fenton oxidation, which in turn effected on PYR sorption and desorption.	[13]
PAH degradation in PAH-contaminated sediments using chemical oxidation	30 g of sediments including 16 PAHs. Oxidant reagents: H <sub>2</sub> O <sub>2</sub> , modified Fenton reagent, activated Na <sub>2</sub> S <sub>2</sub> O <sub>8</sub> , KMnO <sub>4</sub> , KMnO <sub>4</sub> with H <sub>2</sub> O <sub>2</sub> , Na <sub>2</sub> S <sub>2</sub> O <sub>8</sub> with H <sub>2</sub> O <sub>2</sub> . Volume of solution with oxidant: 100 mL. 0.5 mol/L H <sub>2</sub> O <sub>2</sub> (~1.7%) and 0.01 mol/L catechol-chelated Fe <sup>2+</sup> .	High removal efficiency (98%) of total PAHs was obtained using modified Fenton and H <sub>2</sub> O <sub>2</sub> with KMnO <sub>4</sub> . The optimum dosage of oxidant is 100 mmol of oxidant/ 30 g sediment.	[14]

**Table S1.2. (continued)**

Surfactants production during the chemical oxidation of PAH in soil	Three oxidation processes of PAHs in soil were achieved which are hydrogen peroxide-modified Fenton chemistry (HP-MFC), calcium peroxide-modified Fenton chemistry (CP-MFC) and sodium persulfate (SPS) 4.0 kg of field soil including 18 PAHs, 8.5 L water, 1.0 L 50% H <sub>2</sub> O <sub>2</sub> . 200 mg EDTA-Fe <sup>2+</sup> or 500 g Cool-Ox <sup>TM</sup> . Bioremediation was also achieved at room temperature without adjustment of pH.	Biological: 16.5% HP-MF: 71.3 CP-MF: 92.3% SPS: 88.5%. CP-MFC gave a higher removal of HMW PAHs (4-6 rings) than bioremediation.	[15]
Mineralisation of sorbed BAP in soils using Fenton oxidation.	5.0 g of soil spiked by BAP (0.1 mmol BAP per kg of soil). Experimental design was used for three factors, in the case of silica sand, were H <sub>2</sub> O <sub>2</sub> (2400-12,300 mmol/L), slurry volume (0.3-3.7 x 0.31 ml/g, the field capacity of the silica sand), and iron(II) (6.6-23.4 mmol/L). In the case of Palouse loess soil, were H <sub>2</sub> O <sub>2</sub> (1500-14,000 mmol/L), slurry volume (1.0-20.0 x 0.42 mL/g, field capacity of the Palouse loess), and pH (2.0-8.0), with using a native iron. The remediation time is 24 h.	Mineralization percentages of BaP are 70% and 80% in the sand and a Palouse loess soil, respectively.	[16]
Phenanthrene degradation using hydrogen peroxide with goethite.	Soil spiked by PHE (25 mg/kg). 12.5 mL H <sub>2</sub> O <sub>2</sub> (5 mol/L), Goethite 33.5 g/Kg, pH 7	89% removal efficiency of PHE. The reaction follows pseudo-first order kinetics. PHE oxidation was inhibited by the soil contents of organic matter and bicarbonate ions.	[17]

**Table S1.2. (continued)**

Comparative of PAHs removal from soils using iron oxide and H <sub>2</sub> O <sub>2</sub> .	Sand slurries spiked soil by PHE, ANT, and PYR. 5.0 mol/L H <sub>2</sub> O <sub>2</sub> , 33.5 g/kg goethite, neutral pH. Reaction time is 3 h.	Removal percentages of PHE, ANT, and PYR are 73, 60, and 55%, respectively. Removal % is dependent on goethite concentration, H <sub>2</sub> O <sub>2</sub> , bicarbonate, and pH. Reaction follows pseudo-first order kinetics. CO <sub>2</sub> and H <sub>2</sub> O were the final products.	[18]
Chemical/biological remediation of PAHs in PAH-contaminated soils.	Pilot-scale study. Biological remediation then chemical oxidation. 1800 - 2100 gals. 0.5-2.0% v/v H <sub>2</sub> O <sub>2</sub> . Fe <sup>2+</sup> (1-100 mmol/L in slurry) 10-20 days slurry residence time.	Integrated remediation such as chemical/biological remediation gives higher removal efficiency (70%) than bioremediation.	[19]
Fenton/biological treatment of ANTH contaminated soil.	Soil spiked by anthracene (500 mg/Kg). 0.25-1.00 mL of ethanol per g soil was added then agitated for 24 h. Fenton oxidation started by adding 0.30 mL/g soil of 30% H <sub>2</sub> O <sub>2</sub> and 0.20 mL/g 0.5 mol/L Fe <sup>2+</sup> for 24 h, without adjustment of pH. Effect of surfactant (10 mmol/L sodium dodecyl sulfate (SDS)) was investigated.	97% removal efficiency. Ethanol increased the ANTH removal. Biodegradation of 9,10-ANTH is 90%, which faster than of ANTH (30%) in month.	[20]
Benz[a]anthracene (B[a]A) degradation in soil using Fenton/microbial treatment.	Soil was spiked by 500 mg/kg B[a]A. 1.0 mL ethanol /g soil and agitated for 24 h. 0-30 mL of 30% H <sub>2</sub> O <sub>2</sub> /g soil and 0-0.20 mL 0.5 mol/L Fe <sup>2+</sup> /g soil for 24 h, and pH 6.5. Then microbial treatment of product (B[a]7,12-dione) from Fenton reaction was achieved.	The optimum oxidation dosage is 0.30 mL of 30% H <sub>2</sub> O <sub>2</sub> and 0.20 mL of 0.5 mol/L Fe <sup>2+</sup> . 98% of B[A]7,12-dione was removed by biological treatment vs. 12% of B[a]A both in 63 days.	[21]

**Table S1.2. (continued)**

Ethanol-Fenton oxidation of PAHs in an aged gasworks' soil	20 g of soil including 23 PAHs (1608 mg/Kg), 20 mL ethanol, 20 mL of (15%) H <sub>2</sub> O <sub>2</sub> , and 20 mL/g of 5 mmol/L Fe <sup>2+</sup> . The reaction pH was 2-3. The reaction was run for 24 h at 25 °C. Product was extracted by DCM and analyzed by GC-MS.	Removal efficiency was~ 10-20%. Ethanol is effective solvent with Fenton oxidation of PAHs and enhance product accumulation.	[22]
Fenton oxidation of PAHs in contaminated soil in ethanol.	Spiked soil was spiked by 5 PAHs, which are FLUT (50 mg/kg soil), ANT (50 mg/kg soil), PYN (100 mg/kg soil), BBFT (10 mg/kg soil), or BAP (10 mg/kg soil). 220 mg/kg for five PAHs (150 ppm) Soil. Four washing stages of 6.0 g soil was achieved using 18 mL of the first stage and 12 mL of stages 2-4, each stage for 24 h. Fenton oxidation of PAHs using 10 mL of solution, 4 mL of 0.5 mol/L Fe <sup>2+</sup> , and 2.7 mL of 30% H <sub>2</sub> O <sub>2</sub> , pH was 3.5, at 30 °C for 3 h.	73-91% removal of anthracene, benzo[a]pyrene, pyrene, acenaphthylene, acenaphthene, benz[a]anthracene, benzo[j]fluoranthene, or indeno[1,2,3-cd]pyrene. 9.6-27% removal of naphthalene, fluorene, fluoranthene, phenanthrene, or benzo[b]fluoranthene.	[23]

**Table S1.2. (continued)**

Optimization of Fenton oxidation of PAH-contaminated site using vegetable oils	Two field soils: one from New Jersey with 13 PAHs (7700 mg/kg) and the second from Pennsylvania site with (3100 mg/kg PAHs concentration). 10 g of soil, 50 ml of water. pH was 3.0. 100 mg HgCl <sub>2</sub> . 5% (w/w) corn oil (CO) or palm kernal oil (PKO) for 2–3 h. CaO <sub>2</sub> (1% w/w) was also tested as alternative of H <sub>2</sub> O <sub>2</sub> .	5-44% removal efficiencies. Recoveries of HMW PAHs were affected by biotic (non-poisoned)/abiotic (poisoned) reaction system, where in the case of Fenton/CO, recoveries of LMW PAHs is the same in both cases, while recoveries of HMW PAHs was slightly less in biotic reaction. Compared to H <sub>2</sub> O <sub>2</sub> , CaO <sub>2</sub> . Gives higher removal of PAHs.	[24]
PAH removal from creosote-contaminated soil using Fenton oxidation/biological treatment.	4.0 g of sandy creosote oil-contaminated soil with total PAHs concentration in the soil is 1203 mg/kg. 20 mL of H <sub>2</sub> O <sub>2</sub> :Fe <sup>2+</sup> molar ratio of 10:1 to 234:1. Ph was 3.0 and the reaction time was 30 min. An aerobic bench scale sequencing batch reactor was used for achieving the biological treatment.	At using 20:1 H <sub>2</sub> O <sub>2</sub> :Fe mol ratio, the removal % is as follows: 45% (Fenton treatment) and 75% (Fenton/ biological treatment). The reaction kinetic follows a pseudo-first kinetic order.	[25]

**Table S1.3.** Brief summaries of work on PAH degradation using peroxyacetic acid.

<b>Study</b>	<b>Sample and experiential conditions</b>	<b>results</b>	<b>Ref.</b>
Removal of benzo[a]pyrene from contaminated sediments using peroxyacetic acid.	Sediments spiked by benzo[a]pyrene (10-25 mmol/Kg sediments). 2.5 g of contaminated sediments, then 5 mL deionized water, 5 mL of acetic acid or propionic acid, and 5 mL of hydrogen peroxide was added, respectively. Reaction was left for 24 h at room temperature, then 2 ml of 1 mol/L sodium sulfite was added to quench the reaction.	Complete degradation of benzo[a]pyrene was achieved at room temperature within 24 h. Propionic acid shows a faster reaction rate compared to acetic acid. The reason for this behaviour is not clear.	[26]
Removal of PAHs from contaminated Superfund site soil using peroxyacetic acid.	Superfund site soil (5.0 g) including 14 PAHs provided by EPA. Two ratios of hydrogen peroxide:acetic acid:deionized water ( 3:5:7 (v/v/v) and 3:3:9 (v/v/v)) were investigated. Reaction was left at room temperature for 24 h. Products were extracted by 5 mL DCM.	Complete removal of PAHs was achieved using 3:5:7 (v/v/v) ratio.	[27]
PAH degradation using peroxyacetic acid.	Glass beads (0–1.0 g) was spiked by 100 $\mu$ L of benzo[a]pyrene stock solution in acetone (5000 ppm). 3:3:9 v/v/v/ and 5:5:5 v/v/v/ hydrogen peroxide/acetic acid/ deionized water with and without concentrated sulfuric (1.0 mL), and 6:9 v/v commercial peracetic acid/ deionized water were used. The reaction was left for 24 h then quenched using 3 mL of a 1 mol/L sodium sulfite ( $\text{Na}_2\text{SO}_3$ ).	60% removal of when 1.7% peroxyacetic acid was used. The removal % increased to 80% when the peroxyacetic acid increased to 9.2%.	[28]

**Table S1.3.** (continued)

Removal of $\alpha$ -methylnaphthalene from contaminated sediment using peroxy acid.	Three non-contaminated sediments from Lake Macatawa (Holland, MI). 10-25 mmol $\alpha$ -methylnaphthalene /kg sediment. 1.0 g of silty-clay sediment I or 2.5 g sandy sediment II or III. 1:1:1 v/v/v mixture of water/organic acid/hydrogen peroxide solution (15 mL total volume). The reaction was left at room temperature for 24 h, then quenched using 3.0 mL of a 1.0 mol/L sodium sulfite ( $\text{Na}_2\text{SO}_3$ ). Product was extracted by 2.0 mL of isooctane then analyzed by GC-FID.	70% and 100% removal (%) of $\alpha$ -methylnaphthalene when propionic acid and acetic acid were used, respectively.	[29]
--	--	--	------

**Table S1.4.** Some studies that have achieved thermal removal of PAHs from contaminated soils.

<b>Study objective</b>	<b>Experimental conditions</b>	<b>Results</b>	<b>Ref.</b>
Microwave heating for removal of PAHs from contaminated soils.	Field soils (25 g). 0.5-1.5 kW microwave power and N <sub>2</sub> flow rate is 2 L/min. Temperature in the range of 100-300 °C and the residence time is 40 sec.	> 95% removal of PAHs at 100 °C of LMW PAHs and >300 °C of HMW PAHs within 40 sec. Removal of PAHs from contaminated soil is highly dependent on residence time and microwave power.	[30]
Hydrocarbons removal from contaminated soils using microwave heating.	Soil from industrial site (20 g). 5 L/min N <sub>2</sub> flow rate, 1.5 kW microwave power, and 20-110 sec heating time.	The organic contaminants were identified, which are aliphatic, aromatic, and polar compounds. 85-95% removal efficiency using stirred bed system and 30-50% removal efficiency using fixed bed systems.	[31]
Removal of PAHs from contaminated soil using conventional heating	Field soil (2700 mg/kg PAHs). Soil was loaded in a horizontal tubular (length 65 cm x 3 cm wide) then inserted inside the cylindrical furnace. Heating at temperature in the range of 250-650 °C under air flow and the hold time at the final temperature is 60 min. On-line FID analysis of volatile fraction.	Maximum removal of PAHs is 99.7% at 300 - 350 °C.	[32]

**Table S1.3. (continued)**

Degradation of PAHs in soil using microwave heating.	8 g of soil spiked by 1.008 mg of individual PAHs (Benzo[a]pyrene, benzo[b]fluoranthene, dibenzo[a,h]anthracene, Benzo[a]anthracene, 1-nitropyrene and benzo[a,h]quinoline). Sample was heated using open microwave system for 10 min at 37.5 W, 10 min at 75 W, 10 min at 225 W, and 10 min at 750 W.	~55% of PAH compound was removed.	[33]
PAHs extraction from lampblack-contaminated soil by thermal treatment.	Field soil (70 kg) includes 11 PAHs (4100 mg/Kg). Bench scale thermally enhanced soil vapour extraction (SVE) reactor (48 cm <sup>2</sup> x 30 cm). Temperature range is 650-700 °C for 35 days.	PAHs concentration was reduced to be 100 mg/Kg during 10 days at temperature in the range of 250-300 °C.	[34]

## **Appendix B. Supporting information for Chapter 4.**

### **S4.1. Solubility of coal tar in anhydrous ethanol**

The solubility testing of coal tar in anhydrous ethanol was conducted in triplicate at room temperature (~21.5 °C). Different weights of coal tar samples (0.010, 0.020, 0.030, and 0.150 g) were precisely weighed and each was mixed with 4.0 mL of anhydrous ethanol in a 10 mL PTFE sealed tube. The mixture was sonicated for 10 min, then centrifuged for 20 min and filtered using Whatman filter paper (0.45 μm). The undissolved fraction of coal tar was dried at room temperature for 5-7 days in a fume hood until a constant weight was obtained, then the difference in weight was calculated. The results indicated the coal tar was partially soluble in anhydrous ethanol with a solubility of about 4.4 g/L.

### **S4.2. FTIR analysis**

Approximately 0.2 mg of pyrene with biochar (5:1 wt/wt), and residues from the microwave-assisted heating of pyrene with biochar using both open and closed microwave systems were each mixed well with 200 mg of KBr powder using a mortar and pestle, and then pressed using a manual hydraulic press (Specac). The analysis was achieved using an OPUS spectrometer (Thermo Scientific, USA) with a resolution of 4 cm<sup>-1</sup> and 36 scans. The sample was scanned in the wavelength range of 400-4000 cm<sup>-1</sup>.

The FTIR analysis of the pyrene samples with biochar before, and after, microwave heating are shown in Figure S4.1. Two peaks at 1600 cm<sup>-1</sup> and 3200 cm<sup>-1</sup> correspond to the C=C and C-H (sp<sup>3</sup>) stretch, respectively. The presence of these absorption peaks after the microwave heating of pyrene + biochar (C and D) may indicate that some pyrene has become absorbed into the biochar.

### S4.3. SEM analysis

The surface morphologies of biochar and the residues from the microwave heating of pyrene with biochar were investigated using SEM. The SEM model used is a FEI MLA 650 F SEM using an acceleration voltage of 15 kV and a magnification of 50,000. Prior to analysis, samples were coated using a thin layer of gold to improve the secondary electron signal by reducing thermal damage and charging of the sample.

Figure S4.2 shows the SEM analysis of biochar, biochar with pyrene, and residues from microwave heating of pyrene with biochar. Compared to the biochar morphology, some changes can be observed in the residue from the open microwave system, which may indicate that some pyrene has become converted into char, or has become absorbed into the biochar.

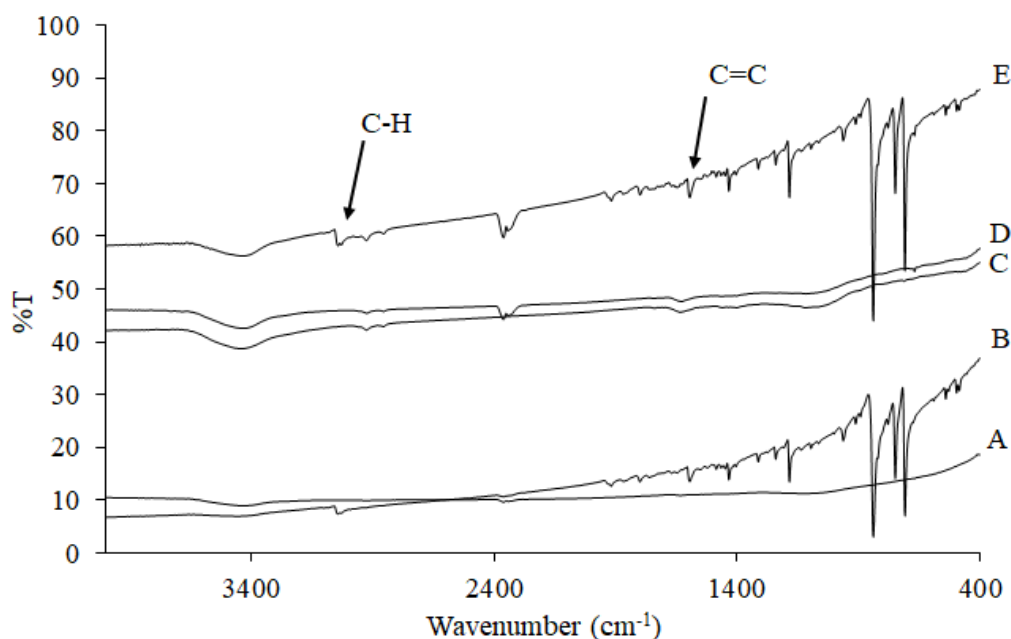


**Figure S4.1.** FT-IR analysis of biochar (A), pyrene (E), pyrene with biochar (B), and residue from microwave-assisted heating of pyrene with biochar using open (C) and closed (D) microwave system.

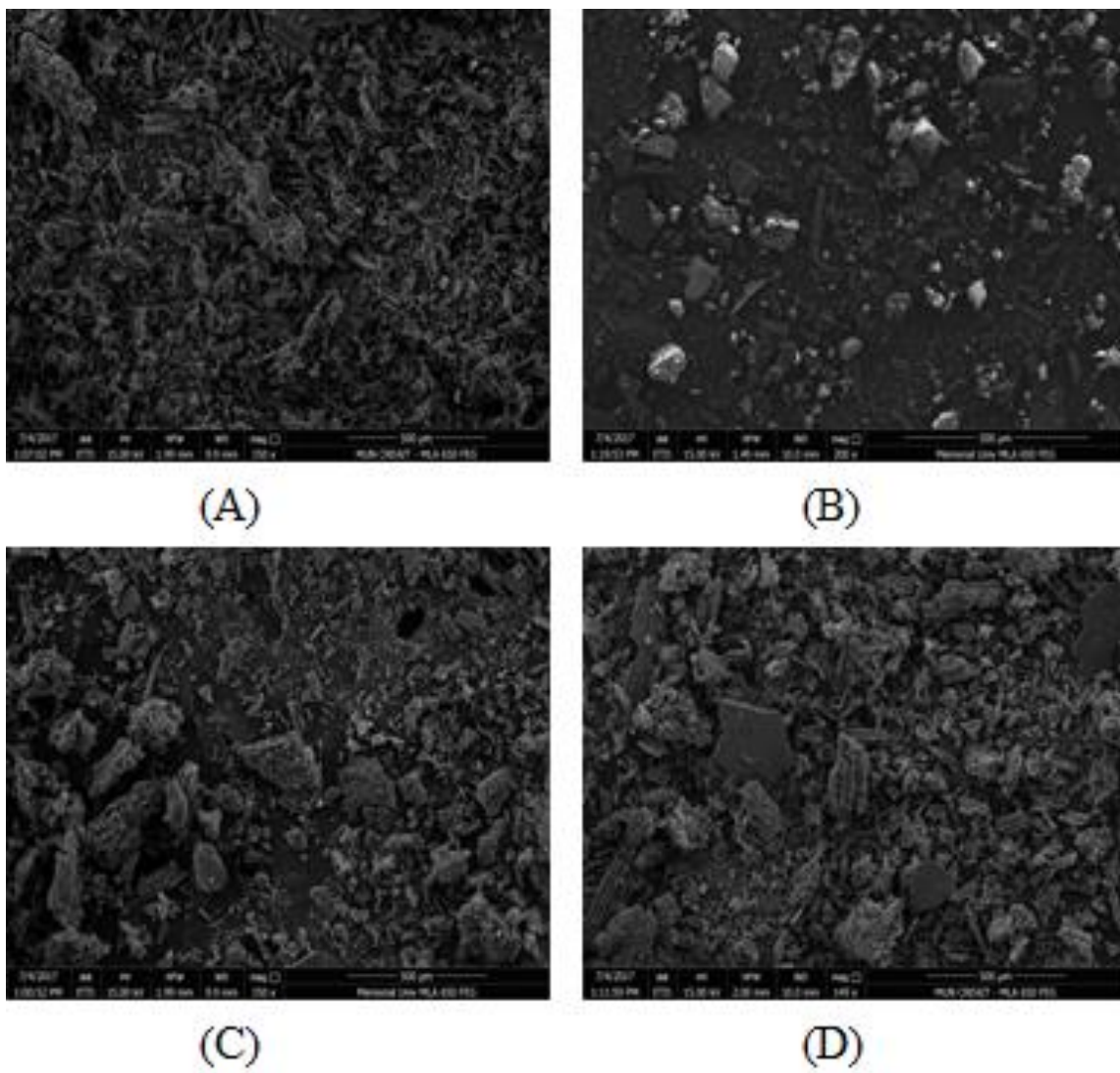


**Figure S4.2.** SEM analysis of biochar (A), biochar with pyrene (B), and residue from microwave heating of pyrene with biochar, using the closed (C), and open (D) microwave systems. Magnification is 150x, and the scale bar is 500 μm.

## Appendix C. Supporting information for Chapter 5.

### S5.1. Computational method to determine the active sites in pyrene

Quantum chemical computations were achieved using density functional theory (DFT) [35] at the Becke3-Lee-Yang-parr (B3LYP) level with 6-31G(d) basis set using the Gaussian 16 program package [36]. The analysis results are listed in Table S5.1. The reactivity of sites in pyrene were estimated using Fukui functions [37], wherein the following equations (S5.1-S5.3) were used:

$$f^+(r) = \rho(r)_{N+1} - \rho(r)_N \quad \text{For nucleophilic attack} \quad (\text{S5.1})$$

$$f^-(r) = \rho(r)_N - \rho(r)_{N-1} \quad \text{For electrophilic attack} \quad (\text{S5.2})$$

$$f^o(r) = \frac{1}{2} [\rho(r)_{N+1} - \rho(r)_{N-1}] \quad \text{For radical attack} \quad (\text{S5.3})$$

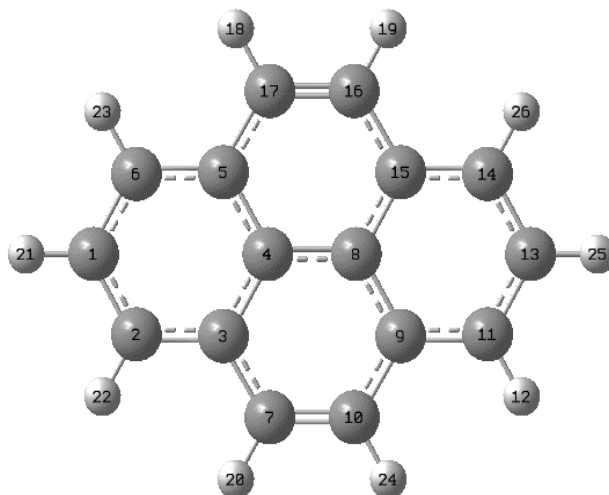
Where,

$\rho(r)_N$ ,  $\rho(r)_{N+1}$ , and  $\rho(r)_{N-1}$  are electronic densities of molecule with  $N$ ,  $N+1$ , and  $N-1$  electrons.

The results indicate that the positions C2, C6, C11, and C14 in the pyrene structure (Figure S5.1) have the highest  $f^o(r)$  values.

**Table S5.1.** Results of Hirshfeld population analysis: Fukui functions ( $f^+$ ,  $f^-$ ,  $f^o$ ) for pyrene.

#	Atom	$\rho(r)_N$	$\rho(r)_{N+1}$	$\rho(r)_{N-1}$	$f^o(r)$	$f^+(r)$	$f^-(r)$
1	C	6.044134	6.081238	6.008405	0.0364165	0.037104	0.035729
2	C	<b>6.042956</b>	<b>6.111335</b>	<b>5.970234</b>	<b>0.0705505</b>	<b>0.068379</b>	<b>0.072722</b>
3	C	6.002946	6.029562	5.976543	0.0265095	0.026616	0.026403
4	C	5.998778	6.006643	5.991072	0.0077855	0.007865	0.007706
5	C	6.002946	6.029562	5.976543	0.0265095	0.026616	0.026403
6	C	<b>6.042956</b>	<b>6.111334</b>	<b>5.970234</b>	<b>0.0705500</b>	<b>0.068378</b>	<b>0.072722</b>
7	C	6.041476	6.095799	5.986952	0.0544235	0.054323	0.054524
8	C	5.998778	6.006643	5.991073	0.0077850	0.007865	0.007705
9	C	6.002946	6.029562	5.976543	0.0265095	0.026616	0.026403
10	C	6.041476	6.095799	5.986951	0.0544240	0.054323	0.054525
11	C	<b>6.042956</b>	<b>6.111334</b>	<b>5.970234</b>	<b>0.0705500</b>	<b>0.068378</b>	<b>0.072722</b>
12	H	0.957430	0.990835	0.925418	0.0327085	0.033405	0.032012
13	C	6.044134	6.081238	6.008405	0.0364165	0.037104	0.035729
14	C	<b>6.042956</b>	<b>6.111334</b>	<b>5.970234</b>	<b>0.0705500</b>	<b>0.068378</b>	<b>0.072722</b>
15	C	6.002946	6.029562	5.976542	0.0265100	0.026616	0.026404
16	C	6.041476	6.095798	5.986951	0.0544235	0.054322	0.054525
17	C	6.041476	6.095798	5.986951	0.0544235	0.054322	0.054525
18	H	0.956092	0.986394	0.927629	0.0293825	0.030302	0.028463
19	H	0.956092	0.986394	0.927629	0.0293825	0.030302	0.028463
20	H	0.956092	0.986394	0.927629	0.0293825	0.030302	0.028463
21	H	0.955280	0.984259	0.926963	0.0286480	0.028979	0.028317
22	H	0.957430	0.990835	0.925418	0.0327085	0.033405	0.032012
23	H	0.957430	0.990835	0.925418	0.0327085	0.033405	0.032012
24	H	0.956092	0.986394	0.927629	0.0293825	0.030302	0.028463
25	H	0.955280	0.984259	0.926963	0.0286480	0.028979	0.028317
26	H	0.957430	0.990835	0.925417	0.0327090	0.033405	0.032013

**Figure S5.1.** The structure of pyrene with the atom labels shown in Tables S5.1.

## References

- [1] Elie, M. R.; Clausen, C. A.; Yestrebky, C. L. Reductive Degradation of Oxygenated Polycyclic Aromatic Hydrocarbons Using an Activated Magnesium/co-Solvent System. *Chemosphere* **2013**, *91*, 1273–1280.
- [2] Elie, M. R.; Clausen, C. A.; Yestrebky, C. L. Multivariate Evaluation and Optimization of an Activated-Magnesium/co-Solvent System for the Reductive Degradation of Polycyclic Aromatic Hydrocarbons. *J. Hazard. Mater.* **2013**, *248–249*, 150–158.
- [3] Garbou, A. M.; Clausen, C. A.; Yestrebky, C. L. Comparative Study for the Removal and Destruction of Pentachlorophenol Using Activated Magnesium Treatment Systems. *Chemosphere* **2017**, *166*, 267–274.
- [4] Zullo, F. M.; Liu, M.; Zou, S.; Yestrebky, C. L. Mechanistic and Computational Studies of PCB 151 Dechlorination by Zero Valent Magnesium for Field Remediation Optimization. *J. Hazard. Mater.* **2017**, *337*, 55–61.
- [5] Elie, M. R.; Williamson, R. E.; Clausen, C. a.; Yestrebky, C. L. Application of a Magnesium/co-Solvent System for the Degradation of Polycyclic Aromatic Hydrocarbons and Their Oxygenated Derivatives in a Spiked Soil. *Chemosphere* **2014**, *117*, 793–800.
- [6] Elie, M. R.; Clausen, C. A.; Geiger, C. L. Reduction of Benzo[a]pyrene with Acid-Activated Magnesium Metal in Ethanol: A Possible Application for Environmental Remediation. *J. Hazard. Mater.* **2012**, *203*, 77–85.
- [7] Kawahara, F. K.; Davila, B.; Al-Abed, S. R.; Vesper, S. J.; Ireland, J. C.; Rock, S. Polynuclear Aromatic Hydrocarbon (PAH) Release from Soil during Treatment with Fenton's Reagent. *Chemosphere* **1995**, *31*, 4131–4142.
- [8] Bogan, B. W.; Trbovic, V. Effect of Sequestration on PAH Degradability with Fenton's Reagent: Roles of Total Organic Carbon, Humic, and Soil Porosity. *J. Hazard. Mater.* **2003**, *100*, 285–300.
- [9] Goi, A.; Trapido, M. Degradation of Polycyclic Aromatic Hydrocarbons in Soil: The Fenton Reagent versus Ozonation. *Environ. Technol.* **2004**, *25*, 155–164.
- [10] Flotron, V.; Delteil, C.; Padellec, Y.; Camel, V. Removal of Sorbed Polycyclic Aromatic Hydrocarbons from Soil, Sludge and Sediment Samples Using the Fenton's Reagent Process. *Chemosphere* **2005**, *59*, 1427–1437.
- [11] Jonsson, S.; Persson, Y.; Frankki, S.; Lundstedt, S.; Van Bavel, B.; Haglund, P.; Tysklind, M. Comparison of Fenton's Reagent and Ozone Oxidation of Polycyclic Aromatic Hydrocarbons in Aged Contaminated Soils. *J. Soils Sediments* **2006**, *6*, 208–214.
- [12] Jonsson, S.; Persson, Y.; Frankki, S.; van Bavel, B.; Lundstedt, S.; Haglund, P.;

- Tysklind, M. Degradation of Polycyclic Aromatic Hydrocarbons (PAHs) in Contaminated Soils by Fenton's Reagent: A Multivariate Evaluation of the Importance of Soil Characteristics and PAH Properties. *J. Hazard. Mater.* **2007**, *149*, 86–96.
- [13] Sun, H. W.; Yan, Q. S. Influence of Fenton Oxidation on Soil Organic Matter and Its Sorption and Desorption of Pyrene. *J. Hazard. Mater.* **2007**, *144*, 164–170.
- [14] Ferrarese, E.; Andreottola, G.; Oprea, I. A. Remediation of PAH-Contaminated Sediments by Chemical Oxidation. *J. Hazard. Mater.* **2008**, *152*, 128–139.
- [15] Gryzenia, J.; Cassidy, D.; Hampton, D. Production and Accumulation of Surfactants during the Chemical Oxidation of PAH in Soil. *Chemosphere* **2009**, *77*, 540–545.
- [16] Watts, R. J.; Stanton, P. C.; Howsawheng, J.; Teel, A. L. Mineralization of a Sorbed Polycyclic Aromatic Hydrocarbon in Two Soils Using Catalyzed Hydrogen Peroxide. *Water Res.* **2002**, *36*, 4283–4292.
- [17] S. R. Kanel. B. Neppolian, H. Choi, J. Y. Heterogeneous Catalytic Oxidation of Phenanthrene by Hydrogen Peroxide in Soil Slurry: Kinetics, Mechanism, and Implication. *Soil Sediment Contam.* **2003**, *12*, 101–117.
- [18] Kanel, S. R.; Neppolian, B.; Jung, H.; Choi, H. Comparative Removal of Polycyclic Aromatic Hydrocarbons Using Iron Oxide and Hydrogen Peroxide in Soil Slurries. *Environ. Eng. Sci.* **2004**, *21*, 741–751.
- [19] Pradhan, S.; Paterek, J.; Liu, B. Y.; Conrad, J. R.; Srivastava, V. J. Pilot-Scale Bioremediation of PAH-Contaminated Soils. *Appl. Biochem. Biotechnol.* **1997**, *63*, 759–773.
- [20] Lee, B. D.; Hosomi, M.; Murakami, A. Fenton Oxidation with Ethanol to Degrade Anthracene into Biodegradable 9, 10-Anthraquinone: A Pretreatment Method for Anthracene-Contaminated Soil. *Water Sci. Technol.* **1998**, *38*, 91–97.
- [21] Lee, B. D.; Hosomi, M. A Hybrid Fenton Oxidation-Microbial Treatment for Soil Highly Contaminated with Benz(a)anthracene. *Chemosphere* **2001**, *43*, 1127–1132.
- [22] Lundstedt, S.; Persson, Y.; Öberg, L. Transformation of PAHs during Ethanol-Fenton Treatment of an Aged Gasworks' Soil. *Chemosphere* **2006**, *65*, 1288–1294.
- [23] Lee, B.-D.; Hosomi, M. Ethanol Washing of PAH-Contaminated Soil and Fenton Oxidation of Washing Solution. *J. Mater.* **2000**, *2*, 24–30.
- [24] Bogan, B. W.; Trbovic, V.; Paterek, J. R. Inclusion of Vegetable Oils in Fenton's Chemistry for Remediation of PAH-Contaminated Soils. *Chemosphere* **2003**, *50*, 15–21.
- [25] Vandekinderen, I.; Devlieghere, F.; De Meulenaer, B.; Ragaert, P.; Van Camp, J. Optimization and Evaluation of a Decontamination Step with Peroxyacetic Acid for Fresh-Cut Produce. *Food Microbiol.* **2009**, *26*, 882–888.

- [26] N'Guessan, A. L.; Levitt, J. S.; Nyman, M. C. Remediation of Benzo(a)pyrene in Contaminated Sediments Using Peroxy-Acid. *Chemosphere* **2004**, *55*, 1413–1420.
- [27] Scott Alderman, N.; N'Guessan, A. L.; Nyman, M. C. Effective Treatment of PAH Contaminated Superfund Site Soil with the Peroxy-Acid Process. *J. Hazard. Mater.* **2007**, *146*, 652–660.
- [28] Alderman, N. S.; Nyman, M. C. Oxidation of PAHs in a Simplified System Using Peroxy-Acid and Glass Beads: Identification of Oxidizing Species. *J. Environ. Sci. Heal. Part A* **2009**, *44*, 1077–1087.
- [29] Levitt, J. S.; N'Guessan, A. L.; Rapp, K. L.; Nyman, M. C. Remediation of Alpha-Methylnaphthalene-Contaminated Sediments Using Peroxy Acid. *Water Res.* **2003**, *37*, 3016–3022.
- [30] Robinson, J. P.; Kingman, S. W.; Snape, C. E.; Shang, H.; Barranco, R.; Saeid, A. Separation of Polyaromatic Hydrocarbons from Contaminated Soils Using Microwave Heating. *Sep. Purif. Technol.* **2009**, *69*, 249–254.
- [31] Robinson, J. P.; Kingman, S. W.; Lester, E. H.; Yi, C. Microwave Remediation of Hydrocarbon-Contaminated Soils - Scale-up Using Batch Reactors. *Sep. Purif. Technol.* **2012**, *96*, 12–19.
- [32] Renoldi, F.; Lietti, L.; Saponaro, S.; Bonomo, L.; Forzatti, P. Thermal Desorption of a PAH-Contaminated Soil: A Case Study. *Ecosyst. Sustain. Dev. Iv, Vols 1 2* **2003**, *18*, 1123–1132.
- [33] Abramovitch, R. A.; Bangzhou, H.; Abramovitch, D. A.; Jiangao, S. In Situ Decomposition of PAHs in Soil and Desorption of Organic Solvents Using Microwave Energy. *Chemosphere* **1999**, *39*, 81–87.
- [34] Thomas C. Harmon, Glenn A. Burks, Anne-Christine Aycaguer, K. J. Thermally Enhanced Vapor Extraction Fro Removing PAHs from Lampblack-Contaminated Soil. *J. Environ. Eng.* **2001**, *127*, 986–993.
- [35] Geerlings, P.; De Proft, F.; Langenaeker, W. Conceptual Density Functional Theory. *Chem. Rev.* **2003**, *103*, 1793–1874.
- [36] Frisch, M. J.; Trucks, G. W.; Schlegel, H. B.; Scuseria, G. E.; Robb, M. A.; Cheeseman, J. R.; Scalmani, G.; Barone, V.; Petersson, G. A.; Nakatsuji, H.; Li, X.; Caricato, M.; Marenich, A. V.; Bloino, J.; Janesko, B. G.; R. G, J. A.; Peralta, J. E.; Ogliar, S. S. Gaussian 16. 2016.
- [37] Raja, M.; Raj Muhamed, R.; Muthu, S.; Suresh, M.; Muthu, K. Synthesis, Spectroscopic (FT-IR, FT-Raman, NMR, UV-Visible), Fukui Function, Antimicrobial and Molecular Docking Study of (E)-1-(3-Bromobenzylidene)semicarbazide by DFT Method. *J. Mol. Struct.* **2017**, *1130*, 374–384.